COOPERATIVE DIVERSITY ARCHITECTURE

FOR WIRELESS NETWORKS

by

M. Sarper Göktürk

Submitted to the Graduate School of Engineering and Natural Sciences
in partial fulfillment of
the requirements for the degree of
Doctor of Philosophy

Sabancı University

June 2011

COOPERATIVE DIVERSITY ARCHITECTURE

FOR WIRELESS NETWORKS

APPROVED BY:

Assoc. Prof. Özgür Gürbüz, (Dissertation Supervisor)

....

Assoc. Prof. Oğuz Sunay

....
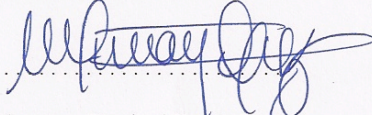
Assoc. Prof. Albert Levi

....
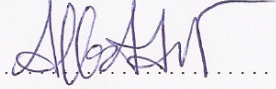
Prof. Elza Erkip

....
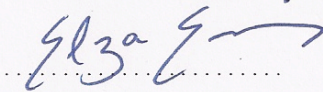
Assoc. Prof. Özgür Erçetin

....
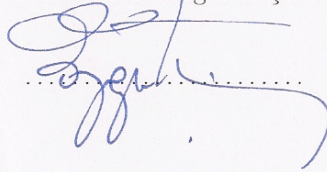
DATE OF APPROVAL: 22. 06. 2011

Abstract

The burgeoning demand for wireless networks necessitates reliable and energy-efficient communication architectures that are robust to the impairments of the wireless medium. Cooperative communication emerges as an appropriate technique that mitigates the severe effects of channel impairments through the use of cooperative diversity. Notwithstanding the fact that cooperative diversity is a very suitable technique to provide robust and reliable communication, the realization of cooperation idea precipitates many technical challenges that are associated with the overhaul of the wireless network design. This dissertation proposes a cooperative diversity architecture for wireless networks, that spans the physical, medium access and routing layers with parameters (jointly) optimized for overall system performance, taking into account the cost of cooperation in each layer.

First, we present a new cooperative MAC protocol, COMAC, that enables cooperation of multiple relays in a distributed fashion. Through the proposed protocol, we investigate and demonstrate at what rate and for which scenarios cooperation brings benefits in terms of throughput and energy-efficiency. Our results demonstrate that cooperation initiation has a significant cost on both the throughput and energy-efficiency, which have been often disregarded in the literature.

We next study the energy minimal joint cooperator selection and power assignment problem under transmit power constraints such that the cooperative transmissions satisfy an average bit error rate (BER) target. We derive the average BER of the cooperative system and we propose a simple yet close approximation to facilitate cooperator selection methods with closed form power assignment solutions. We formulate the joint cooperator selection and power assignment problem, we present the optimal solution (O-CSPA) and we also propose a distributed implementation (D-CSPA). Our results demonstrate that smart cooperator selection is essential, as

it provides efficient resource allocation with reduced overhead leading to improved system performance. Our implementation and simulations of D-CSPA algorithm in COMAC protocol demonstrate that our distributed algorithm causes minimal overhead, yields improved throughput and reduced delay, while reducing the energy consumption.

Finally, we propose a cooperative routing framework and a cross-layer architecture, RECOMAC, for wireless ad hoc networks. The RECOMAC architecture facilitates formation of cooperative sets on the fly in a decentralized and distributed fashion, requiring no overhead for relay selection and actuation, and resulting in opportunistically formed cooperative links that provide robust and reliable end-to-end communication, without the need for establishing a prior non-cooperative route, unlike existing schemes. The results demonstrate that under wireless channel impairments, such as fading and path loss, our cooperative forwarding framework and cross-layer architecture, RECOMAC significantly improve the system performance, in terms of throughput and delay, as compared to non-cooperative conventional layered network architecture with AODV routing over IEEE 802.11 MAC.

Özet

Kablosuz ağlara yönelik giderek artmakta olan talep, kablosuz ortamın kanal bozulmalarına karşı dayanıklı, güvenilir ve aynı zamanda enerji-verimli haberleşme mimarilerini gerektirmektedir. İşbirlikli haberleşme, kanal bozulmalarından kaynaklanan etkilerin işbirlikçi çeşitleme vasıtasıyla azaltılmasına dayanan, uygun bir teknik olarak ortaya çıkmaktadır. İşbirlikli çeşitlemenin, dayanıklı ve güvenilir bir haberleşme yöntemi olmasıyla birlikte, işbirliğinin gerçek bir kablosuz ağda uygulanması kablosuz ağ tasarımı ile ilgili birçok teknik zorluğu beraberinde getirmektedir. Bu tezde, kablosuz ağlar için, fiziksel, ortam erişim ve yol atama katmanlarını kapsayan, tüm sistem başarımını eniyileyen parametrelerin işbirliğinin tüm katmanlardaki maliyeti hesaba alınarak çözümlendiği bir işbirlikçi çeşitleme mimarisi önerilmektedir.

İlk olarak, birden çok röleyle işbirliğini mümkün kılan yeni bir işbirlikli ortam erişim protokolünü sunmaktayız. Önerilen protokol vasıtasıyla, hangi veri iletim hızları ve senaryolarda işbirliğinin sistemin net veri hızına ve enerji-verimliliğine katkı sağladığını incelemekte ve başarım analizlerini sunmaktayız. Sonuçlarımız göstermektedir ki, işbirliğinin başlatılmasının net veri hızı ve enerji-verimliliği üzerinde kayda değer bir etkisi vardır. Bu etki literatürde sıkça gözardı edilmiştir.

Ardından, iletim gücü kısıtlaması ve işbirlikli iletimin belirli bir ortalama bit hata oranını sağlaması kısıtları altında, en düşük enerji harcayan işbirlikçi küme seçimi ve güç ataması problemini incelemekteyiz. İşbirlikli sistemin ortalama bit hata oranını formüle etmekteyiz ve bununla birlikte işbirlikçi küme seçimi ve kapalı-biçimli güç atama sonuçları bulmaya imkan sağlayacak, yalın fakat isabetli bir bit hata oranı yakınsaması önermekteyiz. İşbirlikçi küme seçimi ve güç ataması problemini formüle edip eniyi çözümü (O-CSPA) sunmakta ve ayrıca dağıtık bir uygulamayı (D-CSPA) önermekteyiz. Sonuçlarımız göstermektedir ki, verimli kaynak dağılımını düşük maliyetle gerçekleyerek sistem başarımını iyileştirdiği için akıllı

işbirlikçi röle seçimi vazgeçilmezdir. D-CSPA algoritmamızın COMAC protokolü içerisinde gerçeklemesi ve benzetimleri dağıtık algoritmamızın sistemin net veri hızını arttırdığını, veri gecikmesini azalttığını ve bununla birlikte sistemin enerji harcamasını ve mesajlaşma yükünü de önemli ölçüde azalttığını göstermiştir.

Son olarak, kablosuz tasarsız ağlar için işbirlikçi yol atama yapısı ve katmanlararası bir mimari, RECOMAC, önermekteyiz. RECOMAC mimarisi, literatürdeki mevcut yöntemlerin aksine, dayanıklı ve güvenilir uçtan-uca haberleşmeyi hiçbir önceden saptanmış rotaya gereksinim olmadan, tamamıyla fırsatçı ve dağıtık biçimde oluşturulmuş işbirlikçi röle kümeleri vasıtasıyla, röle seçimi ve harekete geçirilmesi için fazladan hiçbir yük getirmeden sağlamaktadır. Sonuçlar göstermektedir ki, kanal sönümlemesi ve yol kaybı gibi kablosuz kanal bozulmalarında bile, işbirlikçi yönlendirme yapımız ve katmanlararası mimarimiz, RECOMAC, AODV yol ataması ve IEEE 802.11 ortam erişimi kullanan işbirliksiz katmanlı geleneksel ağ mimarilerine kıyasla net veri hızı ve veri gecikmesi açısından sistem başarımını önemli ölçüde arttırmaktadır.

Acknowledgements

I am glad to have the opportunity to thank everybody who supported and encouraged me during my Ph.D. First of all, I would like to express my sincere gratitude to my advisor Prof. Özgür Gürbüz for her tenacious support throughout the development of this dissertation. I deeply appreciate her guiding, inspiration, knowledge, patience, encouragement and perfectionism, which made this dissertation possible.

I would like to express my sincere thanks to Prof. Elza Erkip for providing me the opportunity to collaborate with her laboratory at the Polytechnic Institute of New York University. I am grateful for her enormous support and inspiration, her friendly attitude which made my visit at NYU fruitful and momentous. I also would like to express my sincere gratitude to Prof. Özgür Erçetin for his inspiration, support and many invaluable discussions we held, which contributed to this dissertation. I also would like to thank Prof. Oğuz Sunay and Prof. Albert Levi for being in my thesis committee, and for their time and effort in evaluating my work.

I also would like to thank TUBITAK for the fellowship which supported me during my Ph.D.

I am indebted to several colleagues and friends whose insightful discussions contributed to my research. Many friends and colleagues have made my stay at Sabancı University enjoyable. These include Engin Maşazade, Kayhan Eritmen, Mehmet Karaca, Ali Arsal, Yunus Sarıkaya, Mümin İmamoğlu, Naime Özben Önhon, Mahir Umman Yıldırım, Serkan Çiftlikli. I also would like to thank my longtime great friend Murat Çınar Büyükakça. The thoughts we exchanged, and the laughter we shared made these Ph.D. years fun and memorable.

I owe everything to the unconditional love and support from my family. I am very grateful to my mother Öznur Göktürk, my father Mevlüt Göktürk and my sister H. Sinem Göktürk Büyüknacar for the concern, caring, endless love and support

they provided me throughout my life. I am especially thankful to Elvin Çoban. I probably would not survive the Ph.D. without her love, encouragement, inspiration and support, which cheered me up during the most difficult times. She has also been a great colleague with whom I had the privilege to discuss research.

On a concluding note, the quote below is dedicated to the many people who have helped to inspire and encourage me in pursuing this degree, personally and/or professionally along the way, thank you.

"There is no such thing as a 'self-made' man. We are made up of thousands of others. Everyone who has ever done a kind deed for us, or spoken one word of encouragement to us, has entered into the make-up of our character and of our thoughts, as well as our success." - George Matthew Adams

TABLE OF CONTENTS

List of Tables

List of Figures

List of Abbreviations

ACK   Acknowledgement

ACO   Available to Cooperate

AF   Amplify and Forward

AODV   Ad hoc On Demand Distance Vector

AWGN   Additive White Gaussian Noise

BER   Bit Error Rate

BPSK   Binary Phase Shift Keying

BS   Base Station

C-ACK   Acknowledgement for Cooperative Transmission

C-CTS   Clear to Send in Cooperation

C-MFR   Cooperative MFR

C-RTS   Request to Send in Cooperation

CDMA   Code Division Multiple Access

CF   Cooperative Flooding

CFPR   Cooperative Forwarding within Progress Region

CFPR-DT   CFPR with Dual Threshold

CI   Cooperation Information

CRC   Cyclic Redundancy Check

CSI	Channel State Information
CSMA	Carrier Sense Multiple Access
CSMA/CA	Carries Sense Multiple Access with Collision Avoidance
CTS	Clear to Send
CW	Contention Window
D-CSPA	Distributed Cooperator Selection and Power Assignment
DCF	Distributed Coordination Function
DF	Decode and Forward
DIFS	DCF Inter Frame Spacing
DSTC	Distributed Space-Time Code
EGC	Equal-Gain Combining
F	Conventional Flooding
FC	Frame Control
FCS	Frame Check Sequence
FPR	Forward Progress Region
FSK	Frequency Shift Keying
i.i.d.	Independent and identically distributed
LREP	Location Reply
LREQ	Location Request

MAC	Medium Access Control
MANET	Mobile Ad hoc Network
MFR	Most Forward within the transmission Radius r
MGF	Moment Generating Function
MIMO	Multiple Input Multiple Output
MISO	Multiple Input Single Output
MRC	Maximal Ratio Combining
NAV	Network Allocation Vector
ns-2	Network Simulator version 2
O-CS	Optimal Cooperator Selection without power assignment
O-CSPA	Optimal Cooperator Selection and Power Assignment
OLA	Opportunistic Large Arrays
PDR	Packet Delivery Ratio
PLCP	Physical Layer Convergence Protocol
PSD	Power Spectral Density
PSK	Phase Shift Keying
QAM	Quadrature Amplitude Modulation
QPSK	Quadrature Phase Shift Keying
R-ACK	Routing enabled ACK

R-ACK	Routing enabled Acknowledgement
R-CACK	Routing enabled Cooperative ACK
R-CS	Random Cooperator Selection
R-CTS	Routing enabled Clear to Send
R-RTS	Routing enabled Request to Send
RARA	Random Access Relay Advertisement
RDSTC	Randomized Distributed Space-Time Code
RDSTC	Randomized Distributed Space-Time Code
RECOMAC	Routing Enabled Cooperative MAC
RIFS	Reduced Inter Frame Spacing
RREP	Route Reply
RREQ	Route Request
RTS	Request to Send
SC	Selection Combining
SEP	Symbol Error Probability
SER	Symbol Error Rate
SIFS	Short Inter Frame Spacing
SIMO	Single Input Multiple Output
SISO	Single Input Single Output

SLC	Square-Law Combining
SNR	Signal to Noise Ratio
STBC	Space-Time Block Codes
TC	Threshold Combining
TDD	Time Division Duplex
v-MISO	Virtual MISO
WLAN	Wireless Local Area Network
WMN	Wireless Mesh Network
WSN	Wireless Sensor Network

1   INTRODUCTION

Wireless communications is the fastest growing branch of the communication industry, as it enables mobile communication, reduces the required infrastructure, and thus reduces the deployment costs, and allows for easily expandable networks. With the recent advances in communication technologies, signal processing and hardware design, wireless networks have become ubiquitous. The examples of wireless networks extend from infrastructured wireless local area networks, such as cellular telephone systems, wireless local area networks (WLANs), wide area wireless data systems, satellite systems, to infrastructureless, i.e., ad hoc wireless networks, such as wireless sensor networks (WSNs), wireless mesh networks (WMNs) and mobile ad hoc networks (MANETs) [1].

Today, wireless networks connect smart phones, small handheld computers, tiny sensor nodes and various types of wireless devices. In the near future, almost all devices around us will be connected via self configured wireless networks to provide seamless communication and processing capabilities. The envisioned wireless systems make use of wireless ad hoc networks, in particular, WSNs, which promise various applications, such as monitoring of fire hazards, stress and strain in buildings and bridges, the spread of chemicals and gasses at a disaster site, identification and tracking of enemy targets, surveillance, support of unmanned robotic vehicles, etc. [2]. As such, WSNs facilitate distributed control systems with remote devices, sensors and actuators linked together via wireless communication channels, which foster automated highways, mobile robots, and easily reconfigurable industrial automation.

Unfortunately, the advantages of the wireless networks come together with chal-

lenges. The paramount challenge is the nature of the wireless medium itself. The wireless medium is a shared and unpredictable channel with limited capacity. The wireless medium suffers from channel impairments, such as path loss, shadowing and fading, which diminish the reliability of communication. Moreover, the wireless nodes have to share the same medium for communication, thus requiring efficient methods for wireless transmission, i.e., modulation and coding, and also intelligent methods for node coordination and medium access. In addition to the challenges associated with the wireless medium, each wireless network application can also have its own set of challenges. For example, WSNs require energy-efficient methods for communication, since these networks rely on battery operated small wireless devices with sensing and limited processing capabilities [2]. WLANs, on the other hand, are less energy restricted, but bandwidth is the major design constraint for these networks.

The effects of severe channel impairments can be mitigated through the use of multiple-antennas, i.e., spatial diversity techniques [3]. In spatial diversity, the receiver is provided with multiple copies of the original signal through independent fading paths, thereby the fading of the resultant signal is reduced, leading to reliable and robust communication. Spatial diversity is particularly attractive as it can readily be combined with other forms of diversity, such as time and frequency diversity [1]. However, in order to harness the diversity gains in multi-antenna systems, the antennas are required to be separated by at least half the signal wavelength, translating into 12.5 cm for common wireless equipment, such as IEEE 802.11 [4] or 802.15.4 (ZigBee) [5]. The wireless networks of the near future are envisioned to incorporate many tiny smart wireless nodes that are capable of sensing the medium, communicating with each other and working towards certain tasks. These networks require reliable communication architectures that do not impose size limitations.

Cooperative communication, or user cooperation, has emerged as an appropriate

method for realizing spatial diversity, without employing antenna arrays on the nodes [6,7]. The word "cooperate" derives from the Latin word *cooperari*, from *co-* *'together'* + *operari* *'to work'*, and thus, cooperation connotes acting jointly, working towards the same end. Cooperation exploits the inherent nature of the wireless medium: The wireless transmissions are heard by any node in the transmission range of the sender. The nodes which can successfully receive the source transmission can help the source node in transmitting its data packets to the intended receiver through independent fading channels, thereby providing spatial diversity. The diversity obtained through the cooperative transmissions of multiple nodes is therefore named as *cooperative diversity* [6,8,9].

The basic ideas behind cooperative communication can be traced back to the work of Cover and El Gamal on the information theoretic properties of the relay channel [10]. Cover and El Gamal introduced new schemes to increase the source-destination communication rate with the help of a relay. The information theoretic capacity of the relay channel is still unknown. Nevertheless, numerous schemes have been shown to improve the achievable rate [8]. Following the seminal work of Sendonaris *et. al.* [6,7] and Laneman *et. al.* [8], which demonstrated and analyzed the diversity gains obtainable by user cooperation, with different cooperation protocols, research on cooperative communications has flourished. In the physical layer, the focus has been on investigating the capacity limits and performance of cooperative transmission considering various performance criteria, such as bit-error-rate (BER), outage probability with various cooperation schemes, and with constraints on transmit power, and with different assumptions on the available information. Notwithstanding the fact that cooperative diversity paradigm emerges as a very suitable method to mitigate channel impairments, the realization of cooperation idea precipitates many technical challenges that are associated with the overhaul of the

wireless network design [7, 11].

Cooperation has been shown to provide energy-efficiency as compared to direct transmission, in particular for cases where source-destination channel is not satisfactory for direct transmission [12], [13]. Energy saving is mainly due to the fact that packet retransmissions of the source node are avoided by employing cooperative transmissions, which also boost the signal reception as a result of diversity gain. Distributed implementation of cooperative communication imposes extra challenges on system design, because the energy savings provided by cooperative transmission may degrade as a consequence of the energy cost incurred by cooperation initiation stage, where the cooperation set is formed. That is why, energy-optimal cooperation set selection is essential in harnessing the energy gains promised by cooperative communications. The amount of energy savings provided by cooperation depends on how many and which relays are selected for cooperation and how much transmit power is assigned to each relay. While transmit power allocation is related with the physical layer, initiation and coordination of cooperation is controlled by the Medium Access Control (MAC) layer, and the set of nodes for routing the packets to the destination is discovered by the routing layer. Hence, the optimal cooperative architecture requires a cross-layer approach.

In the literature, cooperator selection and power allocation problems have been studied in [14–24]. A major drawback of the works in [14–20] is that cooperator selection is implicitly carried out by the power allocation process, where nodes assigned with power levels greater than zero get involved in cooperation. However, owing to the fact that this strategy does not take into account the messaging overhead for selection and actuation of the cooperators, and the corresponding energy cost, this strategy may result in acquiring too many cooperators for the sake of improving diversity gain and reducing total transmit power. Some distributed selection mechanisms

4

have also been studied to avoid this problem by using a fixed number of relays [21–23] or by simplifying relay selection via heuristic methods based on instantaneous CSI to select a single best cooperator [25–27] or via a game theoretic approach [24].

While research on cooperative communications in the physical layer is fairly extensive as exemplified above, the higher layer protocols that are essential for the application of cooperation is incommensurate with the available literature in the physical layer. The available literature on cooperative MAC protocols either relies on very complex physical layer models which necessitate compromises at the MAC layer design, thus leading to inaccurate MAC performance analysis, or simplistic physical layer models that obfuscate the underlying challenges on cross-layer MAC design and operation. In [28], the high data rate nodes assist low data rate nodes in their transmissions, where each node maintains a cooperation table that is required to be periodically updated, inducing significant overhead with increased number of nodes in the network. The cooperative MAC protocols proposed in [29,30] do not employ power allocation and explicit relay selection, they use fixed number of relays and exploit the extended transmission range provided by cooperative diversity. In [31], the authors present a distributed cooperative MAC protocol, where a relay node autonomously decides to cooperate to improve the transmission rate. In [32–34], the authors propose cooperative MAC protocols that exploit randomized distributed space time codes (RDSTC) for opportunistic on the fly relay selection. The aforementioned cooperative MAC protocols either disregard the burden of MAC messaging [29,30] or do not investigate the costs of actuating relays, such as energy costs [28,31–34]. However, without a sound MAC messaging and without appropriate quantification of the costs of actuating cooperation, the gains of cooperative diversity can not be fully investigated.

Moreover, the research on cooperative routing is limited with the major studies

relying on conventional routing approaches. A common approach in the literature to incorporate cooperative diversity in multi-hop networks is to employ cooperation on already discovered and established routes. For example, in [35], cooperation is exploited to mediate an unreliable single hop link on the non-cooperative route, such that the original link is kept but its quality is improved by cooperative transmissions of the neighbors. On the other hand, in [36] and [37], an opportunistic cooperative link is formed only when a link fails. As opposed to the schemes that consider single link improvements within non-cooperative routes, in [29] and [38], the objective is to improve the end-to-end performance of a route by utilizing cooperative links in lieu of multiple links, and obtain a route with cooperative links based on a non-cooperative route. Therefore, there is a need for higher layer protocols with accurate physical layer models, and realistic MAC and routing layer operation, which can facilitate cooperation to enhance overall system performance, such as throughput and energy-efficiency.

The design of cooperation-enabled or cooperative networks requires a cooperative diversity architecture that embraces all layers of the protocol stack while taking into account the operation and overhead of employing cooperation in each layer with accurately modeled parameters for each layer, and the application specific performance requirements. In particular, for designing energy-efficient architectures, e.g., for WSNs, the hardware limitations and the power consumption cost of the employed hardware should be taken into account. This is specifically important for cooperative systems, as the cooperative systems require the joint operation of multiple nodes with separate hardwares, each of which consume power. Furthermore, the design of a cross-layer approach requires realistic, simple, yet accurate physical layer models for system optimization. Complex, intricate physical layer models are too involved to be utilized for network-wise optimization problems that are supposed to be run by

energy-constrained wireless nodes, e.g., WSNs. MAC should be build upon a physical layer model that captures the essence of the network and it should be aware of the underlying hardware, at least the power consumption characteristic, so that its operation can be optimized for required system performance criteria, and the cost of employing MAC level messaging can be accurately quantified. The routing layer should be designed such that the route alternatives provided by the robust cooperative transmissions are exploited.

The optimization of overall system performance taking into account the MAC and routing layer operation are often disregarded in the literature. In particular, the cost of initiating and actuating cooperation has been disregarded. However, as shown with various examples and network models in this dissertation, cooperative diversity idea is required to be coupled with intelligently designed MAC and routing layers in order to obtain the promised gains.

1.1 Thesis Contributions

In this thesis, we propose a cross-layer cooperative diversity architecture for wireless networks. The major contributions of this dissertation can be summarized as follows:

- Two cooperative MAC protocols are designed and proposed.

  ◇ Our Carries Sense Multiple Access (CSMA) based cooperative MAC protocol, COMAC, allows for multi-node cooperation and realizes cooperation with minimal overhead. COMAC protocol manifests itself as a general framework, which can be applied over different physical layer settings, and in which different relay selection metrics can be incorporated for realizing cooperation decisions.

  ◇ A slotted ALOHA based cooperative scheme, C-ALOHA, is introduced and its throughput is derived and analyzed.

- The multiple relay cooperative system is analyzed, and the average Bit Error Rate (BER) is derived. A simple yet close approximation to the BER of the multiple relay cooperative system is proposed. As opposed to the approximations available in the literature, the accuracy of our approximation does not degrade for low source-destination SNRs, and holds for a wide range of SNR levels.

- Our BER approximation is utilized in formulating the joint cooperator selection and power assignment problem, for which optimal power assignment solution for multiple relay systems is obtained analytically in closed form. A low complexity, distributed method is also proposed for joint cooperator selection and power assignment, and it is shown to perform similarly to the optimal solution. Our distributed method renders decentralized operation by relying on the individual decisions and computations of the cooperators, different from the available literature that require the source or the destination to carry out cooperator selection and power assignment tasks.

- A novel cooperative routing framework is proposed with a cooperative flooding and two cooperative routing schemes, all of which make use of randomized distributed space-time codes (RDSTC) in cooperative transmissions. A cooperative network architecture, Routing-enabled Cooperative MAC (RECOMAC), is proposed as a cross-layer architecture that spans the physical, MAC and routing layers for wireless ad hoc networks. Cooperative routing within RECOMAC utilizes RDSTC, and it does not require establishing a prior non-cooperative route before cooperative transmissions, as opposed to the existing schemes. This significantly reduces the messaging overhead for route discovery and establishment phases.

For performance analysis, in addition to analytical models and numerical calculations, we have implemented our proposed cooperative protocols and algorithms in

network simulator (ns-2) tool [39], and we have performed extensive simulations in realistic network settings. As performance metrics, we have considered throughput and energy-efficiency, as well as the messaging costs, i.e., overhead involved. We evaluate energy-efficiency in terms of consumed energy per successful bit (energy-per-throughput), which represents the amount of energy consumed to transmit one source bit successfully to the destination node. As opposed to the approaches that consider the energy cost [14,15] or throughput [24] alone, this metric provides a complete quantification for the energy cost of throughput improvement in a cooperative system. In the calculation of energy costs for energy-efficiency analysis, transceiver energy cost is also taken into account through a realistic energy model, and its effect on the energy-efficiency is analyzed, unlike the existing studies that only consider the energy consumption in the transmit amplifier.

1.2   Thesis Organization

This dissertation is organized as follows:

In chapter 2, we present the basics of diversity and cooperative communications, and discuss the challenges and requirements for application of cooperation in wireless networks. Furthermore, each chapter provides the necessary background and a comprehensive summary of the related literature specific for the subject addressed in that chapter.

In chapter 3, first we present our CSMA based cooperative MAC protocol, COMAC. Then, we introduce accommodation of multiple relays and adaptive relay selection into the COMAC protocol. Finally, we present and analyze a second cooperative MAC protocol, Cooperative ALOHA, which enables cooperative transmissions for slotted ALOHA system.

In chapter 4, we consider the energy minimal joint cooperator set selection and

power assignment problem in a cooperation scenario with multiple relays. The average BER of the cooperative system is derived, approximated, and then utilized in the joint optimization problem, for which optimal and approximate distributed solutions are presented.

In chapter 5, we propose a decentralized cross-layer multi-hop cooperative network architecture. Our architecture involves the design of a simple yet efficient cooperative flooding scheme, two decentralized opportunistic cooperative forwarding mechanisms and the design of Routing enabled Cooperative Medium Access Control (RECOMAC) protocol that spans and incorporates the physical, MAC and routing layers for improving the performance of multi-hop communication in wireless ad hoc networks.

In chapter 6, we present our conclusions and directions for future work.

2 BACKGROUND ON COOPERATIVE COMMUNICATIONS

Cooperative communication capitalizes on providing intended receiver with multiple copies of the original signal via the help of the neighboring nodes so called relays (or cooperators) through independent channels, thereby mitigating the effects of fading. The idea of using independent channels of separate nodes stems from the applications in multiple-input-multiple-output (MIMO) systems. In fact, cooperative systems emulate MIMO systems, using nodes with single antenna. Hence, the theoretical background of the cooperative systems can be understood by overviewing the MIMO systems first.

In this chapter, we first visit the spatial diversity concept, diversity combining techniques and their performances. Then, we describe how cooperative diversity is realized at the physical layer, providing different communication protocols and performance gains. Finally, we review the required functionalities at the higher, MAC and the routing layers to realize cooperation in wireless ad hoc networks, and present the state of the art with prominent works in the literature.

2.1 Spatial Diversity

The idea behind diversity is to send the same data over independently fading channels, which are combined in such a way that the probability of fading is reduced for the resultant signal at the receiver. Independent fading channels can be obtained by using multiple antennas, also called an antenna array, at the transmitter and/or the receiver. This type of diversity is referred to as *spatial* or *antenna diversity*. Spa-

tial (antenna) diversity techniques are particularly attractive as they can be readily combined with other forms of diversity, such as time and frequency diversity [1].

Note that, with spatial diversity, independent fading channels can be realized without an increase in transmit signal power or bandwidth. Coherent combining of the diversity signals increases the signal to noise power ratio (SNR) at the receiver. The obtained SNR improvement over the SNR that would be obtained with just a single antenna is named as the *array gain*. In addition to the array gain, spatial diversity also provides *diversity order*, which corresponds to the number of independently faded paths that a signal passes through, i.e., the number of independent fading coefficients that can be averaged over to detect the signal, and is defined as the change in slope of the error probability resulting from the diversity combining [1].

The use of multiple antennas at both the transmitter and receiver combines transmit and receive diversity, and such systems are called multiple input multiple output (MIMO) systems. Receive diversity involves the use of single transmit antenna and multiple receive antennas, and the systems that employ receive diversity are called single input multiple output (SIMO) systems. Likewise, multiple input single output (MISO) systems exploit transmit diversity by the use of multiple transmit antennas and a single receive antenna. Transmit diversity is desirable in systems where more space, power, and processing are available on the transmitter side than the receiver side. In this dissertation, our focus is on transmit diversity obtained via MISO, where the cooperation is realized by the transmitting nodes. In the following section, we will discuss the diversity combining techniques in general, after that, we will concentrate on techniques for MISO systems. Then, we will continue with cooperative diversity paradigm, which capitalizes on the MISO systems and emulates MISO systems with multiple independent nodes with single antenna.

2.1.1 Diversity Combining Techniques

Diversity combining exploits the fact that independent signal paths have low probability of experiencing deep fades simultaneously, if the antennas are spaced sufficiently far apart. The maximum diversity gain for either transmitter or receiver spatial diversity typically requires that the fading amplitudes corresponding to each antenna are (approximately) independent. It is known that [1] in a uniform scattering environment with omnidirectional transmit and receive antennas, the minimum antenna separation required for independent fading on each antenna is 0.38 times the signal wavelength (0.38λ). Diversity combining techniques differ based on where the multiple antennas are employed. Receive diversity combining techniques look after the channel fading that affects incoming signals, and the transmit diversity combining techniques look after the channel fading that affects outgoing signals [40].

There are four major diversity combining schemes: Selection Combining (SC), Equal-Gain Combining (EGC), Square-Law Combining (SLC) and Maximal Ratio Combining (MRC) [1, 40, 41]. Among these combining schemes SC is applicable for only receive diversity. EGC, SLC and MRC can be applied for both the receive and transmit diversity systems [40]. For the application of these techniques in transmit diversity systems, the channel state information should be feedback to the transmitter side [1].

In SC, the combiner outputs the signal on the branch with the largest SNR. With SC, the output from the combiner has an SNR equal to the maximum SNR of all the branches. Moreover, since only one branch output is used, co-phasing of multiple branches is not required; hence this technique can be used with either coherent or differential modulation [1, 41]. Threshold Combining (TC) is a variation of SC. Operation of TC resembles SC in that the combiner outputs the signal on the branch with the largest SNR. Once a branch is chosen, the combiner outputs that signal as long

as the SNR on that branch remains above the desired threshold. If the SNR on the selected branch falls below the threshold, the combiner switches to another branch that is above the threshold. As in SC, co-phasing is not required because only one branch output is used at a time. Although SC and TC are practical since they do not require complex channel gain knowledge, these techniques do not provide full diversity order, thus they are suboptimal diversity combining schemes [1,41]. In EGC, all the complex weighting parameters have their phase angles set opposite to those of their respective multipath branches, but their magnitudes are set equal to some constant value, unity, for simplicity [40]. EGC and MRC rely on the ability to estimate the phase of the different diversity branches and to combine signals coherently. Unlike MRC, SLC is applicable only to certain modulation techniques, in particular, orthogonal modulation including frequency shift keying (FSK) or direct-sequence code division multiple access (CDMA) signals [40], in which different frequencies or sequences are used to represent different data symbols.

Diversity combiner design depends on whether or not the complex channel gain is known at the transmitters. If the gain is known, MRC can be employed to obtain full diversity order [1,41]. However, if the complex channel gain information is not available at the transmitter, a scheme that combines space and time diversity techniques, i.e., space-time codes [42], in particular Alamouti scheme [43], and its extensions are required. In the following section, we overview the two prominent diversity techniques employed by MISO systems, MRC and Alamouti scheme.

2.1.1.1 Maximal Ratio Combining (MRC)

Consider a MISO system with M transmit antennas and one receiver antenna as depicted in Fig. 2.1 [1]. We assume that the path gain $h_i = \kappa_i e^{j\theta_i}$ associated with the ith antenna is known at the transmitter, i.e., channel state information (CSI) is
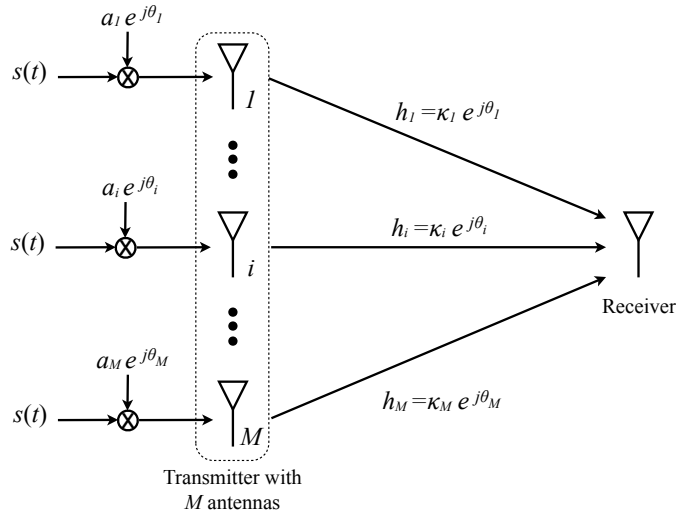
Figure 2.1: A multiple input single output (MISO) system.

available at the transmitter. Let $s(t)$ denote the transmitted signal with total energy per symbol E_s. The signal is multiplied by a complex gain $a_i e^{j\theta_i}$ $(0 \leq a_i \leq 1)$, and then sent through the ith antenna. This complex multiplication performs both co-phasing and weighting relative to the channel gains. Because of the average total energy constraint E_s, the weights must satisfy $\sum_{i=1}^{M} a_i^2 = 1$. The weighted signals transmitted over all antennas are added "in the air", and the received signal is given by

$$y(t) = \sum_{i=1}^{M} a_i \kappa_i s(t). \tag{2.1}$$

Let $N_0/2$ denote the power spectral density (PSD) of the noise at the receiver. The SNR at the receiver is given as

$$\gamma_\Sigma = \frac{y^2(t)}{N_0 B}, \tag{2.2}$$

where B is the received bandwidth in Hz. The optimal transmission strategy is the one which uses a_i that maximizes γ_Σ. Intuitively, the branches with a high SNR should be weighted more than branches with a low SNR, and hence the weights a_i^2

should be proportional to the branch SNRs. a_i^2 that maximize γ_Σ can be found by taking partial derivates of γ_Σ with respect to a_i's and using Cauchy-Schwarz inequality as given in [40]. Solving for the optimal weights yields

$$a_i = \frac{\kappa_i(t)}{\sqrt{\sum_{i=1}^{M} \kappa_i^2(t)}}, \tag{2.3}$$

and the resulting SNR is obtained as [1]

$$\gamma_\Sigma = \frac{E_s}{N_0} \sum_{i=1}^{M} \kappa_i^2(t) = \sum_{i=1}^{M} \gamma_i, \tag{2.4}$$

where $\gamma_i = \kappa_i^2 E_s/N_0$ is equal to the branch SNR between the ith transmitter antenna and the receiver antenna. It is worthwhile to note that the received SNR, γ_Σ is the sum of SNRs of the individual branches, as given in (2.4). In particular, if all paths have the same gain $\kappa_i = \kappa$, then $\gamma_\Sigma = M\kappa^2 E_s/N_0$, so the array gain is equal to M, corresponding to an M-fold increase in SNR over a single antenna transmitting with full power. For fading channels, when the channel gains are not static, the average SNR is calculated as $\bar{\gamma}_\Sigma = \sum_{i=1}^{M} \bar{\gamma}_i$, and for i.i.d. channels the array gain is found as M, from $\bar{\gamma}_\Sigma = M\bar{\gamma}$.

Now, let us observe the diversity order of MRC. When the channel gains are static and known, the probability of symbol error is given as:

$$P_e = \varphi_q Q(\sqrt{\beta_q \gamma_\Sigma}), \tag{2.5}$$

where φ_q and β_q depend on the type of modulation and approximation. For example, when nearest neighbor approximation is considered, φ_q is the number of nearest neighbors to a constellation at the minimum distance and β_q is a constant that relates minimum distance to average symbol energy [3]. Using Chernoff bound [3], it is seen that,

$$P_e \le \varphi_q e^{-\beta_q \gamma_\Sigma/2} = \varphi_q e^{-\beta_q(\gamma_1 + \cdots + \gamma_M)/2}. \tag{2.6}$$

16

Under fading, the average error probability, $\bar{P}_e$ is calculated by averaging P_e over the fading distribution $p(\gamma_\Sigma)$, which is Chi-square distribution [44], χ^2, for γ_Σ, for Rayleigh fading:

$$\bar{P}_e = \int_0^\infty P_e p(\gamma_\Sigma) d\gamma_\Sigma. \tag{2.7}$$

Then, applying the Chernoff bound yields:

$$\bar{P}_e \leq \varphi_M \prod_{i=1}^M \frac{1}{1 + \beta_M \bar{\gamma}_i / 2}. \tag{2.8}$$

In the limit of high SNR and assuming i.i.d. channels with $\bar{\gamma}_i = \bar{\gamma}$, we have [1]:

$$\bar{P}_e \approx \varphi_M \left(\frac{\beta_M \bar{\gamma}}{2} \right)^{-M}. \tag{2.9}$$

Thus, at high SNR, the diversity order of transmit diversity with MRC is M, so transmit MRC achieves full diversity.

The complication of transmit diversity with MRC is to obtain the channel phase and the channel gain values of each antenna path at the transmitter. These channel values can be measured and estimated at the receiver using a pilot technique, and then fed back to the transmitters, or for a time-division duplex system (TDD) [45], the transmitter can perform the estimation while receiving and later use the estimates for the transmit cycle, given that the channel coherence time is sufficiently large.

2.1.1.2 Alamouti Scheme

A simple and prevalent scheme that combines both space and time diversity was developed by Alamouti in [43]. Alamouti's scheme is designed for a digital communication system with two antenna transmit diversity, and provides full diversity order (of two) even in the absence of channel state information.

The Alamouti scheme works over two symbol periods. Over the first symbol period, two different symbols s_1 and s_2, each with energy $E_s/2$, are transmitted simultaneously from antennas 1 and 2, respectively. Over the next symbol period, symbol $-s_2^*$ is transmitted from antenna 1 and symbol s_1^* is transmitted from antenna 2, each again with symbol energy $E_s/2$. The channel is assumed to be constant over the two symbols, hence the received symbol over the first symbol period is $y_1 = h_1 s_1 + h_2 s_2 + n_1$, and the received symbol over the second symbol period is $y_2 = -h_1 s_2^* + h_2 s_1^* + n_2$, where n_i $(i = 1, 2)$ is the additive white Gaussian noise (AWGN) sample at the receiver associated with the ith symbol transmission, and h_i denotes the gain of the channel from antenna i. We assume that the noise sample has zero mean and power N_0. The receiver uses these sequentially received symbols, y_1 and y_2, to form the vector $\mathbf{y} = [y_1 \ y_2^*]^T$, which can be expressed as:

$$\mathbf{y} = \begin{bmatrix} h_1 & h_2 \\ h_2^* & -h_1^* \end{bmatrix} \begin{bmatrix} s_1 \\ s_2 \end{bmatrix} + \begin{bmatrix} n_1 \\ n_2^* \end{bmatrix} = \mathbf{H}\mathbf{s} + \mathbf{n}, \tag{2.10}$$

where $\mathbf{s} = [s_1 \ s_2]^T$, $\mathbf{n} = [n_1 \ n_2]^T$. The receiver is able to estimate the channel matrix $\mathbf{H}$ and form $\mathbf{z} = \mathbf{H}^H \mathbf{y}$, which yields

$$\mathbf{z} = \mathbf{H}^H \mathbf{H}\mathbf{s} + \mathbf{H}^H \mathbf{n} = (|h_1^2| + |h_2^2|)\mathbf{I}\mathbf{s} + \tilde{\mathbf{n}}, \tag{2.11}$$

where $\mathbf{I}$ is identity matrix, and $\tilde{\mathbf{n}} = \mathbf{H}_A^H \mathbf{n}$ is a complex Gaussian noise vector with zero mean and covariance matrix $E[\tilde{\mathbf{n}}\tilde{\mathbf{n}}^*] = (|h_1|^2 + |h_2|^2)N_0 \mathbf{I}$. The diagonal nature of $\mathbf{z}$ effectively decouples the two symbol transmissions, so that each component of $\mathbf{z}$ corresponds to one of the transmitted symbols, i.e., [43]

$$z_i = (|h_1|^2 + |h_2|^2)s_i + \tilde{n}_i, \quad i = 1, 2. \tag{2.12}$$

Thus, the received SNR for z_i is given by

$$\gamma_i = \frac{(|h_1|^2 + |h_2|^2)E_s}{2N_0}, \tag{2.13}$$

where the factor of 2 comes from the fact that s_i is transmitted using half the total symbol energy E_s. Note that, the received SNR per branch is equal to the sum of SNRs on each branch divided by 2; hence, the array gain is 1 [43].

The Alamouti scheme achieves a diversity order of 2, which is the maximum possible diversity order for a two-antenna transmit system, despite the fact that the channel knowledge is not available at the transmitter [43]. In the same setting, with CSI available at the transmitter, MRC can achieve array and diversity gains of 2. The Alamouti scheme can be generalized for $M > 2$, and this is studied in orthogonal space-time block code design [42].

2.1.2 Error and Outage Probability of Spatial Diversity Systems

In this section, we present the derivation of error and outage probabilities for the MISO system. In the derivations, we assume that MRC is employed.

If h_i for $i = 1, \ldots, M$ are known at the receiver, the error probability of the M transmitter diversity system becomes the error probability in an AWGN channel [46]. Assuming coherent modulation, the symbol error probability of a MISO system with M transmitters is given in (2.5) [46]. Under fading, γ_Σ is no longer static, hence we need average symbol error probability or outage probability to assess the performance.

The average symbol error probability is obtained by averaging (2.5) over γ_Σ as follows:

$$\bar{P}_e(\gamma_\Sigma) = \int_0^\infty P_e(\gamma) p_{\gamma_\Sigma}(\gamma) d\gamma, \tag{2.14}$$

where $p_{\gamma_\Sigma}(\gamma)$ is the probability density function (pdf) of γ_Σ.

Furthermore, the outage probability is the probability that the received SNR, γ_Σ of the combined signal falls below a target SNR threshold value, γ_0, and it is given

as [1]

$$P_{out} = P(\gamma_\Sigma \leq \gamma_0) = \int_0^{\gamma_0} p_{\gamma_\Sigma}(\gamma)d\gamma. \tag{2.15}$$

Note that, both the average probability of error and the outage probability expressions for diversity require integration over the distribution $p_{\gamma_\Sigma}(\gamma)$, as obtained in (2.14) and (2.15). However, the distribution of combined SNR, $p_{\gamma_\Sigma}(\gamma)$ is often not in closed form for an arbitrary number of diversity branches especially with different fading distributions on each branch, regardless of the combining technique that is used. In particular, the distribution for $p_{\gamma_\Sigma}(\gamma)$ is often in the form of an infinite-range integral, in which case the expressions (2.14) and (2.15) become double integrals that can be difficult to evaluate numerically. Even when $p_{\gamma_\Sigma}(\gamma)$ is in closed form, the corresponding integrals (2.14) and (2.15) may not lead to closed-form solutions and may also be difficult to evaluate numerically. Expressing the average error probability in terms of the moment generating function (MGF) for γ_Σ instead of its distribution often eliminates these integration difficulties.

The MGF for a nonnegative random variable γ with distribution $p_\gamma(\gamma)$, $\gamma \geq 0$, is defined as [44]:

$$\mathcal{M}_\gamma = \int_0^\infty p_\gamma(\gamma)e^{s\gamma}d\gamma. \tag{2.16}$$

Note that, MGF is just the Laplace transform of the distribution $p_\gamma(\gamma)$ with the argument reversed in sign: $\mathcal{L}[p_\gamma(\gamma)] = \mathcal{M}_\gamma(-s)$ [1]. Thus, the MGF for most fading distributions of interest can be computed either in closed-form using classical Laplace transforms or through numerical integration. In particular, the MGF for common multipath fading distributions are found as follows [47]:

$\diamond$ Rayleigh distribution:

$$\mathcal{M}_{\gamma_s}(s) = (1 - s\bar{\gamma}_s)^{-1}. \tag{2.17}$$

◇ Rician distribution with factor K:

$$\mathcal{M}_{\gamma_s}(s) = \frac{1+K}{1+K-s\bar{\gamma}_s} \exp\left[\frac{Ks\bar{\gamma}_s}{1+K-s\bar{\gamma}_s}\right].$$ (2.18)

◇ Nakagami-m distribution:

$$\mathcal{M}_{\gamma_s}(s) = \left(1 - \frac{s\bar{\gamma}_s}{m}\right)^{-m}.$$ (2.19)

When the diversity fading paths are independent, but not necessarily identically distributed, the average error probability based on the MGF of γ_Σ is typically in closed form or consists of a single finite-range integral that can be easily computed numerically. Here, we follow MGF approach for obtaining a closed form expression for the average symbol error probability, $\bar{P}_e$ of the spatial diversity system.

Note that, with MRC the combined SNR of the MISO system, γ_Σ is the sum of the branch SNRs as given in (2.4). Considering that P_e is in exponential form, i.e., $P_e = c_1 e^{-c_2\gamma}$ [1], the average probability of symbol error for MRC system is given as

$$\bar{P}_e = \int_0^\infty c_1 e^{-c_2\gamma} p_{\gamma_\Sigma}(\gamma)d\gamma.$$ (2.20)

It is assumed that the branch SNRs are independent, so that their joint distribution becomes a product of the individual distributions: $p_{\gamma_1,\dots,\gamma_M}(\gamma_1,\dots,\gamma_M) = p_{\gamma_1}(\gamma_1)\dots p_{\gamma_M}(\gamma_M)$. Using this factorization, substituting $\gamma = \gamma_1 + \dots \gamma_M$ in (2.20), and using the product forms: $\exp[-c_2(\gamma_1 + \dots + \gamma_M)] = \prod_{i=1}^M \exp[-c_2\gamma_i]$ and $p_{\gamma_1}(\gamma_1)\dots p_{\gamma_M}(\gamma_M) = \prod_{i=1}^M p_{\gamma_i}(\gamma_i)$, $\bar{P}_e$ yields

$$\bar{P}_e = c_1 \int_0^\infty \int_0^\infty \cdots \int_0^\infty \prod_{i=1}^M e^{-c_2\gamma_i} p_{\gamma_i}(\gamma_i)d\gamma_i.$$ (2.21)

Switching the order of integration and multiplication, we obtain the following final form:

$$\bar{P}_e = c_1 \prod_{i=1}^M \int_0^\infty e^{-c_2\gamma_i} p_{\gamma_i}(\gamma_i)d\gamma_i = c_1 \prod_{i=1}^M \mathcal{M}_{\gamma_i}(-c_2),$$ (2.22)

where $\mathcal{M}_{\gamma_i}(s)$ is the MGF of the fading distribution for the ith diversity branch.

Similarly, when P_e is in the exponential form of $\int_A^B c_1 e^{-c_2(x)\gamma} dx$, assuming branch SNRs are independent, the average symbol error probability is given as

$$\bar{P}_e = \int_0^\infty \int_A^B c_1 e^{-c_2(x)\gamma} dx p_{\gamma_\Sigma}(\gamma) d\gamma,$$

$$= \int_0^\infty \int_0^\infty \cdots \int_0^\infty \int_A^B c_1 \prod_{i=1}^M e^{-c_2(x)\gamma_i} p_{\gamma_i}(\gamma_i) d\gamma_i,$$

Again, switching the order of integration and multiplication, we obtain the following final form for the average symbol error probability:

$$\bar{P}_e = c_1 \int_A^B \prod_{i=1}^M \int_0^\infty e^{-c_2(x)\gamma_i} p_{\gamma_i}(\gamma_i) d\gamma_i = c_1 \int_A^B \prod_{i=1}^M \mathcal{M}_{\gamma_i}(-c_2(x)) dx. \quad (2.23)$$

Thus, the average probability of symbol error is just a single finite-range integral of the product of MGFs associated with the SNR on each branch. For instance, using (2.23) the average symbol error probability of a MISO system with binary phase shift keying (BPSK) modulation and with Rayleigh fading channel is given as:

$$\bar{P}_e = \frac{1}{\pi} \int_0^{\pi/2} \prod_{i=1}^M \left(1 + \frac{\bar{\gamma}_i}{sin^2\phi}\right)^{-1} d\phi. \quad (2.24)$$

For i.i.d. channels $\bar{P}_e$ is obtained as $\bar{P}_e = \frac{1}{\pi} \int_0^{\pi/2} \left(1 + \frac{\bar{\gamma}}{sin^2\phi}\right)^{-M} d\phi$, which is also plotted in Figure 2.2. It is observed that for a given symbol error rate (SER), the MISO system requires considerably lower average SNR levels as compared to SISO system. The observed difference in SNR is the diversity gain obtained from the MISO system. The average SER for other modulation types can be obtained via the MGF approach as provided in [47].
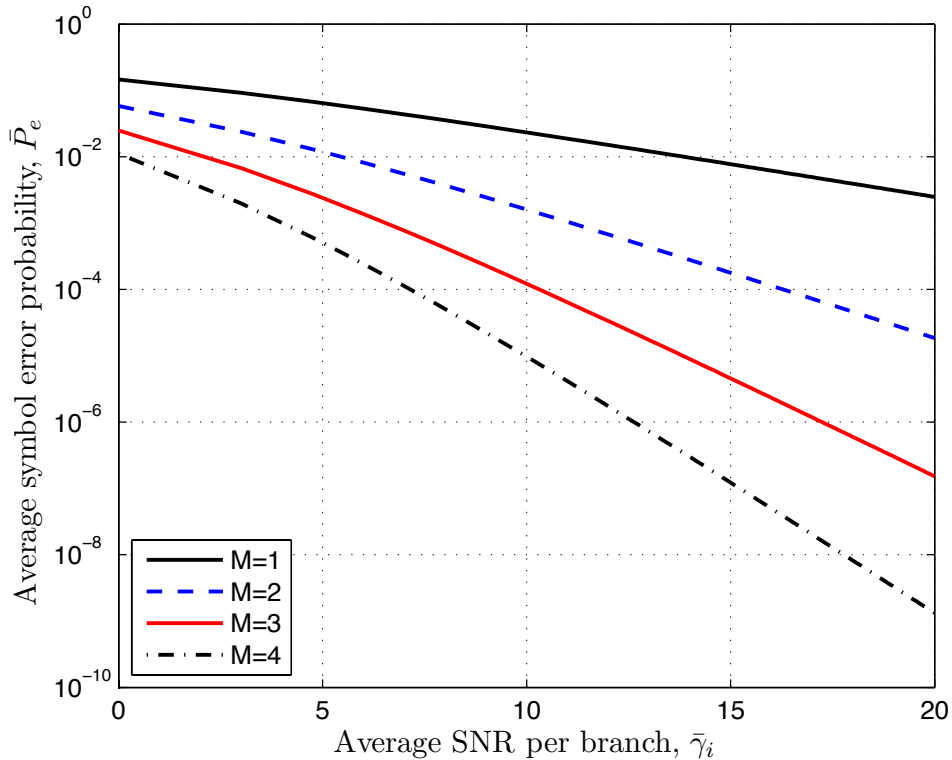
Figure 2.2: Average symbol error probability for M-branch transmit diversity scheme with BPSK modulation.

2.1.3 Benefits of Diversity

It is shown in the previous section that if the fading is independent across antenna pairs, the average error probability can be made to decay like SNR^{-M} at high SNR, in contrast to SNR^{-1} for the single antenna fading channel. This phenomenon implies that at high SNR, the error probability is much smaller. Similar results can be obtained for various modulation schemes and constellations [48]. Since the performance gain at high SNR is dictated by the SNR exponent of the error probability, this exponent is called the *diversity order*. Intuitively, it corresponds to the number of independently faded paths that a symbol passes through, i.e., the number of independent fading coefficients that can be averaged over to detect the symbol. Multiple antenna channels provide spatial diversity, which can be used to improve the relia-

23

bility of the link. The *diversity gain* obtained via multiple antennas over the single antenna systems is defined as the amount of decrease in the required SNR level to achieve the same average symbol probability.

The diversity gain obtained through multiple antenna systems can be exploited to achieve reduced SER levels while keeping the total transmit power the same with the single antenna systems. In the same manner, owing to the diversity gain multiple antenna systems can operate at the same SER levels with the single antenna systems while using less total transmit power. Reduced SER levels imply improved coverage area for multi-antenna wireless transmission with the same transmit power levels with the single antenna systems. Moreover, with multi-antenna systems, the same coverage area with the single antenna systems can be achieved with reduced total transmit power.

Here, we present a simple calculation relating the increase in capacity that results from a multi-antenna system to an equivalent increase in cell coverage. We begin with a general calculation of the increase in cell coverage given a reduction in the required average received power.

Assume that the source is at a distance d meters from the destination node. Let P_{tx} denote the average power transmitted by the node and P_{rx} denote the average power received at the destination node, both in decibels. Then, in a typical wireless channel, we have

$$P_{rx} = P_{tx} - PL(d), \tag{2.25}$$

where $PL(d)$ is the mean path loss at d meters. For modeling the path loss different models are possible, such as the Hata model [49]. Here, we consider a general model to cover a broad range of path loss models. Path loss is modeled as

$$PL(d) = 10\alpha \log_{10}(d) + K(f_c, G), \tag{2.26}$$

where α is the path loss exponent and $K(f_c, G)$ is a constant that depends on the

24

carrier frequency f_c and antenna gain G. Therefore, the required distance to achieve a received power level of P_{rx} with a transmit power level of P_{tx} is given as $\log_{10} d = P_{tx} - P_{rx}$. The coverage area of a transmitter that transmits with power P_{tx} is given by d_{max}:

$$d_{max} = 10^{P_{tx} - P_{rx}}. \tag{2.27}$$

It can be seen that coverage and required average received power are inversely related to each other. The higher the required power, the lower the coverage, and vice versa.

Assume that two different transmission schemes require different received powers in order to operate successfully. That is, let scheme "a" require P_{rx}^a and scheme "b" require P_{rx}^b. Define Γ to be the ratio of the receive power levels these two schemes:

$$\Gamma \triangleq \frac{d_{max}^a}{d_{max}^b} = 10^{\frac{P_{tx} - P_{rx}^a}{P_{tx} - P_{rx}^b}} \tag{2.28}$$

It is known that due to the diversity gain multi-antenna systems can operate at much lower receive threshold values than the direct transmission schemes. Hence, multi-antenna systems result in an increase in the coverage area.

2.2   Cooperative Diversity

In contrast to the conventional forms of spatial diversity obtained with physical antenna arrays employed on a single node [50, 51] as discussed in Section 2.1, in cooperative diversity multiple nodes employed with single antenna transmit cooperatively to form a virtual antenna array, and by this way, spatial diversity can be exploited without the need for implementing multi-antenna arrays on the nodes. This kind of spatial diversity obtained by forming virtual antenna arrays is named as *cooperative diversity* or *user cooperation diversity* [6].

In Figure 2.3, two scenarios in which a source node communicates with the destination node are depicted. In Figure 2.3a, the source node directly communicates

(a) Direct transmission: Source communicates directly to the destination node.

(b) Cooperative transmission: The source communicates to the destination node through the virtual MISO link.
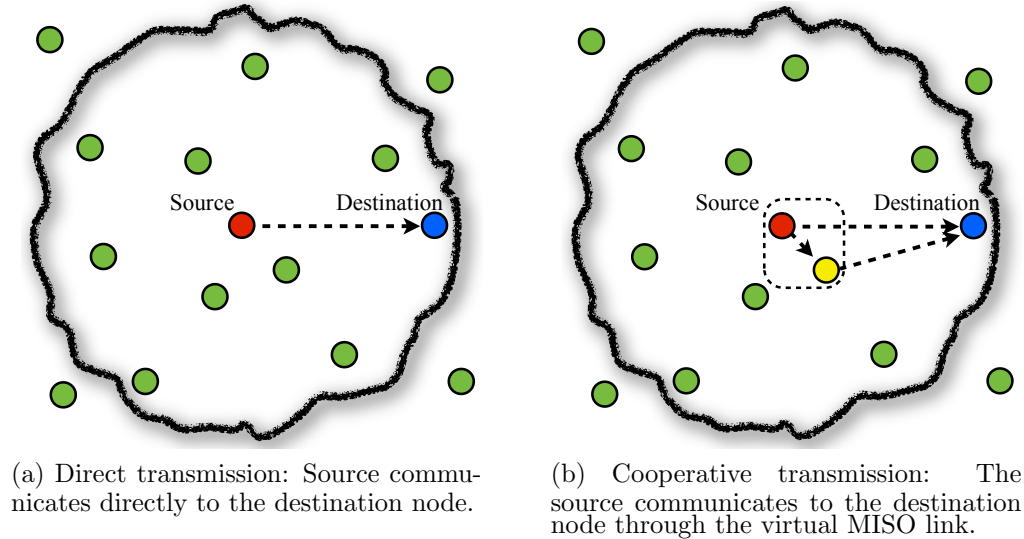
Figure 2.3: Direct and cooperative transmissions.

with the destination node. The nodes in the transmit range of the source node hear the source transmission, but they stay silent during the communication in order to prevent any interference and any possible collisions. Figure 2.3b illustrates the scenario in which the source node and a neighbor node form a cooperation set to emulate a MISO system, and the source communicates to the destination node through the virtual MISO link making use of cooperative diversity. It is assumed in the scenario depicted in Figure 2.3b that the network is designed such that neighbor nodes can help the transmission of the other nodes, and they can access the channel synchronously and/or in coordination with the source and the other cooperating nodes. However, conventional networks were not designed with such cooperative communication in mind. In order to exploit cooperative diversity, the network nodes should be redesigned such that they can assess the need for cooperation, measure the extent and cost of cooperation, and realize and actuate the cooperation autonomously. Furthermore, the decisions of the possible cooperating nodes should be coordinated, such that the nodes in the cooperating set are actuated with optimal gains, while

causing minimal messaging overhead on the network so that they do not obliterate the benefits obtained through cooperation. This problem is further complicated when multi hop routing is considered. Hence, realizing cooperative communication among nodes in a network requires the coordination of multiple network layers and calls for essential modifications on the design of the layers of the protocol stack. In particular, the link, or physical layer, which handles bit level transmissions over the communications medium, the medium access layer, which handles shared access to the communication medium, and the network, or the routing layer, which routes data across the network, should be modified jointly.

In this dissertation, our objective is to design a cross-layer cooperative network architecture that exploits the physical layer findings in cooperative diversity. We assume a transport layer that does not mandate flow control under packet losses, and we assume an application layer that generates packets continuously, (periodically or according to Poisson process). Our aim is to optimize the cooperative network performance considering the physical, MAC and routing layers. In the following, we provide a brief overview of the utilization of the cooperative diversity in the physical, MAC and routing layers.

2.2.1 Physical Layer

There are three fundamental methods, along with their variations, to facilitate cooperative transmissions in the physical layer [8,52]. These cooperative transmission methods are known as *cooperation protocols* or *relay protocols* [6,8]. In Figure 2.4, we illustrate the cooperative system model with C cooperators. Here, it is assumed that cooperative protocols are realized through orthogonal channels, either in time, frequency or code dimension, as depicted in Figure 2.5 [6,8].

The first protocol, sometimes called *observation* [52], is important when the
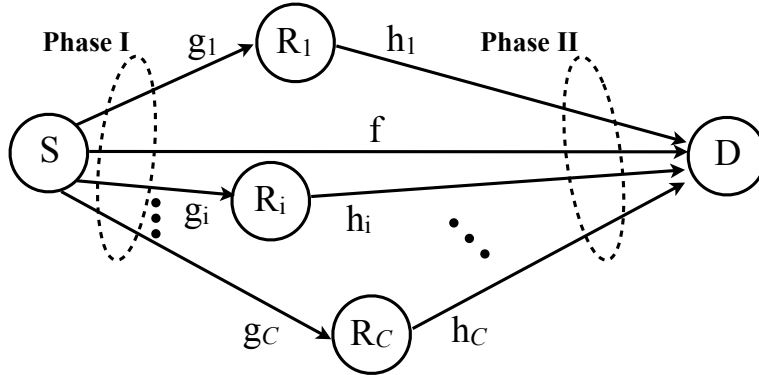
Figure 2.4: Cooperative system model.
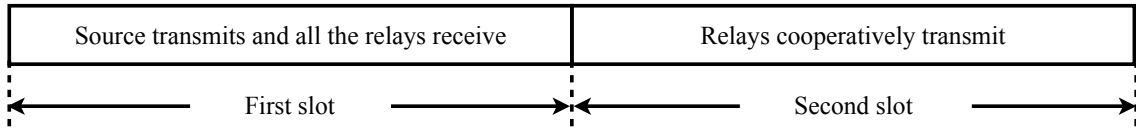
Figure 2.5: Cooperative transmission model.

source-relay and the source-destination channels are comparable, and the relay-destination link is good. In this situation, the relay may not be able to decode the source signal, but nonetheless it has an independent observation of the source signal that can aid in decoding at the destination. Therefore, the relay sends an estimate of the source transmission to the destination. This strategy is known as the *estimate and forward* (also known as *compress and forward* or *quantize and forward*) protocol. The *amplify and forward* (AF) (also sometimes called *scale and forward*) protocol [8] is a special case of the above strategy where the estimate of the source transmission is simply the signal received by the relay, scaled up or down before retransmission.

The second protocol involves decoding of the source transmission at the relay. The relay then retransmits the decoded signal after possibly compressing or adding redundancy. This strategy is known as the *decode and forward* (DF) protocol [8], named after the fact that the relay decodes, regenerates and then forwards the source transmission. The DF protocol is close to optimal when the source-relay channel is

28

excellent, which practically happens when the source and the relay are physically near each other. When the source-relay channel becomes perfect, the relay channel becomes an $M \times 1$ multiple-antenna system.

The third method, known as *facilitation* [52], is mostly of theoretical interest. When the relay is not able to contribute any new information to the destination, it simply tries to stay out of the way by transmitting the signal that would be least harmful to source-destination communication.

There are many other relaying strategies, which are extended versions of the above, namely, partial decode-and-forward, dynamic decode-and-forward, bursty amplify -and-forward, selective relaying, relaying with feedback, etc. Coded cooperation is another scheme proposed for multi node scenarios [11,53,54], where the relay node also wants its own data to be transmitted to the destination, i.e., the source and relay act as partners for each other.

Here, we will elaborate on the AF and DF schemes, as they have practical importance. With the same reasoning, in this dissertation, we design cross-layer cooperative architectures that use DF cooperative systems.

2.2.1.1 Amplify and Forward (AF)

Consider the scenario shown in Figure 2.4, where we have an information source S and a destination D communicating over a channel with fading coefficient f. C relays, namely R_1, ..., R_C are willing to participate in this link providing the destination node, D, with a second copy of the original signal through the complex channels SR_i and R_iD with flat fading coefficients g_i and h_i, respectively. Without loss of generality, we assume that all the AWGN terms, n_{R_i}, n_S and n_D have equal variance N_0. We suppose that the realizations of the random variables f, g_i and h_i have been acquired at the receiver ends, e.g., via training. Note that, no particular assumptions

are made on channel statistics. The relaying model is given in Figure 2.5, and the system model is given in Figure 2.4.

In AF model, relays simply amplify the signal received from the source [8]. Assuming that S and R_i transmit through orthogonal channels, the destination receives two independent copies of the signal x, transmitted by the source, such as

$$y_{SD} = P_S f x + n_{SD}, \tag{2.29}$$

$$y_{SR_i} = P_S g_i x + n_{SR_i}, \tag{2.30}$$

$$y_{R_iD} = h_i A_i(P_S g_i x + n_{SR_i}) + n_{R_iD} = h_i A_i g_i P_S x + n_{R_i}, \tag{2.31}$$

$$y_D = y_{SD} + \sum_{i=1}^{C} y_{R_iD}, \tag{2.32}$$

where $n_{R_i} \triangleq h_i A_i n_{SR_i} + n_{R_iD}$, and A_i is the amplification factor which will be discussed later, and P_S is the source transmit power. We emphasize that the noise terms n_{SD} and n_{R_i} do not have identical power because n_{R_i} includes a noise contribution at the intermediate stage; for this reason, the MRC should be preceded by a noise normalization step. With this combining rule, a decision variable z is formed by weighting the combination with the respective powers. The resulting SNR of the decision variable is given as [55]

$$\gamma_z = |f|^2 \frac{P_S}{\sigma_D^2} + \sum_{i=1}^{C} |A_i g_i h_i|^2 \frac{P_S}{\sigma_{R_i}^2} = \gamma_D + \sum_{i=1}^{C} \gamma_{R_i}, \tag{2.33}$$

where $\gamma_D \triangleq \frac{|f|^2 P_S}{\sigma_D^2}$, and $\gamma_{R_i} \triangleq \sum_{i=1}^{C} |A_i g_i h_i|^2 \frac{P_S}{\sigma_{R_i}^2}$. For fixed f, g_i and h_i realizations, z is Gaussian, and the symbol error probability (SEP) conditioned on the instantaneous SNR γ_z is given by $P_e = Q(\sqrt{k\gamma_z})$, where the constant k depends on the type of modulation ($k = 2$ for phase shift keying , PSK), and $Q(x) = (1/\sqrt{2\pi}) \int_x^\infty e^{-u^2/2} du$ [55].

The term γ_D is the per-hop SNR associated with the direct channel f; that is

$\gamma_D = \gamma_f = \frac{|f|^2 P_S}{N_0}$, but the terms γ_{R_i} requires a bit more elaboration. Expanding n_{R_i}, the term γ_{R_i} takes the form

$$\gamma_{R_i} = |A_i g_i h_i|^2 \frac{P_S}{(1 + |A_i h_i|^2) N_0}. \tag{2.34}$$

Here, we have choices over the amplification factor A_i [55]; a convenient one maintains constant average power output, equal to the original transmitted power

$$A_i^2 = \frac{P_S}{P_S |g_i|^2 + N_0}. \tag{2.35}$$

Substituting (2.35) into (2.34) and (2.33), we obtain

$$\gamma_z = \gamma_f + \sum_{i=1}^{C} \frac{\gamma_{g_i} \gamma_{h_i}}{1 + \gamma_{g_i} + \gamma_{h_i}} \tag{2.36}$$

Given γ_z, the average error probability of cooperative transmission is computed via [1]

$$\bar{P}_e = \int_0^\infty \alpha_C Q(\beta_C \gamma_z) p_{\gamma_z}(\gamma_z) d\gamma_z. \tag{2.37}$$

The exact average error probability do not have closed form solutions. However, there are various approximations in the literature for various cooperation scenarios for the AF protocol, such as [47, 55–57]. The outage probability of AF cooperative protocol is given as $P_{out} = P(\gamma_z \leq \gamma_0) = \int_0^{\gamma_0} p_{\gamma_z}(\gamma) d\gamma$. Furthermore, the capacity of AF protocol, i.e., the maximum average mutual information between the input and the output, achieved by i.i.d. complex Gaussian inputs, is given by [8]

$$I_{AF} = \frac{1}{2} \log(1 + \gamma_z). \tag{2.38}$$

2.2.1.2 Decode and Forward (DF)

AF systems are limited by noise amplification and serious implementation challenges in cooperative systems [1], such as analog and digital distortions like carrier frequency

offset, inaccurate synchronization, and gain control for analog to digital conversion. DF systems, on the other hand, eliminates error propagation and noise amplification [8]. Thus, DF systems are of particular interest. In DF, only the nodes that can successfully decode the source signal can participate in cooperative transmission. Let C denote the number of nodes that have successfully decoded and regenerated the source signal. In this case, the signal received at the destination due cooperative transmission is given as [8]

$$y_{SD} = P_S f x + n_{SD}, \qquad (2.39)$$

$$y_{SR_i} = P_S g_i x + n_{SR_i}, \qquad (2.40)$$

$$y_{R_i D} = P_{R_i} h_i x + n_{R_i D}, \qquad (2.41)$$

$$y_D = y_{SD} + \sum_{i=1}^{C} y_{R_i D}. \qquad (2.42)$$

The received SNR at the destination is given by

$$\gamma_{SD} = \frac{|f|^2 P_S}{N_0}, \qquad (2.43)$$

$$\gamma_{R_i D} = \frac{|h_i|^2 P_{R_i}}{N_0} \qquad (2.44)$$

The resulting SNR at the destination receiver is given as [8]

$$\gamma_z = \gamma_D + \sum_{i=1}^{C} \gamma_{R_i D} \qquad (2.45)$$

Given γ_z, the average error probability of DF cooperative transmission is computed via (2.37), and the outage probability via (2.15). The exact average error probability does not have a closed form solution. However, there are various approximations in the literature for various cooperation scenarios for the DF protocol, such as [22,58–60]. Furthermore, the maximum average mutual information for repetition-

coded DF can be readily shown to be [8]

$$I_{DF} = \frac{1}{2} \min \left\{ \log \left(1 + \gamma_{SD} \right), \log \left(1 + \gamma_z \right) \right\}. \tag{2.46}$$

The first term in (2.46) represents the maximum rate at which the relay can reliably decode the source message, while the second term in (2.46) represents the maximum rate at which the destination can reliably decode the source message given repeated transmissions from the source and the destination. Requiring both the relay and the destination to decode the entire codeword without error results in the minimum of the two mutual information in (2.46).

2.2.2 MAC and Routing Layers

The degree of performance improvement due to cooperative diversity is determined by the channel states of the cooperators. Selection of appropriate cooperators and resource allocation among those cooperators are intrinsically connected problems, solution of which is essential in exploiting cooperative diversity. The cooperative protocols of the physical layer are based on the naive assumptions that the best set of cooperating nodes are preselected, resources are already allocated, and all the transmissions are coordinated [12, 13, 22, 56, 60, 61]. However, selection, resource allocation, coordination and actuation of the cooperating nodes can only be realized with appropriately designed cooperative MAC and routing protocols.

Since node cooperation can take place at multiple levels of the protocol stack, it naturally couples with cross-layer design. For example, consider node cooperation in the physical layer to obtain physical layer diversity. While diversity will improve performance over a given link, node cooperation requires some power and bandwidth to actuate and coordinate the cooperating nodes to achieve this diversity [7,13]. If some bandwidth must be allocated to node cooperation and messaging overhead, then less bandwidth will be available on the channel between the transmit and receive clusters.

Thus, utilizing node cooperation to improve performance requires a joint physical and MAC layer design, such that the cost of realizing cooperation in each layer is taken into account and the overall system performance is optimized. Moreover, if cooperative multi-hop communication is considered rather than single hop communication, then routing layer should be jointly designed for seamless operation with the physical and MAC layers.

In this dissertation, we consider the infrastructured and infractructureless, or ad hoc, networks [62]. Figures 2.6a and 2.7a depict example communication scenarios in infrastructured and ad hoc wireless networks, respectively. In an infrastructured network, a wireless node communicates to any other node in the network through the nearest base station (BS) that is within its communication range. Since the communication between two nodes is carried out via the help of the base stations which are connected through an infrastructure, and node transmissions are carried out in single hop, route discovery is not required for these networks [62]. Typical applications of these networks include WLANs and cellular phone systems [45]. On the other hand, the ad hoc networks have no fixed routers; all nodes can function as routers, which discover and maintain routes to other nodes in the network [62]. In these networks, the routing layer is responsible for discovering the best set of nodes for delivering packets to a specific destination, and configuring and maintaining the nodes so that each node is informed about whom to forward the incoming packets to reach their destinations. Routed packets need to be delivered over the physical link, with the help and coordination of the MAC layer. Example applications of ad hoc networks are WSNs, emergency search and rescue operations, meetings or conventions in which persons wish to quickly share information, and data acquisition operations in inhospitable terrain [62, 63].

For realizing cooperation, the infrastructured wireless networks require the design
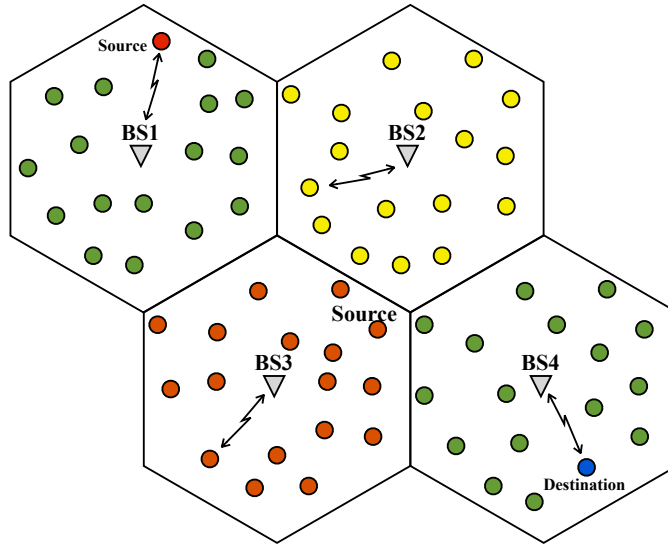
(a) Communication in infrastructured network with direct transmission.
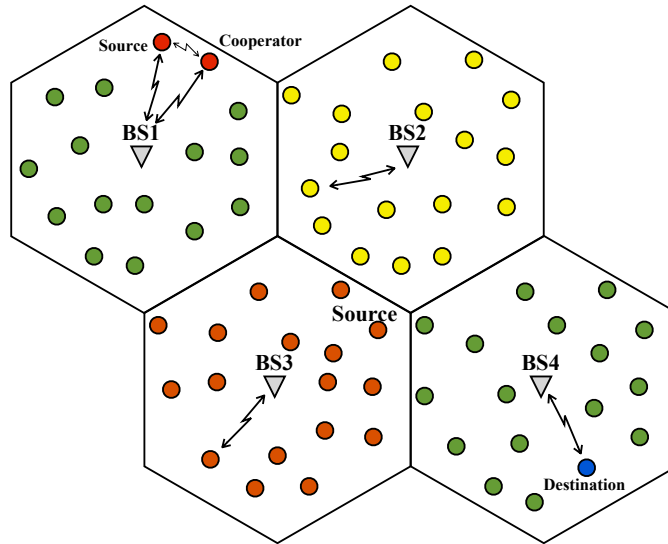
(b) Communication in infrastructured network with cooperative transmissions.

Figure 2.6: Communication in infrastructured network.

of cooperative MAC protocols, whereas wireless ad hoc networks necessitate joint cooperative MAC-routing protocols. In the infrastructured wireless network depicted in Figure 2.6b, a node cooperates with the source node to transmit source's packet to BS1, which sends the data packets to BS4, which delivers the packets to the destina-

(a) Routing with direct transmission.

(b) Routing with cooperative transmissions.
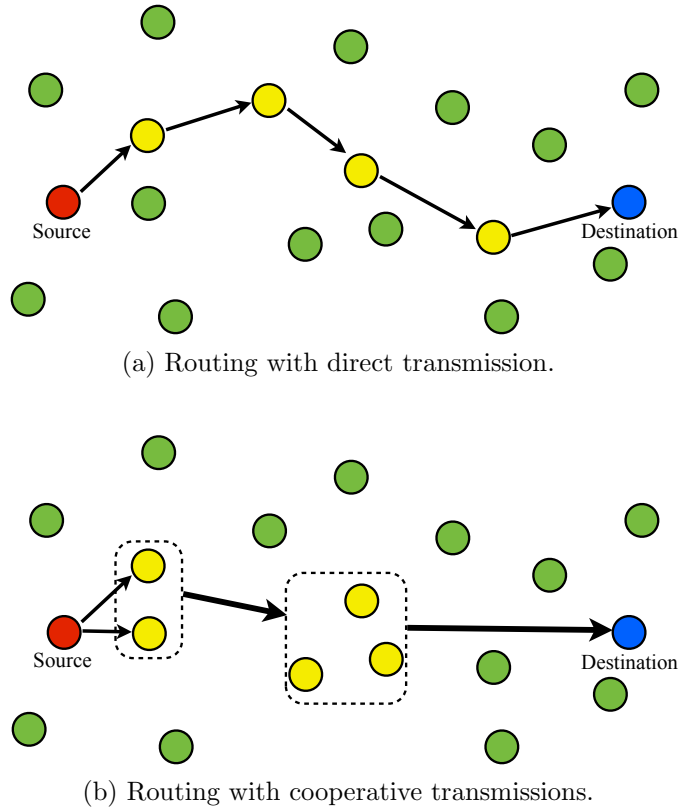
Figure 2.7: Routing with direct and cooperative transmissions.

tion node. For the ad hoc network depicted in Figure 2.7, cooperative diversity opens up a new venue for routing alternatives. Reconsidering the scenario in Figure 2.7a, if cooperation is employed, a subset of the nodes that receive the source transmission can form a cooperation set and they can forward the message towards the final destination. Furthermore, the nodes that receive the cooperation set's transmission can form another subset to forward the message. By this way, multiple cooperation sets can be formed to set up a route between the source and the destination node as illustrated in Figure 2.7b. Cooperation sets can be beneficial, because they provide long haul advantage as well as robust transmissions, which help forming reliable and short routes to the destination.

The literature on multi-hop cooperative protocols is limited, e.g. [29, 35–38]. A

common approach in the literature to incorporate cooperative diversity in multi-hop networks is to employ cooperation on already discovered and established routes. For example, in [35], cooperation is exploited to mediate an unreliable single hop link on the non-cooperative route, such that the original link is kept but its quality is improved by cooperative transmissions of the neighbors. On the other hand, in [36] and [37], an opportunistic cooperative link is formed only when a direct link fails. As opposed to the schemes that consider single link improvements within non-cooperative routes, in [29] and [38], the objective is to improve the end-to-end performance of a non-cooperative route by utilizing cooperative links in lieu of multiple direct links, and obtain a route with cooperative links.

In the following, we will overview the design prerequisites for cooperative MAC and routing protocols.

2.2.2.1 Design Requirements for Cooperative MAC and Routing Protocols

The design of cooperative MAC protocols differs significantly from the conventional MAC protocol design. Conventional protocols aim to schedule and coordinate the transmissions to minimize the collisions and to reserve the medium to only a single user at a given time/frequency/code dimension [45]. However, cooperation idea relies on a different paradigm [6]: Possible cooperators overhear the transmissions of communicating entities and these relay nodes transmit the overheard signal in cooperation with the source node. In other words, cooperation relies on deliberate collisions as opposed to the conventional schemes which avoid collisions. Furthermore, in conventional MAC protocols if a node receives a packet that is not destined to itself, it ignores the packet and stays silent in order to prevent collision or interference. However, in cooperative systems each node is not only responsible for its

own packets but also each node hears the ongoing transmissions, and cooperates with other nodes if needed. Thus, in a cooperative MAC protocol, channel access and network allocation mechanisms need to be modified for utilizing cooperation. Moreover, the assessment of the need for cooperation is necessary, which can be carried out and announced by the source node, or the destination node, or in fully distributed systems this can be carried out autonomously by candidate relays, which also requires substantial modifications in the MAC design.

Having noted the primary design differences between the cooperative and conventional MAC protocols, the primary issues of cooperative MAC protocol design can be summarized as follows: (i) which and how many cooperators should be selected? (ii) how should the resources be allocated among the cooperators? (iii) how should the cooperators be actuated? The MAC protocol should be designed such that these issues are resolved jointly without causing a significant messaging burden on the network.

For exploiting the cooperative diversity, the system parameters should be optimized with respect to the application specific requirements of the network while considering the cost of realizing cooperation. Cooperation requires retransmission of the information, necessitating an extra time/frequency slot [6,7], and requires selection, coordination and actuation of the cooperating nodes, causing messaging overhead [31]. Therefore, cooperation induces extra energy costs and overhead [12,13,31]. A cooperative MAC protocol requires to take into account the messaging required to form a cooperating node set and actuation of the selected set without obliterating the benefits of cooperation. In particular, the network and protocol parameters should be carefully studied for minimizing the cost of cooperation while optimizing the system parameters in accordance with the following objectives:

1. Increased communication reliability over a time-varying channel, which corre-

sponds to reduced average error probability.

2. Increased transmission rate, which corresponds to decreased delay.

3. Increased transmission range, which corresponds to extended coverage area; or reduced transmit power, which corresponds to decreased interference and improved spatial reuse.

4. Reduced energy consumption per reliable communication, which corresponds to achieving required average error probability with reduced energy transmissions.

The quantification of the above mentioned objectives have been provided in our discussion in the physical layer. The network-wise optimization problems require simple yet accurate models for the physical layer. For example, communication reliability can be quantified via outage or error probability of the cooperative system [1]. Although there is vast amount of literature analyzing the outage and error probability of cooperative systems in the physical layer, these works often produce complex models which do not facilitate distributed cooperative MAC protocols, or the findings in these works, [14,15,17,18,24,25,58,59,64–67], lack suitable cooperative MAC protocols for application.

In infrastructured networks, the objective is to solve the single hop optimization problems and schedule the single hop transmissions; however, in infrastructureless networks, the objective is to discover a cooperative route before data communication commences, and to carry out communication through the discovered route, which can be composed of multiple hops. The use of cooperative diversity over multi-hop wireless ad hoc networks is rather involved, because the application of cooperation necessitates a cross-layer MAC-routing protocol, which jointly optimizes the above mentioned objectives for optimal cooperator and route selection simultaneously.

The cooperative MAC protocols in the literature are mainly focused on infrastructured wireless networks [28, 32–34, 68], and these schemes lack generality for application in multi-hop wireless networks, due to the complexity of the relay selection and resource allocation algorithms that do not scale with the network size/density. The application of cooperation in routing layer is rather unexplored, and there is still need for joint MAC-routing protocols to realize cooperation in wireless ad hoc networks. Considering multi-hop cooperative systems, most papers in the literature, e.g., [29, 35–38], assume that an end-to-end path has already been discovered via a conventional routing scheme with direct transmission, and cooperative transmissions are only employed during the packet delivery phase. In such scenarios, cooperative diversity is exploited either to reinforce weak direct links [35], or to replace a failed direct link [36], or to combine multiple direct links in a cooperative transmission to make use of long haul advantage of cooperative diversity [29, 38]. Furthermore, in [30, 37] finding the minimum energy cooperative route is studied, in [21, 69] reliable cooperative multi-hop routing is investigated in energy-constrained densely deployed networks, where cooperation is carried out with fixed number of nodes, and in [70] an ad hoc on demand distance vector (AODV) type of reactive cooperative routing method is presented for densely deployed networks. The above mentioned works in the literature either oversimplify the MAC procedures [30, 69, 70] or totally ignore the required messaging [21, 37], and disregard the effect of messaging on the throughput and energy efficiency.

Although there is fair amount of work in the physical layer, e.g., [6–8, 11–15, 18–20, 22, 24, 53–56, 59–61, 64, 65, 71–74], the works in MAC layer, e.g., [28, 30–34, 68], and in particular, routing layer, e.g., [29, 35–38, 69, 70] are limited, as exemplified in the above mentioned prominent works. In this dissertation, we provide cross-layer MAC and routing protocols that contribute to the cooperative diversity literature.

3 COOPERATIVE MAC PROTOCOL DESIGN AND PERFORMANCE ANALYSIS

In this chapter, we present the design and performance analysis of cooperative MAC protocols for carrier sense multiple access (CSMA) and ALOHA based systems. In particular, this chapter is organized as follows:

In section 3.1, we present our motivation for our work by providing the reader with the state of the art on cooperative MAC protocol design.

In section 3.2, we present a cooperative MAC protocol, COMAC, that enables cooperation in CSMA based systems, in particular, in IEEE 802.11g based systems. Our main effort is to establish the basis for the cooperative MAC design and to determine the conditions under which cooperation is preferable.

In section 3.3, we enhance our protocol design and cooperative MAC architecture to allow for the cooperation of multiple relays, where the relays are selected in a distributed fashion based on the relays' autonomous decisions. Our goal is to quantify and evaluate the throughput and energy cost of actuating multiple relays, taking into account realistic MAC messaging and the corresponding overhead.

In section 3.4, we propose the use of cooperative diversity within the context of an ALOHA system. We present the cooperative ALOHA, C-ALOHA, and we analytically formulate the throughput of C-ALOHA. We show the theoretical performance improvement due to the exploitation of cooperation in an ALOHA based system.

3.1 Background and Related Work

Following the seminal work of Sendonaris *et. al.* [6, 7] and Laneman *et. al.* [8], research on cooperative communications in the physical layer has been fairly extensive with many diverse examples: The symbol error probability of cooperative links with different system set-ups has been studied in [22, 55, 56, 60]. The outage analysis and resource allocation based on the outage analysis have been studied in [14, 15, 19, 20, 54, 61, 64]. The coded cooperation protocols that integrate cooperation into channel coding have been the subject in [11, 53, 54, 71]. The energy-efficiency of cooperative communication has been the subject in [12, 13, 18]. Relay selection methods have been studied with outage criterion [14, 15, 54, 61, 64], and with symbol error probability criterion in [22, 65, 72–74]. Moreover, a buyer/seller game-theoretic relay selection method has been proposed in [24], and SNR threshold based selection techniques have been investigated in [59].

While research on cooperative communications in the physical layer has been fairly extensive as exemplified in the above mentioned prominent works, the higher layer protocols that are essential for the application of the cooperation idea is incommensurate with the available literature in the physical layer. In [28], the authors proposed a cooperative MAC protocol, based on IEEE 802.11, in which high data rate nodes assist low data rate nodes in their transmissions by forwarding their data so that the aggregate throughput can be increased. In that work, each node maintains a cooperation table that is required to be periodically updated, inducing significant overhead with increased number of nodes in the network,. In [30], a CSMA based cooperative MAC protocol is designed for energy-efficient communication. However, in [30], the messaging overhead and the corresponding energy-cost are ignored. Furthermore, in [28,30], the cooperating nodes are selected by the source node, based on the source's knowledge on the network. Jakllari *et. al.* [29] proposed a cooperative

protocol that exploits the extended transmission range provided by cooperative diversity. In [31], the authors present a distributed cooperative MAC protocol, where a relay node autonomously decides to cooperate to improve the transmission rate. In [26], an adaptive method based on distributed timers is proposed to find out and to actuate the best relay among many possible relays. For densely deployed networks, this method requires a long period of silence (no transmission) during the relay selection epoch, which degrades the throughput performance considerably. In [75], cooperative transmissions are employed to provide diversity gain to a collision resolution protocol presented in [76]. In [32–34], the authors propose a cooperative MAC protocol that exploits randomized distributed space time codes (RDSTC) for opportunistic on the fly relay selection.

The aforementioned cooperative MAC protocols either disregard the burden of MAC messaging [29, 30] or do not investigate the costs of actuating relays, such as energy costs [28, 32–34]. However, without a sound MAC messaging and without appropriate quantification of the costs of actuating cooperation, the gains of cooperative diversity can not be fully investigated. For this purpose, in this section, we first design a cooperative MAC protocol to realize cooperation in a realistic network setting, and then we analyze the cost of employing cooperation in various scenarios with different number of cooperators via detailed simulations of the proposed MAC protocols. To our knowledge, the cooperative protocols proposed so far fail to investigate the energy efficiency in its entirety: The proposed protocols have not been investigated considering different transmission ranges and data rates, which are shown to be important parameters for cooperative communications [13]. Also, the effect of circuit energy consumption on the energy efficiency has not been studied, which we attempt to address in this dissertation.

3.2 Cooperative MAC Protocol: COMAC

In this section, we propose a cooperative medium access control protocol, COMAC that enables cooperation in a realistic scenario, using IEEE 802.11g based radios, and leverages cooperative communications by making use of the overheard packets from neighboring nodes of a sender node. In an effort to determine the conditions under which cooperation is preferable, we evaluate COMAC's performance in comparison with standard 802.11 through detailed simulations, considering different data rates, varying transmission ranges, networks of different sizes and various energy consumption models.

This section is organized as follows. The system model is presented in section 3.2.1. COMAC protocol is introduced in section 3.2.2, and the performance analysis is presented in section 3.2.3.

3.2.1 System Model

Consider the example wireless network depicted in Figure 3.1, in which source node, S, disseminates the packet to its neighboring node R in phase-I, and in phase-II, S and R transmit the packet to the destination, D, cooperatively; thus providing transmit diversity at the destination.
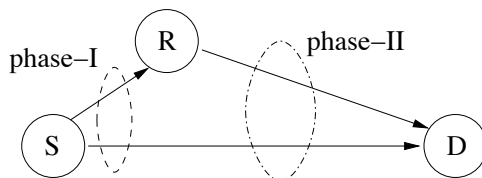
Figure 3.1: System Model

In a typical sensor network, nodes are deployed such that each node has at least one more node in its close vicinity. We assume that the nodes that are close to the source node can assist the source while a packet is being transmitted to another node.

Table 3.1: Data rates, raw modulation schemes, the corresponding receive sensitivities and the SNR thresholds.

Data Rate	Modulation	Receive Sensitivity	SNR Threshold
6 Mbps	BPSK	-90 dBm	10 dB
9 Mbps	BPSK	-84 dBm	16 dB
12 Mbps	QPSK	-82 dBm	18 dB
18 Mbps	QPSK	-80 dBm	20 dB
24 Mbps	16-QAM	-77 dBm	23 dB
36 Mbps	16-QAM	-73 dBm	27 dB
48 Mbps	64-QAM	-72 dBm	28 dB
54 Mbps	64-QAM	-72 dBm	28 dB

The source, relay and destination nodes constitute a cooperating set and the relay nodes are assumed to be in close vicinity of the source node, whereas the destination is relatively far away from the source node as depicted in Figure 3.1.

Each node is assumed to be equipped with identical transmitter and receiver circuitries using the IEEE 802.11g [4] data rates and the raw modulation schemes without error correction. We use the receive sensitivity thresholds given in [77] as summarized in Table 3.1. Here, the noise power is given as -100 dBm. Signals below receive sensitivity can not be received successfully by the receiver. During packet reception in phase-II at the destination, we assume that the diversity receiver implements MRC. MRC receiver obtains the channel state information of source-destination and relay-destination channels via the control packets of COMAC. A packet is received successfully if the average BER is less than or equal to 10^{-5}. The receive threshold is determined by making use of the BER performance of MRC and the modulation schemes under the fading channel. The average BER, $\bar{P}_b$, for the BPSK and Quadrature Phase Shift Keying (QPSK) receiver with M-branch diversity using MRC is given as [1]:

$$\bar{P}_b = \frac{1}{\pi} \int_0^{\pi/2} \left(1 + \frac{\bar{\gamma}}{\sin^2\phi}\right)^{-M} d\phi \qquad (3.1)$$

Similarly, $\bar{P}_b$ for Quadrature Amplitude Modulation (QAM), m-QAM, receiver with M-branch diversity using MRC is given as:

$$\bar{P}_b = \frac{\alpha}{\pi}\left(1 - \frac{1}{\sqrt{M}}\right)\int_0^{\pi/2}\left(1 + \frac{g\bar{\gamma}}{\sin^2\phi}\right)^{-M}d\phi - \frac{\alpha}{\pi}\left(1 - \frac{1}{\sqrt{M}}\right)^2\int_0^{\pi/4}\left(1 + \frac{g\bar{\gamma}}{\sin^2\phi}\right)^{-M}d\phi,$$

$$(3.2)$$

where M designates the number of nodes sending in cooperation, $\alpha = \frac{4}{\log_2 m}$ and $g = \frac{3\log_2 m}{2(m-1)}$ and the average SNRs, $\bar{\gamma}$, of cooperating nodes are independent and identically distributed (i.i.d.) .

Given $\bar{P}_b^*$ and the raw modulation scheme, the corresponding required SNR for an MRC receiver, $\gamma_M(\bar{P}_b^*)$, can be calculated via the expressions (3.1), (3.2). Let $\gamma_1(\bar{P}_b^*)$ and $\gamma_M(\bar{P}_b^*)$ denote the SNR levels required for a transmission with a given $\bar{P}_b^*$, for non-cooperative ($M=1$) and cooperative transmissions ($M > 1$), respectively. The ratio $\frac{\gamma_1}{\gamma_M}$ is called as the diversity gain, which also reflects into a decrease in the sensitivity threshold at the receiver. In other words, receive threshold of an M-branch MRC receiver, Υ_M, can be found in terms of the receive threshold of a receiver without a combiner, Υ_1, as $\Upsilon_M = \frac{\Upsilon_1\gamma_M(\bar{P}_b)}{\gamma_1(\bar{P}_b)}$. The advantage of the decreased receive threshold is two folds: 1) The transmission range is extended while the transmit power is kept constant, 2) The transmit power is decreased while serving the same transmission range with the non-cooperative scheme.

Here, we propose a cooperative MAC protocol that takes advantage of the decreased receive threshold through longer transmission ranges and improved packet success rates compared to the non-cooperative transmission, while keeping the transmit power constant. The mode of transmission, cooperative or non-cooperative, can be determined by the source and the relay nodes with the help of the received signal strength measurements of the source-relay, relay-destination channels from the previous transmissions. However, investigation of possible methods for cooperation

decision and relay selection is considered in the next chapter. Here, we design a MAC protocol to enable cooperative communications and evaluate its performance in detail.

3.2.2 A Cooperative MAC protocol: COMAC

COMAC is backward compatible with the IEEE 802.11 MAC, so that it can be used together with the existing MAC protocol. In the original IEEE 802.11 standard, if a node receives a packet that is not destined to itself, it ignores the packet and sets its Network Allocation Vector (NAV) according to the duration specified in the packet header. The proposed MAC protocol exploits the fact that each transmitted packet is overheard by the neighboring nodes and makes use of the overheard packets. For this purpose, the COMAC protocol makes use of the reserved bit in the Frame Control Field of the MAC header to indicate whether the transmission is in cooperative mode or not.

Frame Control	Duration	RA	TA	Coop Info	FCS
16	16	48	48	k	32

Bits:

(a) C-RTS frame format

Frame Control	Duration	RA	FCS
16	16	48	32

Bits:

(b) C-CTS, C-ACK and ACO frame formats

Frame Control	Duration/ ID	Address 1	Address 2	Address 3	Sequence Control	Address 4	Frame Body	FCS
16	16	48	48	48	16	48	n	32

Bits:
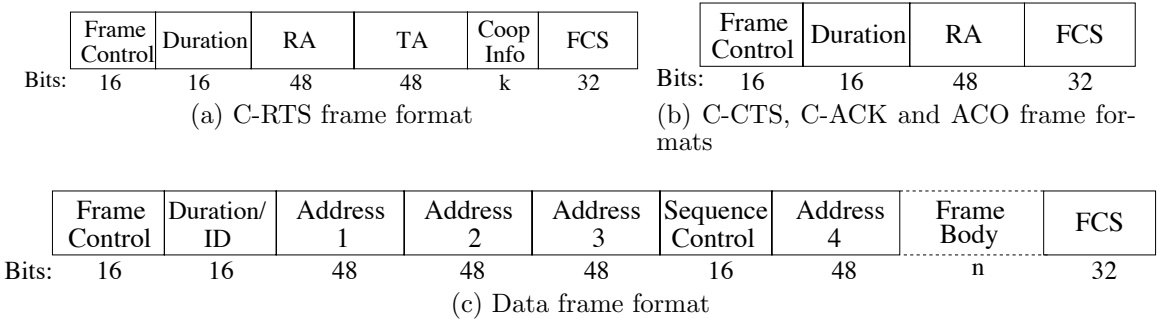
(c) Data frame format

Figure 3.2: COMAC frame formats

The modified packet structures are depicted in Figure 3.2 and Figure 3.3 depicts the frame exchanges in the cooperative mode. Cooperative transmission is initiated by the source via sending a Request to Send in Cooperation (C-RTS) packet. The C-RTS packet includes a field called "Cooperation Information" (CI), which is specifically used to announce the number of relays being selected and their IDs. The CI
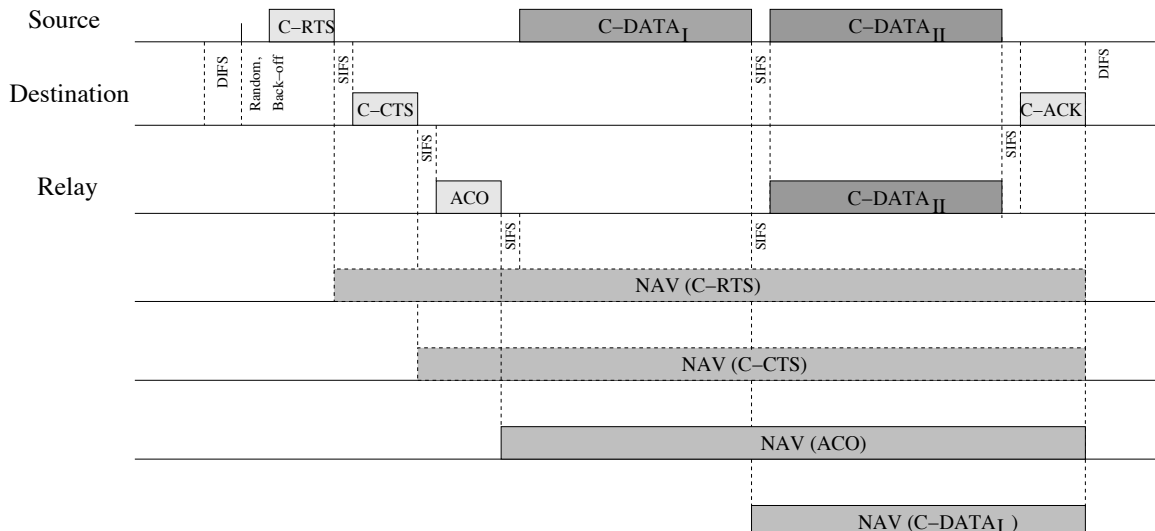
Figure 3.3: Frame exchange and NAV settings for COMAC

field has a variable size, k, which varies depending on the number of relays being selected. While describing the protocol operation we assume that only one relay is selected by the source, and the CI field is set accordingly. The destination node replies to the C-RTS with a Clear to Send in Cooperation (C-CTS) packet. The relay sends an ACO (Available to Cooperate) packet following the C-CTS to announce its availability for cooperation. Upon reception of the ACO, the source disseminates the data packet (phase-I), C-DATA$_I$ and in phase-II, the source and the relay nodes repeat the data packet, C-DATA$_{II}$. The destination acknowledges the successful reception of C-DATA$_{II}$ by a C-ACK. The C-RTS packet reserves the medium for the duration of one cooperative packet transmission and the neighboring nodes update their NAVs, upon the reception of C-CTS, ACO, C-DATA$_I$, C-DATA$_{II}$ and C-ACK, making use of the duration field in all packets. C-RTS and ACO packets also assist the channel estimation procedure for the MRC receiver.

We describe the protocol operation by explaining the procedures followed by the sensor nodes in different roles, namely source, relay and destination nodes.

Source node, S : Operation of the source node is depicted in Figure 3.4. The
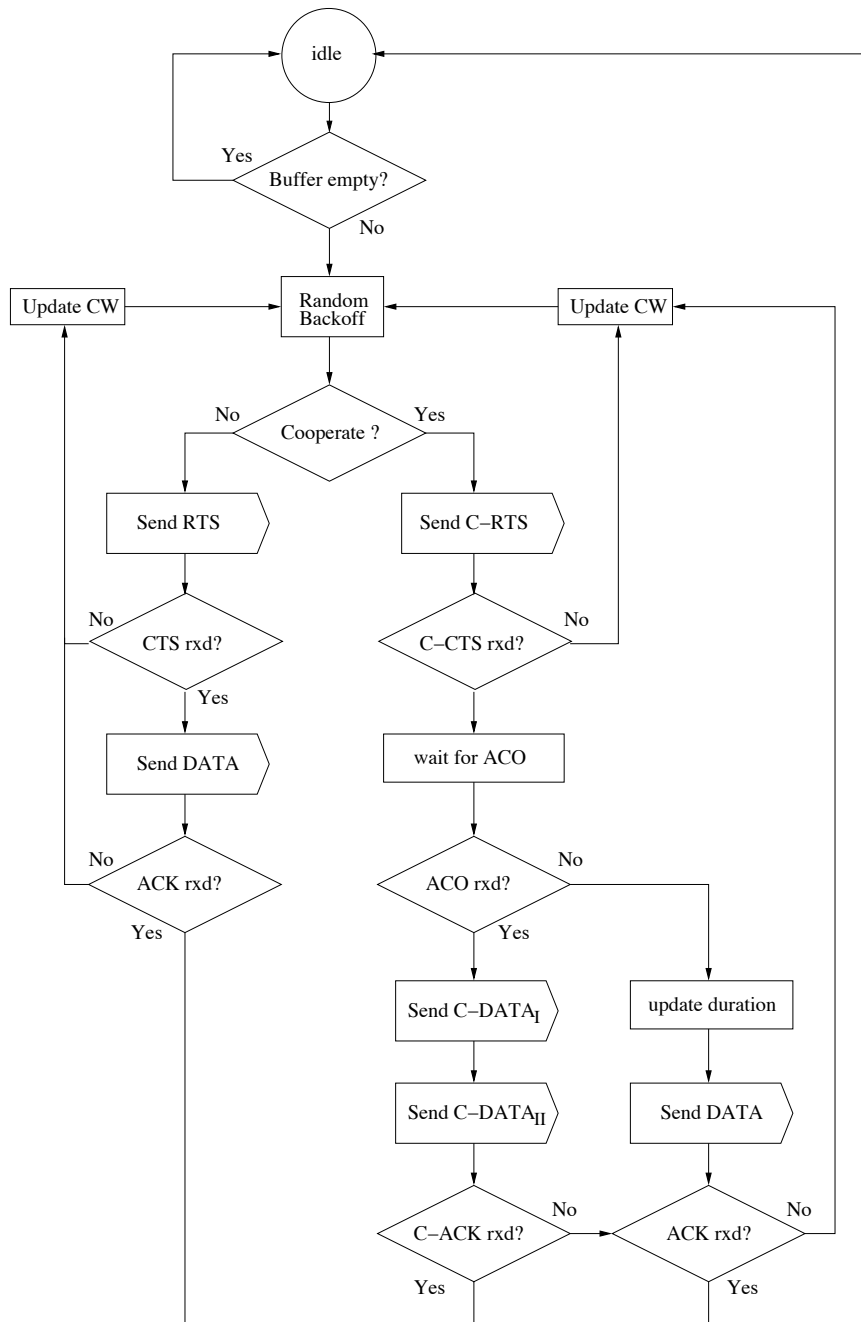
Figure 3.4: Flow chart at the source node

source node initially determines the mode of transmission.

1) If the source decides not to cooperate, the packet exchanges are carried out as in IEEE 802.11 in RTS/CTS mode. However, if the source decides to coop-

erate, then a C-RTS is sent to the destination. The C-RTS packet informs the neighboring nodes about the expected duration of the cooperative transmission, as designated in its duration field. The duration field of the C-RTS is set so that $D_{C\text{-}RTS} = 5T_{SIFS}+T_{C\text{-}CTS}+T_{ACO}+2T_{DATA}+T_{C\text{-}ACK}+6T_{prop}$, where T_{SIFS} is the duration of one short inter frame spacing (SIFS), $T_{C\text{-}CTS}$, T_{ACO}, $T_{C\text{-}ACK}$, T_{DATA} denote the duration of a C-CTS, ACO, C-ACK and DATA frame, respectively. The transmission duration values for C-CTS, ACO, C-ACK, DATA packets, $T_{C\text{-}CTS}$, T_{ACO}, $T_{C\text{-}ACK}$, T_{DATA}, are obtained by dividing the lengths of the respective packet types with the transmission rates of those packets, as given in Table 3.2. T_{prop} designates the maximum propagation delay.

2) If C-CTS is received in response to the C-RTS packet, then the source waits for an ACO packet. If C-CTS is not received, the source updates its contention window (CW), backs off and restarts from step 1 again.

3) If an ACO is received after a SIFS period following the C-CTS, cooperation is feasible, so the source disseminates the data, C-DATA$_\text{I}$, after a SIFS period. The duration field in the C-DATA$_\text{I}$ is set as the remaining time from the duration $D_{C\text{-}RTS}$ and the nodes that hear C-DATA$_\text{I}$ packet update their NAVs accordingly, as depicted in Figure 3.3. After a SIFS period following C-DATA$_\text{I}$ transmission, the source repeats the data packet, C-DATA$_\text{II}$. After the C-DATA$_\text{II}$ transmission, the source waits for a C-ACK packet.

If an ACO message is not received after a SIFS period following the C-CTS, the source assumes that the relay is not available, and initiates the transmission of the DATA packet. The transmission reverts to non-cooperative mode and the duration field is set according to direct data transmission as: $D_{DATA} = T_{SIFS} + T_{DATA} + T_{ACK} + 2T_{prop}$.

4) If a C-ACK is received in response to C-DATA$_\text{II}$, the source declares the suc-

cess of the cooperative transmission and returns to the idle position. If an ACK is received, the source declares successful packet transmission but failed cooperative transmission. If neither ACK nor C-ACK is received, the source initiates retransmission with updated CW and returns to step 1. The source keeps track of the failures in cooperative transmission while cooperating with a relay node. If a relay node fails to cooperate for more than a predefined number of times, the source may decide not to cooperate with this node next time, and exclude this node from its cooperating list.

Relay node, R : Operation of the relay node is depicted in Figure 3.5 (a). A node receiving a C-RTS message with its ID in the CI field, deduces that cooperative transmission is requested and waits for the C-CTS packet. If a C-CTS is received, the node determines the mode of transmission.

1) If the relay node decides to cooperate, an ACO message is sent to the source node after a SIFS period following the reception of the C-CTS. Otherwise, the relay returns to the idle state.

2) If a C-DATA$_\mathrm{I}$ packet is received after the transmission of ACO, the relay repeats the received data packet after a SIFS period. The relay node does not expect an acknowledgement, but defers its transmission and remains passive until the end of the frame exchange. If a DATA packet is received after the transmission of ACO, the relay assumes that cooperative transmission was aborted. In this case, the relay updates its NAV according to the duration field of the DATA packet.

Destination node, D : Operation of the destination node with MRC is depicted in Figure 3.6 (b).

1) A node receiving a C-RTS message deduces that cooperative transmission is requested and sends a C-CTS message.

2) If an ACO message is received, the destination expects a C-DATA$_\mathrm{I}$ packet.
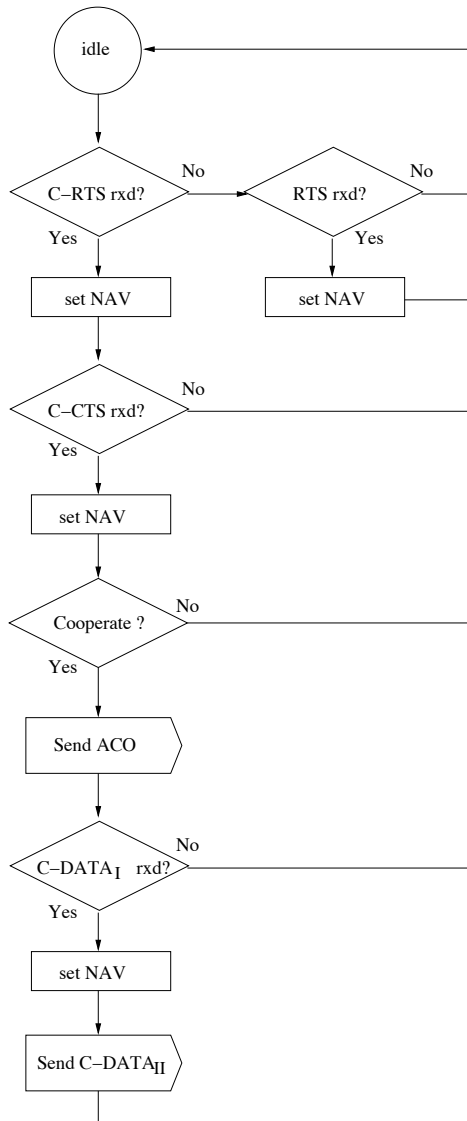
Figure 3.5: Flow chart at the relay.

If the C-DATA$_I$ packet is received after the ACO packet, the destination waits for the C-DATA$_{II}$ packets. If the C-DATA$_{II}$ is received from both the relay and the source, the destination replies back with a C-ACK designating that the cooperative transmission was successful. If the C-DATA$_{II}$ packet is received neither from the source nor the relay, but the C-DATA$_I$ was successfully decoded, then the destination sends an ACK and returns to the idle state. If DATA packet is received after the ACO packet instead of C-DATA$_I$, then the destination node assumes that the cooperative
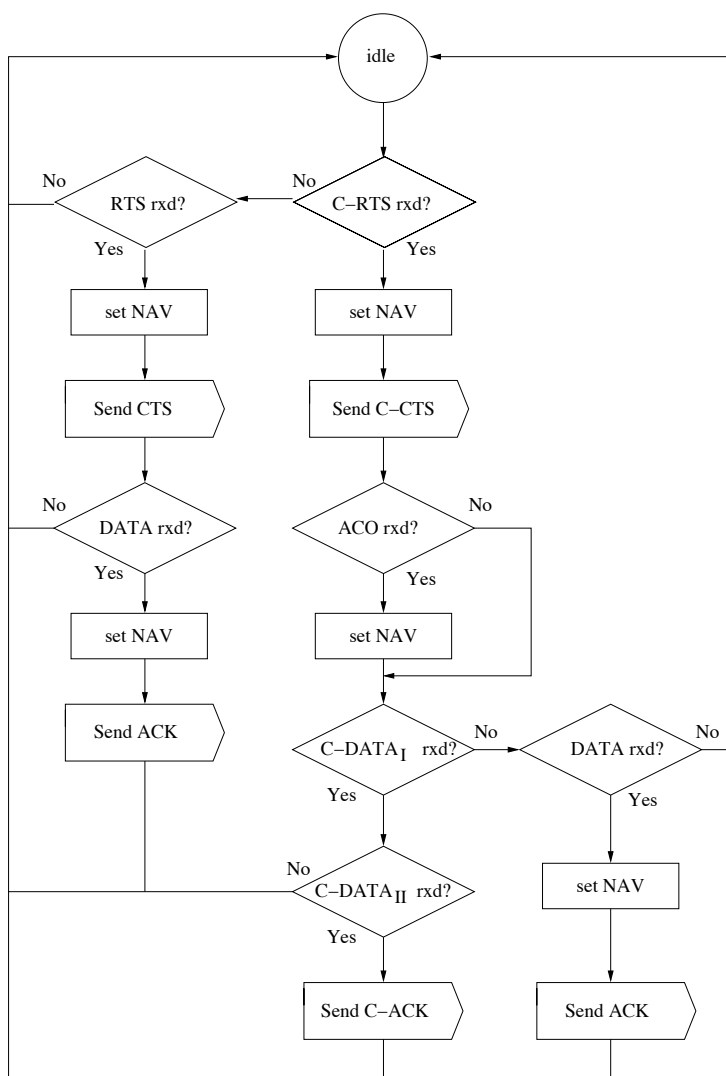
Figure 3.6: Flow chart at the destination.

transmission was aborted. In this case, the destination replies with an ACK packet after SIFS period following the DATA packet denoting the successful non-cooperative transmission.

3) If an ACO message is not received after a SIFS period following the C-CTS transmission, the destination assumes that direct data transmission will be carried out. However, if C-DATA$_I$ packet is received without receiving an ACO, the destination deduces that cooperative transmission has been initiated although ACO packet

had not been received. The destination updates the NAV according to the duration field of the C-DATA$_I$ packet and proceeds with cooperative diversity reception as described in step 2.

3.2.3 Performance Analysis

We have modeled and implemented our COMAC protocol in ns-2 environment [39]. Our COMAC implementation in ns-2 comprises modifications in the physical layer model of ns-2, and the design and implementation of our COMAC protocol in the MAC layer of ns-2 in accordance with the descriptions in section 3.2.2. Below, we first summarize our modifications in the physical layer model of ns-2, and we describe the primary components of our cooperative MAC implementation in ns-2, and then we continue with the performance analysis.

Ns-2 is a packet-level discrete event simulator [39]. The physical layer implemented in ns-2 is an abstraction of the operation of the receiver, where actual bit transmissions are not considered. A transmitted packet is assumed to be successful or erroneous based on whether the received signal power is above or below a certain threshold, respectively, which is determined by the receiver specifications. The conventional ns-2 physical layer model does not incorporate the fading channel, but it only includes the path-loss model. In order to have a realistic wireless channel model, and to observe the effect of fading channel, we have implemented Rayleigh fading in the physical layer model. In particular, in our implementation, received power is an exponentially distributed random variable whose mean is determined by path-loss. Furthermore, physical and MAC layer models of ns-2 has been updated so as to allow for synchronous transmissions of cooperating nodes, to realize cooperative diversity gain in case of cooperative transmissions, and also to differentiate between simultaneous transmissions of non-cooperating and cooperating nodes. Since a practical

cooperative diversity receiver is not readily available, for implementing and realizing the cooperative diversity gain, we have modified the receive threshold values of the considered receiver chip in accordance with the receive sensitivity values provided in Table 3.1, considering the theoretical diversity gain, as described in section 3.2.1. In the MAC layer of ns-2, we have modeled and implemented our COMAC protocol as a CSMA based protocol, as detailed in section 3.2.2. The conventional protocols are designed such that only a single node accesses the medium at a given time slot, and otherwise packet collisions occur at the receiver. However, our protocol relies on concurrent transmissions of the cooperating nodes, which should be differentiated from the collision event. In order to differentiate the operation of the receiver under concurrent transmissions of cooperating nodes and overlapping transmissions of non-cooperating nodes, the cooperation mode and the ID of the cooperators are included in the packet headers. The node emulates the cooperative diversity receiver given that the packets are in cooperation mode and the channel gains are obtained through the C-RTS - C-CTS - ACO messaging of our COMAC protocol. If the simultaneously received packets are not in cooperation mode, then the packets undergo collision.

We conducted detailed performance analysis of the COMAC protocol via simulations in ns-2 environment. Specifically, standard IEEE 802.11 protocol is compared to COMAC, in scenarios where cooperation is always enabled between a source and a relay node that is in close vicinity of the source. In the simulations, IEEE 802.11g settings are considered as the physical layer and a two ray ground model with Rayleigh fading and path loss exponent 4 is used to model the wireless channel. We assume slow fading so that channel condition does not vary for the duration of one frame exchange, and the MRC receiver obtains the source-destination and the relay-destination channel information by the C-RTS and ACO transmissions, respectively. A packet is received successfully if its power at the receiver is above the receive threshold. For

the non-cooperative scheme, we use the receive threshold (Υ_1) values provided in [77] for an average BER of 10^{-5}. The receive threshold (Υ_2) applied at the MRC receiver at the given BER requirement is calculated as described in section 3.2.1, and the threshold values used in the simulations are summarized in Table 3.1. Control packets are transmitted at 6 Mbps and Table 3.2 lists the other system parameters used by COMAC and IEEE 802.11g protocols. All the data and control packets are transmitted with a power of 1 mW and 30 mW, respectively, and no power control is applied.

Our goal with simulations is to determine at what rate and at what distance should cooperation be preferred to improve the system performance both energy-efficiency and throughput wise. We define the throughput as the number of successfully transmitted data bits per second. A data packet is successfully transmitted if the source node receives an acknowledgement from the destination. Furthermore, we consider the energy-efficiency by defining *energy-per-throughput* which is the energy consumed in the system for successfully transmitting one data bit to the destination.

Table **3.2**: COMAC System Parameters

RTS	92 bytes
C-RTS	98 bytes
CTS, C-CTS, ACO, ACK, C-ACK	86 bytes
Pay load	1044 bytes
MAC header	34 bytes
PLCP preamble and header	72 bytes
Data rate for MAC and PHY header	6 Mbps
Slot time	9 μs
SIFS	10 μs
DIFS	28 μs
PLCP short preamble time	24 μs
PLCP header time	72 μs

In the first set of simulations, we evaluate the performance in a point-to-point

scenario, where a single source generates data packets according to a Poisson distribution and transmits the packets to a destination node over a fading channel. For a lossless channel, where packets are assumed not to undergo channel errors, i.e., every packet is assumed to be successfully received at the destination, and considering data rate of 54 Mbps and control packet transmission rate of 6 Mbps, the maximum point-to-point throughput of IEEE 802.11g with RTS/CTS exchange can be calculated as 10.4 Mbps, while the maximum throughput for COMAC with RTS/CTS/ACO exchange is obtained as 7 Mbps. Here, the loss in the throughput of COMAC is due to the increased overhead. Although the throughput of the non-cooperative scheme in the lossless channel is higher than COMAC's, the opposite is observed in practice in the fading channel.

In Figure 3.7, we observe the point-to-point throughput measured at the destination receiver with and without cooperation, considering the fading channel, different physical data rates and by varying the separation between the source and the destination. We observe that the maximum achievable throughput of the non-cooperative scheme is available for only a very short range and as the separation distance is increased, the throughput is decreased sharply especially at higher data rates. In the meantime, COMAC outperforms the non-cooperative scheme after a short distance, and provides a flat throughput curve, 0.70 - 6 times better than direct 802.11 within medium to long transmission ranges. Figure 3.7 also depicts the highest throughput curve considering all transmission modes and rates, allowing the best decisions for data rates and whether to cooperate or not. Specifically, up to 26 m the non-cooperative scheme can be preferred to operate at 54 and 48 Mbps. Starting from 26 m up to 205 m, COMAC provides the highest throughput at 54 Mbps. After 205 m, COMAC operates at lower date rates, 24 and 18 Mbps, while providing significant throughput gains over the direct scheme, which can only operate at the basic rate

of 6 Mbps. The overall range, 315 m is limited by the range of the control packets. The throughput improvements measured in this experiment is due to the diversity gain obtained by cooperative transmission, which makes the channel more robust to errors and brings the long haul transmission advantage. Cooperative transmission is enabled by the proposed COMAC protocol, which provides higher throughput at a longer range despite the additional overhead introduced.
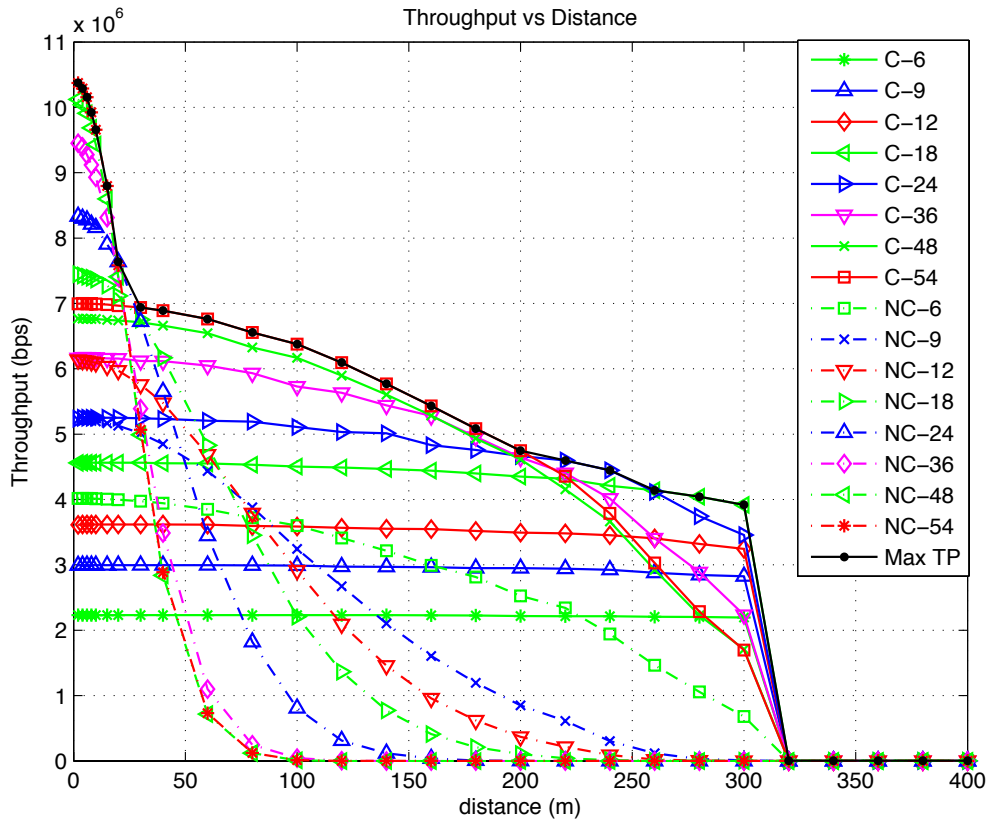
Figure 3.7: Throughput vs distance, for COMAC (C) and non-cooperative scheme (NC), i.e. 802.11g, at data rates of 6, 9, 12, 18, 24, 36, 48, 54 Mbps.

Next, we compare the energy-efficiency of the COMAC protocol in the above point-to-point scenario. We consider the data rates of 54 and 18 Mbps, as the modes that provide the highest throughput for most ranges, and also two data rates distinct enough to reflect the differences in transmission times and receiver sensitivity levels.
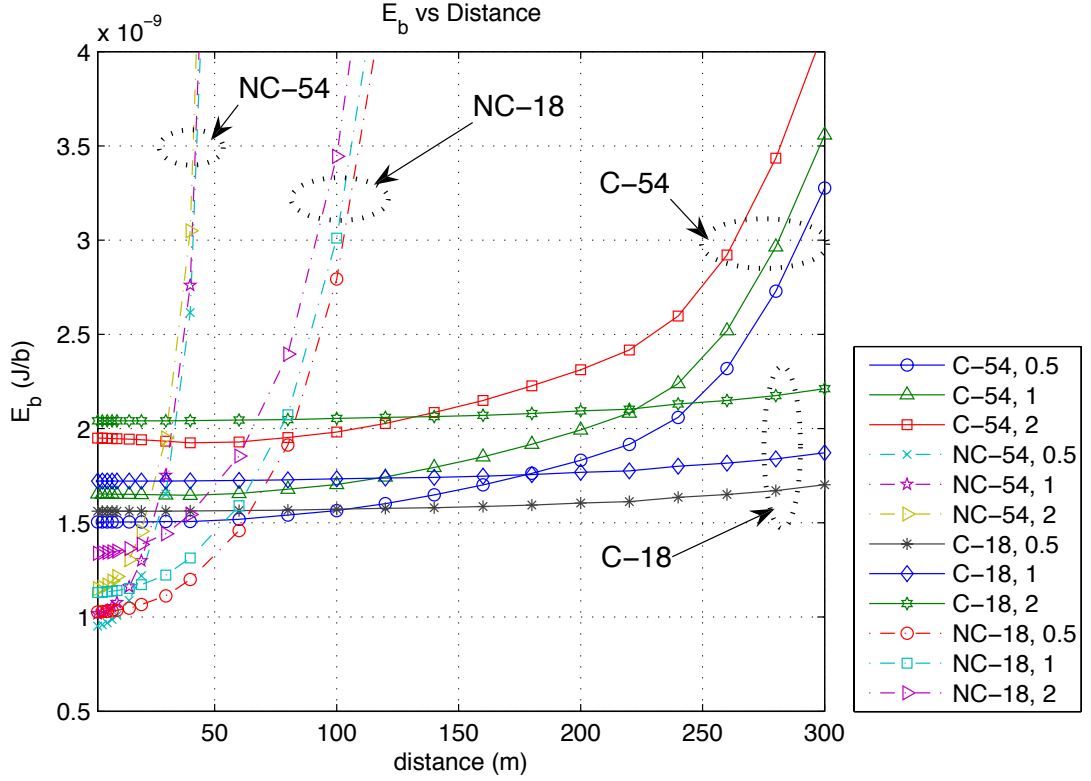
Figure 3.8: Energy-efficiency vs distance, at data rates of 18 and 54 Mbps, for $P_c = 0.5P_t$, $P_c = P_t$ and $P_c = 2P_t$ for COMAC (C) and non-cooperative (NC) scheme.

We model the energy consumption for transmitting a packet as $E_t=(P_c+P_t)T$ and for receiving a packet as $E_r=P_cT$, respectively. P_t refers to power consumption at the transmit amplifier. The power consumption at the transmit circuitry and the receive circuitry are assumed to be equal [78] and denoted as P_c, and T designates the packet duration. In fact, the actual circuit energy consumption values may vary depending on the technology used, so in our simulations we also investigate the effect of circuit energy consumption on the energy efficiency of the protocols. In Figure 3.8, we compare the energy-efficiency of the cooperative and non-cooperative schemes, for cases $P_c/P_t = 0.5, 1, 2$. For short ranges, the non-cooperative 802.11 protocol is energy efficient in all cases, and COMAC consumes more energy, which

is due to the additional energy consumption at the relay node. However, the energy consumption of direct 802.11 is dramatically increased after a short distance (around 40 m for 54 Mbps and 80 ms for 18 Mbps), while the energy spent using cooperative COMAC remains in the same level up to farther distances (up to 200 m for 54 Mbps and 300 m for 18 Mbps). The energy consumption of COMAC is significantly below direct 802.11 for medium to long range distances, considering both rates and effect of circuit energy. In all curves, it is observed that the effect of circuit energy consumption on the energy-efficiency is increased, as source-destination separation is increased. The simulation results prove that in both high and relatively low data rates, all circuit energy levels, and despite the energy consumption at the relay node, COMAC significantly improves the energy-efficiency, especially for medium to long range transmissions due to robustness to the channel conditions.
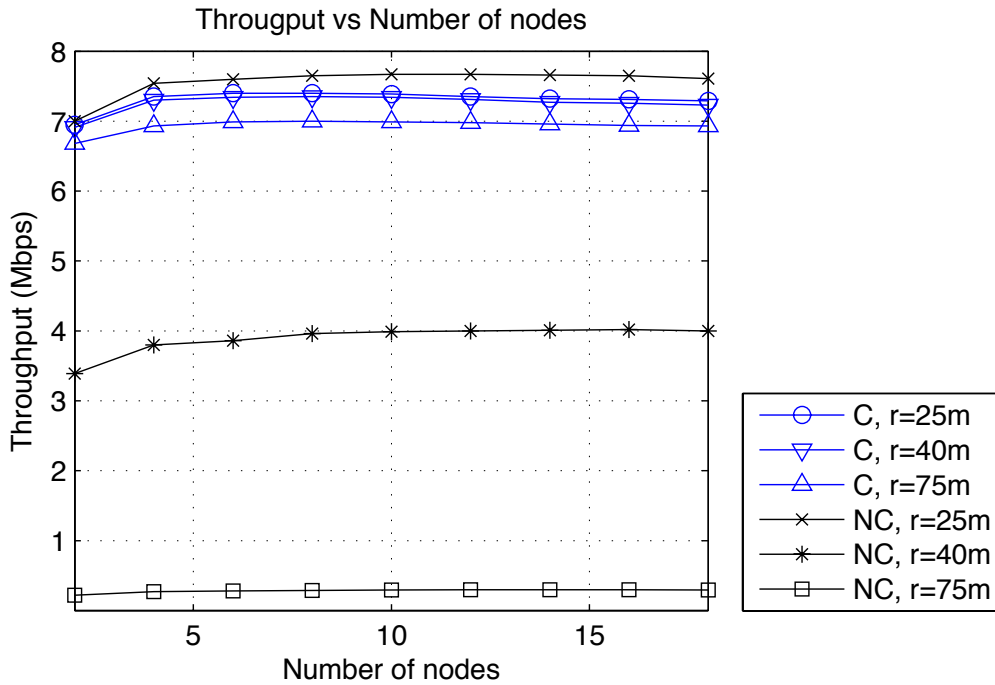
Figure 3.9: Throughput vs number of nodes, at a data rate of 54 Mbps for r=25m, r=40m, and r=75m for COMAC (C) and non-cooperative scheme (NC).

Now, we consider the non-cooperative 802.11 and COMAC protocols in a multi-

point-to-point scenario, where both protocol overhead and transmissions are increased. Multiple source nodes are placed on a circle with a radius of r and the destination node is located at the center. Both schemes operate at the data rate of 54 Mbps and r is varied. Each source node generates data packets according to a Poisson distribution, and can serve as a relay when necessary. In Figure 3.9, we observe the throughput as a function of the number of source nodes in the network. For a relatively small range, $r = 25$ m, we observe that cooperative and non-cooperative schemes achieve similar throughput performance.

As the transmission distance is increased, the aggregate throughput of the non-cooperative scheme is decreased dramatically, while COMAC's performance is only slightly degraded. These results confirm that the throughput performance of COMAC is not affected by increased number of contending nodes in the network, and in fact, COMAC can improve the aggregate throughput by a factor that increases with increasing range, which is observed to be as large as 23 for $r = 75$ m.

Finally, in Figure 3.10, we observe the energy-efficiency performance for the above multi-point-to-point scenario with varying number of nodes, also considering different circuit energy consumption levels. The transmission range is fixed as $r = 40$ m and data rate is set as 54 Mbps. For these settings, the simulations indicate that COMAC's total energy consumption is half of the non-cooperative scheme for all circuit energy consumption levels. Further savings are obtained for longer transmission range. Last but not least, energy-efficiency of COMAC is not affected by the increased number of contending nodes as much as non-cooperative 802.11. This is due to improved packet success rate of COMAC, so that packet retransmissions, hence repeated usage of transmit and receive circuitries are avoided.

In this section, it is shown that the amount of performance improvement depends on the transmission range, data rate and components of energy consumption.
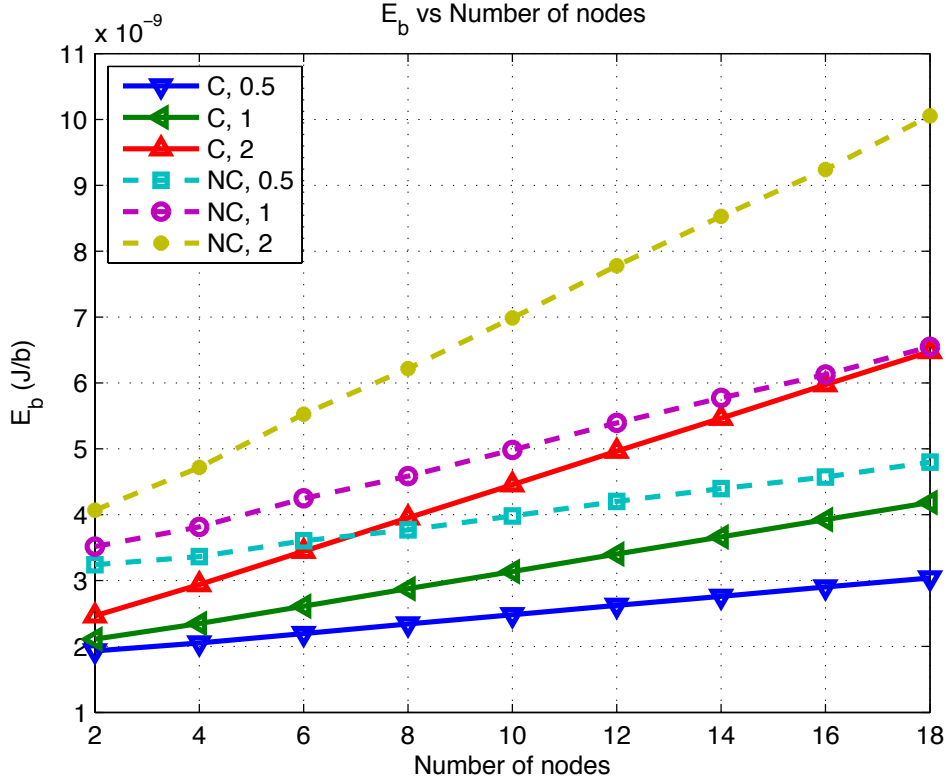
Figure 3.10: Energy-efficiency vs number of nodes, at $r=40$m and at a data rate of 54 Mbps for $P_c = 0.5P_t$, $P_c = P_t$ and $P_c = 2P_t$ for COMAC (C) and non-cooperative (NC) scheme.

Despite the introduced overhead and extra transmissions, cooperative transmission realized through the COMAC protocol is proven to provide significant throughput enhancements in both point-to-point and multi-point-to-point scenarios, especially for medium to long range transmission. For the same transmission ranges, energy savings of about 50 percent is obtained, irrespective of increased number of users or circuit energy consumption.

In the next section, we consider employing multiple relays for cooperative transmissions to further improve the system performance. For this purpose, we introduce adaptive relay selection into the COMAC protocol, where the selection and actuation of multiple relays is carried out through a method that relies on slotted ALOHA

based relay advertisements.

3.3   COMAC with Multiple Relays

In this section, we introduce adaptive relay selection into the COMAC protocol, where relays autonomously decide whether to get involved in the cooperative transmission or not. Here, we extend COMAC to operate with multiple relays, and we propose and analyze a relay selection mechanism based on random access relay advertisements. We analytically evaluate the performance of COMAC in a scenario where multiple possible relay nodes contend to announce their availability for cooperation and actuate cooperative transmission without any explicit selection carried out by either the source or the destination. We provide the analysis of the throughput gain provided by the proposed scheme and obtain the optimum relay actuation probability maximizing the throughput gain.

This section is organized as follows. In section 3.3.1, the system model is presented. In section 3.3.2, the operation of the COMAC protocol with multiple relays and relay actuation are introduced. The analysis of the protocol and the proposed relay actuation scheme is provided in section 3.3.3. Simulation results are presented in section 3.3.4.

3.3.1   System Model

Figure 3.11 illustrates the cooperative system model with multiple relays. In phase I, the source node, S, disseminates the packet to its neighboring nodes $R_1, R_2, ..., R_N \in \mathcal{R}$, where $\mathcal{R}$ denotes the set of candidate relays. In phase II, S and a subset of relays from $\mathcal{R}$, transmit the packet to the destination, D, cooperatively; thus providing transmit diversity at the destination.

Each node is assumed to be equipped with identical receiver and transmitter
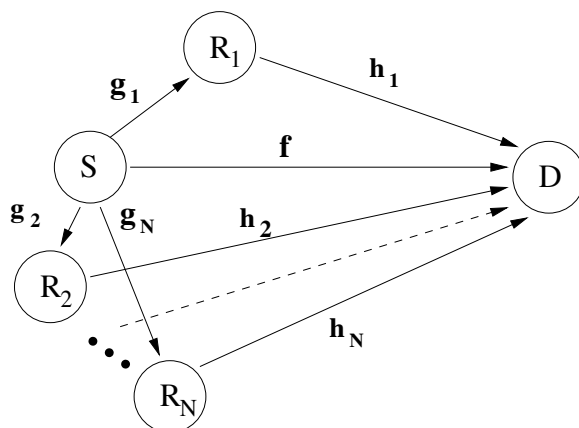
Figure 3.11: COMAC with multiple relays: System model.

circuitries using the IEEE 802.11g [4] data rates and the raw modulation schemes without error correction. A packet is received successfully by the receiver if the signal is above the receive sensitivity level. We use the receive sensitivity thresholds given in [77] and summarized in Table 3.1. During the cooperative packet reception at the destination, we assume that the diversity receiver implements MRC. The diversity receiver obtains the CSI of source-destination and relay-destination channels via the control packets employed by COMAC, and the receive threshold of the diversity receiver is determined by making use of the average BER performance of MRC with the specified modulation schemes under the fading channel, as explained in subsection 3.2.1.

3.3.2 COMAC with Multiple Relays

The COMAC protocol with multiple relays provides a general framework to initiate and actuate cooperative transmissions when specific relay nodes are not explicitly assigned for each source node. The protocol consists of three main stages, namely the cooperation request by the source node, declaration of availability for cooperation by the candidate relays and the cooperative data transmission, which is composed of phases I and II, as depicted in Figure 3.12. As shown in this figure, the source

node sends a C-RTS message to the destination node to initiate cooperative data transmission and to reserve the medium. Although C-RTS message is destined to a specific node, cooperative mode transmission makes the message accessible to every node that can hear it. The C-RTS message has two different uses depending on who receives the message: Any node that receives a C-RTS packet, which is not destined to itself, deduces that the sender requests assistance for an upcoming data transmission, and keeps listening to the channel to hear the response of the intended receiver. The intended receiver (destination) replies back to the source node by sending a C-CTS message, announcing that the medium is reserved for the cooperative transmission of the source node. If a node receives the C-CTS packet without having heard the C-RTS message, it deduces that cooperative transmission will be carried out, and sets its NAV according to the duration field of the C-CTS message.
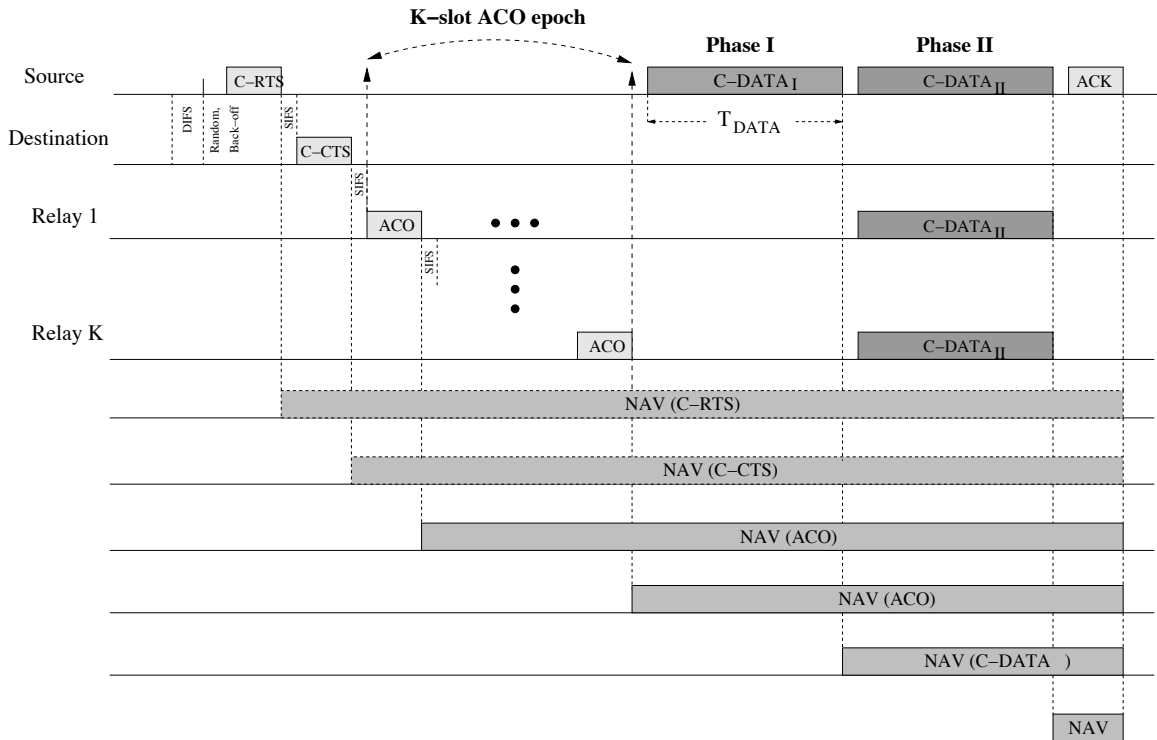
Figure 3.12: Frame exchange and NAV settings for COMAC when cooperation initiation is successful, i.e., at least 1 ACO slot is successful.
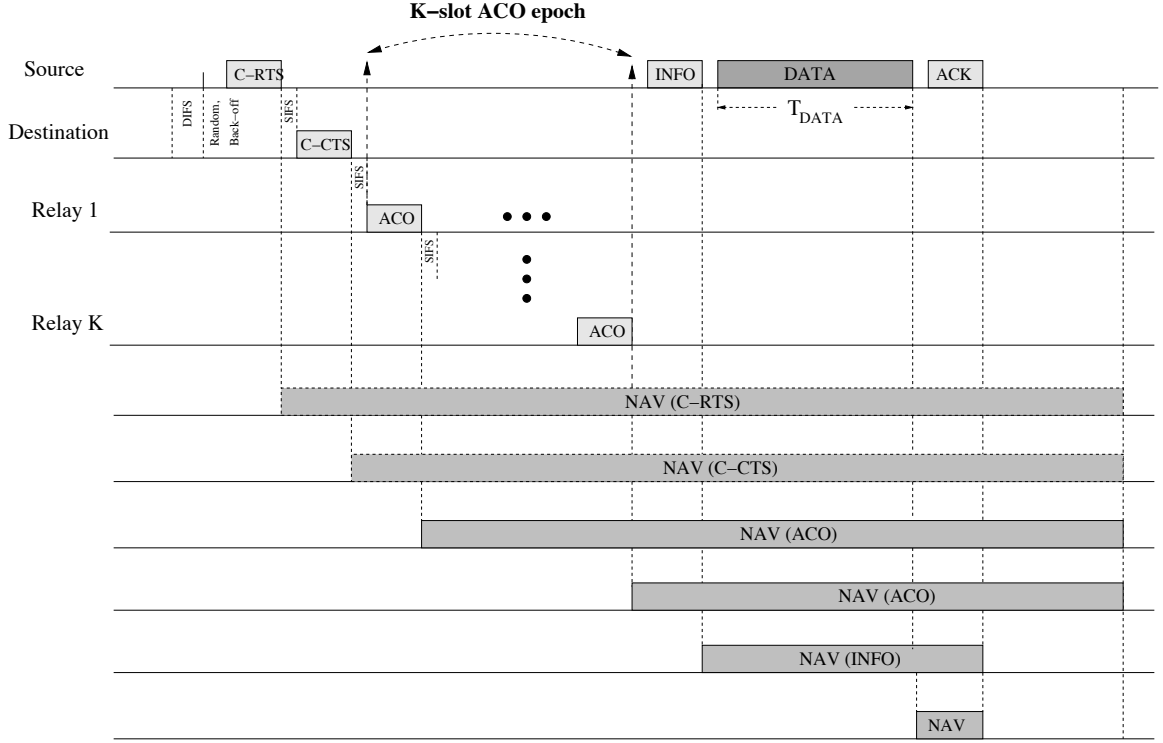
Figure 3.13: Frame exchange and NAV settings for COMAC when cooperation initiation fails, i.e., entire ACO epoch is lost due to collisions or no transmission.

A node that has received both the C-RTS and C-CTS messages is regarded as a candidate relay for the cooperative transmission and $\mathcal{R}$ denotes the set of the candidate relays. A subset from $\mathcal{R}$ is required to form the cooperating node set and actuate the cooperative data transmission. Actuation of individual nodes is explained in the next subsection. A node in $\mathcal{R}$ which decides not to get involved in cooperation sets its NAV according to the duration field of the C-CTS packet, and keeps listening to the channel for any updates about the status of the cooperative transmission. A node that wants to cooperate announces its decision with an ACO message within a predetermined period of time, namely *ACO-epoch*. This duration is calculated as $K(T_{ACO} + T_{SIFS})$, where K denotes the number of ACO transmission slots, and T_{ACO} and T_{SIFS} are the duration of one ACO packet transmission and one SIFS, respectively. Note that the parameter K also limits the number of relays involved in

cooperative transmission.

A node in $\mathcal{R}$ selects its ACO transmission slot randomly, where each slot has equal probability, q_a, for selection. For an ACO-epoch with length K, a node in $\mathcal{R}$, transmits at slot $i, \forall i = 1, 2, ...K$, with probability $q_a = 1/K$. If at least one node can successfully announce its availability to cooperate, the ACO-epoch is regarded as successful and in the upcoming slot the source node disseminates the data packet to the available relay node(s), so that the source and the relay(s) can cooperatively transmit the data packet in the following slot(s). The operation of the protocol in case of a successful ACO-epoch is depicted in Figure 3.12.

ACO transmissions are based on random access so the ACO-epoch is prone to collisions. If none of the ACO slots are successful, the cooperation initiation fails, since retransmissions or collision resolution are not allowed in the ACO-epoch (so as to limit the overhead of ACO-epoch). In such a case of failed cooperation initiation, the source node should revert to direct transmission. Recalling that source reserves the medium for cooperative transmission at the beginning of the control packet exchanges, the failure of the cooperation initiation should be immediately feedback to all nodes so that the period reserved for cooperative transmission is not wasted. For this purpose, we modify the initial COMAC protocol, so that upon a failed ACO-epoch, the source node transmits an INFO message, which has a packet structure similar to the C-CTS packet, for announcing the failure of the cooperation initiation. Figure 3.13 depicts the frame exchange sequence and the NAV updates in case of a failed cooperation initiation. Direct data transmission is done by the source node after an SIFS period of time following the INFO message. The destination node replies back with an ACK message, if data is successfully received. Note that, the NAV update provided by the INFO message decreases the initially reserved packet transmission time by $T_{DATA} - T_{INFO}$.

3.3.3 Relay Actuation

Various relay actuation mechanisms can be incorporated into the general framework of the COMAC protocol, where ACO transmissions can provide not only the nodes' intention for cooperation but CSI as well. Here, we propose and analyze a slotted ALOHA type ACO transmission scheme, namely Random Access Relay Advertisement (RARA) to actuate cooperative transmission. We provide an analysis of the throughput gain that can be obtained with the RARA scheme when all the nodes in the candidate relay set accesses the ACO-epoch with equal probability, and we obtain the optimum ACO transmission probability to maximize the throughput gain with COMAC cooperation.

We denote the probability that a node is actuated, i.e., a node decides to cooperate as q_c. Any node decides not to join the cooperating node set with probability $1 - q_c$, sets its NAV according to the duration designated in C-CTS message. We would now like to find the optimum relay actuation probability, q_c, that maximizes the throughput gain, $\mathcal{T}_G$, provided by COMAC over direct transmission. For a given ACO-epoch length, the throughput gain is given as

$$\mathcal{T}_G = L_D \left[\frac{P_{s,fc}}{T_{fc}} + \frac{P_{s,sc}}{T_{sc}} \right] - L_D \frac{P_{s,d}}{T_d}, \tag{3.3}$$

where throughput obtained by COMAC is represented by the first term and the second term accounts for the throughput of direct transmission. L_D is the length of the data packet in bits. $P_{s,fc}$, $P_{s,sc}$, $P_{s,d}$ are the probability of successful data transmission in case of failed cooperation initiation (fc), probability of successful cooperation initiation (sc) and probability of success in direct transmission (d), respectively. T_{fc}, T_{sc}, T_d, represent the durations of the successful packet transmission for the corresponding cases. These durations are found as follows: $T_d = T_{RTS} + T_{CTS} + T_{DATA} + T_{ACK} + 3T_{SIFS}$, $T_{fc} = T_d + KT_{ACO} + T_{INFO} + (K+1)T_{SIFS}$, and

$T_{sc} = T_{fc} + T_{DATA} - T_{INFO}$. The transmission duration values for RTS, CTS, DATA, ACK, C-RTS, C-CTS, ACO, INFO packets, T_{RTS}, T_{CTS}, T_{DATA}, T_{ACK}, $T_{C\text{-}RTS}$, $T_{C\text{-}CTS}$, T_{ACO}, T_{INFO}, are obtained by dividing the lengths of the respective packet types with the transmission rates of those packets.

Let $P_s(k) = [1 - P_b(\bar{\gamma}, k)]^{\mu}$ denotes the probability that a packet transmitted cooperatively by k nodes is successfully received at the MRC receiver (assuming uniform bit errors and no forward error correction). Note that, $k = 1$ refers to direct transmission, and the probability of success of the direct transmission is given as $P_{s,d} = P_s(1)$. Next, we define the probability that n nodes among N nodes decide to join the cooperating node set as $Q_c(n, N) = \binom{N}{n} q_c^n (1 - q_c)^{N-n}$, where N is the number of nodes in the candidate relay set, $\mathcal{R}$. Also, the success probability of a single slot in the ACO-epoch, when n nodes decide to transmit ACO is $p_s(n) = n q_a (1 - q_a)^{n-1}$. Given the probability of failure of the entire ACO-epoch with length K as $Q_f = [1 - (1 - p_s(n))^K]$, the probability of success in case of failed cooperation initiation, $P_{s,fc}$, can be calculated as:

$$P_{s,fc} = P_s(1) \left[1 - \sum_{n=1}^{N} Q_c(n, N) Q_f \right], \qquad (3.4)$$

since in this case, the source node reverts to direct transmission and probability of successful data packet reception at the receiver is equal to $P_s(1)$.

Defining the success probability of k ACO slots in an ACO-epoch of length K as $Q_a(n, k, K) = \binom{K}{k} (p_s(n))^k (1 - p_s(n))^{K-k}$, the probability of success of the cooperative transmission in case of successful cooperation initiation can be obtained as:

$$P_{s,sc} = \sum_{n=1}^{N} Q_c(n, N) \sum_{k=1}^{K} Q_a(n, k, K) P_s(k + 1). \qquad (3.5)$$

Thus, the throughput gain provided by the RARA scheme can be computed by substituting (3.4), (3.5), and $P_{s,d}$ into equation (3.3). Next, we search for the optimum

q_c that maximizes the throughput gain, i.e., expression (3.3).

For $K = 1$, the single slot ACO-epoch case, the probability of success of the ACO-epoch simplifies to $Q_a = Nq_c(1 - q_c)^{N-1}$, and the probability of success of cooperative transmission in case of failed and successful cooperation initiation is given as $P_{s,fc} = P_s(1)(1 - Q_a)$, and $P_{s,sc} = P_s(2)Q_a$, respectively. Thus, the throughput gain, $\mathcal{T}_G$, for the single slot ACO-epoch case is given as

$$\mathcal{T}_G = L_D \left[\frac{P_s(1)}{T_{fc}} - \frac{P_s(1)}{T_{sd}} + Q_a \left(\frac{P_s(2)}{T_{sc}} - \frac{P_s(1)}{T_{fc}} \right) \right]. \tag{3.6}$$

The expression in (3.6) is maximized when Q_a is maximized, which corresponds to $q_c = 1/N$, and results in $Q_a = (1 - 1/N)^{N-1}$. Note that, as $N \to \infty$, $Q_a \to e^{-1}$, which is the maximum throughput of slotted ALOHA.
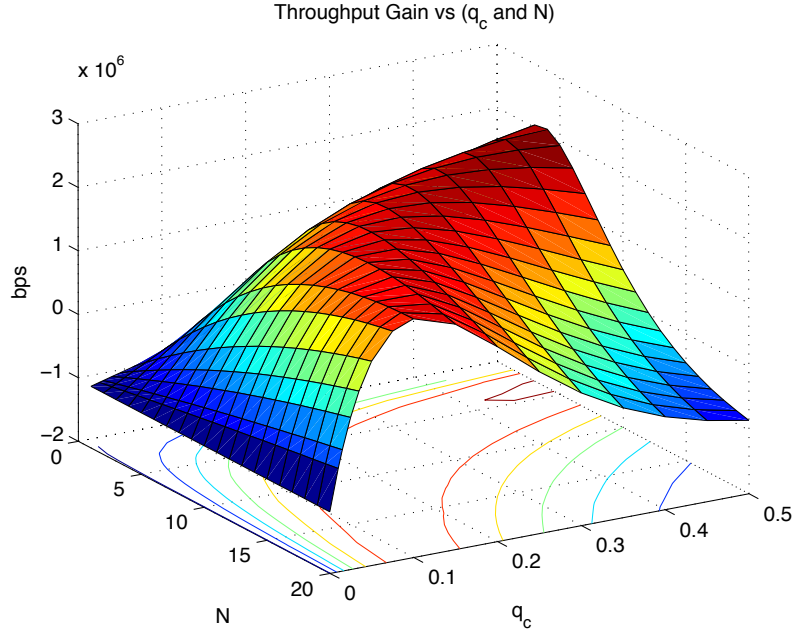
Figure 3.14: Throughput gain, $\mathcal{T}_G$, vs (q_c, N) provided by COMAC with $K = 2$.

For $K > 1$, i.e., the multiple relays case, a closed form solution for q_c that maximizes the expression (3.3) is not available. However, we can obtain family of surfaces as a function of N and q_c for varying K values. Figure 3.14 depicts the surface and the

Table 3.3: Optimum q_c for varying N (number of candidate relays) and K (ACO-epoch length)

K/N	4	8	12	16	20
1	0.25	0.13	0.08	0.06	0.05
2	0.52	0.26	0.17	0.13	0.10
3	0.77	0.39	0.26	0.20	0.16
4	1	0.52	0.35	0.26	0.21

contour diagram for $K = 2$. It is observed that given K and N values, the throughput gain is a convex function of q_c; thus, the optimum value of q_c that maximizes the throughput gain provided by the RARA scheme can be computed numerically. In Table 3.3, we provide the values of the optimum q_c that maximizes the expression (3.3) for varying K and N values. It is seen that for a given K value, i.e., length of ACO-epoch, q_c decreases logarithmically with increasing N, number of candidate nodes, and for a given N value, q_c increases linearly with increasing K.

Successful operation of the RARA scheme requires the knowledge of only two parameters: N, the number of candidate nodes in the vicinity of the source node, and K, the ACO-epoch length. K is a system parameter, and N can be found easily via neighbor discovery methods such as [79]. The values for K and N can be announced by the source node in the C-RTS packet, thus providing the necessary inputs to the candidate relays to compute the relay actuation probability, i.e., q_c.

3.3.4 Performance Evaluation

We have modeled and implemented our COMAC protocol with RARA scheme in ns-2 environment [39]. Our implementation in ns-2 shares the same physical and MAC layer models as described in 3.2.3. Moreover, in COMAC with RARA implementation, the ACO-epoch is incorporated into our model following the descriptions in sections 3.3.2 and 3.3.3. Specifically, each possible cooperator generates a random variable from uniform distribution, and compares this number with the predetermined

71

q_c value. If the generated random variable is smaller than q_c, the node transmits its ACO packet in one of the slots of the ACO-epoch with equal probability.

We evaluate the performance of COMAC with RARA scheme via simulations in ns-2 environment by observing the throughput and energy performance for varying ACO-epoch lengths, K, and relay actuation probability values, q_c. We quantify the performance for realistic scenarios, and also verify the validity of the analytically computed q_c values.
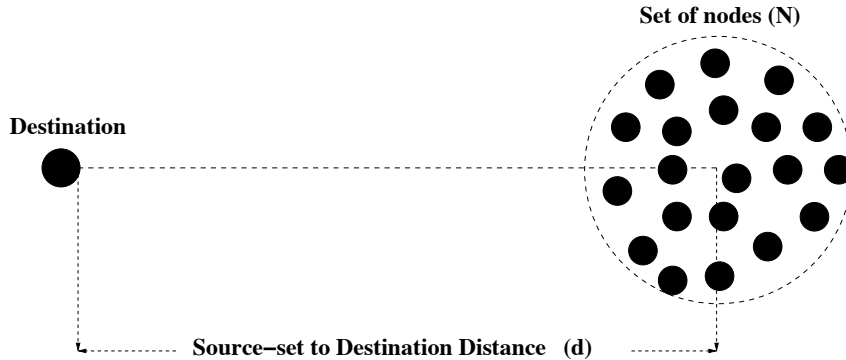
Figure 3.15: A set of nodes residing in a circular region contend for the medium to send their packets to the destination node that is located d meters away from the center of the source-set.

In the simulations, IEEE 802.11g settings are considered for the physical layer and a two ray ground model with path loss exponent of 4 and Rayleigh fading is used to model the wireless channel. We assume slow fading so that channel state does not vary for the duration of one frame exchange, and the MRC receiver obtains the source-destination and the relay-destination channel information by the C-RTS and ACO transmissions, respectively. Data packets of 1024 bytes are transmitted at 54 Mbps, and control packets are transmitted at 6 Mbps. Data packets are transmitted with a power of 1 mW and control packets are sent at 30 mW, and no power control is applied. We evaluate the performance in a multi-point-to-point scenario, where 20 sources inside a circular region of radius 10 m, generate data packets according to a Poisson distribution and they contend with each other to send their data packets

over the fading wireless channel to a destination node located $d = 50$ m away from the center of the circular region, as depicted in Figure 3.15.
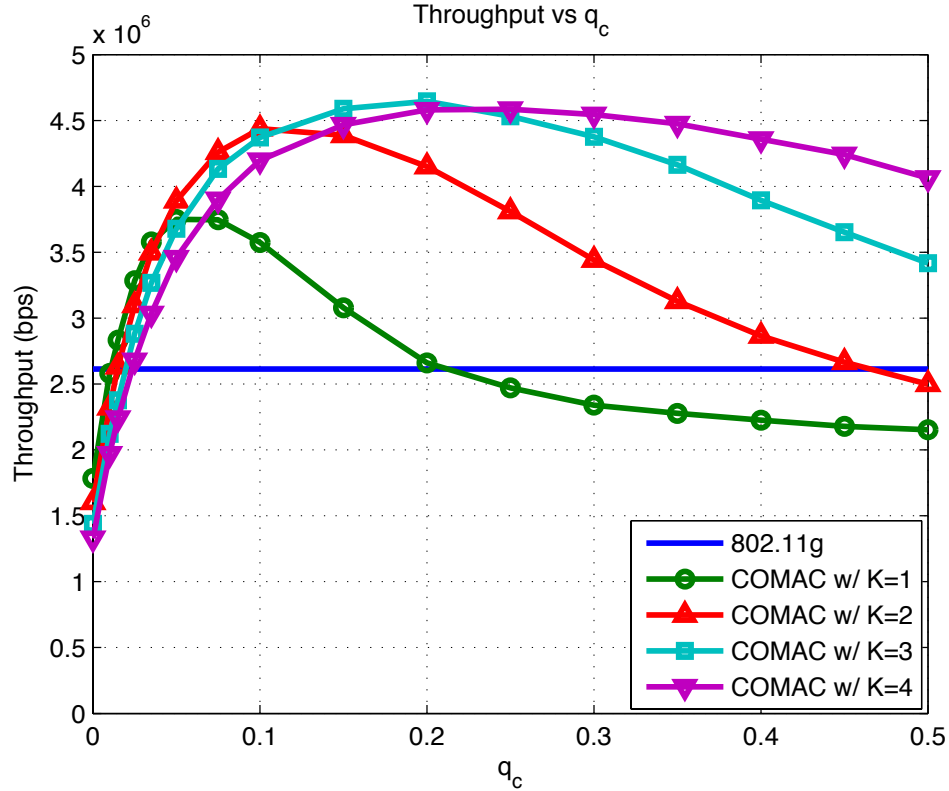
Figure 3.16: Throughput vs q_c for COMAC with RARA scheme, and varying K.

The throughput vs q_c performance of COMAC with the RARA scheme with different ACO-epoch lengths (K) is compared with the direct 802.11g transmission (with RTS/CTS mode on) in Figure 3.16. It is observed that COMAC improves the throughput of the network significantly. As shown in Figure 3.16, COMAC with RARA scheme provides up to 79% improvement in the aggregate throughput for the optimum value of q_c considering the observed K values. It is verified in Figure 3.16 that the optimum value of q_c which is obtained via simulations is consistent with the analytically obtained q_c values which are provided in Table 3.3. Note that, the throughput gain is increased with increasing K for $K \leq 3$, and an ACO-epoch longer than 3 slots does not improve the throughput performance further, but degrades the

performance. This is due to the increased overhead imposed by the longer ACO-epoch. The probability of collisions during the ACO-epoch is decreased by using longer ACO-epochs; however the increased probability of success does not pay off unless the throughput gain provided by adding an extra node into the cooperating node set is greater than the overhead introduced by increasing the ACO-epoch length.
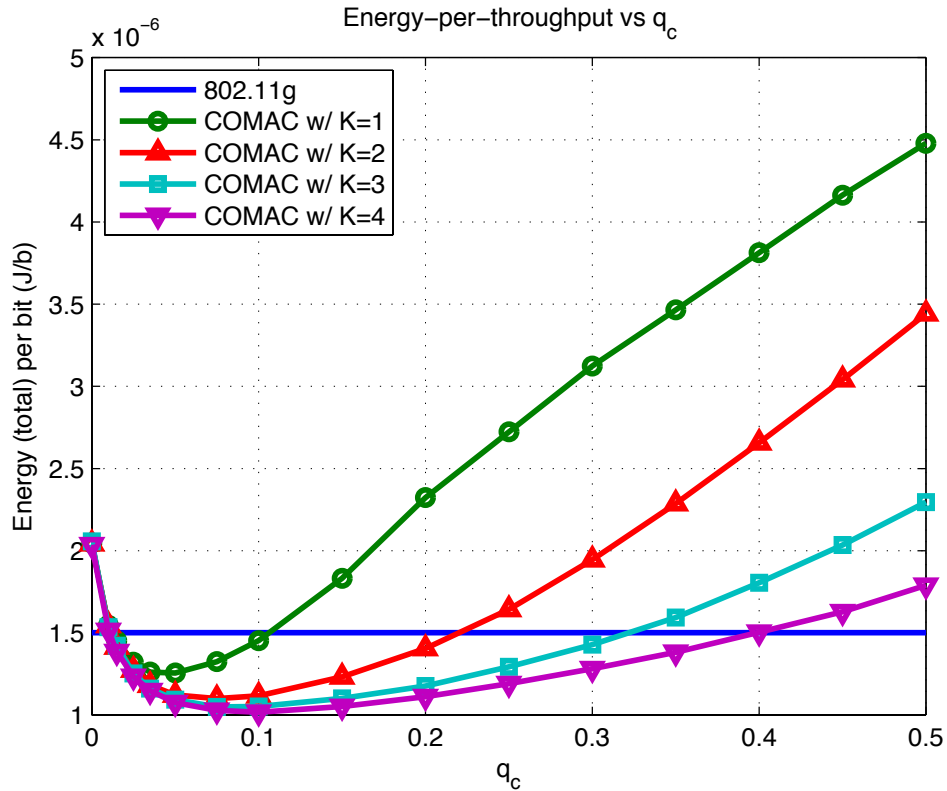
Figure 3.17: Energy-per-throughput vs q_c for COMAC with RARA scheme.

Next, we evaluate the energy-efficiency performance of COMAC with RARA scheme. Energy-efficiency is observed by defining *energy-per-throughput*, which is the energy consumed in the system for successful transmission of one data bit to the destination. We model the energy consumption for transmitting a packet as $E_t = (P_c + P_t)T$ and for receiving a packet as $E_r = P_cT$, respectively, where T designates the packet duration. P_t refers to power consumption at the transmit amplifier. The power consumption at the transmit circuitry and the receive circuitry

are assumed to be equal [78] and denoted as P_c. Figure 3.17 depicts the energy-per-throughput performance of the COMAC protocol with different ACO-epoch lengths as compared to direct 802.11g for the above test scenario using $P_c = 250$ mW, as in [78]. For direct transmission, the transmission of one bit of data packet and successful reception at the destination node results in an average energy consumption of 1.5 $\mu J/b$ in the network. COMAC with RARA scheme reduces this energy consumption by 17%, 27%, 30%, 32%, when $K = 1, 2, 3,$ and 4, respectively as shown in Figure 3.17. The improvements in the energy savings provided by the cooperative scheme is lower than the gains in the aggregate throughput. This is because of the fact that, in the cooperative scheme all the nodes in the vicinity of the source node keeps listening to the channel, which also consumes energy and degrades the energy efficiency. Despite the overhead, it is worthwhile to note that COMAC schemes still provide significant energy savings over the direct transmission.

In an effort to investigate the effect of the transceiver circuitry energy consumption (P_c) in the energy efficiency of the system, in Figure 3.18, we have obtained the maximum energy savings provided by the COMAC protocol with optimum q_c setting over direct transmission considering varying circuit power consumption values (P_c) and keeping the transmit power level the same (i.e., $P_t = 1$ mW for data transmission), and different ACO-epoch lengths, K. We observe that the degree of the energy savings provided by the COMAC protocol becomes independent of the transceiver circuitry power consumption as the power consumed at the transmit amplifier becomes much less than the power consumed at the transceiver circuitry.

As observed in Figure 3.16 and Figure 3.17, length of the ACO epoch plays an important role in the performance of the COMAC RARA scheme. The longer the ACO-epoch, the smaller the probability of having collisions during the ACO-epoch, thus increasing the probability of successful cooperation initiation and leading to more
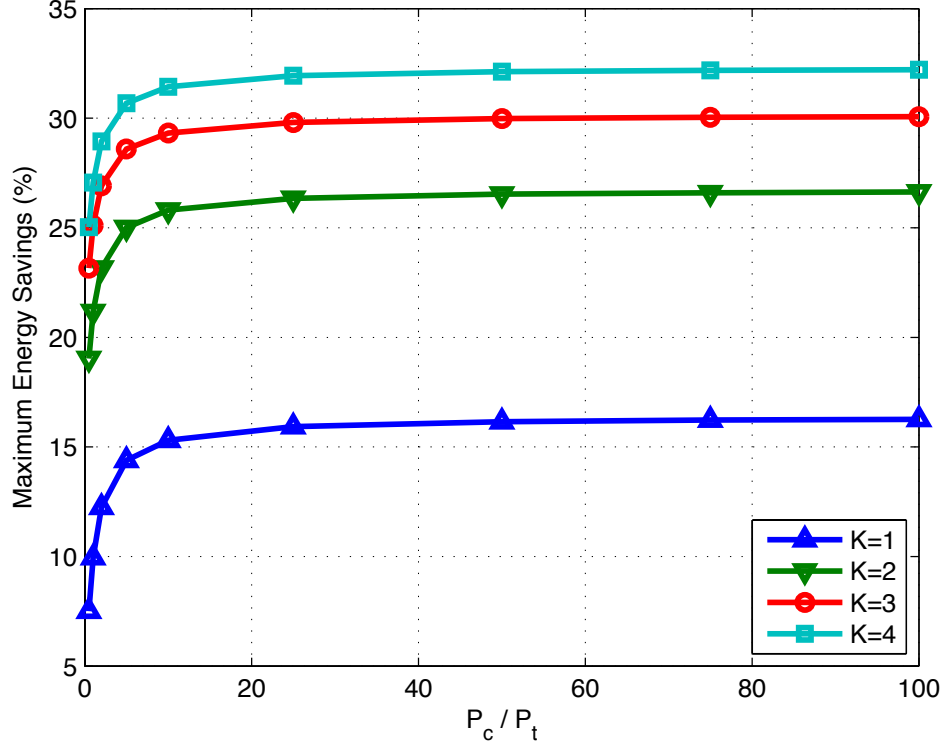
Figure 3.18: Percentage of maximum energy savings provided by COMAC for varying circuit energy consumption values and for optimum q_c.

robust transmissions. It is seen that COMAC RARA scheme can perform worse than direct transmission for certain q_c values depending on the values of K and N. It is worthwhile to note that the energy-efficiency performance of COMAC RARA scheme is more sensitive to the changes in q_c than the throughput performance, especially for smaller K values, which is due to the additional reception and transmission energy cost induced by the ACO-epoch. Our simulations show that the energy savings and the throughput improvements provided by the COMAC RARA scheme increases further as the source to destination separation is increased, which is due to the robust long haul transmissions made available by cooperation, as also validated in section 3.2.

The COMAC protocol with multiple relays provides a general framework, in which

new relay selection metrics can be incorporated for realizing multi-node cooperation in WSNs. In the next section, we propose and analyze multi-node cooperative scheme within the context of a slotted ALOHA system.

3.4 Cooperative Slotted ALOHA: C-ALOHA

In a wireless network, transmission errors occur either due to packet collisions or due to channel fading/noise. Recently in [80], a practical technique is presented for differentiating collisions and channel errors. We exploit the collision/error differentiation capability presented in [80], and we propose and analyze slotted ALOHA [81] based random access scheme, C-ALOHA, which enables cooperative transmissions in case of erroneous packet receptions to provide robustness to channel errors and improve the packet success probability.

In C-ALOHA, initial transmission of a packet is carried out as in the slotted ALOHA system. We assume that the receiver recognizes whether packet transmission failure is due to a collision or channel noise, and sends immediate *collision* or *error* feedbacks, respectively. In case of an *error* feedback, cooperative transmissions are invoked, so that some of the nodes that have correctly overheard the transmission can retransmit together with the source node in the next slot. Consequently, the packet success probability is improved and the number of retransmissions is decreased significantly as compared to a non-cooperative system.

This section is organized as follows. In section 3.4.1, we describe our system model. We introduce and analyze our C-ALOHA protocol in section 3.4.2. The performance analysis is provided in section 3.4.3.

3.4.1 System Model

We consider a wireless network of m nodes, where nodes transmit over a Rayleigh fading channel to a single receiver employing MRC. Packets arrive for transmission at each node according to an independent Poisson process with overall rate of λ, i.e., with rate λ/m at each transmitting node. Each packet is of equal size and requires one time slot for transmission. All transmitters are assumed to be synchronized, and reception of each packet starts at an integer time and ends before the next integer time as assumed in the analysis of slotted ALOHA in [82]. We also assume that at the end of every slot, each node obtains immediate feedback from the receiver through an error-free channel specifying whether: 1) the slot was *idle* (i), 2) a transmission occurred but the packet could not be successfully decoded due to *error* (e), 3) multiple transmissions resulted in *collision* (c), 4) a packet was received *success*fully (s). Error-free feedback can be approximated by applying error control coding to the feedback packet. Furthermore, although not essential for correct protocol operation, immediate feedback is assumed to simplify the analysis.

In cooperative networks, the nodes that have correctly overheard the source transmission may cooperate with the source by retransmitting the overheard packet to the receiver, so that the receiver can be provided with multiple copies of the same signal, resulting in diversity gain. We quantify the improvement in successful packet reception probability due to cooperative transmission for varying number of cooperating nodes, when BPSK modulation is employed. The approach followed here does not depend on the modulation scheme and any modulation scheme can be used instead of BPSK.

The average BER, $\bar{P}_b$, under Rayleigh fading for the BPSK receiver with k-branch diversity using MRC is given by [1] $\bar{P}_b(\bar{\gamma}, k) = \frac{1}{\pi} \int_0^{\pi/2} \left(1 + \frac{\bar{\gamma}}{sin^2\phi}\right)^{-k} d\phi$, where $\bar{\gamma}$ refers to the average SNR per link, and k denotes the number of cooperating nodes. Assum-

ing uniform bit errors and no forward error correction, the success probability of a μ bit packet can be obtained as $P_s(k) = [1 - \bar{P}_b(\bar{\gamma}, k)]^\mu$, and the probability of packet error as $P_e(k) = 1 - P_s(k)$. Channel SNR is assumed to be estimated at the receiver for each node-receiver link, and to remain constant for a time slot. Synchronization among transmitting nodes can be provided via techniques such as [83], and in case of imperfect synchronization, one of the methods reviewed in [29] can be employed so that full diversity gain can still be achieved.

3.4.2 Analysis of C-ALOHA

In this subsection, we present the throughput analysis of the C-ALOHA protocol in detail. We assume that each node has two separate buffers, and each buffer is assumed to be of one packet size for analysis purposes. Each generated packet directly goes to buffer B_1; discarded if B_1 is full or stored otherwise. A transmitted packet is kept in B_1 until success feedback is received. All nodes in the network overhears the transmission of other nodes. In case a packet is correctly overheard, it is stored in buffer B_2, replacing the current packet in B_2. Otherwise, B_2 is emptied. Thus, B_2 always stores the correctly overheard packet in the previous slot. When the intended receiver sends an e feedback, each node that correctly overheard the transmission independently transmits the packet in B_2 with probability q_c. In case of a c feedback, each node independently transmits the packet in B_1 with probability q_r.

We define the state of the system with respect to the total number of backlogged packets in the network, i.e., total number of packets in B_1. The probability that a packet arrives at a node in x slots is $q_a(x) = 1 - e^{x\lambda/m}$. We assume that each new arrival is not directly transmitted but backlogged. When the system is at state n, a successful packet reception occurs with probability $P_n(s)$, which can be written by

conditioning on the feedback from the receiver as

$$P_n(s) = P_n(s|f_c)P_n(f_c) + P_n(s|f_i)P_n(f_i) + P_n(s|f_e)P_n(f_e) + P_n(s|f_s)P_n(f_s), \quad (3.7)$$

where $P_n(f_c)$, $P_n(f_i)$, $P_n(f_e)$, $P_n(f_s)$ refer to the probability that c, i, e, s feedbacks are received at state n. These probabilities are also interpreted as the probability that *collision* occurred in the previous slot, the previous slot was *idle*, *erroneous* or *success*, respectively. First, we derive $P_n(s)$ for ALOHA considering channel errors, and then, derive $P_n(s)$ for C-ALOHA.

3.4.2.1   ALOHA

The probability of successful transmission at state n is independent of the received feedback, but only dependent on the current state. Therefore, the probability of success given the feedback, is same for each feedback, i.e., $P_n(s|f_i) = P_n(s|f_e) = P_n(s|f_c) = P_n(s|f_s) = nq_r(1 - q_r)^{n-1}P_s(1)$.

Let n be the number of backlogged nodes at an arbitrary time t_0. The system can be at any state between 0 and n in the previous slot, $t_0 - 1$, depending on the number of packet arrivals during that slot. Assuming that packets arrive at the system at the end of each slot, we define the probability that j arrivals occurred in x slots in transition to state n as $Q_{a,x}(n, j) = \binom{m-(n-j)}{j}q_a(x)^j(1 - q_a(x))^{m-n}$. Also, probability that k nodes choose to transmit packets in the previous slot, $t_0 - 1$ is $Q_r(n, j, k) = \binom{n-j}{k}q_r^k(1 - q_r)^{n-j-k}$, where q_r is the probability that a node transmits the packet in B_1. Having quantified $Q_{a,x}$ and Q_r, we can give the probability of

receiving i, c, s, e feedbacks when the system is at state n.

$$P_n(f_i) = \sum_{j=0}^{n} Q_{a,1}(n,j)Q_r(n,j,0), \tag{3.8}$$

$$P_n(f_c) = 1 - P_n(f_i) - \sum_{j=0}^{n} Q_{a,1}(n,j)Q_r(n,j,1), \tag{3.9}$$

$$P_n(f_s) = \sum_{j=0}^{n} Q_{a,1}(n,j)Q_r(n,j,1)P_s(1), \tag{3.10}$$

$$P_n(f_e) = \sum_{j=0}^{n} Q_{a,1}(n,j)Q_r(n,j,1)P_e(1), \tag{3.11}$$

where $P_s(1)$ and $P_e(1)$ refer to the success and error probabilities of a single node transmission over a noisy fading channel, respectively. The intuition behind the derivation of (3.8), (3.9) and (3.10) are the same in the analysis of slotted ALOHA [82]. However, (3.11) is derived by noting that error feedback is received when there is a single transmission but it is corrupted due to channel noise.

3.4.2.2 C-ALOHA

The operation of the C-ALOHA system would be best explained by describing the response of the system to each feedback. In case of i, c and s feedbacks, each node transmits its packet in B_1 with probability q_r. However, in case of an e feedback each node that has correctly overheard the source packet transmits the packet in B_2 together with the source node in the upcoming slot with probability q_c. Note that, the first occurrence of e feedback is always after a single node (direct) transmission, whereas the following occurrences can be after either a direct or a cooperative transmission. It can be easily shown that the probability of receiving an i and a c feedback are still given by (3.8), (3.9), respectively. The success probability given c, i and s feedback is $P_n(s|f_c) = P_n(s|f_i) = P_n(s|f_s) = nq_r(1-q_r)^{n-1}P_s(1)$, since after collision,

idle and success events C-ALOHA operates in the same way as ALOHA.

In case of an e feedback, the probability of success depends on whether or not cooperation is invoked. A packet may be received successfully after multiple erroneous trials, which may involve either cooperative or direct transmissions. We define the period between the first occurrence of the e feedback and the time s feedback is received as an *error epoch*. An error epoch may consist of multiple erroneous transmissions but can have only one successful transmission, which also designates the end of the error epoch. Let $Q_h(t)$ represent the probability that t nodes correctly overhear the source packet, $Q_h(t) = \binom{m}{t} P_s(1)^t P_e(1)^{m-t}$, and $Q_c(t,k)$ represent the probability that k out of t nodes choose to involve in cooperation, and the cooperative packet transmission is successful $Q_c(t,k) = \binom{t}{k} q_c^k (1-q_c)^{t-k} P_s(k+1)$.

A transmission may be successful without requiring cooperation, in which case error epoch has length 1. The probability of having an error epoch of length 1 is $P(l=1) = \sum_{j=0}^{n} Q_{a,1}(n,j) P_s(1)$. For $x \geq 2$, in order to simplify the analysis we assume that once a set of nodes chooses to cooperate with a source node, the same set of nodes continue to retransmit the packet until the end of the error epoch. Then $P(l=x)$ for $x \geq 2$ can be given

$$P(l=x) = \sum_{j=0}^{n} Q_{a,x}(n,j) P_e(1) \sum_{t=1}^{m} Q_h(t) \sum_{k=1}^{t} Q_c(t,k) P_e(k+1)^{l-2}$$

$$+ \sum_{j=0}^{n} Q_{a,x}(n,j) P_e(1) \sum_{t=0}^{m} Q_h(t) (1-q_c)^t P_s(1). \tag{3.12}$$

In the derivation of (3.12), we differentiate among the cases of cooperation and direct transmission employed within the epoch. The expected length of an error epoch is $E\{L\} = \sum_{x=1}^{\infty} x P(l = x)$. The proportion of time the system is in error epoch is $1 - P_n(f_i) - P_n(f_c)$. Since only one out of $E\{L\}$ slots is a success, by renewal-reward

theory the probability of receiving s feedback can be given as

$$P_n(f_s) = \frac{1}{E\{L\}} \left[1 - P_n(f_i) - P_n(f_c)\right].$$

(3.13)

Furthermore, $P_n(f_e)$ is also equal to $1 - P_n(f_s) - P_n(f_c) - P_n(f_i)$, and $P_n(s|f_e)$ is

$$P_n(s|f_e) = \sum_{t=1}^{m} Q_h(t) \sum_{k=1}^{t} Q_c(t,k) + \sum_{t=0}^{m} Q_h(t) \left(1-q_c\right)^t P_s(1),$$

where the first and second terms represent the probabilities of success with cooperative transmission and direct transmission, respectively. Thus, the probability of successful transmission in C-ALOHA can be determined by (3.7).

3.4.3 Numerical Results
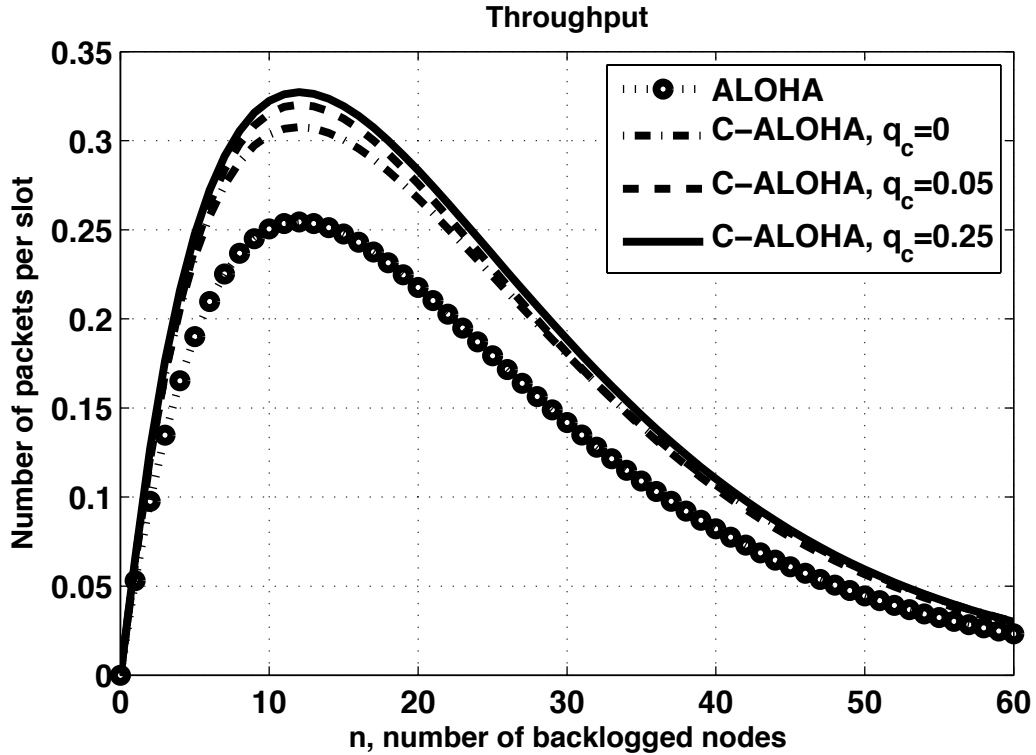
Figure 3.19: Throughput of C-ALOHA for varying number of backlogged nodes.

In this subsection, we compare the throughput of C-ALOHA with slotted ALOHA over a noisy fading channel. We consider i.i.d. node-receiver links, with Rayleigh fading, average SNR of 25 dB, and coherence time equal to a time slot. The packet size is set as 512 bits. The throughput is calculated for varying number of backlogged nodes and different q_c as depicted in Figure 3.19. It is clearly seen that ALOHA suffers from the channel errors, and the maximum throughput is decreased dramatically to 0.255. C-ALOHA reaches a maximum of 0.33 under the same channel conditions, slightly below the maximum throughput of slotted ALOHA in error-free channel (0.367). It is observed that the maximum throughput of slotted ALOHA can be improved by 20% by enabling error detection capability and immediate source retransmission upon error feedback. This corresponds to C-ALOHA with no cooperating nodes, i.e., $q_c = 0$. User cooperation provides a further 10% increase in the throughput, and thus, resulting in a 30% increase in the maximum throughput of slotted ALOHA. Note that, for a given channel state and network of size m, there is a q_c value below which the system is underutilized, and above which the throughput can not be increased further. This is due to the fact that for a given channel state the cooperative transmission is almost always successful when the number of cooperating nodes is above a certain number, and adding additional nodes in the cooperating set does not provide any further gain.

In Figure 3.20, we investigate the effect of average SNR on the throughput and the q_c value, when the network size, m, is 10. It is observed that as the channel quality degrades q_c value is needed to be increased to improve the packet success probability. This is because of the fact that as the channel degrades larger number of cooperating nodes, i.e., larger number of diversity branches, are required so that transmitted packet can be successfully received at the MRC receiver.
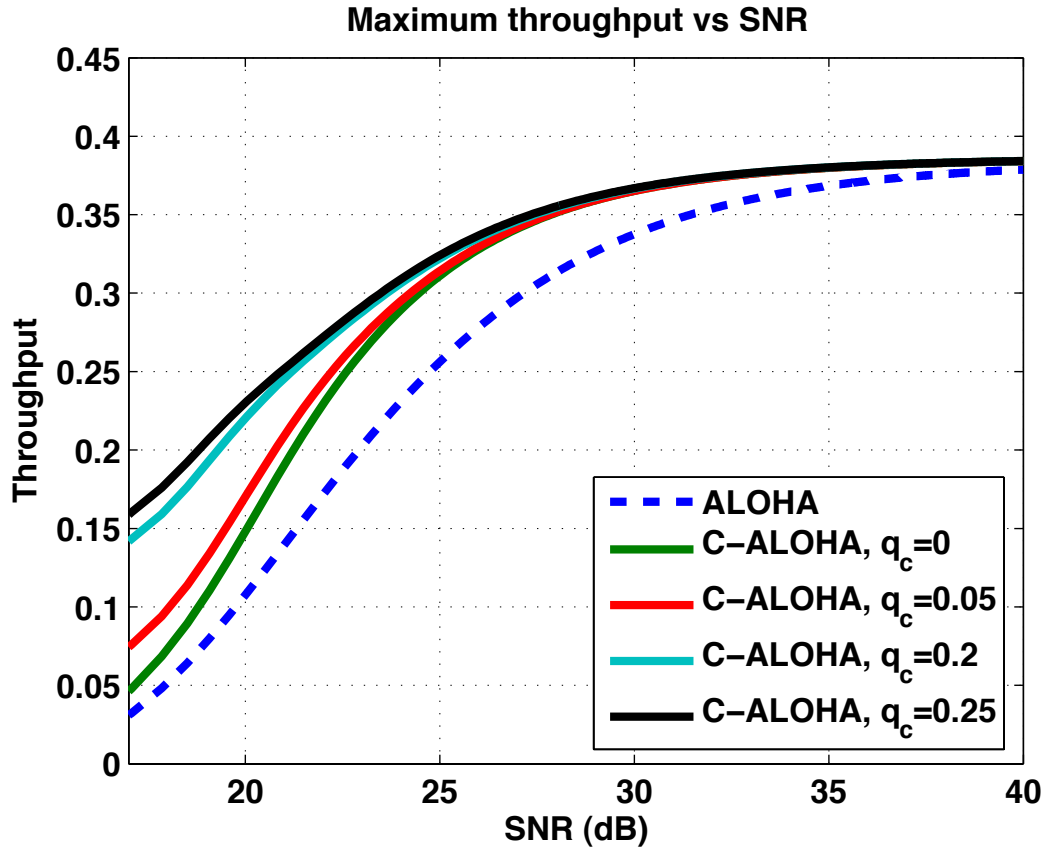
Figure 3.20: Throughput of C-ALOHA for varying SNRs

3.5 Discussion

In this chapter, we have presented two cooperative MAC protocols, COMAC and C-ALOHA. Through COMAC, which is CSMA based, we have demonstrated and quantified the throughput and energy gains that can be achieved by cooperative transmission in a WSN. It is shown that the amount of performance improvement depends on the transmission range, data rate and components of energy consumption. Despite the introduced overhead and extra transmissions, cooperative transmission via the COMAC protocol is proven to provide significant throughput enhancements in both point-to-point and multi-point-to-point scenarios, especially for medium to long range transmission. For the same transmission ranges, energy savings of about

50 percent is obtained, irrespective of increased number of users or circuit energy consumption.

We have also proposed and analyzed a distributed relay selection and actuation scheme based on random access relay advertisements for our COMAC protocol. The proposed scheme renders simple distributed operation, which makes it suitable especially for densely deployed WSNs. We have evaluated the throughput performance of COMAC with relay selection through analytical derivation and ns-2 simulations, and we have also observed the energy efficiency. The results are promising as significant throughput enhancements, of up to 79% and energy savings of up to 32% are observed over direct transmission. The COMAC protocol with multiple relays provides a general framework, in which new relay selection metrics can be incorporated for realizing cooperation in WSNs.

We have also presented a cross-layer random access method that incorporates cooperative transmissions into the well known ALOHA system. We have derived analytical expressions for the successful packet transmission probability for this protocol and analyzed the effect of random cooperation decision on the system performance. We have shown that by exploiting the robustness of cooperative transmissions against channel impairments, the throughput of the ALOHA system in a noisy fading channel can be improved by 30%.

The degree of the performance improvement provided by the cooperative transmission depends on the channel conditions of the nodes participating in cooperation. Intelligent methods for selecting the most appropriate relays among many possible candidates and allocating the resources among the possible relays optimally can further improve the system performance. In the following chapter, we study incorporating channel state information into the relay selection mechanism, rather than relying merely on random relay decisions. We consider optimal cooperation set formation

while system parameters, such as transmit powers of relay nodes, are optimized such that a predetermined level of reception quality is guaranteed, i.e., a predetermined average BER level is maintained.

The results of this chapter have been presented and published in [84–86].

4 OPTIMAL COOPERATOR SELECTION AND POWER ASSIGNMENT

In this chapter, we consider the energy minimal joint cooperator set selection and power assignment problem in a cooperation scenario with multiple relays, under transmit power constraints, while satisfying a realistic metric, target average BER at the destination receiver. We first derive the average BER of a cooperative system with multiple relays, and propose a simple, yet close approximation to the BER. Our BER approximation facilitates a tractable joint solution for our problem, resulting in Optimal Cooperator Selection and Power Assignment (O-CSPA) algorithm, which involves the selection of the best cooperator set and closed form solutions for the optimal power levels for the cooperators. O-CSPA requires centralized operation, entailing extra bandwidth and complexity costs, due to the need of exchanging and considering channel states for all involved nodes. Hence, next we study the properties of the optimal solution, and we propose a distributed method, namely Distributed Cooperator Selection and Power Assignment (D-CSPA) algorithm, in which the relays can individually decide to become a cooperator and they can determine their power levels themselves. We evaluate the performance of O-CSPA and D-CSPA algorithms considering several network topologies, varying target BER levels and different power consumption models, by taking into account the energy dissipated in the transceiver circuits and amplifiers of all involved nodes.

This chapter is organized as follows. In Section 4.1, we provide a summary of the related work from the literature. In Section 4.2, we describe our system model, including cooperation and energy consumption models. In Section 4.3, we provide the problem formulation, we derive the average BER of the cooperative system and

its approximation and we present the joint optimal solution for cooperator selection with power assignment, namely O-CSPA. In Section 4.4, we introduce our distributed approach and algorithm, D-CSPA, and we describe the implementation of D-CSPA embedded in the COMAC protocol [84, 85], described in the previous chapter. Performance analysis is provided in Section 4.5, followed by our conclusions in Section 4.6.

4.1 Related Work

The degree of performance improvement due to cooperative diversity is determined by the channel states of the cooperators. Selection of appropriate cooperators and resource allocation among those cooperators are intrinsically connected problems, solution of which is essential in exploiting cooperative diversity.

In the literature, energy efficient cooperator selection and power allocation have been studied via different approaches: In [14], Chen *et al.* study the optimum distributed power allocation strategy that minimizes total transmit power while providing a target instantaneous SNR at the destination with a target outage probability for a DF system. Zhao *et al.* [15] investigate optimal power allocation for an AF system, and Li *et al.* [17] explore transmit power allocation strategies for multiple relays considering SNR upper bounds to maximize instantaneous SNR at the destination for AF and DF systems. These schemes require the knowledge of instantaneous CSI for all the links that are involved in cooperation, introducing significant overhead, which can obliterate the benefits of cooperative diversity, as shown in [18]. As a means to reduce the burden of exploiting instantaneous CSI, in [19] and [20], the authors minimize the outage probability based on average CSI, in [21–23], the authors study optimal power allocation and cooperator selection based on the average BER criterion.

A major drawback of the works in [14, 15, 17–23] is that cooperator selection is implicitly carried out by the power allocation process, where nodes assigned with power levels greater than zero get involved in cooperation. This selection strategy may end up acquiring too many cooperators for the sake of improving diversity gain and reducing total transmit power, but the overhead and energy consumed for actuating the cooperators are totally ignored. Some distributed selection mechanisms try to avoid this problem by using a fixed number of relays [21–23] or by simplifying selection [24, 25, 27]. [25] analyzes a distributed method based on instantaneous CSI to select the single best cooperator from a set of multiple available relays, [27] employs a threshold method based on instantaneous SNR for multiple cooperator selection in a DF system, and [24] studies a distributed buyer/seller game theoretic framework with power allocation based on instantaneous channel measurements. Last but not least, the existing schemes [14, 15, 17–25, 27] merely impose a constraint on total transmit power and disregard the individual transmit power constraints. However, sensor nodes are each constrained by maximum transmit power levels due to hardware limitations. Furthermore, in the existing schemes the transceiver circuitry energy cost of the cooperators is totally neglected, so they fail to address the energy cost of cooperation its entirety.

BER is advantageous in terms of evaluating the overall performance of cooperative systems, however the major disadvantage of BER-based optimization is its complexity that requires the multi-relay optimization problems to be solved numerically at a central node and that does not allow closed form power allocation solutions [21–23]. A simple yet close approximation to the average BER can facilitate distributed solution for relay selection and power allocation.

4.2 System Model

We consider a source-destination (SD) pair, and a neighbor node set $\mathcal{N}$ of N nodes ($R_i, i = 1, ..., N$), as depicted in Figure 3.11. We define the "best" cooperation set, out of all possible subsets of $\mathcal{N}$, as the set of nodes that minimizes the total energy consumed for successfully transmitting one source bit to the intended destination at a desired target average BER level. In order to form such an energy-minimizing reliable cooperation set, one needs to optimally determine: (i) how many cooperators are required, (ii) which cooperators should be used, (iii) how much resource should be assigned to each cooperator, to achieve the required level of reliability. These problems are intrinsically connected, so they have to be solved simultaneously. Next, we present our cooperation model and energy consumption model that incorporates these intrinsically connected subproblems.

4.2.1 Cooperation Model

A cooperation set is looked upon for an SD pair when the direct channel between the source and its intended destination cannot be relied on for direct transmission. We presume that if the direct link between the SD pair provides the required level of reliability, cooperation is not required. Neighboring nodes in $\mathcal{N}$ can be arranged in $2^N - 1$ different possible cooperation sets to help the source. Let us consider the possible sets with r cooperators, which makes up $\binom{N}{r}$ different sets. Let $\mathcal{C}_{r,j}$ be the jth cooperation set with r relays such that $j = 1, 2, ..., \binom{N}{r}$, and r denotes the cardinality of the cooperation set, i.e., $r = |\mathcal{C}_{r,j}|$, and $r = 1, \ldots, N$. As an example, $\mathcal{C}_{1,1} = \{R_1\}$, $\mathcal{C}_{1,2} = \{R_2\}$, ..., $\mathcal{C}_{1,N} = \{R_N\}$, and likewise $\mathcal{C}_{2,1} = \{R_1, R_2\}$, $\mathcal{C}_{2,2} = \{R_1, R_3\}$, ..., $\mathcal{C}_{2,\binom{N}{2}} = \{R_{N-1}, R_N\}$.

The cooperative system considered in this work has two phases: In phase 1, S transmits its signal with an energy-per-bit level of E_b Joules/bit. We assume that the

nodes that receive the source transmission with a power level that is above a hardware determined receive threshold can successfully decode-and-regenerate the source signal. In phase 2, the nodes in the selected cooperation set, say $\mathcal{C}_{r,j}$, cooperatively transmit the decoded-and-regenerated signal to D through orthogonal channels using CDMA. While cooperatively transmitting, we assume that the cooperators in $\mathcal{C}_{r,j}$ can adjust their transmit power levels, such that each cooperator uses a transmit energy level of $\rho_{r,j}(i)E_b$ J/b, where $\rho_{r,j}(i)$ denotes the relay's relative power level with respect to the power level of the source, $0 \leq \rho_{r,j}(i) \leq 1$, $\forall R_i \in \mathcal{C}_{r,j}$. The cooperation set, $\mathcal{C}_{r,j}$, is assigned a power vector, $\boldsymbol{\rho}_{r,j}$, where each entry is the relative power level of the corresponding cooperator. For instance, considering the set $\mathcal{C}_{3,1} = \{R_1, R_4, R_7\}$, the power vector is obtained as $\boldsymbol{\rho}_{3,1} = [\rho_{3,1}(1)\ \rho_{3,1}(4)\ \rho_{3,1}(7)]$.

We assume that the direct and neighbor channels, namely SD, SR_i and R_iD channels (from Figure 3.11), undergo independent Rayleigh fading with coefficients f, g_i and h_i, respectively. The mean channel gains for these channels are obtained as $E[|f|^2] = \sigma_f^2$, $E[|g_i|^2] = \sigma_{g_i}^2$ and $E[|h_i|^2] = \sigma_{h_i}^2$, respectively, where $E[\cdot]$ denotes expectation. We assume that the additive white Gaussian noise at all channels have equal variance, N_0. The instantaneous SNR of the transmitted signal by the source, observed at node R_i is $\gamma_{g_i} = \frac{E_b}{N_0}|g_i|^2$, and observed at the destination is $\gamma_f = \frac{E_b}{N_0}|f|^2$. Likewise, the instantaneous SNR of the transmitted signal by cooperator R_i at the destination is $\gamma_{h_i} = \rho_{r,j}(i)\frac{E_b}{N_0}|h_i|^2$. In this work, we assume that the channel statistics are available in terms of the average SNRs of SD, R_iD and SR_i channels, which are given as $\bar{\gamma}_f = \frac{E_b}{N_0}\sigma_f^2$, $\bar{\gamma}_{h_i} = \rho_{r,j}(i)\frac{E_b}{N_0}\sigma_{h_i}^2$ and $\bar{\gamma}_{g_i} = \frac{E_b}{N_0}\sigma_{g_i}^2$, respectively. Here, we define relative measures for ease of notation such as: $\delta_i \triangleq \sigma_{h_i}^2/\sigma_f^2$ and $\eta_i \triangleq \sigma_{g_i}^2/\sigma_f^2$, and obtain the average SNR of R_iD and SR_i channels as $\bar{\gamma}_{h_i} = \rho_{r,j}(i)\delta_i\bar{\gamma}_f$ and $\bar{\gamma}_{g_i} = \eta_i\bar{\gamma}_f$, respectively.

Note that, the analysis carried out in this work is valid for both when transmissions

are uncoded, and when orthogonal space time block codes (STBC) are employed. In the case of STBC, the destination node, D, with the knowledge of the complex channel fading coefficients between the source-destination (SD) and cooperator-destination (R_iD) channels, can linearly combine the multiple signals to recover the symbols; and in case of uncoded cooperative transmissions, D can combine the signals received in phase 1 and phase 2 using a MRC and can perform detection based on the combined signal.

4.2.2   Energy Consumption Model

In order to thoroughly investigate the energy-efficiency of cooperation, in our energy consumption model, we take into account the energy dissipated at the transmitter and receiver circuitries of all the nodes that participate in the cooperative transmission in addition to their transmit amplifier energy consumptions. For the transmitter and receiver circuitries, energy cost per bit can be calculated as $E_t = w_t/r_b$, $E_r = w_r/r_b$, respectively. w_t and w_r are the power consumption of the transmitter and the receiver circuitries, respectively, and r_b is the transmission bit rate. We assume that all the nodes in the network are identical in their circuitries, i.e., w_r, w_t and r_b are the same for all nodes. Each node transmits at a constant bit rate of r_b, with no rate adaptation.

In the previous chapter, our energy consumption model incorporated constant transmit power levels for the quantification of the power consumption at the transmit amplifier, as the protocols considered in the previous chapter did not facilitate power assignment. Here, we quantify the energy per bit cost at the transmit amplifier to take into account the energy cost of using varying transmit power levels due to power assignment. We assume that the source node always transmits with an energy-per-bit level of E_b, which is assumed to be the maximum transmit energy-

per-bit level available at each node in the network. Following the transmit energy model in [87], $E_b = \epsilon_{ta} d^\alpha$, where ϵ_{ta} is the energy-per-bit-per-meter$^\alpha$ $(J/b/m^\alpha)$ at the transmit amplifier and α is the path loss coefficient. Given a predetermined average BER target (P_{th}) and maximum transmit energy level (E_b), d represents the maximum source-destination separation that allows for successful communication. In this work, we consider cases where SD separation, d, is such that direct SD channel is not reliable. The selected cooperators help the source node, each spending an energy level of $E_b \rho_{r,j}(i)$ at their transmit amplifiers. The total energy-per-bit cost of the cooperative system with the cooperation set, $\mathcal{C}_{r,j}$, and the power vector $\boldsymbol{\rho}_{r,j}$ is given as

$$\mathcal{E}_{r,j}(\boldsymbol{\rho}_{r,j}) = (1 + \sum_{R_i \in \mathcal{C}_{r,j}} \rho_{r,j}(i))E_b + (r+1)E_t + (2r+1)E_r. \tag{4.1}$$

The first term in (4.1) is the energy consumed in the transmit amplifiers of the source and the cooperator nodes, and the second term is the transmit circuitry energy consumption in these nodes. The third term involves the energy consumed at the receiver circuitries, considering receptions at r cooperators during phase 1 and $(r+1)$ receptions at the destination in phase 2. Since only the nodes that can successfully decode the source transmission can participate in cooperation, energy cost due to error propagation is obliterated, and hence it is not considered in (4.1). Our quantification of the total energy per bit cost of the cooperative system given in (4.1) is not specific to the energy model used. Other energy models, such as [88] can be used as well, without requiring any modification in our protocol operation.

The optimal power assignment vector that minimizes the term $\sum_{R_i \in \mathcal{C}_{r,j}} \rho_{r,j}(i)$ for a given cooperation set $\mathcal{C}_{r,j}$ subject to the average BER threshold is denoted as $\boldsymbol{\rho}_{r,j}^*$. Among all possible cooperation sets, $\mathcal{C}_{r,j}$, $j = 1, \ldots, \binom{N}{r}$ and considering all possible r, i.e., $r = 1, \ldots, N$, each with optimal power vector $\boldsymbol{\rho}_{r,j}^*$, one set, $\mathcal{C}^*$, minimizes the total energy cost for cooperative transmission. Here, our objective is to obtain the

best cooperation set, $\mathcal{C}^*$, and the corresponding optimal power assignment vector, $\boldsymbol{\rho}^*$.

4.3   Optimal Cooperative Set Selection and Power Assignment

Our goal is to find the energy minimal cooperation set such that the *average BER of the cooperative transmission* satisfies a given *average BER target, P_{th}*. Total energy cost of a cooperation set with r cooperators can be minimized only by optimal assignment of transmit power levels, because the transceiver energy terms depend merely on the number of cooperators as shown in (4.1). Denoting the average BER as $\bar{P}_b(\mathcal{C}_{r,j}, \boldsymbol{\rho}_{r,j})$, our goal is to solve the following problem:

$$\underset{\mathcal{C}_{r,j}, \boldsymbol{\rho}_{r,j}}{\operatorname{argmin}} \mathcal{E}(\boldsymbol{\rho}) \tag{4.2}$$

$$s.t. \quad \bar{P}_b(\mathcal{C}_{r,j}, \boldsymbol{\rho}_{r,j}^*) \leq P_{th}, \tag{4.2a}$$

$$0 \leq \rho_{r,j}(i) \leq 1, \quad \forall R_i \in \mathcal{C}_{r,j}, \tag{4.2b}$$

$$0 \leq r \leq N, \quad \forall \mathcal{C}_{r,j} \subseteq \mathcal{N}, \quad r \; integer. \tag{4.2c}$$

We formulate this problem in two intrinsically connected parts. Given a set $\mathcal{C}_{r,j}$, we obtain the optimal power vector $\boldsymbol{\rho}_{r,j}^*$ from:

$$\min \sum_{R_i \in \mathcal{C}_{r,j}} \rho_{r,j}(i) \tag{4.3}$$

$$s.t. \quad \bar{P}_b(\mathcal{C}_{r,j}, \boldsymbol{\rho}_{r,j}) \leq P_{th}, \tag{4.3a}$$

$$0 \leq \rho_{r,j}(i) \leq 1, \quad \forall R_i \in \mathcal{C}_{r,j}.$$

Next, we obtain the best cooperation set via:

$$\underset{\mathcal{C}_{r,j},0<r\leq N}{\operatorname{argmin}} \ \mathcal{E}(\boldsymbol{\rho}) \tag{4.4}$$

$$s.t. \quad \bar{P}_b(\mathcal{C}_{r,j},\boldsymbol{\rho}^*_{r,j}) \leq P_{th}, \tag{4.4a}$$

$$r = 1,\cdots,N \quad integer.$$

The problem defined in (4.4) is in the form of a mixed integer non-linear program, and (4.3) is a non-linear constrained optimization problem, where (4.3a) is convex. The average BER constraint (4.3a) is always active, and the minimizer for the objective (4.3) satisfies (4.3a) with equality. Obviously, the minimizer for (4.3) satisfies the average BER constraint (4.4a) with equality, too. Thus, once the optimal solution for (4.3) is found, finding the solution for (4.4) turns into finding the optimal r^* via a search method. Later in the sequel, we will present an intelligent search algorithm to find the optimal r^* without looking for all possible cooperation set alternatives.

4.3.1   Average BER of the Cooperative System

In this part, we derive the average bit error probability of the cooperative transmission given r cooperators are involved and letting $\mathcal{C}_{r,j}$ is the selected cooperation set. The success event for the cooperative transmission by the set $\mathcal{C}_{r,j}$ means: All the nodes in $\mathcal{C}_{r,j}$ successfully decode the source transmission in phase 1, and cooperative transmission in phase 2 is successfully received by the destination. The error event for the cooperation occurs either when all the nodes in $\mathcal{C}_{r,j}$ cannot successfully decode-and-regenerate the source signal, or when the nodes in $\mathcal{C}_{r,j}$ successfully decode-and-regenerate the source transmission but the cooperative transmission fails. Note that, partial relaying is not allowed in our cooperation model; hence it is not considered in the error analysis[1]. We define these events as: $\mathbb{E}_1 = \{$All cooperators in

---

[1]Despite improved signal quality, a partial set cannot satisfy reliability (BER) requirement, and causes further energy costs as will be demonstrated later.

$\mathcal{C}_{r,j}$ decode-and-regenerate the source transmission}, $\mathbb{E}_2 = \{$Error occurs in the combined signal of r cooperators and the source node}, $\mathbb{E}_3 = \{$Not all of the cooperators in $\mathcal{C}_{r,j}$ can decode-and-regenerate the source transmission}, $\mathbb{E}_4 = \{$Error occurs in the direct transmission}. Based on the event probabilities, we formulate the average bit-error probability for the cooperative system realized via the cooperation set $\mathcal{C}_{r,j}$ and the power vector $\boldsymbol{\rho}_{r,j}$ as:

$$\bar{P}_b(\mathcal{C}_{r,j}, \boldsymbol{\rho}_{r,j}) = P(\mathbb{E}_2|\mathbb{E}_1)P(\mathbb{E}_1) + P(\mathbb{E}_4|\mathbb{E}_3)P(\mathbb{E}_3). \tag{4.5}$$

Given γ_{th} as the SNR threshold for successful decode-and-regenerate operation, and assuming that all channels undergo independent[2] fading, we can write $P(\mathbb{E}_1) = P(\gamma_{g_i} \geq \gamma_{th}, \forall R_i \in \mathcal{C}_{r,j}) = \prod_{R_i \in \mathcal{C}_{r,j}} P(\gamma_{g_i} \geq \gamma_{th})$. Furthermore, for Rayleigh fading, $P(\mathbb{E}_1)$ is given as

$$Q(\mathcal{C}_{r,j}) \triangleq P(\mathbb{E}_1) = \prod_{R_i \in \mathcal{C}_{r,j}} \exp\left(-\gamma_{th}/\bar{\gamma}_{g_i}\right), \tag{4.6}$$

and $Q'(\mathcal{C}_{r,j}) \triangleq P(\mathbb{E}_3) = 1 - \prod_{R_i \in \mathcal{C}_{r,j}} \exp\left(-\gamma_{th}/\bar{\gamma}_{g_i}\right)$.

Assuming binary phase shift keying, BPSK modulation, the average BER of the direct SD channel is found as [1]

$$\bar{P}_b(\bar{\gamma}_f) \triangleq P(\mathbb{E}_4|\mathbb{E}_3) = \frac{1}{2}\left(1 - \sqrt{\bar{\gamma}_f/(1 + \bar{\gamma}_f)}\right). \tag{4.7}$$

(Our work and framework can also easily be extended for other modulation schemes.)

For a DF system, with orthogonal STBC or with an MRC at the receiver, $P(\mathbb{E}_2|\mathbb{E}_1)$ is equivalent to the average error probability of a MISO system with $(r+1)$ transmitters [1, 46]. With Rayleigh fading and BPSK modulation assumption, average BER of an $(r+1)$x1 MISO system, $\bar{P}_b(\bar{\gamma}_\Sigma) \triangleq P(\mathbb{E}_2|\mathbb{E}_1)$, is given as [1]:

$$\bar{P}_b(\bar{\gamma}_\Sigma) = \frac{1}{\pi} \int_0^{\pi/2} \frac{\sin^2 \phi}{\sin^2 \phi + \bar{\gamma}_f} \prod_{R_i \in \mathcal{C}_{r,j}} \frac{\sin^2 \phi}{\sin^2 \phi + \bar{\gamma}_{h_i}} d\phi. \tag{4.8}$$

---

[2]Independence assumption may change with geographical correlation models as demonstrated in [89]. However, investigation of cooperative systems under correlated channels is out of the scope of this work.

Placing the event probabilities in (4.5), $\bar{P}_b(\mathcal{C}_{r,j}, \boldsymbol{\rho}_{r,j})$, the cooperative system's average BER is obtained as

$$\bar{P}_b(\mathcal{C}_{r,j}, \boldsymbol{\rho}_{r,j}) = \bar{P}_b(\bar{\gamma}_\Sigma)Q(\mathcal{C}_{r,j}) + \bar{P}_b(\bar{\gamma}_f)Q'(\mathcal{C}_{r,j}). \qquad (4.9)$$

Although the power assignment problem stated in (4.3) is convex and bears optimal solution, an analytical solution cannot be obtained due to the complexity involved with the MISO error probability term, (4.8), in (4.9). In the mean time, sensor nodes require distributed operation and simple computations. Due to this reasoning, an accurate approximation for (4.8) is essential to obtain simple analytical solutions for $\boldsymbol{\rho}_{r,j}^*$.

An alternative exact expression for the MISO average error probability is provided in [46, eqn. 5A.75], which simplifies the average BER expression, (4.8), by converting the integration terms to summations. However, due to the summations, that expression is again not suitable for obtaining simple power assignment solutions. In the literature, such as [58] and [56], approximations to the average BER of the cooperative systems are derived assuming high SNR on SD channels. Accuracy of these approximations degrades significantly when SD SNR is low, which is in fact when cooperation is required. In order to obtain analytical closed form solutions for $\boldsymbol{\rho}_{r,j}^*$, here we have derived a simple yet a very close approximation for the MISO average error probability, (4.8).

Proposition 4.3.1. *Average BER of an $(r+1)$x1 MISO system with BPSK modulation subject to Rayleigh fading can be approximated by*

$$\bar{P}_b(\bar{\gamma}_\Sigma) \approx \left[\frac{1}{\pi} \int_0^{\pi/2} \frac{(\sin\phi)^{2(r+1)}}{\sin^2\phi + \bar{\gamma}_f} d\phi \right] \prod_{R_i \in \mathcal{C}_{r,j}} \frac{1}{1 + \bar{\gamma}_{h_i}}. \qquad (4.10)$$

Proof. We first relieve $\bar{\gamma}_{h_i}$ terms from the integral in (4.8). By letting $\phi = \pi/2$ in (4.8), we obtain the Chernoff bound: $\bar{P}_{b,cher} = 0.5(1 + \bar{\gamma}_f)^{-1} \prod_{R_i \in \mathcal{C}_{r,j}} (1 + \bar{\gamma}_{h_i})^{-1}$.

The difference between $\bar{P}_{b,cher}$ and $\bar{P}_b(\bar{\gamma}_\Sigma)$ can be formulated as a function of $\bar{\gamma}_f$ as:

$\mathcal{D}_p \triangleq \log_{10}(\bar{P}_{b,cher}) - \log_{10}(\bar{P}_b(\bar{\gamma}_\Sigma)) = 10\zeta\log_{10}(\bar{\gamma}_f) + \mu$, via which, exact average BER of a MISO system, (4.8), can be rewritten as

$$\bar{P}_b(\bar{\gamma}_\Sigma) = \bar{\gamma}_f^{-10\zeta} 10^{-\mu} \bar{P}_{b,cher}, \tag{4.11}$$

where μ and ζ are obtained as

$$\zeta = \log_{\bar{\gamma}_f}\left(\frac{2\int_0^{\pi/2}\Phi(1)\prod_{R_i\in\mathcal{C}_{r,j}}(1+\kappa_i)\Phi(\kappa_i)d\phi}{(1+\bar{\gamma}_f)\int_0^{\pi/2}\Phi(\bar{\gamma}_f)\prod_{R_i\in\mathcal{C}_{r,j}}(1+\kappa_i\bar{\gamma}_f)\Phi(\kappa_i\bar{\gamma}_f)d\phi}\right),$$

$$\mu = \log_{10}\left(\frac{\pi}{4\int_0^{\pi/2}\Phi(1)\prod_{R_i\in\mathcal{C}_{r,j}}(1+\kappa_i)\Phi(\kappa_i)d\phi}\right),$$

where $\kappa_i \triangleq \rho_{r,j}(i)\delta_i$ and $\Phi(x) \triangleq \frac{\sin^2(\phi)}{\sin^2(\phi)+x}$. Note that μ is computed by substituting $\bar{\gamma}_f = 1$ in $\mathcal{D}_p$. ζ is obtained by substituting μ into $\mathcal{D}_p$.

We obtain the approximation to (4.8) by investigating the behavior of $\mathcal{D}_p$ when $\bar{\gamma}_f$ is low and the contribution from the cooperation set, $\mathcal{C}_{r,j}$, is high. It is observed in the exact average BER, (4.8), that the contribution of the SD branch is exhibited in the term $(\sin^2\phi + \bar{\gamma}_f)$, and the contribution of $\mathcal{C}_{r,j}$ is revealed in the term $\prod_{R_i\in\mathcal{C}_{r,j}}(\sin^2\phi + \kappa_i\bar{\gamma}_f)$. By extending the product term, it is seen that the largest contribution of $\mathcal{C}_{r,j}$ is due to the term $\bar{\gamma}_f^r(\sin\phi)^{2r}\prod_{R_i\in\mathcal{C}_{r,j}}\kappa_i$. In fact, when $\bar{\gamma}_f$ is small, $\mathcal{K} \triangleq \prod_{R_i\in\mathcal{C}_{r,j}}\kappa_i$ is expected to be very large, so that the predetermined average BER level is achieved. Hence, we consider the behavior of $\mathcal{D}_p$ when $\mathcal{K}$ is sufficiently large, which is mathematically equivalent to analyzing the behavior of ζ and μ as $\mathcal{K} \to \infty$. By noting that $\lim_{\mathcal{K}\to\infty}[\mathcal{D}_p] = 10\log_{10}\bar{\gamma}_f\lim_{\mathcal{K}\to\infty}[\zeta] + \lim_{\mathcal{K}\to\infty}[\mu]$, we define and obtain $\tilde{\zeta}$ and $\tilde{\mu}$ as follows:

$$\tilde{\zeta} = \lim_{\mathcal{K}\to\infty}\zeta = \log_{\bar{\gamma}_f}\left[\frac{2\int_0^{\pi/2}\Phi(1)(\sin\phi)^{2r}d\phi}{(1+\bar{\gamma}_f)\int_0^{\pi/2}\Phi(\bar{\gamma}_f)(\sin\phi)^{2r}d\phi}\right]$$

$$\tilde{\mu} = \lim_{\mathcal{K}\to\infty}\mu = \log_{10}\left[\frac{4}{\pi}\int_0^{\pi/2}\Phi(1)(\sin\phi)^{2r}\right]d\phi.$$
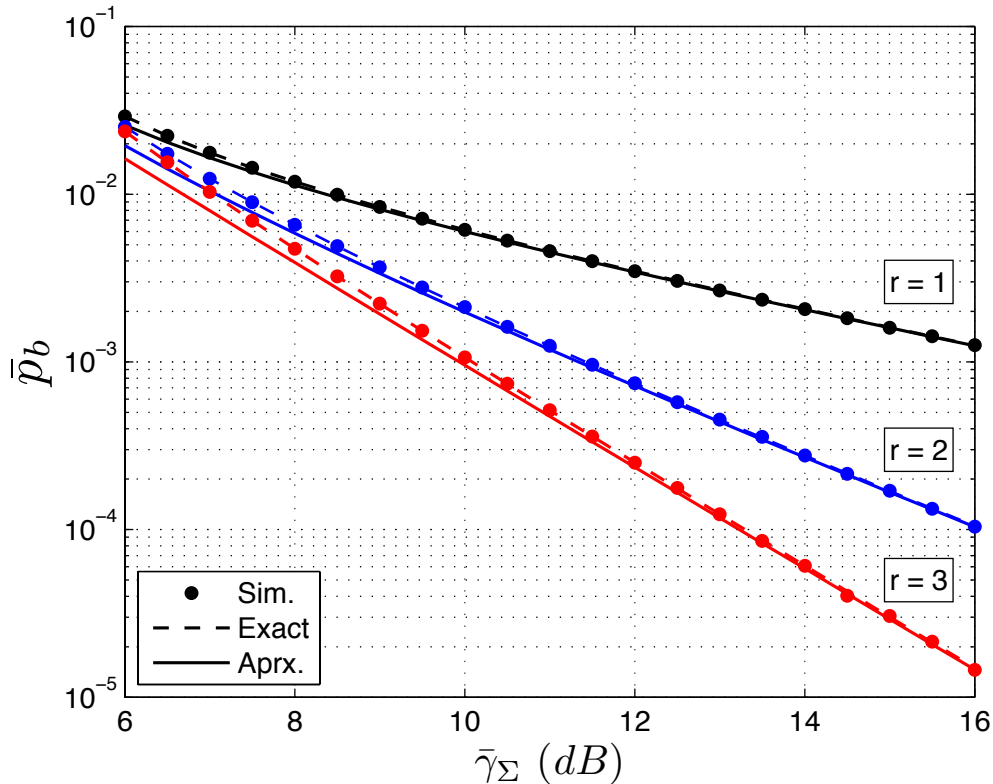
Figure 4.1: Performance of the proposed approximation in comparison to the simulations and the exact analytical formula (4.8), for varying number of cooperators, r.

The approximation (4.10) is obtained by substituting $\tilde{\zeta}$ and $\tilde{\mu}$ for ζ and μ, respectively in (4.11).

In Figure 4.1, we depict the performance of our BER approximation in comparison to the exact MISO average BER formulation [1] and the bit-level simulations for different number of cooperators, r, when total average SNR, $\bar{\gamma}_\Sigma$ is varied. It is observed that for the target BER levels of practical interest, i.e., BER levels smaller than 10^{-3}, our approximation holds tightly with the theoretical and the simulation results.

Furthermore, in Figure 4.2 we demonstrate the accuracy of our approximation in comparison to the approximation given in [56], specifically for low SD average
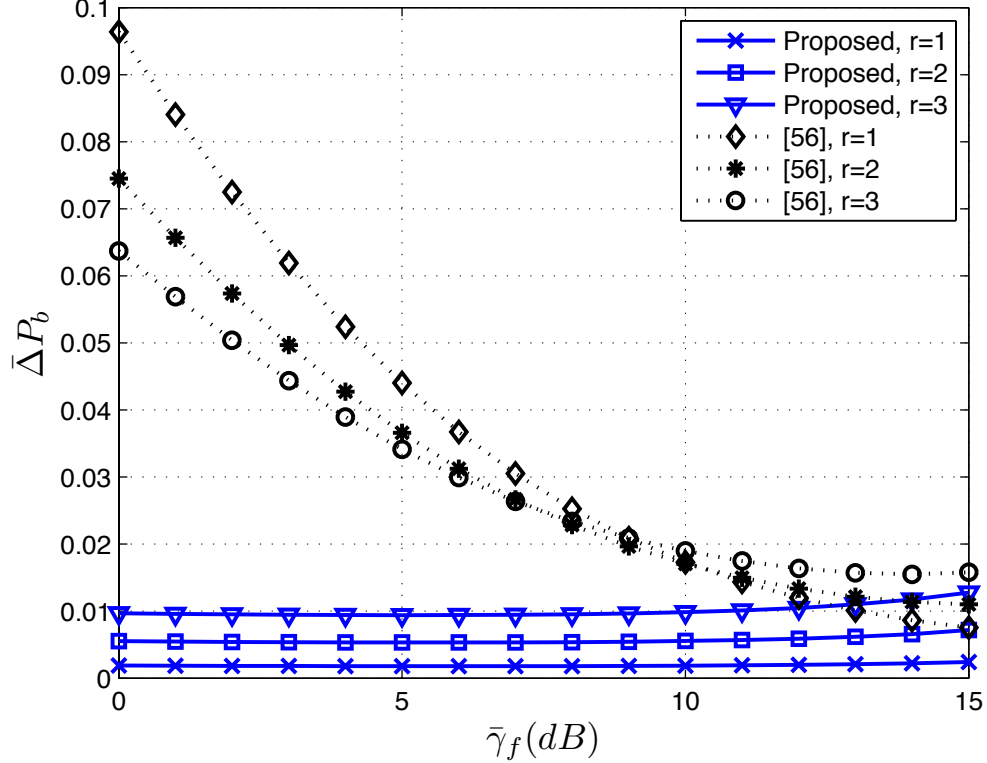
Figure 4.2: Accuracy comparison with the approximation in [56] for low SD average SNR levels, $\bar{\gamma}_f$, and for varying number of cooperators, r.

SNR levels. Figure 4.2 depicts the normalized discrepancy between the exact and approximate average BER of the cooperative link for both our approximation and the approximation in [56], for varying average SD SNR, $\bar{\gamma}_f$, and varying number of cooperators, r, when total average SNR is kept as $\bar{\gamma}_\Sigma = 15$ dB. The results reveal that for the average SD SNR values at which cooperation is really needed, our approximation is more accurate than the approximation in [56]. $\qquad\square$

Using Proposition 4.3.1, we reformulate the cooperative average error probability, $\bar{P}_b(\mathcal{C}_{r,j}, \boldsymbol{\rho}_{r,j})$, as

$$\bar{P}_b(\mathcal{C}_{r,j}, \boldsymbol{\rho}_{r,j}) \approx \Lambda(r, \bar{\gamma}_f) Q(\mathcal{C}_{r,j}) \prod_{R_i \in \mathcal{C}_{r,j}} (1 + \rho_{r,j}(i)\delta_i\bar{\gamma}_f)^{-1} + \bar{P}_b(\bar{\gamma}_f) Q'(\mathcal{C}_{r,j}), \qquad (4.12)$$

where

$$\Lambda(r, \bar{\gamma}_f) \triangleq \frac{1}{\pi} \int_0^{\pi/2} \frac{(\sin \phi)^{2(r+1)}}{\sin^2 \phi + \bar{\gamma}_f} d\phi. \tag{4.13}$$

4.3.2 Power Assignment for Minimizing Energy Cost

In this part, we study the optimal power assignment problem for a given cooperation set $\mathcal{C}_{r,j}$. We solve the power assignment problem stated in (4.3) by exploiting the average BER approximation given in Proposition 1.

We reformulate the constraint (4.3a) by substituting (4.12) as follows:
$\Lambda(r, \bar{\gamma}_f) Q(\mathcal{C}_{r,j}) \prod_{R_i \in \mathcal{C}_{r,j}} (1 + \rho_{r,j}(i) \delta_i \bar{\gamma}_f)^{\text{-}1} + \bar{P}_b(\bar{\gamma}_f) Q'(\mathcal{C}_{r,j}) \leq P_{th}$, and we define

$$\Omega(\mathcal{C}_{r,j}, \bar{\gamma}_f) \triangleq \frac{\Lambda(r, \bar{\gamma}_f) Q(\mathcal{C}_{r,j})}{P_{th} - \bar{P}_b(\bar{\gamma}_f) Q'(\mathcal{C}_{r,j})}. \tag{4.14}$$

The power assignment problem for the set $\mathcal{C}_{r,j}$ is obtained as:

$$\min \sum_{R_i \in \mathcal{C}_{r,j}} \rho_{r,j}(i) \tag{4.15}$$

$$s.t. \quad \Omega(\mathcal{C}_{r,j}, \bar{\gamma}_f) \leq \prod_{R_i \in \mathcal{C}_{r,j}} 1 + \rho_{r,j}(i) \delta_i \bar{\gamma}_f \tag{4.15a}$$

$$0 \leq \rho_{r,j}(i) \leq 1, \quad \forall R_i \in \mathcal{C}_{r,j}. \tag{4.15b}$$

The optimization problem (4.15) is convex and non-linear. It should be noted that, at optimality, the inequality constraint (4.15a) must be satisfied with equality, because $\bar{P}_b(\mathcal{C}_{r,j}, \boldsymbol{\rho}_{r,j})$ is a monotonically decreasing function of $\boldsymbol{\rho}_{r,j}$. That is to say, minimizer for the objective function (4.15), maximizes $\bar{P}_b(\mathcal{C}_{r,j}, \boldsymbol{\rho}_{r,j})$ subject to P_{th}. In particular, at the optimal power solution $\boldsymbol{\rho}_{r,j}^*$, $\bar{P}_b(\mathcal{C}_{r,j}, \boldsymbol{\rho}_{r,j})$ attains its maximum value, P_{th}. Constraint (4.15b) defines the feasible region for $\boldsymbol{\rho}_{r,j}^*$.

This problem, (4.15), can be solved analytically, when the feasible region for $\boldsymbol{\rho}_{r,j}$, (4.15b), is relaxed to include all non-negative power assignments, i.e., $0 \leq$

$\rho_{r,j}(i), \forall R_i \in \mathcal{C}_{r,j}$. For the moment, we consider only the non-negativity constraint for $\rho_{r,j}(i)$, i.e., ignore the upper limit for $\rho_{r,j}(i)$. In Lemma 1, we present the optimal relative power assignment solution without the upper limit.

Lemma 4.3.2. *The optimal relative power assignment for the cooperative system with the cooperation set $\mathcal{C}_{r,j}$ is given as*

$$\rho_{r,j}^*(i) = \frac{1}{\bar{\gamma}_f} \left(\Omega(\mathcal{C}_{r,j}, \bar{\gamma}_f) \prod_{R_k \in \mathcal{C}_{r,j}} \frac{\sigma_f^2}{\sigma_{h_k}^2} \right)^{1/r} - \frac{\sigma_f^2}{\sigma_{h_i}^2 \bar{\gamma}_f}. \tag{4.16}$$

Proof. We solve the problem analytically, via the Lagrange relaxation method. The Lagrangian is formed as

$$\mathcal{L}(\boldsymbol{\rho}_{r,j}, \lambda) = \lambda[\Omega(\mathcal{C}_{r,j}, \bar{\gamma}_f) - \prod_{R_i \in \mathcal{C}_{r,j}} (1 + \rho_{r,j}(i)\delta_i\bar{\gamma}_f)] + \sum_{R_i \in \mathcal{C}_{r,j}} \rho_{r,j}(i).$$

Partial derivatives of $\mathcal{L}(\boldsymbol{\rho}_{r,j}, \lambda)$ with respect to $\rho_{r,j}(i)$, $\forall R_i \in \mathcal{C}_{r,j}$ and λ give

$$\frac{\partial \mathcal{L}}{\partial \rho_{r,j}(i)} = 1 - \lambda \delta_i \prod_{R_k \in \mathcal{C}_{r,j}, k \neq i} \bar{\gamma}_f(1 + \rho_{r,j}(k)\delta_k) = 0, \tag{4.17}$$

$$\frac{\partial \mathcal{L}}{\partial \lambda} = \prod_{R_i \in \mathcal{C}_{r,j}} (1 + \rho_{r,j}(i)\delta_i\bar{\gamma}_f) = \Omega(\mathcal{C}_{r,j}, \bar{\gamma}_f). \tag{4.18}$$

Solving for $\rho_{r,j}(i)$ in (4.17), we obtain $\rho_{r,j}(i) = \rho_{r,j}(1) + \frac{1}{\bar{\gamma}_f}(\delta_1 - \delta_i)$. By substituting $\rho_{r,j}(i)$ in (4.18), we obtain $(1 + \rho_{r,j}(1)\delta_1\bar{\gamma}_f)\delta_1^{(r-1)} \prod_{R_i \in \mathcal{C}_{r,j}, i \neq 1} \delta_i = \Omega(\mathcal{C}_{r,j}, \bar{\gamma}_f)$. Finally, the optimal relative power solution, $\rho_{r,j}^*(i)$, is obtained as given in (4.16). $\qquad\square$

Note that, the optimal power assignment (4.16) is a *water-filling solution*, in which $\Lambda(r, \bar{\gamma}_f)$, P_{th}, $\bar{P}_b(\bar{\gamma}_f)$, $Q(\mathcal{C}_{r,j})$, $\prod_{R_i \in \mathcal{C}_{r,j}} \delta_i^{-1}$, r are the common terms that set the top level for the water-filling analogy with exactly the same values for each node in $\mathcal{C}_{r,j}$. Cooperators with large σ's are assigned with higher power levels than the other cooperators. Since $\sigma_{h_i}^2 \propto d_{R_iD}^{-\alpha}$, it is deduced that the cooperators which are assigned with higher power levels are the ones that are closer to the destination.

Recalling the upper limit in the inequality constraint, (4.15b), we propose to obtain the optimal solution by repetitive application of (4.16) as follows: The optimal power assignment is obtained via (4.16) for all the cooperators in $\mathcal{C}_{r,j}$. If there are relative power assignments, $\rho_{r,j}^*(i)$, violating the upper limit (i.e., greater than 1), the relative powers of these nodes are set to the upper limit, and the power assignment problem (4.15) is solved again. This procedure is continued until a feasible solution is found, such that $\rho_{r,j}^*(i) \leq 1$, $\forall R_i \in \mathcal{C}_{r,j}$. Otherwise, it is deduced that there is no feasible solution for the considered cooperation set, $\mathcal{C}_{r,j}$, under the given constraints. This procedure is summarized in Algorithm 1.

Algorithm 1 Optimal power assignment

Relay set: $\mathcal{C}_{r,j}$; $\mathcal{C}_j = \mathcal{C}_{r,j}$; $k = |\mathcal{C}_j|$; $\mathcal{F} = \{\emptyset\}$
while $k \neq 0$ **do**
  for $R_i \in \mathcal{C}_j$ **do**
    Compute $\rho_{r,j}^*(i)$ for $\mathcal{C}_j$ via eqn. (4.16)
    if $\rho_{r,j}^*(i) > 1$ **then**
      $\rho_{r,j}^*(i) = 1$
      $\mathcal{F} \leftarrow \mathcal{F} \cup R_i$
    end if
  end for
  $\mathcal{C}_j \leftarrow \mathcal{C}_j - \mathcal{F}$; $k = |\mathcal{F}|$; $\mathcal{F} = \{\emptyset\}$
end while

4.3.3   Cooperator Selection with Power Assignment

In this part, we revisit the overall energy minimization problem in (4.4) and propose a solution that jointly determines the optimal cooperation set and the corresponding optimal power levels.

In Section 4.3.2, the optimal power assignment, $\boldsymbol{\rho}_{r,j}^*$, has been derived for a given cooperation set, $\mathcal{C}_{r,j}$. Among the sets with r cooperators, one of the cooperation sets minimizes the total energy cost. We denote this set, its relative power assignment and its total energy cost as $\mathcal{C}_r^*$, $\boldsymbol{\rho}_r^*$ and $\mathcal{E}_r^*(\boldsymbol{\rho}_r^*)$, respectively. Furthermore, we denote

the energy-minimizing cooperation set as $\mathcal{C}^*$, corresponding power assignment vector as $\boldsymbol{\rho}^*$ and the minimal energy cost as $\mathcal{E}^*(\boldsymbol{\rho}^*)$. Here, our goal is to find $\mathcal{C}^*$ and $\boldsymbol{\rho}^*$.

The search for the optimal cooperation set requires that the energy consumption of each possible cooperation set is calculated and compared with the energy cost of the other sets, which can be computationally intense. However, owing to the relation between the transceiver circuitry and the transmit amplifier energy consumption, the search for the optimal cooperation set can be simplified. In the following, we present an observation that is useful in simplifying the search.

Proposition 4.3.3. *In a cooperative system that uses optimally selected relative power levels, the total energy-per-bit cost of the cooperation set, $\mathcal{E}_r^*(\boldsymbol{\rho}_r^*)$, is increased as the cardinality (r) of the cooperation set is increased.*

Specifically, $\mathcal{E}_r^*(\boldsymbol{\rho}_r^*) < \mathcal{E}_{r+1}^*(\boldsymbol{\rho}_{r+1}^*)$ holds true, when the following inequality is satisfied

$$\sum_{R_i \in \mathcal{C}_r^*} \rho_r^*(i) - \sum_{R_i \in \mathcal{C}_{r+1}^*} \rho_{r+1}^*(i) < \frac{E_t + 2E_r}{E_b}. \tag{4.19}$$

□

Corollary 4.3.4. *Observing (4.19), as the cooperation set is expanded, i.e., as r is increased, $\sum_{R_i \in \mathcal{C}_r^*} \rho_r^*(i)$ is decreased as a consequence of the diversity gain. Hence, the left hand side of (4.19) is positive and the difference is reduced as r is increased.*

□

For practical values of E_b, E_t and E_r, the right hand side of (4.19) can get much larger than the transmit power difference attained by the diversity gain. Due to this fact, the optimization problem stated in (4.4) does not require a search among all the possible cooperation set combinations. Cooperator search process can start with the sets with one cooperator and the number of cooperators can be increased until a set

that minimizes the total energy cost while satisfying the average BER target is found. In fact, in WSNs typical transmit amplifier power consumption values are around 1 mW, whereas the current typical transmitter and receiver circuitries consume around 50 mW [90], which also demonstrates the validity of the Proposition 4.3.4.

Making use of the Corollary 4.3.4, the search for the optimal cooperation set with the optimal power assignment can be performed in a reduced sample space, and in an incremental fashion. Algorithm 2 summarizes the joint framework for the optimal cooperation set selection with power assignment. This algorithm is named as, Optimal Cooperator Selection and Power Assignment (O-CSPA).

Algorithm 2 Optimal Cooperator Selection and Power Assignment (O-CSPA)

$r = 1$, $\mathcal{C}^* = \{\emptyset\}$,
  while $\mathcal{C}^* = \{\emptyset\}$ **do**
    find $\boldsymbol{\rho}^*_{r,j}$, $\forall \mathcal{C}_{r,j}$, $j = 1, \ldots, \binom{N}{r}$ $\Rightarrow$ find $\boldsymbol{\rho}^*_r$, $\mathcal{C}^*_r$
    if $\boldsymbol{\rho}^*_r$ is not feasible, i.e., $\exists R_j \in \mathcal{C}_r$ s.t. $\rho^*_r(j) > 1$ **then**
      $r = r + 1$
    else
      find $\boldsymbol{\rho}^*_{r+1,j}$, $\forall \mathcal{C}_{r+1,j}$, $j = 1, \ldots, \binom{N}{r+1}$ $\Rightarrow$ find $\boldsymbol{\rho}^*_{r+1}$, $\mathcal{C}^*_{r+1}$
      if (4.19) is satisfied **then**
        $\mathcal{C}^* = \mathcal{C}^*_r$, $\boldsymbol{\rho}^* = \boldsymbol{\rho}^*_r$
      else
        if $\mathcal{E}_{r+1}(\boldsymbol{\rho}^*_{r+1}) < \mathcal{E}_r(\boldsymbol{\rho}^*_r)$ **then**
          $\mathcal{C}^* = \emptyset$
        else
          $\mathcal{C}^* = \mathcal{C}^*_r$, $\boldsymbol{\rho}^* = \boldsymbol{\rho}^*_r$
        end if
      end if
    end if
  end while

Note that O-CSPA algorithm is centralized, because the computation of $\Omega(\mathcal{C}_{r,j}, \bar{\gamma}_f)$ in (4.14) requires the knowledge of $Q(\mathcal{C}_{r,j})$, which involves the channel statistics of all the links in the network, namely σ^2_f, $\sigma^2_{g_i}$, $\sigma^2_{h_i}$ $\forall R_i \in \mathcal{C}_{r,j}$. While implementing this approach, it is assumed that all channel information is available at a central node, e.g. the source node, which searches among all subsets $\mathcal{C}_{r,j}$ to find $\mathcal{C}^*_r$, where $j = 1, \cdots, \binom{N}{r}$, computes the optimal power assignment vectors for $\binom{N}{r}$ different co-

operation sets, computes the energy consumption corresponding to these sets/vectors and finds the energy-minimizing set/vector. Hence, the worst case complexity of O-CSPA is $O(N2^N)$.

WSNs usually need to operate in a distributed fashion. Despite being optimal, the solution stated in this section is difficult to be realized in a distributed fashion. In O-CSPA, all channel statistics are required to be known by every node, and dissemination of CSI and formation of a multi-relay set requires an immense amount of information to be exchanged among nodes, which can steal not only from the network bandwidth but from energy as well.

4.4 Distributed Cooperator Selection and Power Assignment (D-CSPA)

4.4.1 Description of D-CSPA

Here, we present our distributed joint cooperation set selection and power assignment (D-CSPA) method, in which each node makes its own decision whether to get involved in cooperation or not. In D-CSPA, cooperation set is formed in an iterative fashion, and cooperative transmission is carried out only after a reliable cooperation set is found. After the source transmission, each neighboring node that has successfully decoded the source signal computes the required power allocation via (4.16) to satisfy the target reliability level with cooperative transmission. If the node deduces that its inclusion in the cooperation set can help achieving the required average BER, it announces its decision to the neighboring nodes. Here, we envision that the candidate nodes send their announcements in an order that can be determined based on a channel quality metric, such as the $R_i D$ channel statistics ($\sigma_{h_i}^2$). The pseudocode of our distributed algorithm D-CSPA is given in Algorithm 3 and its operation is

summarized in the steps below:

1. Let R_1 be the first node to announce its availability. R_1 constitutes the initial cooperation set, $\{R_1\}$, with relative power assignment vector $\boldsymbol{\rho}_{1,1}^*$. R_1 informs neighbor nodes about its channel statistics, namely $\sigma_{g_1}^2$, $\sigma_{h_1}^2$, via the announcement message.

2. Upon hearing R_1's announcement, each node R_i computes the power assignment vector, $\boldsymbol{\rho}_{2,j}$, for the set $\{R_1, R_i\}$. Assume that next node to announce its decision is R_2, the updated set is $\{R_1, R_2\}$ and the updated relative power assignment vector is given as $\boldsymbol{\rho}_{2,1}^* = [\rho_{2,1}^*(1) \ \rho_{2,1}^*(2)]$. R_2 announces its availability for cooperation in the following cases: $\boldsymbol{\rho}_{1,1}^*$ is not feasible or energy-per-bit cost can be decreased by the inclusion of this relay, i.e., $\mathcal{E}_{2,1}(\boldsymbol{\rho}_{2,1}^*) < \mathcal{E}_{1,1}(\boldsymbol{\rho}_{1,1}^*)$.

3. After R_2's message, all neighbor nodes have the following information: $\sigma_{h_1}^2$, $\sigma_{h_2}^2$, $\sigma_{g_1}^2$, $\sigma_{g_2}^2$. Each node R_i computes the power assignment vector for the set $\{R_1, R_2, R_i\}$, and the node is added to the cooperation set if the energy cost is smaller than the previous cost, as explained in step 2. The same procedure is repeated for the rest of the nodes, i.e., each time a node announces its availability for cooperation, the other nodes compute the optimal power assignment and the energy cost for the set and compare it to the energy cost of the previous set. The algorithm continues until energy-per-bit cost cannot be decreased further.

4. In case there are no relay nodes available for cooperation, or in case the average BER requirement cannot be met with the cooperation of the available nodes, cooperation is aborted.

D-CSPA mandates that the cooperators are selected one by one and in order of their mean channel gains to the destination. Although SR channel statistics, σ_g^2, are

108

Algorithm 3 Distributed Cooperator Selection and Power Assignment (D-CSPA) algorithm run by node R_i

---

if $\gamma_{g_i} \geq \gamma_{th}$ **then**
    $r = 0$, Decision $= \emptyset$
    while Decision $= \emptyset$ **do**
        if a cooperator's decision, say, R_l, is received **then**
            $r = r + 1$, $\mathcal{C}_r \leftarrow \mathcal{C}_{r-1} \cup R_l$
            Compute $\rho_r^*(j), \forall R_j \in \mathcal{C}_r$ via **Algorithm 1**
            if $\boldsymbol{\rho}_r^j$ is not feasible, i.e., $\exists R_j \in \mathcal{C}_r$ s.t. $\rho_r^*(j) > 1$ **then**
                Decision = Cooperate
            else
                if (4.19) is satisfied **then**
                    Decision = Do not cooperate
                else
                  if $\mathcal{E}_r(\boldsymbol{\rho}_r^*) < \mathcal{E}_{r-1}(\boldsymbol{\rho}_{r-1}^*)$ **then**
                    Decision = Cooperate
                  else
                    Decision = Do not cooperate
                  end if
                end if
            end if
        else
            Decision = Cooperate
        end if
    end while
end if

---

not exploited when adding cooperators into the set, this information is used to find the optimal power assignment via (4.16). Here, we assume that nodes are identical in their circuitries. In case of networks with different circuitries, each node can announce its transceiver energy cost together with $\sigma_{g_i}^2$ and $\sigma_{h_i}^2$ information, while announcing its availability for cooperation.

The worst case complexity is found as $O(N^3)$, which can lead to significant reduction in the total number of required computations as compared to O-CSPA, especially when N is large. Surprisingly, reduced complexity comes together with energy-efficiency, as shown in the performance analysis section.

4.4.2 D-CSPA in COMAC Protocol

We have implemented D-CSPA algorithm within our cooperative MAC protocol, COMAC, presented in Section 3.3. Cooperative packet exchange with D-CSPA in COMAC consists of three main stages as depicted in Figure 4.3: i) Reservation stage, where cooperative data transmission request is made by the source node, ii) ACO epoch, where the announcements of the candidate relays are sent and the cooperation set is formed and power levels are assigned in accordance with the D-CSPA algorithm, and iii) The cooperative data transmission stage, which includes phases 1 and 2 of cooperation. The operation of the COMAC protocol with D-CSPA algorithm can be summarized as follows:

The source node starts the cooperative packet exchange by sending a C-RTS packet to reserve the medium, and the destination node replies by a C-CTS packet, agreeing on the reservation period, which is set to the entire time duration of cooperative transmission, including three stages. The nodes that have received both C-RTS and C-CTS are regarded as candidate relays for cooperative transmission. From these packets, each candidate node i can estimate the average SNR of SR_i and
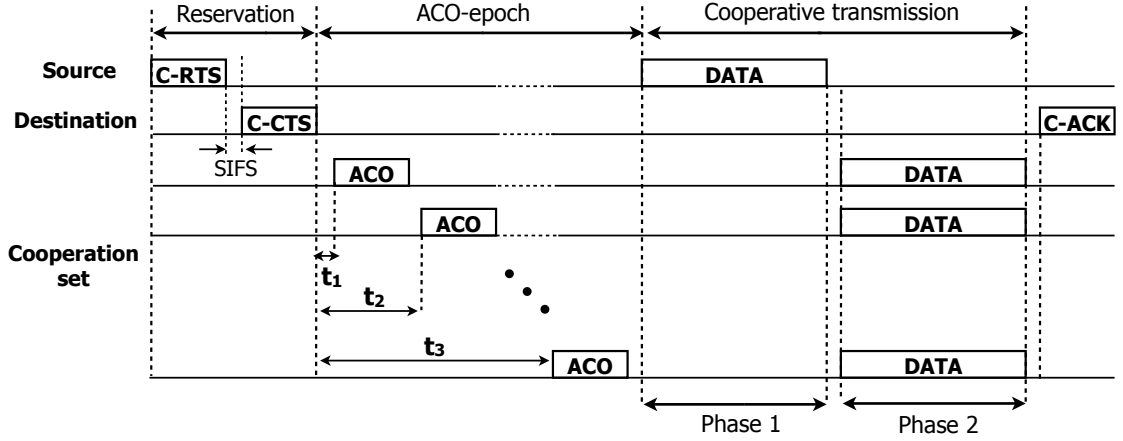
Figure 4.3: Packet exchanges for COMAC with D-CSPA.

$R_i D$ channels ($\sigma_{g_i}^2$ from C-RTS and $\sigma_{h_i}^2$, from C-CTS). Furthermore, the C-CTS packet contains the average SNR of the SD channel (σ_f^2), which was obtained by the destination node while receiving C-RTS. Following the reservation phase, candidate cooperators announce their availability for cooperation via ACO packets during the ACO-epoch. Each candidate relay node i, makes use of the channel information provided through C-RTS and C-CTS packets to compute the required power allocation vector considering itself for cooperation, via (4.16), and computes and starts a timer, t_i, based on its initial power assignment value, ρ_i (which is observed to perform better than $\sigma_{h_i}^2$), given as $t_i = f(\rho_i, \tau_{aco})$, where τ_{aco} is the total ACO-epoch duration. The timer values help differentiate the candidate relays and provide the transmission order envisioned by the D-CSPA algorithm, so that each node i sends its ACO, when its timer t_i expires. In each ACO packet, node i includes the average SNR levels of the $R_i D$ and SR_i channels, ($\sigma_{h_i}^2$ and $\sigma_{g_i}^2$). When a node j receives ACO packets before the expiration of its own timer, t_j, it computes and updates the power allocation vector for the most up-to-date cooperation set, including the nodes that have already sent their ACO packets and itself. If the current cooperation set (without node j) satisfies the required average BER level, then node j checks if its inclusion

111

in the cooperation set can decrease the energy-per-bit cost of cooperation (which is implementation of steps 2 and 3 in D-CSPA operation). If the current cooperation set (without node j) does not satisfy the required average BER level, or if inclusion of node j decreases the energy cost, then node j waits to announce its availability with its ACO packet. If node j deduces that its inclusion cannot decrease the energy cost, it cancels its timer. This way, the cooperation set is incrementally selected and the optimal power levels are calculated during the ACO-epoch period. ACO collisions are avoided with appropriate selection of the timer and the ACO-epoch length.

When a reliable cooperation set can be formed by the end of the ACO-epoch, the source node disseminates the data packet (phase 1 of cooperation), then in phase 2, the nodes in the cooperation set cooperatively transmit the data packet to the destination node over orthogonal channels at the assigned optimal power levels. The destination node replies with a C-ACK message, if it can successfully decode the cooperative transmission[3]; otherwise a retransmission is invoked as described in CO-MAC protocol [85]. When a reliable cooperation set cannot be found within the ACO-epoch, the source node reverts to direct transmission, setting the duration field of the transmitted data packet to the updated transmission duration. This way, the reservation duration is shortened and the neighboring nodes are informed. If the destination node can successfully decode the data packet, it replies with an ACK packet; otherwise a retransmission is invoked.

4.5 Performance Analysis

In this section, we present performance analysis in two parts: In the first part, we provide a thorough numerical analysis for the energy-efficiency of the proposed

---

[3]Here, it is assumed that the destination node stores the source transmission in phase 1 in memory, and combines this signal with the cooperation set transmissions in phase 2, similar to COMAC operation.

centralized and distributed algorithms, O-CSPA and D-CSPA, considering different node deployment scenarios, varying SD channel conditions ($\bar{\gamma}_f$), varying target average BER levels (P_{th}), and varying (transceiver) power consumption models. In the second part, we evaluate the implementation of D-CSPA in COMAC, and via an event-driven network simulator (ns-2), we analyze the energy-efficiency, throughput and delay performance, as well as overhead cost by taking into account actual packet sizes, instantaneous channel conditions, collisions and retransmissions in a realistic network setting.

4.5.1 Energy Efficiency of Proposed Schemes

In this part, we evaluate the energy cost of cooperation employing our cooperator selection and power allocation schemes, O-CSPA and D-CSPA via numerical experiments and analysis, without taking into account the MAC layer. In our experiments, all channels, SD, SR_i and R_iD, are assumed to be undergoing independent Rayleigh fading, and values for E_b, r_b, N_0 and maximum SD separation for direct communication are chosen in accordance with the data sheet in [90].

As benchmarks for comparison, we consider the following two schemes, random cooperator selection (R-CS) and optimal cooperator selection without power assignment (O-CS). R-CS scheme randomly selects a cooperator among the neighbors. If the transmission with the selected cooperator cannot satisfy the desired average BER threshold, another cooperator is randomly selected and added into the cooperation set until the average BER threshold is achieved. R-CS uses fixed power levels for the cooperators, i.e., $\boldsymbol{\rho}_{r,j} = 1$. O-CS employs the same algorithm for the cooperation set selection as O-CSPA except that O-CS uses fixed power levels for all the nodes, i.e., $\boldsymbol{\rho}_{r,j} = 1$. Comparison of O-CS with O-CSPA and D-CSPA reveals how much energy can be saved by adjusting the transmit power levels of the cooperators.

4.5.1.1 Effect of Node Deployment

Different node deployments can be encountered in sensor network applications depending on the event monitored and the specific requirements of the applications [2]. Node deployment (topology) determines the limits of many intrinsic properties of WSNs, such as energy-efficiency. Depending on the topology, the performance of the distributed cooperative schemes may vary, which can alter the energy-efficiency presumptions.

Here, in an effort to analyze the effect of node deployment on the performance of our distributed scheme, we evaluate and compare the energy-per-bit performances of the distributed and the centralized (optimal) schemes under varying network topologies that correspond to the best, worst and random (averaged) instances. For this purpose, we consider the following topologies: nodes deliberately placed on vertically or horizontally aligned grids, nodes deliberately located in a square grid, as shown in Figures 4.4, 4.6, 4.8, respectively; and randomly deployed relays.

We evaluate the energy-per-bit cost performance of our schemes D-CSPA and O-CSPA for varying $\bar{\gamma}_f$ values by considering the energy consumed at the transmit amplifiers and also the energy consumed at the transceivers. For the following scenarios, we set the average BER threshold as $P_{th} = 10^{-4}$, decode-and-regenerate threshold as $\gamma_{th} = 20$ dB and $E_t = E_r = 10^4 \epsilon_{ta}$, according to [90]. We assume that no two nodes have exactly the same channel statistics $\{\sigma_h^2, \sigma_g^2\}$ pair.

4.5.1.1.1 Vertically Aligned Nodes   Neighbors of the source node are assumed to be placed on an axis that is vertical to the axis connecting S and D, as depicted in Figure 4.4. This kind of node deployment can be encountered in pipeline, bridge monitoring and border surveillance applications [2].

This topology corresponds to the best instance for the operation of D-CSPA,
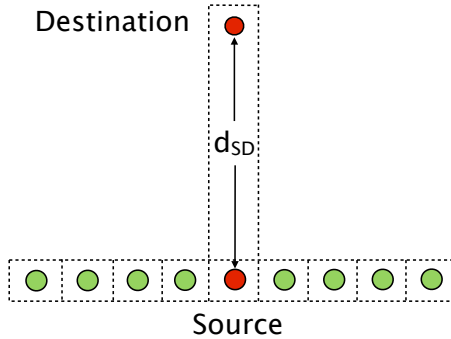
Figure 4.4: Vertically aligned nodes.

since the node with the best average SR channel also has the best average RD channel. As $\bar{\gamma}_f$ is increased, D-CSPA and O-CSPA reduces the energy-per-bit cost polynomially owing to the transmit power assignment that exploits the diversity gain. The abrupt changes in the energy cost are due to cooperation set updates, which occur at $\bar{\gamma}_f = 10.1$ dB and 16.2 dB as depicted in Figure 4.5. As the cooperation set is enlarged, the transmit amplifier energy cost is decreased owing to the diversity gain, and in the mean time, total energy cost is increased considerably because of the transceiver energy consumption of the added cooperator. It is observed that O-CS assigns the optimal cooperation set, but it does not exploit the diversity gain to reduce the transmit amplifier energy consumption.

Both O-CSPA and D-CSPA provide 82% decrease in the transmit amplifier energy consumption as compared to O-CS at $\bar{\gamma}_f = 15$ dB. When the transceiver energy cost is also taken into account, the reduction in the energy-per-bit cost is observed as 20.5%. The results demonstrate that for vertically aligned nodes, almost the same performance can be obtained by employing D-CSPA scheme in place of O-CSPA.

4.5.1.1.2 Horizontally Aligned Nodes Neighbors of the source node are assumed to be horizontally aligned on the axis that connects S and D. As depicted in Figure 4.6, 4 nodes are located between S and D and 4 nodes are on the other
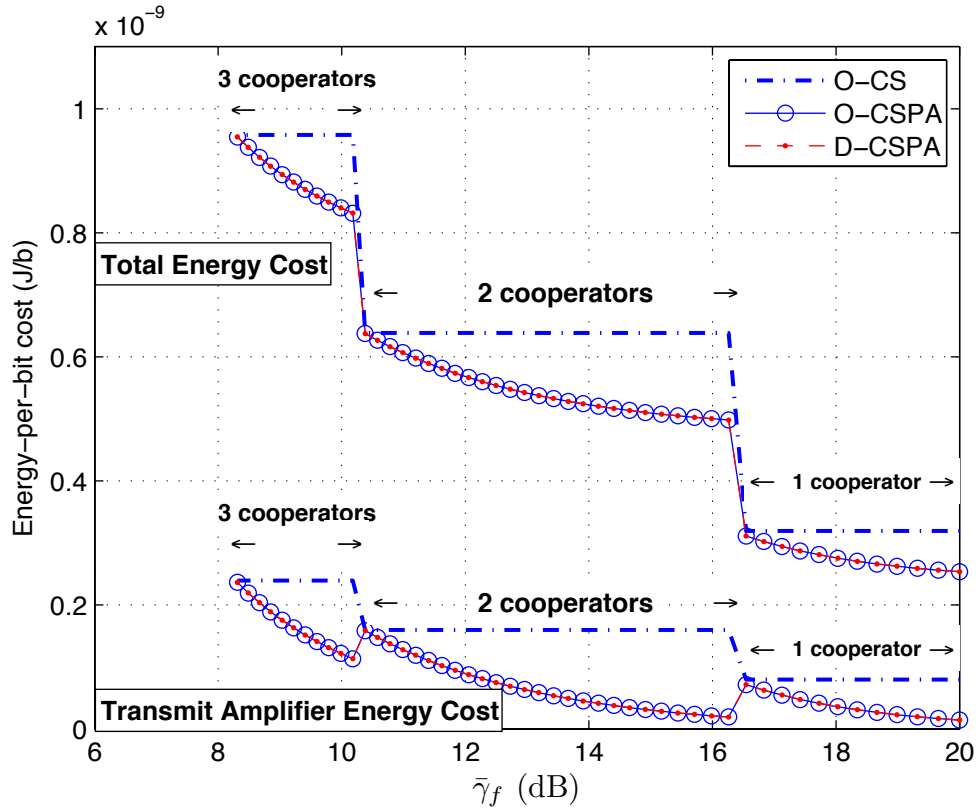
Figure 4.5: Vertically aligned nodes: Energy-per-bit cost vs Average SD SNR; total energy cost and transmit amplifier energy cost.
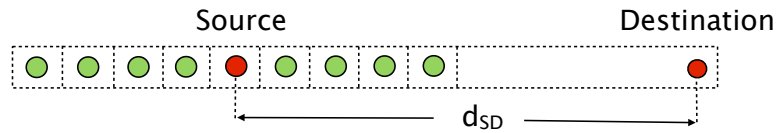
Figure 4.6: Horizontally aligned nodes.

side of S. This kind of node deployment can be encountered in pipeline or border surveillance applications, where nodes are communicating with another node on the path to the base station [2].

It is observed that the performance of D-CSPA deviates from O-CSPA for certain ranges of SD SNR. D-CSPA finds suboptimal cooperation sets owing to using σ_h^2 when adding a cooperator to the set. Nonetheless, D-CSPA assigns the optimal transmit power levels to the cooperators, since it makes use of σ_g^2 at the power assignment

stage. Cooperation set updates of the D-CSPA scheme are distinguished as glitches in Figure 4.7. It is observed that the effect of glitches on the energy performance of D-CSPA is smoothened when the transceiver circuit energy consumption is also taken into account. Since D-CSPA and O-CSPA assign the same number of cooperators for the cooperation set, the effect of transceiver energy consumption is the same for both of the schemes.

It is observed that, considering only the energy cost of the transmit amplifiers, at $\bar{\gamma}_f = 15$ dB, D-CSPA reduces the energy consumption with respect to O-CS by 81.5%, while O-CSPA reduces the energy cost by 87%; considering the total energy cost, D-CSPA and O-CSPA provides a reduction by 20.4% and 21.8%, respectively, with respect to O-CS. Note that in horizontal alignment, the node with the best average RD channel has the worst average SR channel among all neighbors. Due this fact, horizontally aligned relays correspond to the most troublesome topology in terms of the operation of D-CSPA. However, D-CSPA still outperforms O-CS significantly, and furthermore, converges to O-CSPA as cooperation set is enlarged.

4.5.1.1.3 Square Grid Deployment Having compared the best and worst instance performances of the distributed and the optimal schemes, now, we provide performance analysis for another frequently encountered, general topology, where neighbors are assumed to be located in a square gridded region around the source, as depicted in Figure 4.8. This kind of node deployments are typical for habitat monitoring applications [2, 91].

As observed in Figure 4.9, in this topology, D-CSPA and O-CSPA perform equally well, with up to 86.8% reduction in the transmit amplifier energy cost and around 20.7% reduction in the total energy cost over O-CS algorithm. The results demonstrate that as SD channel gets poorer, cooperative system gets help from closely located neighbors. It is seen that D-CSPA exploits diversity advantage without de-
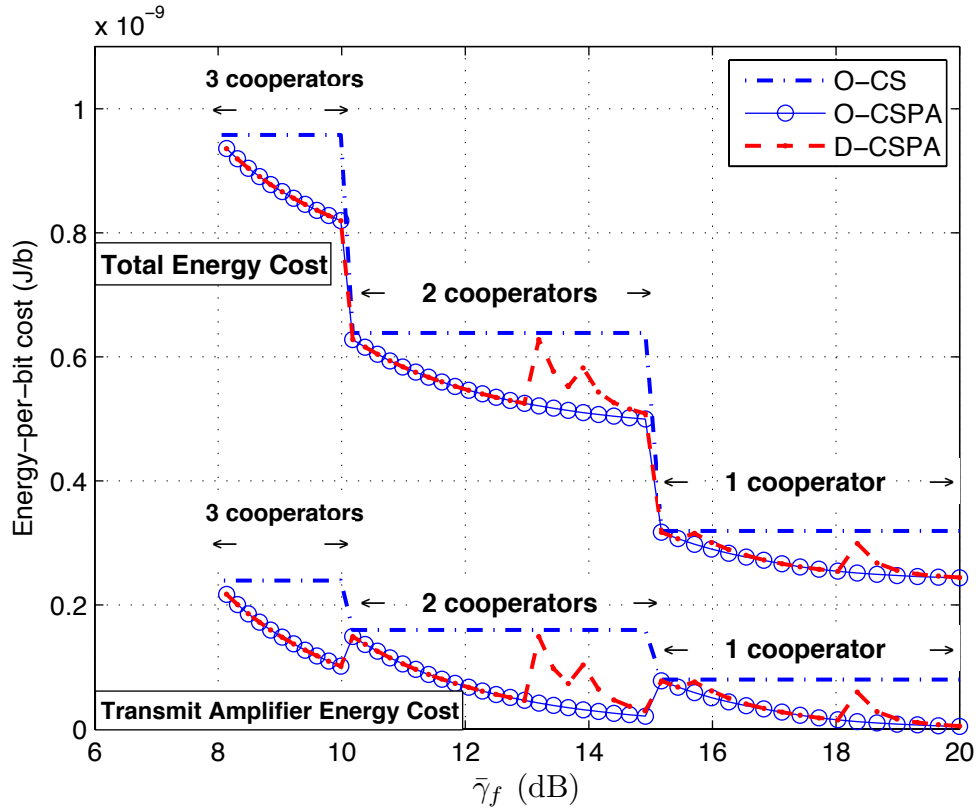
Figure 4.7: Horizontally aligned nodes: Energy-per-bit cost vs Average SD SNR; total and transmit amplifier energy cost.
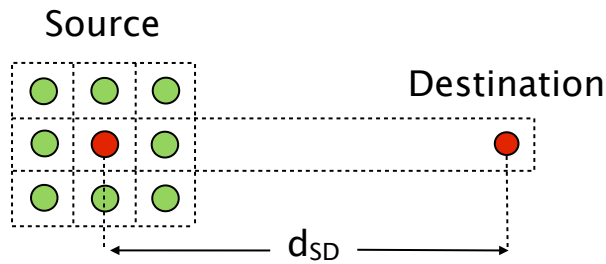
Figure 4.8: Nodes deployed on a regular square grid.

grading the energy performance.

4.5.1.1.4 Random Deployment Having demonstrated the best, worst and general instances, now, we consider the cases where node deployment (topology) is not predetermined. This kind of scenario can be encountered in surveillance applications
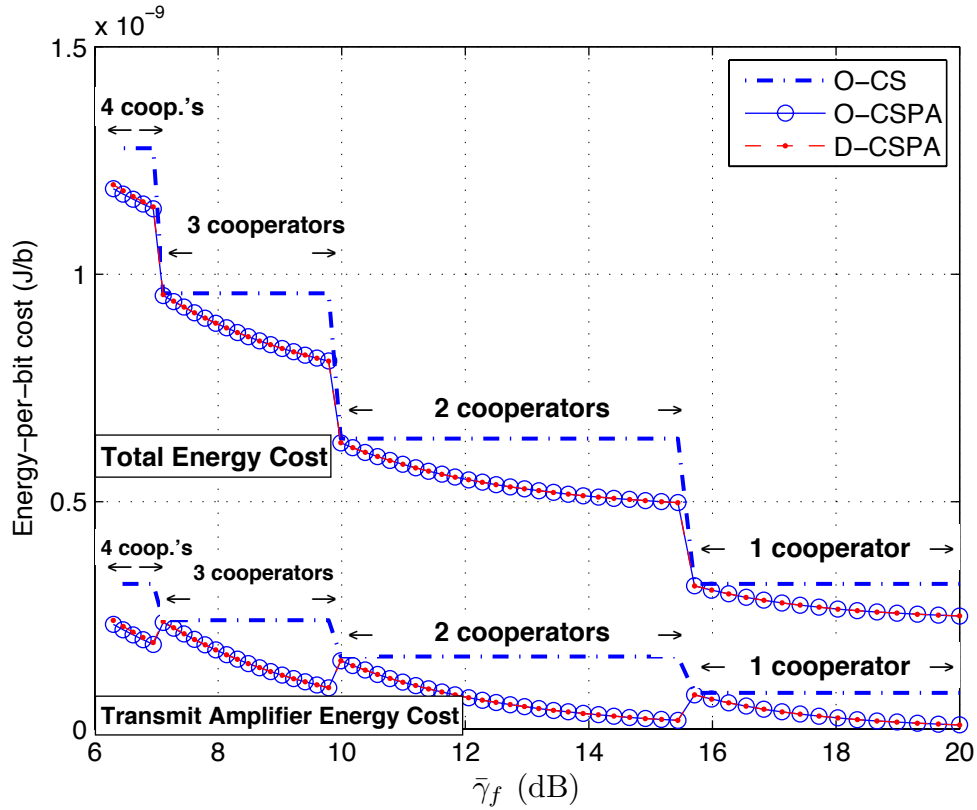
Figure 4.9: Square grid deployment: Energy-per-bit cost vs Average SD SNR; total energy cost and transmit amplifier energy cost.

in hostile environments, where nodes are dispersed randomly in the region of interest. We consider randomly deployed nodes and we analyze the average energy-per-bit performance of the distributed and centralized (optimal) schemes. Eight nodes are randomly deployed in the square area depicted in Figure 4.8 with S located in the center. 20 simulations are carried out and the results are averaged.

As depicted in Figure 4.10, R-CS operates poorly when the average SD SNR is low and cannot find feasible cooperation sets for some of the simulations, particularly for $\bar{\gamma}_f < 12.5$ dB. However, the cooperation schemes with smart selection, namely O-CS, O-CSPA and D-CSPA, enable communication even for very low $\bar{\gamma}_f$ at the designated average BER level, $P_{th} = 10^{-4}$. It is observed that D-CSPA does not cause any performance degradation as compared to O-CSPA for $\bar{\gamma}_f$ greater than

13 dB. D-CSPA's performance deviates from the optimal point for low $\bar{\gamma}_f$, in which case more than 2 cooperators are required. However, even for those cases D-CSPA's maximum deviation from the optimal operating points (O-CSPA) are only 1.91%, 2.90% and 2.92%, at the average SD SNRs of 12 dB, 10 dB and 9 dB, respectively. D-CSPA operates at the optimal points for moderate $\bar{\gamma}_f$ and deviates only a little at low average SD SNRs. This makes D-CSPA an appropriate energy-efficient scheme for cooperative system implementations.

The results demonstrate that although D-CSPA scheme's performance may deviate from the optimal for extreme topologies, performance improvement due to the joint cooperation selection and power assignment scheme is not specific to a certain node deployment, as similar energy-per-bit cost reductions are obtained for diverse set of topologies.

4.5.1.2 Effect of Target Average BER Level

Wireless networks are expected to operate at predetermined levels of reliability and quality-of-service that reflect application specific requirements. Depending on the required level of reliability, i.e., target average BER level, the minimum number of cooperators needed and the power allocated to the cooperators change, which effects the energy-per-bit performance considerably. In this part, we evaluate and compare the effect of target average BER level on the average energy cost performance of D-CSPA, O-CSPA, O-CS and R-CS schemes. We use the same random topology as described in Section 4.5.1.1.4.

In Figure 4.11, we observe that, for stringent target average BER levels, multiple cooperators are required and the energy cost of transmission is increased. As target average BER level is increased, D-CSPA and O-CSPA try to reduce the number of cooperators and adjust the transmit power levels to save energy while still satisfying
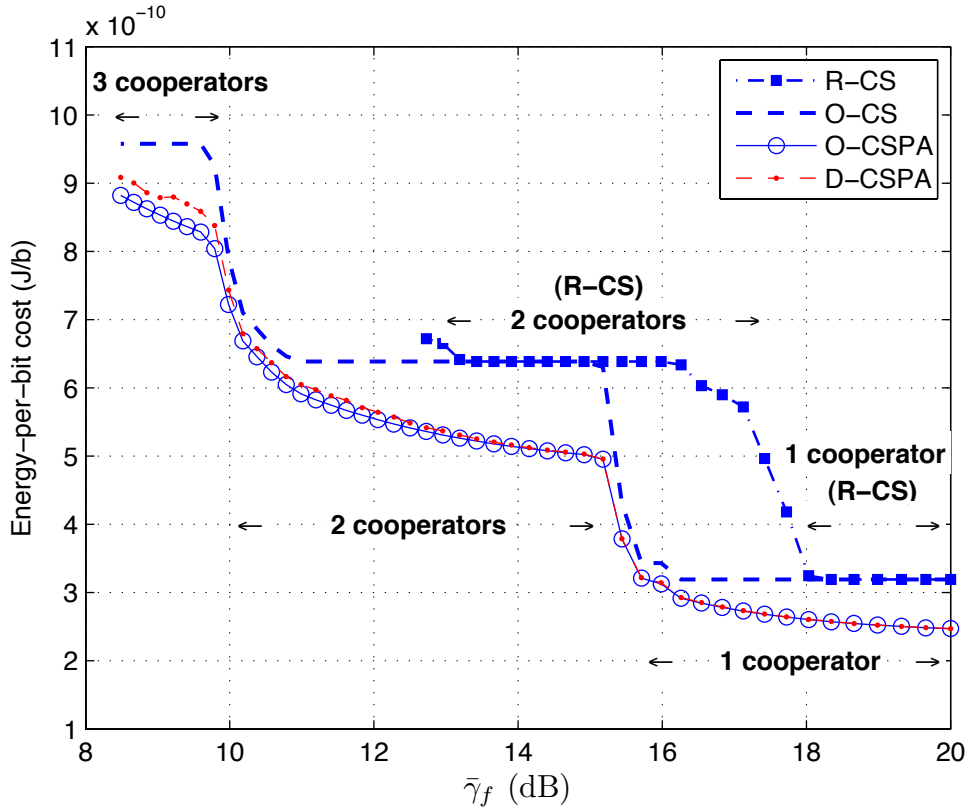
Figure 4.10: Random deployment: Average energy cost vs Average SD SNR $(\bar{\gamma}_f)$; total energy cost.

the target average BER. In all cases, D-CSPA and O-CSPA significantly outperform O-CS and R-CS algorithms. Even when $P_{th} = 2 \cdot 10^{-5}$, D-CSPA exceeds the optimal energy cost only by 3.26%, whereas it still provides a reduction by 7.31% in the total energy cost as compared to O-CS.

The results reveal that unlike R-CS, which fails to even actuate cooperation below the BER levels of 6.10^{-5}, D-CSPA guarantees reliable communication while still providing significant energy-savings. Furthermore, the results demonstrate the need for smart cooperator selection for reliable communication, and D-CSPA is shown to provide the required level of reliability with minimal number of cooperators with the assigned transmit power levels very close to the power levels of O-CSPA, even for
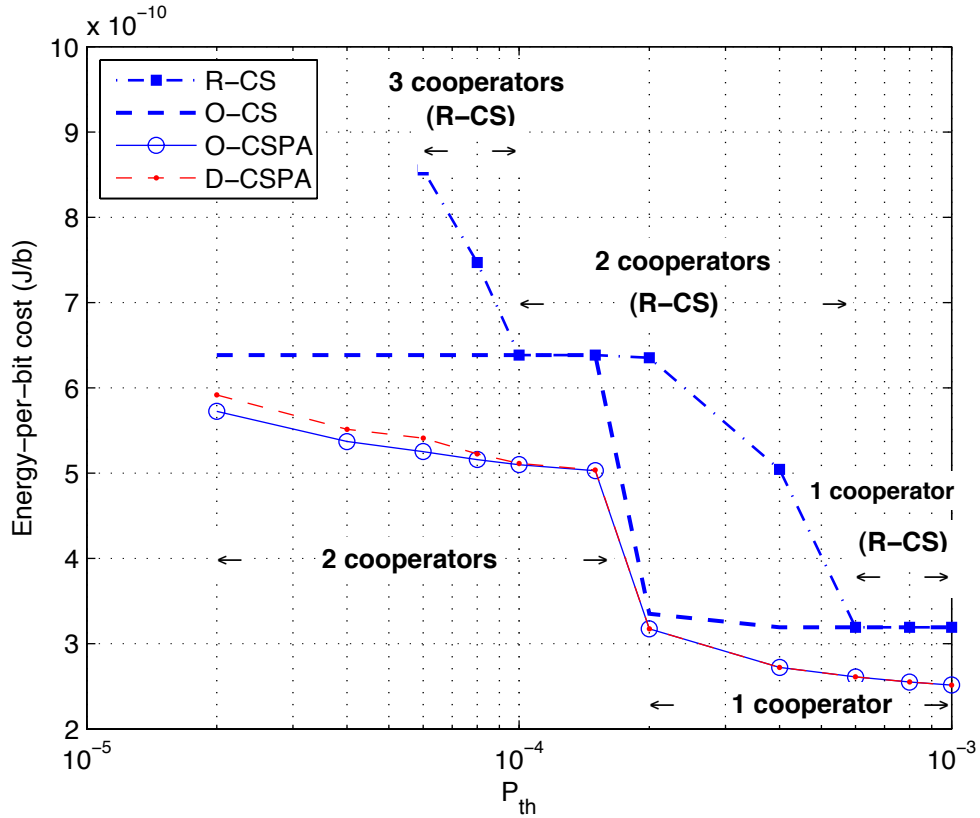
Figure 4.11: Effect of target average BER level: Average energy cost vs Average BER threshold (P_{th}).

very low target BER levels.

4.5.1.3 Effect of Power Consumption Model

The energy dissipated at the circuitries of the cooperators has a significant effect on the energy-efficiency of the multi-relay cooperative systems as the transceiver energy consumption increases polynomially with the increased number of cooperators. Solution to the minimum energy cooperation set selection problem depends on the power consumption model employed. We know from (4.1) that the amount of energy consumed at the transceiver circuitry is invariable regarding which cooperators are selected, but vary with respect to the number of cooperators. Besides, the amount of transceiver energy consumption depends on the technology used, and as technology

progresses energy-efficient sensor node implementations become available [92, 93].

For a thorough energy-efficiency analysis of our joint cooperator selection and power assignment method with respect to random cooperator selection, here, we evaluate the performance of D-CSPA and O-CSPA as compared to R-CS when the transceiver energy consumption level is varied in a broad range, with respect to ϵ_{ta}. We calculate the percentage of energy saved by D-CSPA with respect to R-CS as $[\mathcal{E}(\text{R-CS}) - \mathcal{E}(\text{D-CSPA})]/\mathcal{E}(\text{R-CS})$. Figure 4.12 depicts the energy savings offered by D-CSPA and O-CSPA for representative average SD SNR levels, namely $\bar{\gamma}_f = 10$ dB, 14 dB and 18 dB, when the average BER level is set as $P_{th} = 10^{-4}$ and the decode-and-regenerate threshold is set as $\gamma_{th} = 20$ dB.

It is observed that as the amount of transceiver circuitry energy cost is decreased, energy savings provided by smart cooperation set selection is increased significantly. It can be said that as less energy consuming circuitries become available, the energy savings offered by D-CSPA and O-CSPA schemes are expected to increase further. Note that, for low $\bar{\gamma}_f$, R-CS operates poorly, and D-CSPA and O-CSPA always outperforms R-CS. Due to this fact, for low $\bar{\gamma}_f$, D-CSPA's and O-CSPA's energy savings over R-CS scheme become independent of the transceiver circuitry energy cost.

The results indicate that for the currently available transceiver circuitries [90], 20% energy saving can be obtained using D-CSPA. Furthermore, it is revealed in Figure 4.12 that as the energy aware sensor node implementations become available [93], energy savings around 90% can be attained by employing D-CSPA.

4.5.1.4 Effect of Error in Channel State Information

Wireless networks are prone to errors in CSI, which may render the network inoperable. Considering the performance of distributed algorithms, errors can have a
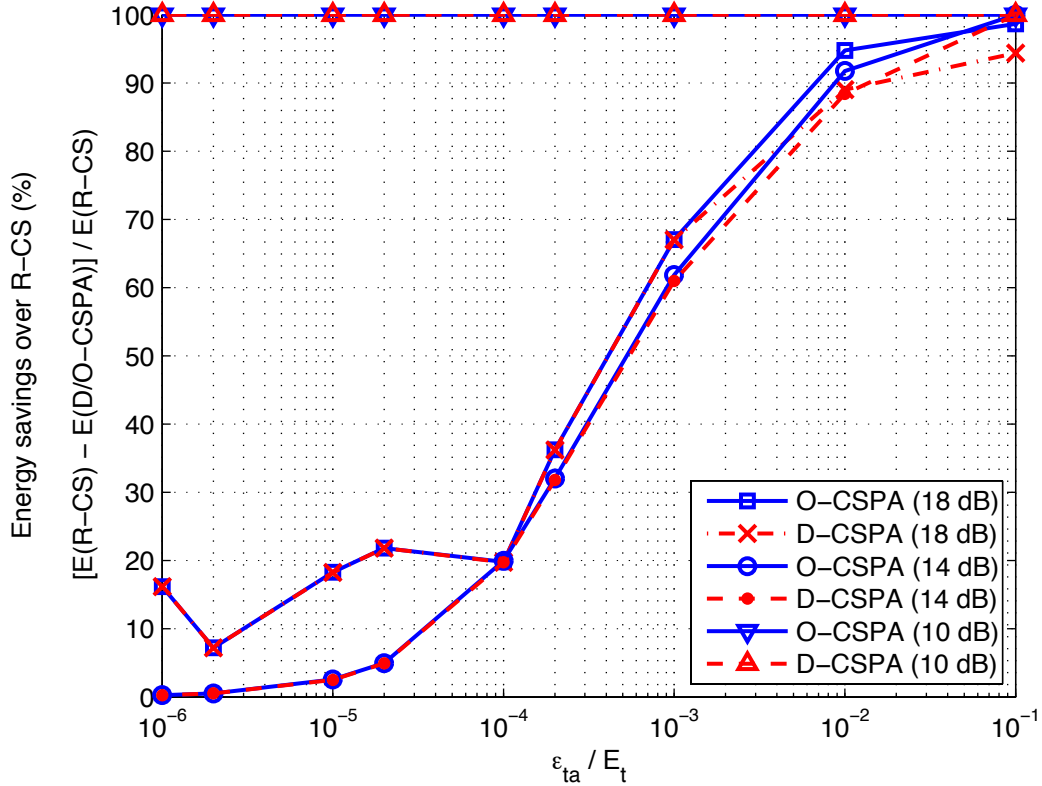
Figure 4.12: Effect of power consumption model: Energy savings over R-CS vs Transceiver energy cost, for $\bar{\gamma}_f = 10, 14, 18$ dB.

significant impact on cooperator selection and power assignment solutions owing to the accumulation of error.

Here, we evaluate the sensitivity of D-CSPA to the errors in the channel state information. We define σ_e^2 as the amount of error in the channel statistics of a given channel. Specifically, when the error variance is given as $\sigma_e^2 = 0.2$, it should be interpreted as all the nodes in the network compute/retrieve all the statistics with 20% error. Note that, assuming each node computes/retrieves all the channel statistics erroneously represents a worst case scenario. Figure 4.13 depicts the deviation of the average energy performance of D-CSPA with errors from the performance of O-CSPA without errors for different average SD SNR, as the amount of error, σ_e^2, is varied. For the simulations, the following system parameters are used: $P_{th} = 10^{-4}$,

$\gamma_{th} = 20$ dB, σ_e^2 is varied between 0 and 0.2.

It is observed in Figure 4.13 that for average SD SNR values that require one or two cooperators, D-CSPA is immune to errors; D-CSPA deviates from the optimal operation point by at most 11%, but still outperforms R-CS without error. When $\bar{\gamma}_f$ is decreased, D-CSPA becomes more sensitive to errors. This is because for very low $\bar{\gamma}_f$, more than 2 cooperators are needed, in which case error may sum up and obfuscate the joint cooperation set selection and power assignment process. Nevertheless, it is important to note that, despite the increased CSI sensitivity with decreased $\bar{\gamma}_f$, D-CSPA still provides significant energy savings over R-CS scheme.
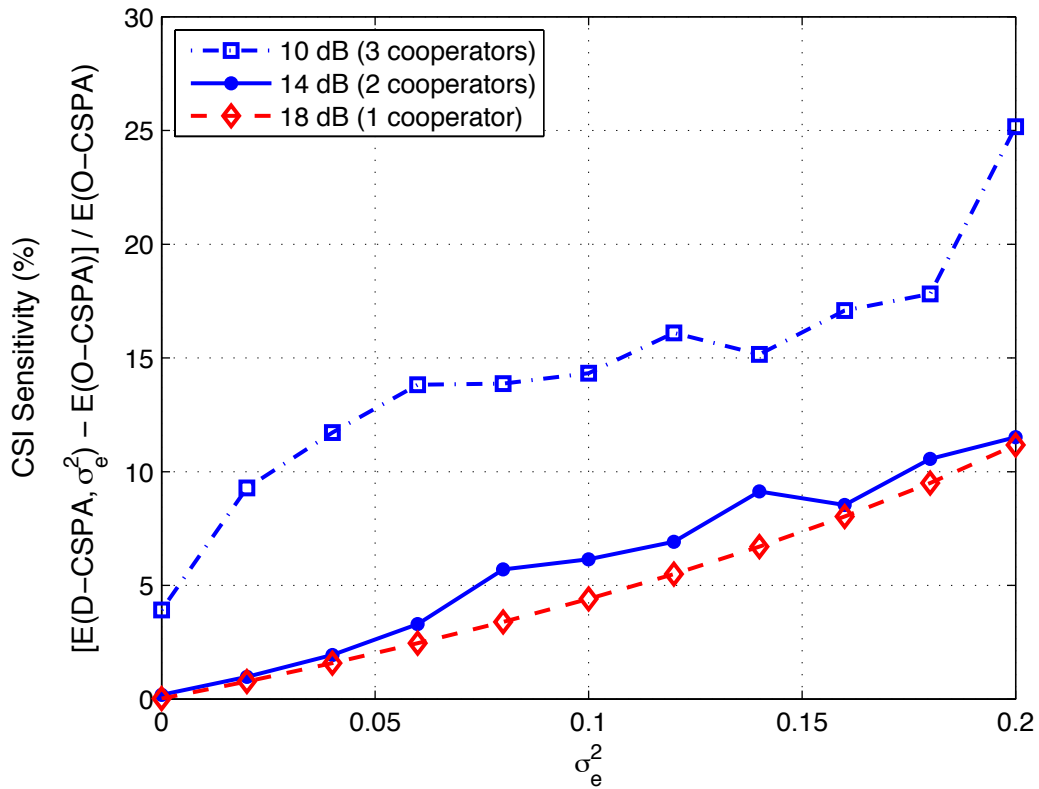
Figure 4.13: Effect of error in channel statistics information: CSI sensitivity vs σ_e^2, for $\bar{\gamma}_f = 10, 14, 18$ dB.

The results reveal that the operation of D-CSPA is not degraded even under

extortionate levels of CSI misinformation, and it is demonstrated that D-CSPA is a robust distributed method suitable for WSN applications.

4.5.2 Performance of D-CSPA in COMAC Protocol

In this section, we provide the ns-2 simulation results that depict the performance of D-CSPA within COMAC, in comparison to direct transmission. We have modeled and implemented our COMAC protocol with D-CSPA in ns-2 environment [39]. Our implementation in ns-2 shares the same physical and MAC layer models as described in 3.2.3. Moreover, D-CSPA algorithm is incorporated into our ns-2 model following the descriptions in section 4.4.2. For direct transmissions, we assumed IEEE 802.15.4's MAC [94] with additional RTS/CTS feature [4], so that the MAC schemes of the compared algorithms are similar (i.e., both are based on CSMA/CA with reservations).

In the simulations, the source node generates packets according to Poisson distribution with an average rate of 125 kbps, such that the source node always has a packet in its buffer to send to the destination node. We used the following physical layer settings in accordance with IEEE 802.15.4 standard [94]: Each node uses data transmission rate of 250 kbps. The data packet size is set as 128 bytes, C-RTS is of 15 bytes long, while C-CTS, ACO and ACK packets are of 13 bytes. All control packets have been set to these given sizes, which are large enough to carry the desired information (channel information, duration fields etc.), hence the overhead measurements reflect accurate values. In the simulations, we assumed a maximum transmission power level of 1 mW in accordance with [90]. For the wireless channel, we implemented the two-ray ground path loss model with exponent 4, and we modeled each data packet to undergo independent Rayleigh fading. It is assumed that a packet is successfully received if its instantaneous SNR is above 20 dB. All

results depict the averages of the results obtained from 20 realizations and each run for simulation duration of 50 seconds.
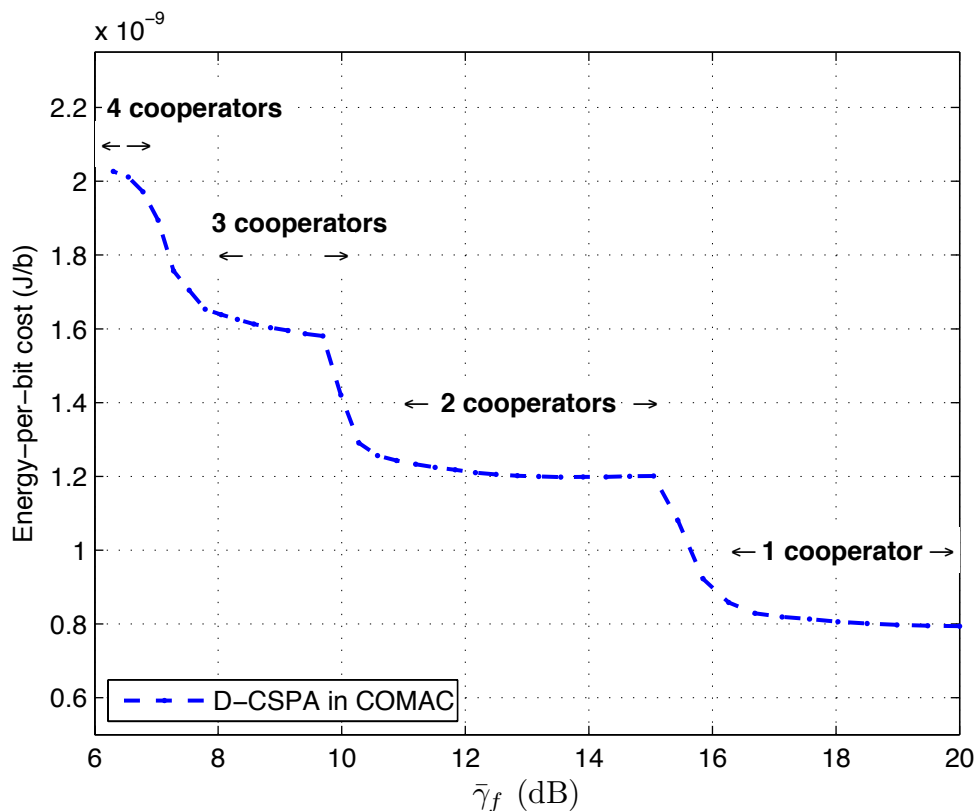
Figure 4.14: Energy-per-bit cost of D-CSPA in COMAC.

In Figure 4.14, we depict the energy-per-bit cost of the D-CSPA algorithm realized in COMAC protocol. By this experiment, we have observed that the energy behavior of D-CSPA algorithm in the random topology (shown in Figure 4.10) is perfectly repeated for the practical implementation of D-CSPA within COMAC protocol; except that this time, the energy cost is about doubled when the costs of realistic MAC implementation is considered. When the energy cost of D-CSPA is compared to direct transmission in Table 4.1, we observe that the energy cost of D-CSPA is 1/2 - 1/94 times the energy cost of direct transmission, due to improved channel quality and reduced number of retransmissions owing to diversity gain provided by cooperation,

which is enabled with minimized energy costs, thanks to optimal cooperator selection and power allocation by D-CSPA.

Table 4.1: Energy Cost (nJ/b)

$\bar{\gamma}_f(dB)$	6	8	10	12	14	16	18	20
Direct	∞^{a}	∞	124	31	12	5.40	2.88	1.80
D-CSPA	2.03	1.64	1.31	1.21	1.20	0.88	0.81	0.79

[a] Significantly high value.

Table 4.2: Throughput, Delay, MAC overhead Performance

$\bar{\gamma}_f$ (dB)	Throughput (b/s)		Average Delay (s)		MAC Overhead (b/s)	
	Direct	D-CSPA	Direct	D-CSPA	Direct	D-CSPA
6	~ 0 [b]	61658	∞	0.0044	∞	991
8	~ 0	61385	∞	0.0046	∞	838
10	185	61140	3.99	0.0045	431	758
12	730	60700	1.01	0.0046	433	690
14	1800	59250	0.38	0.0047	436	687
16	4300	61483	0.15	0.0044	442	556
18	8047	62199	0.065	0.0043	453	552
20	13106	62159	0.031	0.0042	469	556

[b] Significantly low value.

In Table 4.2, we provide the throughput and delay performance as well as overhead cost of D-CSPA in COMAC again together with direct transmission in IEEE 802.15.4 MAC. It is observed that the throughput of D-CSPA is 4 - 300 times that of direct transmission, and the delay of direct transmission is 8 - 800 times higher than that of D-CSPA, since retransmissions are prevented by robust cooperative transmissions. MAC overhead is measured around 1% of achieved throughput for D-CSPA, and for direct transmission, constant overhead is observed, which is at least 4% of achieved throughput.

The results presented in this section prove that our proposed D-CSPA algorithm in a practical MAC implementation, not only offers significant energy savings, but

also provides significant throughput improvement and delay reduction with minimal overhead, depicting a promising potential as a practical cooperative scheme as compared to standard direct transmission.

4.6   Discussion

In this chapter, we have studied the energy minimal joint cooperator selection and power assignment problem under transmit power constraints such that the cooperative transmissions satisfy a predetermined average BER target. We have derived the average BER of the cooperative system, and we have proposed a simple yet close approximation to facilitate simple cooperator selection methods with closed form power assignment solutions.

We have formulated the joint cooperator selection and power assignment problem using our BER approximation, we have presented the optimal solution (O-CSPA) and proposed a distributed implementation (D-CSPA). The performance of O-CSPA and D-CSPA algorithms are evaluated considering various network topologies, target average BER levels and different power consumption models. Our results demonstrate that smart cooperator selection is essential, as it provides efficient resource allocation with reduced overhead leading to improved system performance. It is further observed that with optimal transmit power assignment, energy dissipated at the transmit amplifiers can be reduced by 80%, while maintaining long-haul transmissions at the demanded average BER level. Also, it is shown that total energy cost of communication can be reduced by 20% considering current transceivers. As less energy consuming circuitries become available, the energy savings offered by cooperative systems can be improved up to 90%. We also demonstrate that our distributed method, D-CSPA provides similar energy savings with the optimal scheme, O-CSPA, with much lower (worst case) complexity and with a robust performance even under

errors in channel statistics. Our implementation and simulations of D-CSPA algorithm in our COMAC protocol demonstrate that our distributed algorithm causes minimal overhead, yields improved throughput and reduced delay, while significantly reducing the energy consumption.

Note that, in the above performance analysis the computational cost is not considered in terms of energy, but in terms of complexity only. The inclusion of the exact energy cost due to the algorithm computations is not possible as the available data sheets of the considered receiver circuitries lacked this information. Nevertheless, it is safe to deduce that the relative complexity results also reflect the relative energy costs of the algorithms, and lower complexity implies lower energy cost for computations.

The results of this chapter have been submitted for publication in [95].

5 A CROSS-LAYER MULTI-HOP COOPERATIVE NETWORK ARCHITECTURE

In the previous chapters, we have considered cooperation in a single hop, and proposed solutions for implementing cooperation over a single hop. In this chapter, multiple hop ad hoc networks are considered, and a novel decentralized cross-layer multi-hop cooperative network architecture is proposed for improving the performance of multi-hop communication via cooperation. In this architecture, we present a cooperative routing framework with three cooperative forwarding schemes, a cooperative flooding scheme and two decentralized opportunistic cooperative forwarding methods, as well as the design of Routing Enabled Cooperative Medium Access Control (RECOMAC) protocol, which incorporates the physical, MAC and routing layers. The proposed architecture exploits randomized distributed space-time codes (RDSTC) at the physical layer to realize cooperative diversity. In our architecture, routing layer functionality is submerged into the MAC layer to provide seamless cooperative communication while the messaging overhead to set up routes, select and actuate relays is minimized.

This chapter is organized as follows. In section 5.1, we present our motivation for our work by providing the reader with the state of the art on cooperative routing literature. In section 5.2, we describe the system model, consisting of the network model and the physical layer model, specifically RDSTC. In section 5.3, we present our cooperative forwarding strategies with RDSTC that form the framework for our cross-layer architecture, and in section 5.3.3, we present the performance analysis of our cooperative forwarding strategies. Next, we introduce our cooperative cross-layer architecture, RECOMAC, in section 5.4. In section 5.4.4, we provide the performance

analysis of RECOMAC, followed by the discussion in section 5.5.

5.1   Background and Related Work

Wireless ad hoc networking has recently become popular with applications, such as wireless mesh networks, wireless sensor networks and mobile ad hoc networks, owing to their attributes such as, minimal configuration requirements, quick deployment and decentralized operation. Different from centralized wireless networks, where nodes communicate with a base station or an access point via single hop links, in wireless ad hoc networks, the end-to-end communication is carried over multiple hops, realized through intermediate nodes.

Despite many potential applications as exemplified above, the performance of wireless ad hoc networks is still limited because: i) The end-to-end path consists of multiple concatenated unicast links along specified nodes on a predetermined path. Those unicast links suffer from errors due to channel impairments, caused by fading, and failure of even a single link can make the entire end-to-end path inoperable, requiring route rediscovery and maintenance procedures. In case of harsh environmental conditions, the route discovery phase may need to be repeated several times causing heavy messaging burden, thereby leading to wasted network bandwidth and degraded throughput. ii) Routing messages are delivered by contending for the available medium. In addition to the burden for rediscovery, the contention avoidance and resolution mechanisms also steal from the network bandwidth that could otherwise be used for data communication. Moreover, as the network size is increased, the message overhead of routing strategies is also increased, resulting in further degradation in throughput and delay performance.

As discussed in the previous chapters, there is vast amount of literature on cooperation in the physical layer [8, 9, 11, 19, 52], and there is increasing interest

on MAC layer architectures supporting cooperative diversity for single hop networks [28,84,85,96,97]. However, the literature on multi-hop cooperative protocols is still limited [29,35–38]. A common approach in the literature to incorporate cooperative diversity in multi-hop networks is to employ cooperation on already discovered and established routes. For example, in [35], cooperation is exploited to mediate an unreliable single hop link on the non-cooperative route, such that the original link is kept but its quality is improved by cooperative transmissions of the neighbors. On the other hand, in [36] and [37], an opportunistic virtual MISO (v-MISO) link is formed only when a link fails. As opposed to the schemes that consider single link improvements within non-cooperative routes, in [29] and [38], the objective is to improve the end-to-end performance of a route by utilizing cooperative links in lieu of multiple links, and obtain a route with cooperative links based on a non-cooperative route.

The aforementioned schemes restrict packet forwarding to be completed on a prior non-cooperative route, hence they do not make use of all the route alternatives that can be realized for end-to-end communication between a source-destination pair. Furthermore, in these schemes, the number of relays participating in cooperation is fixed due to the fixed dimension of the underlying distributed space-time code (DSTC) or for reducing the computational complexity. Since realization of cooperative diversity requires extra messaging for cooperative set selection and actuation, under realistic wireless network scenarios, the throughput of the aforementioned systems will further degrade. This automatically raises the problem of how to select and actuate the relays in a decentralized, distributed fashion without obliterating the benefits of cooperation.

A cooperative routing scheme that circumvents the relay selection and actuation problem by use of opportunistic large arrays (OLA) [98] at the physical layer has

been presented in [70]. OLA relies on the idea that each node accumulates energy from multiple transmissions of a packet, and relays this packet when the accumulated energy is above a predetermined threshold. However, the authors of [70] consider a perfect MAC protocol, which provides flawless coordination among the nodes, while packets are routed through the network. Furthermore, although OLA can be favorable for network flooding, its operation for unicast routing is problematic without an appropriately designed MAC protocol. If transmissions are not coordinated via a MAC protocol, OLA can result in multiple nodes to transmit different packets at overlapping periods, resulting in significantly degraded system performance. The proper design of multi-hop cooperative protocols with cooperative diversity involves optimizing the behavior and performance of various layers jointly.

In this chapter, we propose a cross-layer cooperative network architecture that involves *cooperative flooding* and *cooperative forwarding* mechanisms for packet forwarding, and Routing-Enabled Cooperative Medium Access Control (RECOMAC) protocol, which facilitates these mechanisms by incorporating physical, MAC and routing layers. Our architecture exploits randomized coding via RDSTC [71], at the physical layer. Randomized coding alleviates relay selection and actuation mechanisms, as a specific antenna index is not allocated per relay, and therefore the coordination among the relays is reduced. In our cooperative forwarding mechanisms, the coded packets are forwarded from a cooperative set to a consecutive cooperative set in the direction towards the final destination, while no messaging is required among the relays of a cooperative set.

5.2 System Model and RDSTC Preliminaries

We consider a wireless ad hoc network with nodes equipped with a single antenna. It is assumed that each node, i, has the capability to acquire its location information,

namely its coordinates (x_i, y_i), via a positioning system, such as Global Positioning System (GPS) [99, 100]. We assume that there are N nodes in the network, and the nodes are assumed to know the node density, υ, of the network. In this network, a source node, S, generates packets to be delivered to a destination node, D. It is presumed that S and D are located in the network such that multiple wireless hops are required for the end-to-end communication.

It is assumed that transmission of node i is attenuated by a path-loss exponent of α, and the instantaneous channel is affected by slow, flat Rayleigh fading, which is independent from other channels. In particular, the channel fading between nodes i and j is denoted as ζ_{ij}, and the instantaneous channel gain, $|h_{ij}|^2$, between nodes i and j is given as $|h_{ij}|^2 = |\zeta_{ij}|^2 d_{ij}^{-\alpha}$. Note that, $|h_{ij}|^2$ is exponentially distributed with mean $d_{ij}^{-\alpha}$, where d_{ij} is the distance between the nodes i and j, and $d_{ij}^{-\alpha}$ represents the path-loss model [49]. The fading coefficients remain the same during one packet duration. It is also assumed that the additive white Gaussian noise at all receivers have equal power spectral density, $N_0/2$. Below, we describe the direct and cooperative transmission models, which are depicted in Figures 5.1 and 5.2.
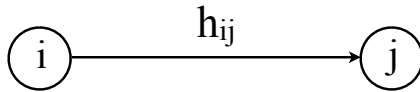
Figure 5.1: System model: Direct transmission.

5.2.1 Direct Transmission

The direct transmission of node i results in an instantaneous SNR of $\gamma_{ij} = \frac{P|h_{ij}|^2}{N_0}$ at node j, where P is the transmission power (depicted in Figure 5.1). It is assumed that the packet transmitted by node i can be successfully decoded by node j if $\gamma_{ij} \geq \gamma_{th}$, where γ_{th} corresponds to an SNR level for correct reception of a packet with a certain level of reliability, and it depends on modulation and channel coding used. Alternately, we can consider this threshold as arising from the outage probability formulation for fixed transmission rate [101].
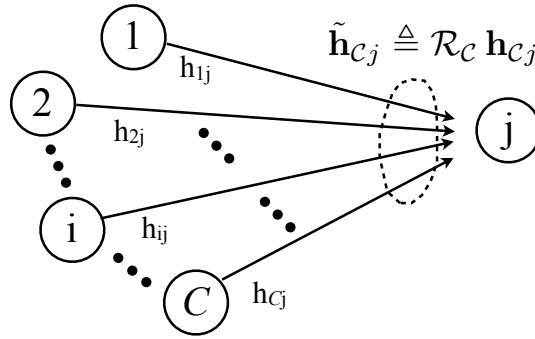
Figure 5.2: System model: Cooperative transmission with RDSTC.

5.2.2 Cooperative Transmission with Randomized Distributed Space-Time Codes

In this work, cooperative transmissions are realized via RDSTC. Here, we provide a brief description of RDTSC and their application in cooperation. In Figure 5.2, we depict the cooperative transmission model with RDSTC. For a comprehensive description, the reader is referred to [71].

Let $\mathbf{z} = [z_0 \; z_1 \ldots z_{n-1}]$ be the block of symbols to be transmitted from node i to node j via cooperation of multiple intermediate nodes. We denote the node set that has successfully decoded the symbols, $\mathbf{z}$, as $\mathcal{C}$, and $C \triangleq |\mathcal{C}|$ represents the number of nodes in this set. The main idea is that the nodes in $\mathcal{C}$ can form a cooperative set

136

to forward data towards node j. In the following, we describe the processing at each cooperating node and analyze the decoding at node j.

At each node, in $\mathcal{C}$, $\mathbf{z}$ is mapped onto a matrix $\mathcal{G}(\mathbf{z})$, as in standard space-time coding: $\mathbf{z} \to \mathcal{G}(\mathbf{z})$, where $\mathcal{G}(\mathbf{z})$ is an $n \times L$ space-time code matrix, and L denotes the number of antennas in the underlying space-time code. Then, each node in $\mathcal{C}$ transmits a random linear combination of columns of $\mathcal{G}(\mathbf{z})$. Let $\mathbf{r}_k$ be the $L \times 1$ random vector that contains the linear combination of coefficients for the kth node in the set $\mathcal{C}$. Then, RDSTC can be expressed as the following mapping:

$$\mathbf{z} \to \mathcal{G}(\mathbf{z})\,\mathcal{R}, \tag{5.1}$$

where $\mathcal{R} = [\mathbf{r}_1\ \mathbf{r}_2 \dots \mathbf{r}_C]$ is an $L \times C$ matrix, named as *the randomization matrix.* Since node processing is intended to be local, $\mathbf{r}_k$'s are independently assigned for each $k \in \mathcal{C}$. This property allows RDSTC to be implemented in a decentralized fashion. We assume that entries of $\mathcal{R}$ are identically and independently distributed (i.i.d.), chosen according to a given distribution. In [71], distributions which provide maximal diversity are identified.

We denote the vector that represents the channel coefficients between the nodes in $\mathcal{C}$ and the receiver node j as $\mathbf{h}_{\mathcal{C}j} = [h_{1j}\ h_{2j}\ \dots\ h_{Cj}]$. The signal received by node j is given as

$$\mathbf{y} = \mathcal{G}(\mathbf{z})\,\mathcal{R}\,\mathbf{h}_{\mathcal{C}j} + \mathbf{w}, \tag{5.2}$$

where $\mathbf{w} \sim \mathcal{N}_c(\mathbf{0}, (N_0/2)\mathbf{I})$, and $\mathbf{h} \sim \mathcal{N}_c(\mathbf{0}, (N_0/2)\boldsymbol{\Sigma}_{h_{\mathcal{C}j}})$. We assume that node j employs coherent detection which requires channel estimation. Note that, the received signal can be interpreted to have passed through an effective channel of $\tilde{\mathbf{h}}_{\mathcal{C}j} \triangleq \mathcal{R}_{\mathcal{C}}\,\mathbf{h}_{\mathcal{C}j}$, as depicted in Figure 5.2. Thus, instead of estimating the channel vector $\mathbf{h}_{\mathcal{C}j}$ and the randomization matrix $\mathcal{R}_{\mathcal{C}}$, separately, the receiver can estimate the effective channel coefficients of $\tilde{\mathbf{h}}_{\mathcal{C}j}$, and it does not need to know the identity of

the nodes in $\mathcal{C}$. For orthogonal space-time codes, $\mathcal{G}(\mathbf{z})$, the instantaneous SNR of the cooperatively transmitted signal received at node j is given as [71]

$$\gamma_{\mathcal{C}j} = \frac{P||\,\mathcal{R}_\mathcal{C}\,\mathbf{h}_{\mathcal{C}j}\,||^2}{N_0}.$$

Hence, the cooperative transmission can be successfully decoded by node j, if $\gamma_{\mathcal{C}j} \geq \gamma_{th}$. At this point, it is assumed that all nodes use the same data rates, i.e., coding and modulation schemes.

For the cooperative transmissions, we require that for each cooperative set, the total transmit power is approximately equal to direct transmission, and the total power of P is equally distributed among the relays via power normalization. The power normalization ensures that the average transmit power of a cooperative set and direct transmission are similar, so that the signal quality improvement due to cooperative diversity is observed, while maintaing the total interference approximately the same as the direct scheme. The details on power normalization is provided in section 5.3.2.1.

Note that, unlike regular DSTC [53] used in previous cooperative schemes [11, 28, 29, 35, 36, 38, 96], RDSTC does not allocate an antenna index to each relay, which means relay selection and actuation mechanisms are not necessary. This alleviates the coordination requirement among the source and the relays (which can cause potential reduction in the signaling overhead for initiation of cooperative transmission). Furthermore, in the schemes using DSTC, the number of cooperating nodes is constrained by the dimension of the underlying space-time code. However, in RDSTC, addition of more relays is possible without a bound on the total number of nodes in the cooperative set, which can further improve the overall signal quality.

5.3 Cooperative Routing Framework using RD-STC

In this section, we present three cooperative packet forwarding mechanisms that exploit RDSTC in ad hoc networks. The proposed cooperative forwarding schemes form the basis for our cooperative cross-layer architecture, RECOMAC, which will be discussed in detail in Section 5.4. For the cooperative transmissions, we require that each node in the cooperative set uses a normalized power level. The power normalization ensures that the average transmit power of a cooperative set and a non-cooperative transmission is the same. This way, we are able to observe the signal quality improvement due to cooperative diversity, while maintaing the total transmit power cost and interference approximately the same as a non-cooperative scheme. The details on power normalization is provided in Section 5.3.2.1.

5.3.1 Cooperative Forwarding Strategies

Consider the network realization given in Figure 5.3, where the operation of different forwarding schemes are demonstrated for the same realization. In Figure 5.3a, a direct route between S and D is shown. Direct (non-cooperative) routes require each node to know by whom the packet is to be received at the next hop, and over each hop they also necessitate MAC mechanisms to coordinate transmissions of the nodes, avoid and resolve collisions, if any. The three proposed cooperative forwarding schemes are explained in detail next.

5.3.1.1 Cooperative Flooding (CF)

In Cooperative Flooding, CF, the source node, S initiates flooding by direct transmission, and then successive packet forwarding takes place using cooperative transmissions with RDSTC. The transmission of the source node is in broadcast mode and

(a) Direct route

(b) Cooperative flooding (CF)

(c) CFPR
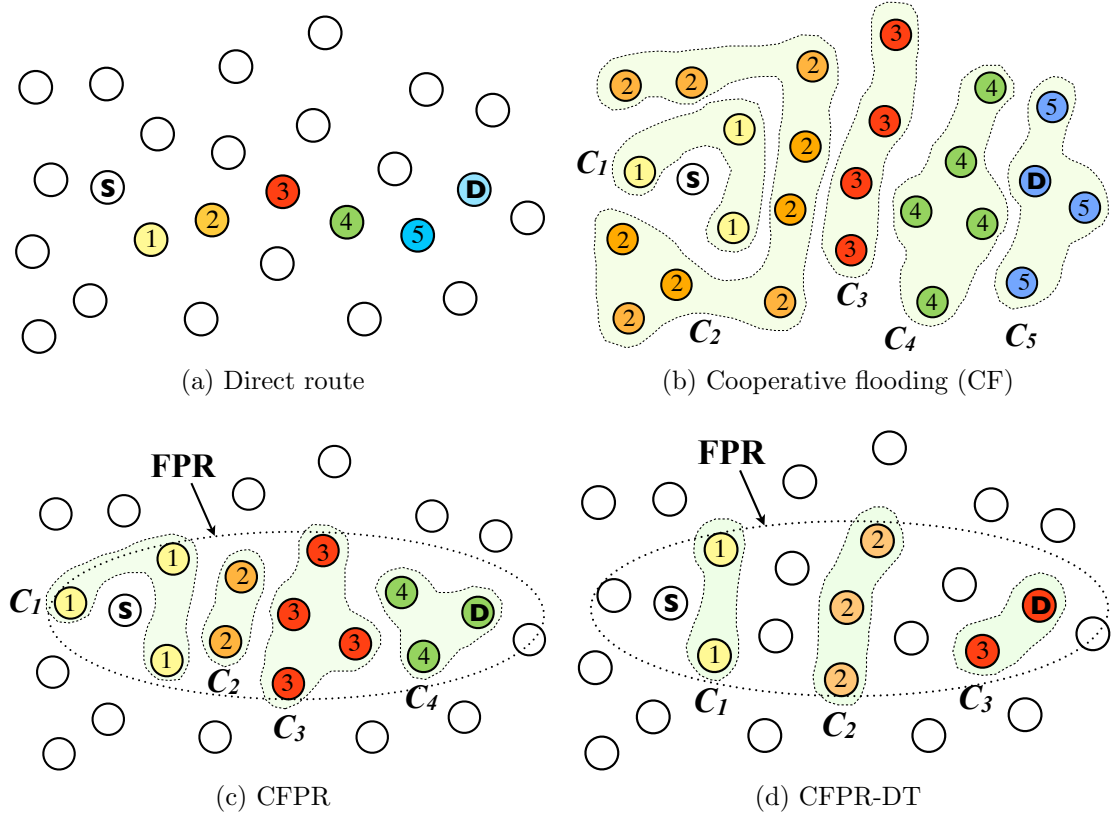
(d) CFPR-DT

Figure 5.3: Packet forwarding via direct (non-cooperative) routing, CF, CFPR, CFPR-DT.

it is received by multiple neighboring nodes. Let $\mathcal{C}_1 = \{j | \gamma_{Sj} \geq \gamma_{th}\}$ denote the set of first hop nodes that receive the source's transmission. Each node in $\mathcal{C}_1$ re-encodes the packet via RDSTC and the packet is cooperatively transmitted. In particular, after the received symbols are successfully decoded, each node i in $\mathcal{C}_1$ maps the received symbols onto the space-time code matrix $\mathcal{G}(\mathbf{z})$, multiplies this matrix with its randomization vector, $\mathbf{r}_i$, chosen from complex Gaussian distribution, and then sends the resulting matrix, $\mathcal{G}(\mathbf{z})\,\mathbf{r}_i$. The overall resulting symbol matrix due to the cooperative transmissions of all the nodes in $\mathcal{C}_1$ is given as (5.1), and the received signal is given as (5.2). The set of nodes that successfully receive the packet cooperatively transmitted by $\mathcal{C}_1$ form the second hop cooperative set, represented by $\mathcal{C}_2$. Now, each

node in $\mathcal{C}_2$ re-encodes the information received from $\mathcal{C}_1$ using RDSTC and forwards it cooperatively to the next set, as explained above, and this is carried out until the destination is reached, as depicted in Figure 5.3b. In general, the cooperative set at hop k can be written as

$$\mathcal{C}_k = \{j | \gamma_{\mathcal{C}_{(k-1)}j} \geq \gamma_{th}, j \notin \cup_{i=1}^{k-1} \mathcal{C}_i\},$$

where $\mathcal{C}_0 = \{S\}$. Note that, in CF, for the cooperative transmission decision, each node only checks whether the received SNR is above the predetermined threshold γ_{th}, and whether it has forwarded the same packet before. The nodes do not need any instantaneous information about the network, and furthermore, topology, channel states or the cooperation decisions of the other nodes. Cooperative sets are formed in a distributed manner based on the received instantaneous SNR levels, which change as a result of fading and mobility for each transmitted packet. Hence, each packet may be flooded by a different set of relays. For brevity of notation, we omit to represent the dependency of cooperative sets on instantaneous channel conditions and node locations.

CF can be used for data transfer to a particular destination, or for dissemination of common information throughout the network, such as dissemination of query packets. Due to cooperative transmission via RDSTC, CF does not require contention resolution mechanisms as conventional flooding with direct transmission. CF floods the network faster than conventional flooding, thanks to cooperative diversity gain. This will be further illustrated in Section 5.3.3.2.1.

CF policy is similar to the OLA approach of [98], as both schemes flood the network by cooperative transmissions. However, different from OLA and conventional flooding, in CF, the total transmit power is kept approximately normalized at each hop (see Section 5.3.2.1). Furthermore, in OLA, the cooperative transmissions are actuated when enough energy is accumulated at a node, while in CF, the nodes only

decode based on their reception from the previous cooperative set. Note that, when energy accumulation is considered, the transmission synchronization is essential, and a MAC protocol is required for handling firing times. However, none of these have been addressed in [98].

5.3.1.2   Cooperative Forwarding within Progress Region (CFPR)

In this scheme, the packets are progressively forwarded from the source, S to the destination, D, by RDSTC cooperative transmissions of the nodes, which reside in a predefined region, as depicted in Figure 5.3c.

Suppose that S has acquired the location information of D via a flooding algorithm, for example via our CF method, which will be discussed in detail later in this chapter. We propose the use of this destination location information to set up a regional route between S and D such that the progress of packets towards D is enhanced. We define forward progress as the progress made by a packet in the direction towards D at each hop, and we define the forward progress region (FPR) as a specific region between S and D. In Cooperative Forwarding within Progress Region, CFPR, only the nodes that reside in FPR are candidate relays for cooperative transmission. The use of FPR assures that the packet moves closer to D at each traversed hop.

Our aim in defining FPR is to improve the signal strength of the cooperative transmissions using RDSTC with normalized transmit power levels. Due to power normalization, the transmission range of nodes in a cooperative set concentrated in a small region close to the destination, can achieve higher average SNR levels at the next hop receivers, as compared to the range of nodes in cooperative sets with dispersed nodes in a large region, which is the case in CF.

In our studies, we have observed that the size and shape of the FPR affects the end-to-end performance of cooperative packet forwarding. Although various FPR

forms are possible, here, our aim is to utilize a simple FPR that is controlled via a few parameters, which can be adjusted to obtain a desired system performance depending on the node density. While large FPR may be required for end-to-end connectivity in sparse networks, dense networks may benefit from small FPR. In particular, FPR should be such that in order to guarantee sustained progress of forwarding, at each hop, sufficient number of cooperating nodes is included in the FPR. This calls for a sufficiently large region around S and between S and D. Moreover, in some cases, D may not be able to decode a packet due to a deep fade in its channel, although it resides in FPR. Hence, a sufficiently large region around D is also required to be included in the FPR, so that there are sufficiently many neighbor nodes around D, and these nodes can cooperatively transmit the packet when necessary. Here, we propose to use an elliptical FPR, as it satisfies the aforementioned requirements. The elliptical FPR has S and D located at its two foci, and its denoted by $\mathcal{F}(\Delta_1, \Delta_2)$, where Δ_1 and Δ_2 are semi minor and semi major axis of the elliptical region, respectively. The size and shape of the FPR can be controlled via Δ_1 and Δ_2 for optimizing the performance.

In CFPR, only the nodes that reside in the FPR and that receive the signal with an instantaneous SNR level above the threshold (γ_{th}) are actuated for cooperative transmission. Here, we assume that the location information of S and D, and the FPR parameters (Δ_1, Δ_2) are carried within each packet to be forwarded, so each node that successfully decodes the packet, can autonomously compute the FPR boundaries and decide whether it belongs to the FPR or not based on its own location (x, y). In CFPR, the cooperative set at hop k is given as:

$$\mathcal{C}_k = \{j | \gamma_{\mathcal{C}_{(k-1)}j} \geq \gamma_{th}, j \notin \cup_{i=1}^{k-1} \mathcal{C}_i, (x_j, y_j) \subseteq \mathcal{F}(\Delta_1, \Delta_2)\}$$

with $\mathcal{C}_0 = \{S\}$. Each node only determines whether it belongs to $\mathcal{C}_k$ or not, but it is unaware of the other nodes. Cooperative sets at each hop are again formed on the

fly, according to instantaneous channel conditions and node locations.

CFPR reduces the number of cooperating nodes at each hop as compared to CF, and also, since cooperative transmissions are normalized in power and the transmitters are concentrated in a region towards D, CFPR results in longer transmission ranges, leading to fewer hops as compared to CF, as illustrated in Section 5.3.3.2.1.

It is worthwhile to note that the idea of limiting packet forwarding to a specific elliptical region has been considered previously in [102] and [103], considering direct transmissions. These works try to improve the performance of conventional routing schemes with direct transmissions, and cooperation is not considered. Here, however, our setting and purpose is to come up with cooperative routing schemes that make use of RDSTC, and we propose the FPR approach for enhancing cooperative forwarding.

5.3.1.3   CFPR with Dual Threshold (CFPR-DT)

We have observed that the randomized coded cooperative transmissions of the nodes that use normalized power levels can provide high average received SNR levels, if they are concentrated in a small region. Hence, the forward progress of a packet can be further improved by constraining the size of the cooperative sets.

In CFPR with Dual Threshold, CFPR-DT, we propose that the nodes autonomously decide whether or not to participate in cooperative forwarding, by checking if the received SNR is above the minimum required SNR level, γ_{th}, and also below a predetermined upper threshold level, γ_d, in addition to checking whether they are in the FPR. Consider two consecutive cooperative hops of CFPR formed as $\mathcal{C}_{k-1} \to \mathcal{C}_k \to \mathcal{C}_{k+1}$, as depicted in Figure 5.3c. $\mathcal{C}_k$ consists of the nodes that receive the cooperatively transmitted signal from $\mathcal{C}_{k-1}$ at varying SNR levels (all certainly are above γ_{th}). Due to the effect of path-loss, the nodes that are close to $\mathcal{C}_{k-1}$ receive the signal with large

144

SNR levels with high probability; likewise the nodes that are far away from $\mathcal{C}_{k-1}$ receive the signal with lower, yet still sufficient SNR levels to decode the packet. This suggests that the transmission range of $\mathcal{C}_k$ can be further improved by preventing the nodes that receive the signal with high SNR levels from participating in cooperative transmission with set $\mathcal{C}_k$. In particular, our aim in employing the dual threshold is, at each hop, to form cooperation sets that include only the nodes that are closer to the destination node. This leads to CFPR-DT illustrated in Figure 5.3d.

For CFPR-DT, the cooperative set at hop k is given as:

$$\mathcal{C}_k = \{j | \gamma_{th} \leq \gamma_{\mathcal{C}_{(k-1)}j} \leq \gamma_d, j \notin \cup_{i=1}^{k-1} \mathcal{C}_i, (x_j, y_j) \subseteq \mathcal{F}(\Delta_1, \Delta_2)\}, \qquad (5.3)$$

where γ_d is the upper threshold value for the received instantaneous SNR. Similar to CF and CFPR, in CFPR-DT each node only determines whether it belongs to $\mathcal{C}_k$ or not, but it is unaware of the status of the other nodes. It is assumed that all FPR parameters (Δ_1, Δ_2) and SNR threshold γ_d, are carried within the packet as a part of the packet header.

CFPR-DT reduces the number of cooperating nodes per hop, as compared to CFPR, by further restraining the inclusion of a node in the cooperative set via γ_d. Cooperating nodes concentrated towards D provide longer transmission ranges, which leads to fewer hops in comparison with CFPR, as shown later in Section 5.3.3.2.1.

5.3.2 Power Normalization and FPR Parameter Selection

The performance of CF, CFPR and CFPR-DT strategies depend on power normalization and the selected FPR parameters, namely Δ_1, Δ_2 and γ_d. In this section, we address the criteria for power normalization and FPR parameter selection.

5.3.2.1 Power Normalization

The purpose of power normalization is to limit the total transmit power of a co-operative set, $\mathcal{C}_k$, to that of a system which employs direct transmission, such that gains of cooperative diversity is attained without increasing the power cost and the interference level as compared to direct transmission.

It is presumed that power normalization is carried out by equally dividing the available power budget, P among the cooperating nodes. In order to realize such power assignment in a decentralized fashion, it is necessary that each node in the cooperative set knows the number of actuated nodes in the set. However, acquiring this information instantaneously is impractical. Even if this can be realized under some oversimplified network and channel assumptions, solutions such as immediate feedbacks can cause substantial messaging overhead, which may reduce the benefits obtained by cooperation. Hence, here, for power normalization, we propose to use the average number of relays included or actuated in a cooperative set, instead of the exact instantaneous number. Our cooperative forwarding strategies suggest that the nodes which are actuated at hop k, i.e., $\mathcal{C}_k$, depend on the previous cooperative set, $\mathcal{C}_{k-1}$. Thus, the average number of relays at the kth hop, can be calculated conditioned on the previous relay set, $\mathcal{C}_{k-1}$ and then averaged over randomization matrix, fading and node location distributions, as $\bar{C}_k = E[C_k | \mathcal{C}_{k-1}]$.

The average number of nodes that participate in cooperative forwarding of the packet at the first hop of CFPR-DT, or equivalently, the average number of nodes that successfully receive the source transmission, and satisfy the FPR conditions and the upper threshold γ_d, can be computed as:

$$\bar{C}_1 = \iint_{(x,y) \in \mathcal{F}(\Delta_1, \Delta_2)} v[e^{-\gamma_{th}\Gamma_s(x,y)} - e^{-\gamma_d\Gamma_s(x,y)}]dxdy, \tag{5.4}$$

where $1/\Gamma_s(x,y)$ is the received average SNR at location (x,y) such that $\Gamma_s(x,y) =$

146

$(N_0/P)[(x - x_s)^2 + (y - y_s)^2]^{(\alpha/2)}$. Here, the nodes are assumed to be uniformly distributed with density υ, and fading coefficients are Rayleigh distributed, which result in exponentially distributed received SNR levels with mean values obtained as a function of the distance and path loss coefficient α, i.e., $|\zeta_{ij}|^2 d_{ij}^{-\alpha}$, as described in the system model, section 5.2. Thus, the exponential terms represent the probability of the received SNR at location (x, y) to remain between the two thresholds, γ_{th} and γ_d. Note that, for CFPR, (5.4) is updated such that $\gamma_d \to \infty$; for CF, (5.4) is updated such that FPR is the entire network and $\gamma_d \to \infty$.

Computation of the average number of relays for $k \geq 2$ is intricate not only due to randomized coding, which does not yield a closed form probability density function for the cooperatively transmitted signal [104], but also due to the dependency of each cooperative set on the previous set. Due to this fact, in this work, we obtain $\bar{C}_k$ $(k \geq 2)$ via simulation experiments, as provided in Section 5.3.3.1. Note that, the source node can compute the average number of nodes based on the node density and the FPR parameters prior to communication and tabulate results. Then, this information can be forwarded within the source initiated packet.

5.3.2.2   Selection of FPR parameters and SNR threshold

The performance of the cooperative forwarding schemes is dependent on the selection of the FPR parameters, namely Δ_1, Δ_2 and γ_d. For example, if Δ_1, Δ_2 and γ_d are large, the FPR covers a large region, causing cooperative forwarding to be carried out by many cooperating nodes dispersed in a large area, yielding reduced forward progress, and also causing increased number of nodes affected by cooperative forwarding. However, if the FPR covers a small area and γ_d is very small, there may not be sufficient number of nodes to exploit the cooperative diversity gain at each hop, which obliterates the benefits of cooperation.

The FPR parameters, Δ_1, Δ_2 and γ_d can be determined so that the system performance is optimized. Here, we consider two objectives for optimizing Δ_1, Δ_2 and γ_d: *Minimum hop count* and *minimum spatial footprint*. Minimized hop count objective provides improved throughput and reduced end-to-end delay, as the packets are made to traverse fewer number of hops to reach the destination. Minimum spatial footprint objective aims at reducing the interference caused by cooperating nodes on the surrounding nodes.

5.3.2.2.1 Minimum hop count: With this approach the FPR parameters are selected such that the average number of hops to reach D is minimized. Since we do not assume rate adaptation, minimized average hop count results in maximized end-to-end throughput and minimized end-to-end delay. Let $K(\Delta_1, \Delta_2, \gamma_d)$ denote the total number of hops between S and D for a single network realization, considering a single realization of node locations, fading channels between nodes and randomization matrix for RDSTC, and let $\bar{K}(\Delta_1, \Delta_2, \gamma_d)$ represent the average number of hops carried out over multiple node distributions, fading channel and randomization matrix realizations. The optimal FPR parameters are found via the following optimization problem:

$$\min_{\Delta_1, \Delta_2, \gamma_d} \bar{K}(\Delta_1, \Delta_2, \gamma_d) \tag{5.5}$$

$$s.t. \quad D \notin \cup_{k=1}^{K(\Delta_1, \Delta_2, \gamma_d)-1} \mathcal{C}_k, \ D \in \mathcal{C}_K, \tag{5.5a}$$

$$\gamma_{th} < \gamma_d. \tag{5.5b}$$

Constraint (5.5a) indicates that the destination, D does not belong to an active cooperative transmission set, but it belongs to the last relay set, i.e., $\mathcal{C}_K$. Note that in (5.5), the objective is to minimize the total number of hops averaged over multiple network realizations, while the constraint (5.5a) should hold for the cooperative sets for each single realization of the network. The optimization problem is given for

CFPR-DT, the optimal FPR parameters for CFPR can be obtained similarly using (5.5) by setting $\gamma_d \to \infty$.

Note that, these optimal parameters only depend on the node density, υ and the locations of S and D. We envision that $\bar{K}(\Delta_1, \Delta_2, \gamma_d)$ and the optimal parameters are to be computed offline, prior to actual data transfer. Once calculated, the resulting optimal choice of $(\Delta_1, \Delta_2, \gamma_d)$ can be stored at the source node, and these values can be included within the packet header generated by the source headed towards the destination.

5.3.2.2.2 Minimum spatial footprint: Cooperative forwarding may involve many nodes in packet relaying. While the total power is kept constant, allowing a large number of relays in the cooperation set would radiate that power to a wider geographical area. Reducing the total number of relays participating in cooperation helps to control the spatial footprint of the cooperative transmissions, therefore reduces the interference and improves the spatial reuse of the network. Let $N_{\mathcal{C}}(\Delta_1, \Delta_2, \gamma_d) \triangleq \sum_{k=1}^{K(\Delta_1, \Delta_2, \gamma_d)-1} |\mathcal{C}_k|$ represent the total number of nodes that participate in cooperative forwarding for one realization of the network, and let $\bar{N}_{\mathcal{C}}(\Delta_1, \Delta_2, \gamma_d)$ represent the average total number of cooperating nodes, with averaging calculated over node distributions, fading channel and randomization matrix realizations. The optimal FPR parameters are obtained by the following optimization problem:

$$\min_{\Delta_1, \Delta_2, \gamma_d} \bar{N}_{\mathcal{C}}(\Delta_1, \Delta_2, \gamma_d)] \tag{5.6}$$

$$s.t. \quad D \notin \cup_{k=1}^{K(\Delta_1, \Delta_2, \gamma_d)-1} \mathcal{C}_k, \ D \in \mathcal{C}_K, \tag{5.6a}$$

$$\gamma_{th} < \gamma_d. \tag{5.6b}$$

As in minimum hop count, network connectivity is assured by constraint (5.6a). Similarly, the optimal FPR parameters for CFPR can be obtained by setting $\gamma_d \to$

∞ in (5.6). Again, we assume that $\bar{N}_C(\Delta_1, \Delta_2, \gamma_d)$ is computed and the optimal parameters are obtained offline prior to actual communication. The optimal FPR parameters, $(\Delta_1, \Delta_2, \gamma_d)$ are assumed to be included within the header of the packet generated by the source.

5.3.3   Performance Analysis

In this section, we present the performance analysis of our cooperative forwarding framework. We first evaluate our power normalization method, then we assess the performance of our cooperative forwarding schemes under minimum hop count and minimum spatial footprint objectives, and finally, we present the performance of our cooperative schemes in mobile scenarios.

In the simulations, we consider a network of N nodes randomly and uniformly distributed in a square region. The lower left corner is located at (0,0) coordinates, and upper right corner is at (100 m, 100m). In order to avoid edge effects, S and D are assumed to be located inside the network, where S is at $(20, 50)$ and D is at $(80, 50)$. Path-loss exponent is set as $\alpha = 4$, and each packet and each link undergoes independent flat, slow Rayleigh fading. At each node Alamouti scheme [43] is assumed as the space-time code of RDSTC. Each node forms its randomization matrix, $\mathcal{R}$, with the coefficients drawn from complex Gaussian distribution. Furthermore, the transmit power, P, is selected such that average direct transmission range is 15 m in accordance with the specifications in [90]. The SNR threshold for successful packet decoding is set as $\gamma_{th} = 10$ dB considering an IEEE 802.15.4 transceiver [90].

5.3.3.1   Power normalization

The aim of power normalization is to limit the total transmit power of a cooperative set to the direct transmission power level P. For power normalization, in our work,
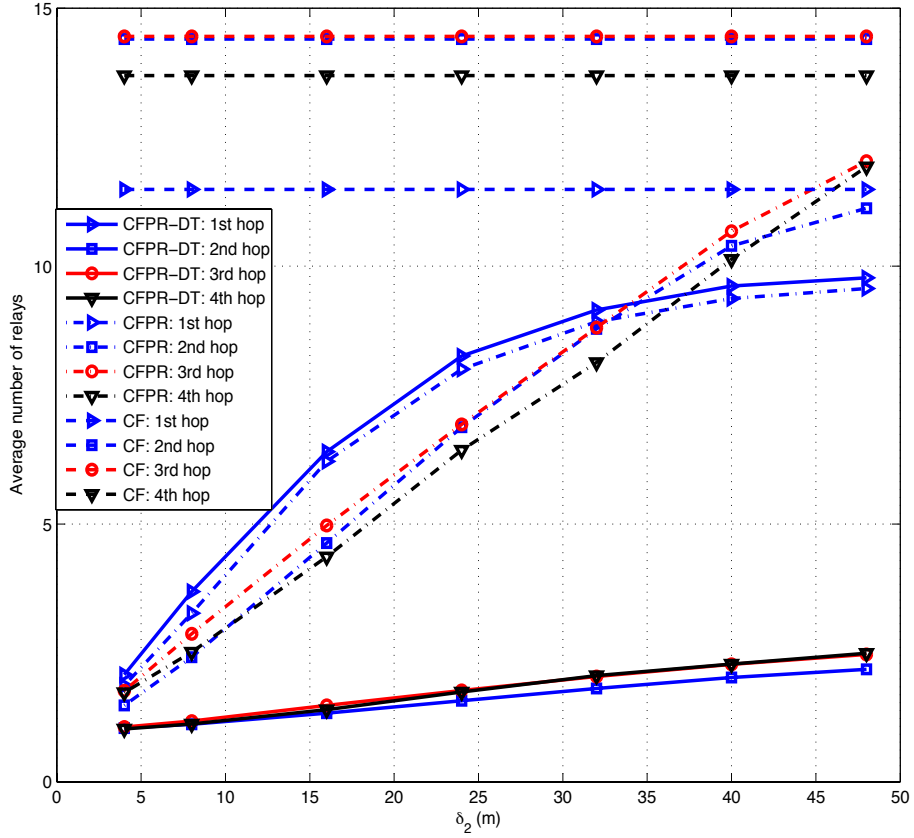
Figure 5.4: Average number of relays at the first, second, third and the fourth hops for CF, CFPR and CFPR-DT schemes, when $N = 100$.

it is assumed that the total transit power budget, P is equally divided among all the cooperating nodes. The relays at hop k normalize their power levels with respect to the expected (average) number of nodes in $\mathcal{C}_k$. $\bar{\mathcal{C}}_k$ is assumed to be indicated in the header of the source's packet. In Figure 5.4, we present the simulation results depicting the average number of cooperating nodes in the first four hops after the source node, namely $\bar{C}_1$, $\bar{C}_2$, $\bar{C}_3$, $\bar{C}_4$, when $N = 100$, Δ_2 is varied from 4 to 48 m and Δ_1 is selected such that S-D connectivity is assured. For CFPR-DT, upper SNR threshold is set as $\gamma_d = 15$ dB.

It is observed in the results of CF that although the number of relays in the first hop can be smaller than the ones' in the other hops due to direct transmission, the

average number of relays tends to be similar as the hop count is increased, which is a consequence of the power normalization and uniform node distribution. As depicted in Figure 5.4, for CFPR and CFPR-DT schemes, $\bar{C}_2$, $\bar{C}_3$ and $\bar{C}_4$ are approximately the same for relatively small Δ_2. Our further experiments with larger number of nodes N, i.e., denser networks, also reveal the same behavior. Due this observation, we assume that source node only computes and forwards $\bar{C}_1$ and $\bar{C}_2$ within its packet, rather than computing and forwarding each $\bar{C}_k$, $\forall k \in K$. It is presumed that the nodes which receive the packet from the source node normalize their transmit power levels with $\bar{C}_1$, and, the nodes at the other hops $k \geq 3$, i.e., the nodes that receive the packet through cooperative transmission, normalize their transmit power levels using $\bar{C}_2$.

5.3.3.2 Performance Analysis of the Cooperative Forwarding Schemes

We next present simulation results to evaluate the performances of CF, CFPR and CFPR-DT schemes. We also compare our forwarding framework with the best (in terms of minimum hop count [105]) location-based greedy direct forwarding scheme, namely the Most Forward within the transmission Radius r (MFR) scheme of [106]. We implement a genie aided version of MFR, where each node is assumed to know the instantaneous channel gain to its neighbor nodes [106], and the position of all the nodes in the network. As such, given a packet and its final destination, in MFR, a node sends (using direct transmission) the packet to its far most neighbor (among the neighbors that can successfully decode packet) in the direction of the final destination, thus achieving most forward progress at each hop. Note that, since MFR corresponds to the best direct forwarding scheme in terms of minimizing the hop count [105], it indicates an upper bound for the performance of schemes based on direct transmission.

Furthermore, in an effort to compare our proposed routing schemes with cooperative schemes that build on existing direct routes (such as [29, 38]), we consider a cooperative routing scheme that builds on the best direct route found out by the MFR scheme. In cooperative diversity enabled version of MFR, which we name as Cooperative MFR (C-MFR), the packet is cooperatively forwarded by two relays that are far most in the direction of the final destination. It is assumed that relays use Alamouti space-time codes. Total transmit power per hop is kept fixed as P and equally allocated among the relays. Note that, MFR and C-MFR require that each node knows the instantaneous channel state information to its neighbors, as well as every other node's location, none of which are required by our cooperative schemes CF, CFPR and CFPR-DT.

As another benchmark for comparison, we also consider the conventional flooding (F) scheme with direct transmission.

5.3.3.2.1 Cooperative Forwarding with Minimum Hop Count Metric: In this part, we evaluate the performance of our proposed schemes, CF, CFPR and CFPR-DT with their parameters optimized with respect to minimum hop count criterion. We compare our schemes with MFR, C-MFR and F, in terms of the average number of hops required to reach the destination node. The FPR parameters (Δ_1, Δ_2, γ_d, $\bar{C}_1$, $\bar{C}_2$) of CFPR and CFPR-DT schemes are determined by the solution of the problem given in (5.5) prior to communication. The simulation results depict the average number of hops to reach the destination for the considered schemes for varying network sizes, N, as given in Figure 5.5.

It is seen that CF can significantly reduce the number of hops to reach the destination, especially for sparse networks, as compared to direct conventional flooding. It is also observed that our CFPR scheme provides slightly larger number of hops as compared to MFR and C-MFR, whereas our CFPR-DT scheme with the best dual
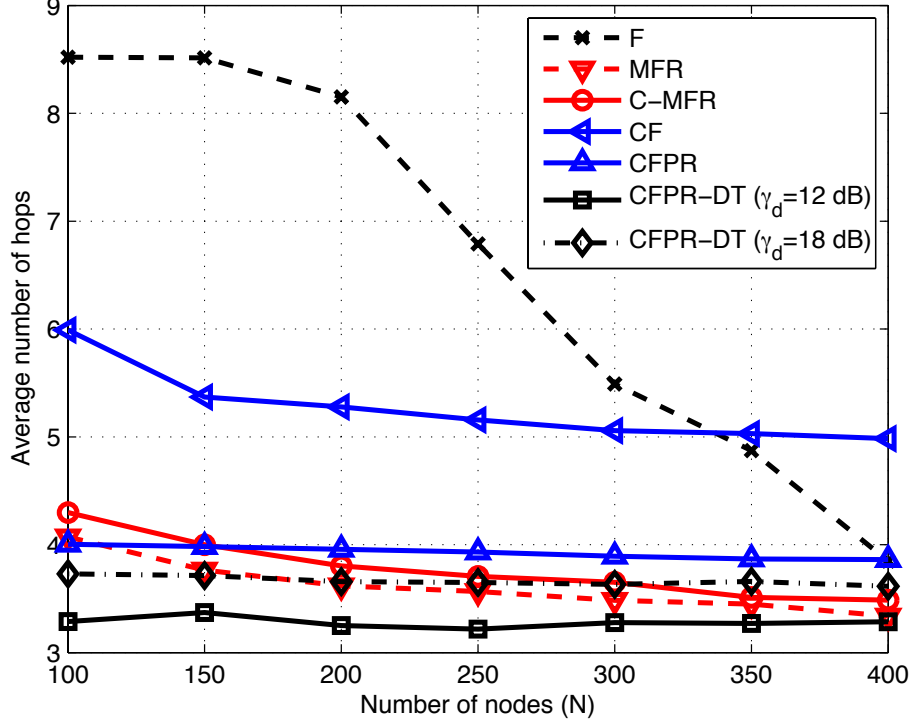
Figure 5.5: Average number of hops. For each N, the FPR parameters, Δ_1, Δ_2, γ_d are optimized via (5.5), and the corresponding $\bar{C}_1$ and $\bar{C}_2$ are obtained as explained in Section 5.3.3.1.

threshold, i.e., $\gamma_d = 12$ dB, results in smaller total number of hops to reach the destination as compared to all other schemes. As γ_d is increased, the number of hops to reach the destination using CFPR-DT is increased due to the relays' being dispersed in large regions. Of note, our cooperative forwarding schemes achieve reduced total hop count with much less channel information as compared to MFR and C-MFR.

These results also demonstrate that our cooperative forwarding framework can exploit the long haul advantage of cooperative transmissions by actuating the relays in a specific region. On the contrary, C-MFR fails to exploit the long haul advantage, by relying on the cooperative transmissions of the nodes which are on the already established best direct path. The results indicate that constraining the cooperating nodes to be selected on a best direct path not only reduces the route alternatives but

also does not necessarily result in improved end-to-end performance.
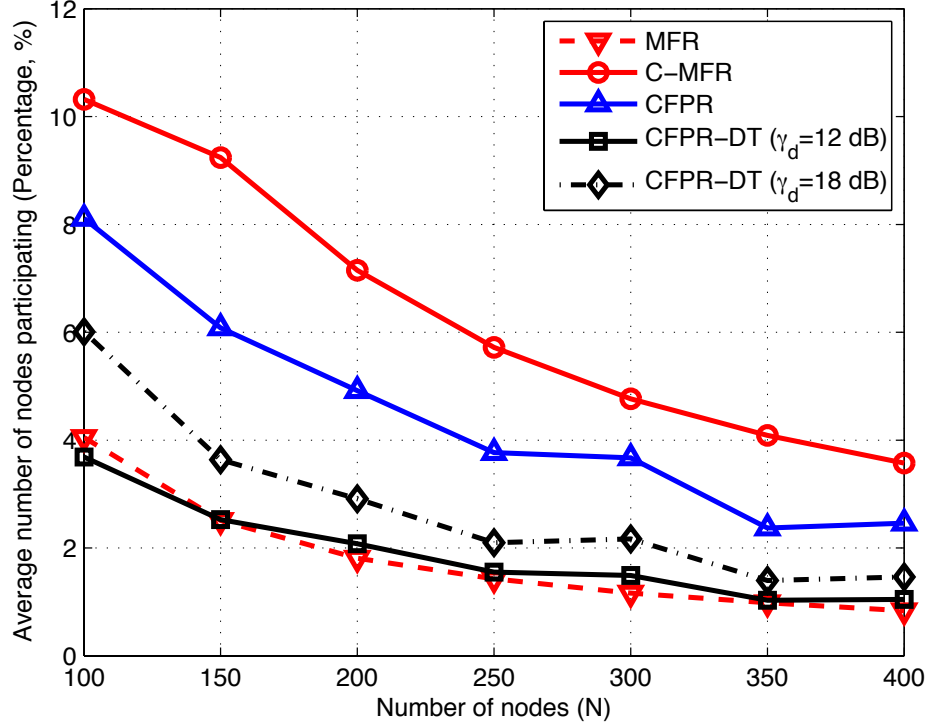
Figure 5.6: Average number of nodes participating in routing (in percentage). For each N, the FPR parameters, Δ_1, Δ_2, γ_d are optimized via (5.6), and the corresponding $\bar{C}_1$ and $\bar{C}_2$ are obtained as explained in Section 5.3.3.1.

5.3.3.2.2 Cooperative Forwarding with Minimum Spatial Footprint Metric: In this part, we evaluate the performance of our CFPR and CFPR-DT schemes with parameters selected according to minimum spatial footprint criterion, in comparison to MFR and C-MFR schemes in terms of the average number of relays that actually participate in the packet forwarding process, and also in terms of the average number of nodes which are affected by the ongoing routing process. The FPR parameters $(\Delta_1, \Delta_2, \gamma_d, \bar{C}_1, \bar{C}_2)$ of CFPR and CFPR-DT schemes are determined by the solution of the problem given in (5.6) prior to communication. The simulation results that depict the average number of relays (represented as a percentage of the
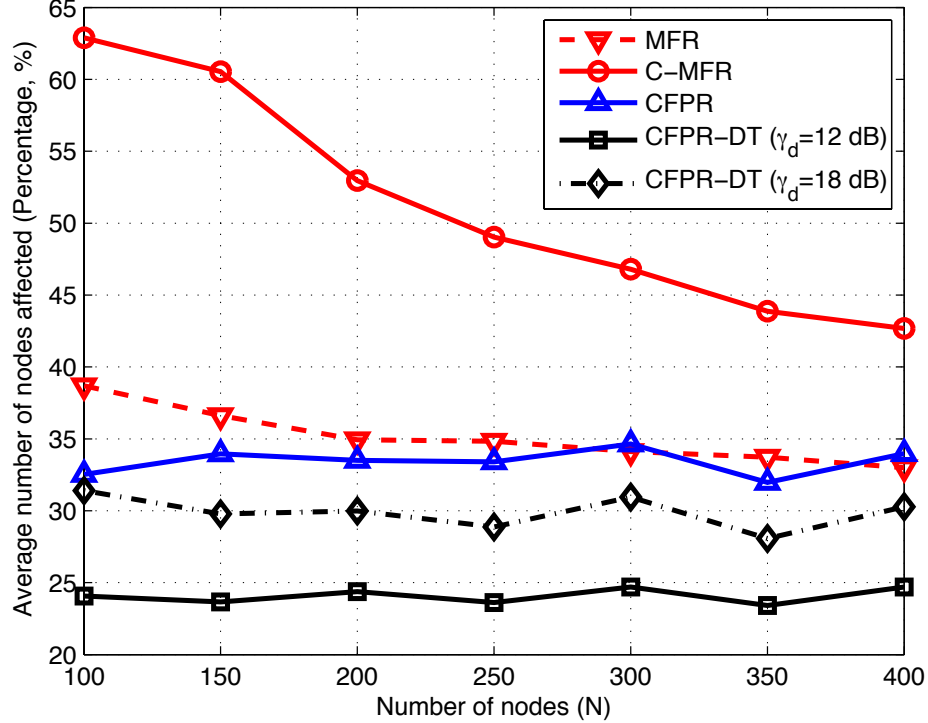
Figure 5.7: Average number of nodes affected by routing (in percentage). For each N, the FPR parameters, Δ_1, Δ_2, γ_d are optimized via (5.6), and the corresponding $\bar{C}_1$ and $\bar{C}_2$ are obtained as explained in Section 5.3.3.1.

total number of nodes) that actually participate in the packet forwarding process are given in Figure 5.6, and the results that depict the total number of nodes (in percentage) that successfully decode the transmissions including the nodes which do not participate due to the location and/or SNR constraints are provided in Figure 5.7.

It is observed in Figure 5.6 that the average number of nodes participating in the forwarding process with CFPR-DT (with the best γ_d) is almost the same with the one of MFR. Moreover, the number of nodes affected by the ongoing packet forwarding with CFPR-DT is 10% less than that of MFR. Note that, although MFR recruits smaller number of intermediate nodes as compared to CFPR, it is shown in Figure 5.7 that CFPR leaves a smaller footprint on the network than MFR. It is deduced

from the results of C-MFR that employing cooperation on an already established best route diminishes the spatial reuse in the network. The results demonstrate that our cooperative routing framework can significantly improve the spatial reuse as compared to both direct routing and cooperative scheme, C-MFR that build on direct route.

A comparison of the optimal FPR parameters found using minimum hop count objective and minimum spatial footprint objective reveals that minimum spatial footprint objective forces the FPR to remain in a smaller region as compared to minimum hop count objective, which benefits from a larger FPR for improved diversity gain and long haul advantage. Also, it is observed that increasing the dual threshold of CFPR-DT results in larger spatial footprint, leading to increased number of participating and affected nodes. Furthermore, a comparison of the achieved average number of hops for system parameters optimized using the minimum hop count and minimum node count objectives reveals that CFPR-DT with the best dual threshold provides almost the same average hop count for both metrics for all considered node densities, whereas in CFPR minimizing the node count does not necessarily correspond to minimized hop count especially for dense networks.

Note that, the results provided above do not take into account any MAC protocol operation, overhead for node coordination, collisions or contention resolution are not considered. Such MAC operations degrade the performance of direct routing and cooperative routing schemes that build on direct routes significantly, while our proposed cooperative routing schemes require neither contention resolution nor relay selection mechanisms. The cooperative framework is revisited for MAC protocol operation and messaging costs in Section 5.4.

5.3.3.2.3 Mobile Scenarios: In this part, we evaluate the performance of our CFPR and CFPR-DT schemes in comparison to MFR and C-MFR in terms of their

packet delivery ratios (PDR) under mobility. We adopt the random walk mobility model in [107], where a mobile node moves in a uniformly randomly chosen direction from $(0, 2\pi)$ and with a uniformly randomly chosen speed from an interval 0-5 m/s. In our simulations, the mobile node starts moving at time $t = 1$ second, and at the end of every 5 seconds, it picks a new random direction and speed, and continues moving towards its new direction.

In the mobility experiments, we consider a network with 300 nodes, and we evaluate the performance for two scenarios: i) Only D is mobile, ii) All the nodes in the network are mobile. For the CFPR and CFPR-DT schemes, it is assumed that during the entire simulation period S uses the initial location information of D, i.e., D's location at time $t = 0$ to calculate FPR parameters and to forward its packets.

In Figure 5.8, we depict the PDR, i.e., the ratio of the packets delivered to D to the packets initiated by S, for CFPR and CFPR-DT schemes considering both of the mobility scenarios. It is observed that without any FPR updates for 10 s, PDR is above 95% for both CFPR and CFPR-DT when D is mobile, and PDR is still above 90% when all nodes are in motion. The reduced PDR performance of CFPR-DT is due to the upper threshold constraint, which makes finding an appropriate relay in the falsely assigned FPR more difficult as compared to CFPR. Note that, the main performance degradation is due to the stale information on D's exact location, which causes the use of a false FPR, yielding 10% loss in PDR without any FPR parameter updates for 10 seconds. On the other hand, the mobility of the cooperating nodes causes only an additional 5% degradation in PDR.

In Figure 5.9, we depict the PDR for MFR and C-MFR schemes for varying CSI update periods. In the simulations of MFR and C-MFR, it is assumed that all nodes are mobile, a route is established based on the knowledge of the current CSI and the location information of all nodes in the network, and packets are forwarded
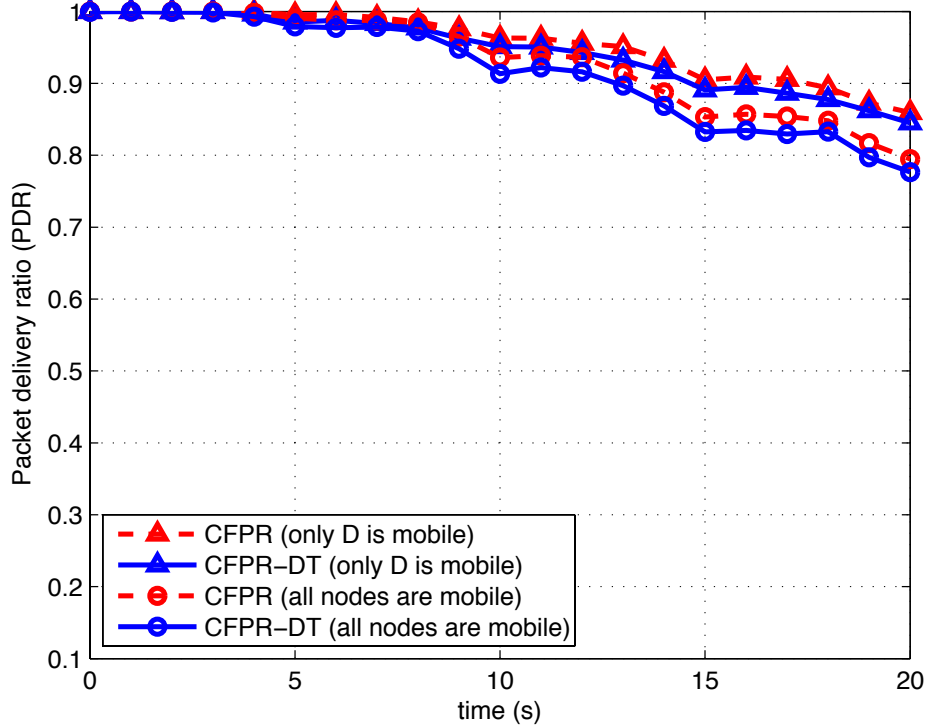
Figure 5.8: Packet delivery ratio of CFPR and CFPR-DT when nodes move according to the random walk mobility model. The FPR parameters, Δ_1, Δ_2, γ_d are optimized via (5.5), and the corresponding $\bar{C}_1$ and $\bar{C}_2$ are obtained as explained in Section 5.3.3.1.

through the established route. It is presumed that CSI and the location information are updated and the route is rediscovered on predetermined periods in multiples of the coherence interval. The results demonstrate that the PDRs of MFR and C-MFR schemes degrade significantly if the CSI and the location information are not updated once every coherence interval. This is mainly due to the fact that these schemes continue forwarding the packets through the nodes which were selected based on the stale CSI. If at least one of the links on the route fails, the entire end-to-end path fails, requiring route rediscovery. The situation for C-MFR is even worse than MFR, because for C-MFR at each hop there are two predetermined nodes that are expected to forward the packet. If at least one of these predetermined cooperating
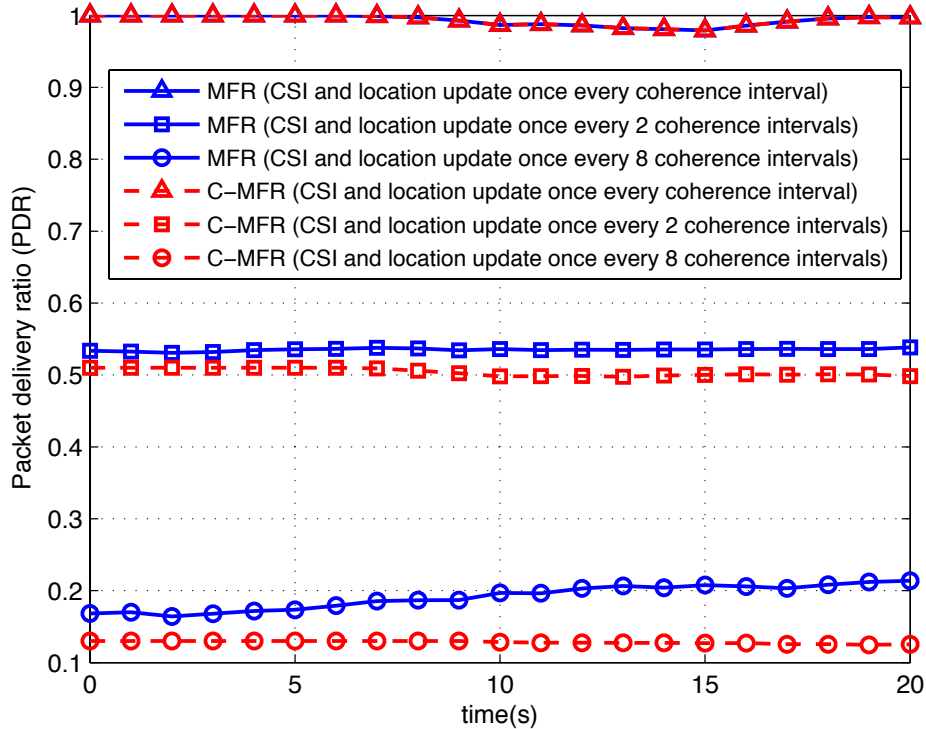
Figure 5.9: Packet delivery ratio of MFR and CMFR, for varying CSI update periods, when all nodes move according to the random walk mobility model.

nodes happen to observe a degradation in its channel gain due to mobility or a deep fade, cooperation is not actuated, and the cooperative link fails with high probability. The simulation results indicate that, as the channel conditions and the node locations change, MFR and C-MFR routes must be rediscovered such that always the best set of nodes for packet forwarding can be used. However, this implies a heavy messaging burden on the network.

Considering IEEE 802.15.4 settings [94] (128 byte packets and 250 kbps data rate) and taking into account our mobility model, the duration of single hop packet transmission is around 4 ms, and the channel coherence time can be computed approximately as 100 ms. This suggests that MFR and C-MFR schemes necessitate CSI updates at least once every 25 packets. If the CSI is updated once every 50 pack-

ets, the PDR observes a dramatic drop to around 50% for both MFR and C-MFR schemes. Frequent and periodic messaging is required to acquire and disseminate the current CSI for MFR and C-MFR schemes, which potentially steal from the available network resources.

Unlike MFR and C-MFR, none of our cooperative forwarding schemes (CFPR, CFPR-DT) rely on the CSI, and hence they do not require any CSI updates. The degradation in PDR of CFPR and CFPR-DT schemes is mainly due to the stale knowledge on the location information of the destination node. Note that, the coordinates of the source and the destination nodes form the loci of the FPR. The stale knowledge on the destination location information can result in wrongly formed FPR, and sometimes, it can leave the destination node out of the FPR. The PDR of our schemes can be maintained at a desired level with significantly few location update messages. For example, if a PDR of at least 95% is required, the destination location information is required to be updated once every 10 s for CFPR and CFPR-DT, as depicted in Figure 5.8. Of note, considering the IEEE 802.15.4 settings and our mobility model, this means that CFPR and CFPR-DT schemes require destination location updates only approximately once every 2500 packets, which is 1% the frequency of CSI updates in MFR and C-MFR schemes. It is worthwhile to note that CFPR and CFPR-DT require only the update of the destination location information, whereas MFR and C-MFR require frequent periodic CSI updates for each link in the network, which brings a heavier messaging burden on the network. The results demonstrate that our schemes show resilience to mobility and fading, while imposing reduced messaging overhead as compared to MFR and C-MFR.

5.4 Routing Enabled Cooperative MAC Protocol: RECOMAC

In conventional wireless networks that are based on a layered architecture, the job of the routing layer is to discover the best set of nodes for delivering packets to a specific destination, and to configure and maintain the nodes so that each node is informed about whom to forward incoming packets to reach their destinations. Routed packets need to be delivered over physical links, with the help and coordination of the MAC layer. Since the wireless medium is shared, simultaneously transmitted packets have a high chance of collision, and once a collision occurs, it should be resolved as the packets are retransmitted. The job of the MAC layer is to coordinate the transmissions from multiple nodes, avoiding and resolving collisions, so that all packets are successfully delivered on each link along the path, as they are forwarded to their next destinations.
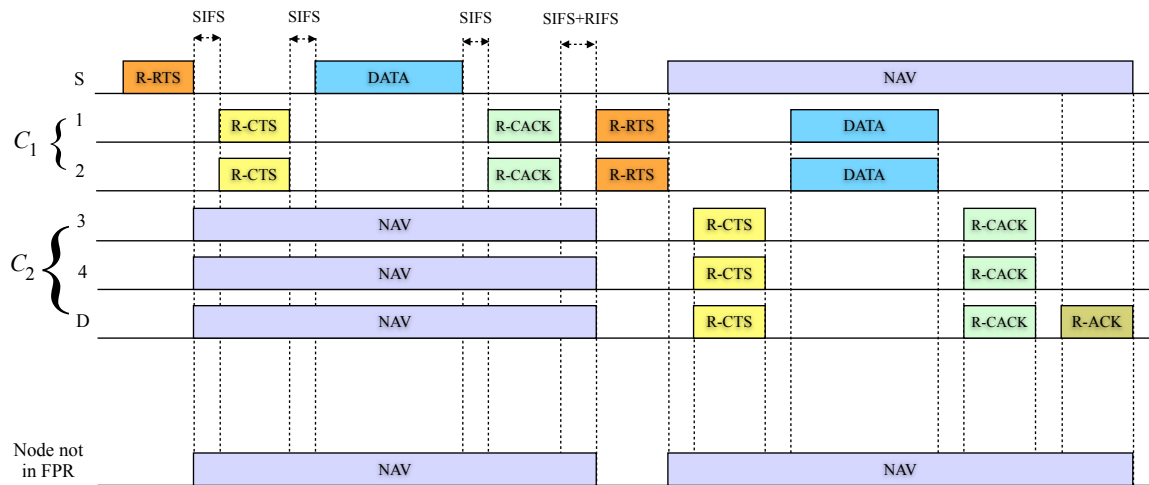
Figure 5.10: RECOMAC packet exchange procedure: For the transmission of S, cooperation bit of the frame control field is set as 0, while it is set as 1 for all other transmissions which are carried out in cooperative mode.

In the proposed cooperative cross-layer architecture, Routing Enabled Cooperative MAC, RECOMAC, the functions of physical, MAC and routing layers are

162
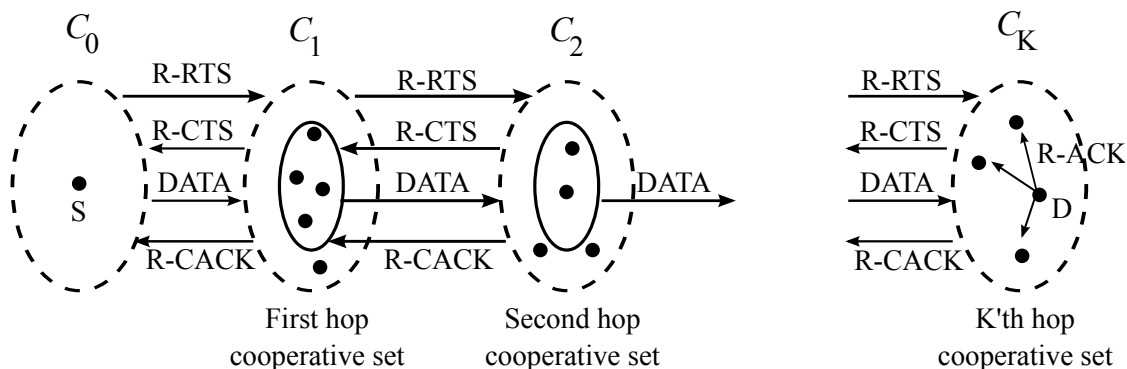
Figure 5.11: Cooperative forwarding and cooperative set formation within packet exchanges of RECOMAC.

combined to provide seamless cooperative communication, while the the messaging overhead to set up routes, select and actuate relays is minimized. Our architecture achieves this by incorporating the routing layer functions into the MAC layer. RECOMAC builds upon our cooperative forwarding framework presented in Section 5.3, and it employs a modified version of IEEE 802.11 protocol [4] for medium access and data delivery. In particular, we introduce new functionalities to IEEE 802.11's MAC, such as cooperative packet transmission and routing for realizing CFPR-DT for data delivery.

In RECOMAC, end-to-end communication is realized in two phases, namely the destination location discovery phase and the data delivery phase. In the destination location discovery phase, source node, S obtains the location information of the destination node, D. Then, in the data delivery phase, S uses the location information of D for data delivery via a multi-hop cooperative protocol that relies on CFPR-DT strategy.

Each data packet transmission is carried out after Routing enabled Request to Send (R-RTS) and Routing enabled Clear to Send (R-CTS) packet exchange between the sender and the receiver nodes. After the R-RTS and R-CTS message exchange, the cooperative set sends the data packet to the receiving node set. The receiving

node set replies back with a Routing enabled Cooperative ACK (R-CACK) to acknowledge the successful progress of the data packet. If the final destination node belongs to the receiving node set, it declares the successful packet delivery by sending a Routing enabled ACK (R-ACK) message following the R-CACK. The RECOMAC packet exchange is illustrated in Figure 5.10.

It is worthwhile to note that, in RECOMAC, the sender of a packet is not a single node but a group of cooperating nodes, and similarly, the receiver of a packet is also a group of nodes, as depicted in Figure 5.11. Although the sender side and the receiver side consists of multiple nodes, in RECOMAC, we utilize only transmit side cooperation, i.e., v-MISO links, but not receiver side cooperation. At each hop, the nodes in the sender cooperation group form a cooperative (v-MISO) link with each single node in the receiving side node set. That is to say, in RECOMAC, at each hop, multiple v-MISO links are formed between the sending cooperative set and the receiving node set, where the number of v-MISO links is determined by the number of nodes in the receiving node set. It is also important to note that every packet transmission in RECOMAC, excluding the source transmission, is in cooperative mode and the packets are RDSTC encoded. Specifically, after the received symbols are successfully decoded by the nodes in the receiving node set, the nodes in this set form the cooperative transmission set for the next hop progress of the packet. For this purpose, each node i in the cooperative set maps the received symbols onto the space-time code matrix $\mathcal{G}(\mathbf{z})$, multiplies this matrix with its randomization vector, $\mathbf{r}_i$, chosen from complex Gaussian distribution, and then sends the resulting matrix, $\mathcal{G}(\mathbf{z})\,\mathbf{r}_i$. The overall resulting symbol matrix due to the cooperative transmissions of all the nodes in the cooperative set is given as (5.1), and the received signal is given as (5.2), as discussed in section 5.2. Next, we describe the structures of the packet types employed by the RECOMAC protocol.

5.4.1 RECOMAC Packet Structures

We introduce new modified packet structures for RECOMAC with additional fields to support our cooperative forwarding strategies. In Figure 5.12, we depict the structures of the packets used in RECOMAC, namely LREQ, LREP, R-RTS, R-CTS, R-ACK, R-CACK and DATA packets.

Frame Control	Final Destination Address	Source (Originator) Address	Source Location	Hop Count	Sequence Control	FCS
16	48	48	48	8	16	32

Bits:

(a) LREQ message format

Frame Control	Final Destination Address	Source (Originator) Address	Final Destination Location	Source Location	FPR parameters	Hop Count	Sequence Control	FCS
16	48	48	48	48	32	8	16	32

Bits:

(b) LREP message format

Frame Control	Duration	Final Destination Address	Source (Originator) Address	Final Destination Location	Source Location	FPR parameters	Hop Count	Sequence Control	FCS
16	16	48	48	48	48	32	8	16	32

Bits:

(c) R-RTS message format

Frame Control	Duration	Final Destination Address	Source (Originator) Address	Hop Count	Sequence Control	FCS
16	16	48	48	8	16	32

Bits:

(d) R-CTS, R-ACK and R-CACK message formats

Frame Control	Duration/ ID	Address 1	Address 2	Address 3	Hop Count	Sequence Control	Address 4	Frame Body	FCS
16	16	48	48	48	8	16	48	n	32

Bits:

(e) DATA packet format

Figure 5.12: RECOMAC packet structures. FPR parameters field is reserved for Δ_1, Δ_2, γ_d, $\bar{C}_1$ and $\bar{C}_2$ information.

Each packet includes Frame Control (FC) and Frame Check Sequence (FCS) fields, as defined in IEEE 802.11 [4]. FC field specifies the form and function of the frame by defining the protocol version, the packet type, i.e., control, management, data, and various other functions as detailed in [4]. Note that, in the original IEEE 802.11 standard, if a node receives a packet that is not destined to itself, it ignores the packet and sets its NAV according to the duration specified in the packet

header. RECOMAC makes use of the reserved bit in the FC field to allow the nodes to differentiate between the cooperative and non-cooperative transmissions. If the transmission is in cooperative mode, then the neighboring nodes receive the packet even it is not destined to themselves, but they set their NAV if they reside out of the FPR and/or if they do not satisfy the dual threshold criteria. FCS is used to verify that the frame is received without loss or error. The method used for verification is known as Cyclic Redundancy Check (CRC) [45].

Each packet also includes hop count field which designates the number of hops the packet has traversed, as well as the address fields for final destination and the source (data originator). The hop count field is used by the cooperating nodes to identify the cooperative set in which they belong to, i.e., $\mathcal{C}_i$, where i is defined by the hop count field. The hop count field is set as zero by the data originator, and it is incremented by one by each node that forwards the packet. The sequence control field is used to control if the packet is duplicate or out of date. In addition to the aforementioned fields, Location Reply (LREP) and R-RTS packets include two extra fields that hold the location information for the final destination and the source nodes in terms of (x, y) coordinates, and an extra field to hold the FPR parameters, namely the Δ_1, Δ_2, γ_d, $\bar{C}_1$ and $\bar{C}_2$ values, as depicted in Figures 5.12b and 5.12c. The FPR parameters together with the location information of the source and the destination nodes, provide an intermediate node with necessary information to compute the FPR and to check whether it belongs to the FPR or not. $\bar{C}_1$ and $\bar{C}_2$ are used for power normalization by the cooperating nodes, as explained in section 5.3.3.1.

5.4.2   Destination Location Discovery Phase

Destination location discovery is pursued by the source node, S before data delivery to the destination node, D starts. The goal in this phase is to obtain the location

information for D. S first inquires the location of D with a Location Request (LREQ) message which is sent by cooperative flooding, CF method, as described in Section 5.3.1.1. Note that, when the location of D is not known, CFPR or CFPR-DT cannot be used. Figure 5.12a depicts the structure of the LREQ packet, including the source (S) and the destination (D) addresses, the source's location, the hop count field that designates how many hops this LREQ message has traversed, and the sequence control field which is used to avoid dissemination of stale LREQ messages. The hop count is initialized to 0 at S and incremented by one at each hop.

When D receives the LREQ message, it obtains the location information of S. In response to LREQ, D initiates the cooperative forwarding of the Location Reply (LREP) message, via CFPR-DT method. The FPR parameters and the upper threshold, γ_d, are calculated based on the density of the network, the source and the destination locations according to the optimization problem given in (5.5). LREP message involves address and location information, as well as FPR parameters, hop count and sequence control as given in Figure 5.12b. The LREP message is forwarded through the selected FPR by CFPR-DT. When S receives this LREP message, it obtains the location information of D, which concludes the destination location discovery phase.

5.4.3 Data Delivery Phase

Having completed the destination discovery phase successfully, the cooperative forwarding for data delivery can be initiated. A data packet is sent after a successful routing-enabled-request-to-send (R-RTS) and routing-enabled-clear-to-send (R-CTS) message exchange between the sender and the receiver node sets. A packet is forwarded through the FPR via cooperative sets in multiple hops until it reaches the destination node. Following a successful data delivery, a routing-enabled ac-

knowledgement (R-ACK) is sent by D. We have named the cooperative and non-cooperative acknowledgements as R-CACK and R-ACK, respectively, due to their different functions as described below. In the following, we present the operation of source, intermediate cooperating nodes and destination, in detail.
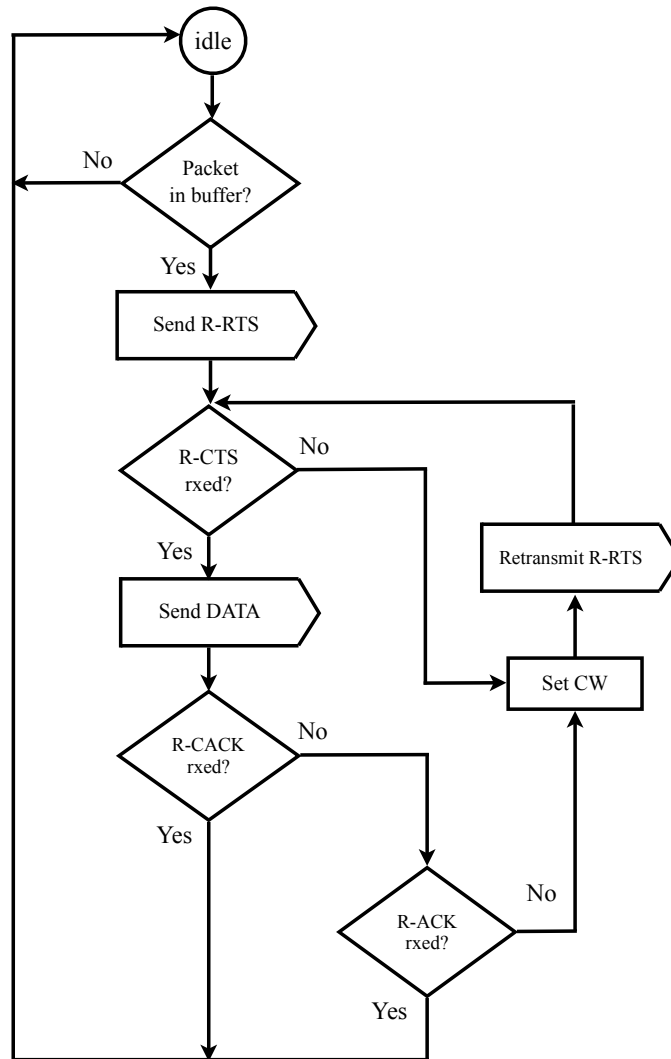

Figure 5.13: Flow chart for the source node.

5.4.3.1 Source node

The source node can compute the optimal FPR parameters via the optimization problem given in (5.5) or can make use of the information obtained from LREP message by the destination. The operation of S is depicted in the flow chart given in Figure 5.13, and summarized below.

(i) Whenever there is a packet in the source node's buffer, it initiates the data transmission by broadcasting an R-RTS message. The R-RTS packet structure is consistent with IEEE 802.11 RTS structure, but here we introduce additional fields to realize RECOMAC. As depicted in Figure 5.12c, the R-RTS message includes fields that hold the location information of S and D, and the FPR parameters (Δ_1, Δ_2, γ_d, including $\bar{C}_1$ and $\bar{C}_2$) and the number of hops that the message has traversed.

The source node broadcasts the R-RTS message, with FPR parameters, the upper threshold, γ_d, and location information set, the cooperation bit turned off and the hop count field set to 0. The R-RTS message informs the neighboring nodes about the expected duration of the single-hop transmission as specified in the duration field. The duration field of R-RTS is set to a value $\mathcal{D}_{R-RTS}$, which is calculated as $\mathcal{D}_{R-RTS} = 4T_{SIFS} + 4T_{R-CTS} + T_{DATA} + T_{R-CACK} + T_{R-ACK} + 5T_{prop} + T_{RIFS}$, where T_{SIFS} is the duration of one short interframe spacing (SIFS), T_{RIFS} is the duration of one reduced interframe spacing (RIFS), T_{R-CTS}, T_{R-CACK}, T_{R-ACK}, T_{DATA} denote the duration of R-CTS, R-CACK, R-ACK and DATA frames, respectively, and T_{prop} designates the maximum propagation delay. The nodes which receive the R-RTS and do not belong to the FPR or do not satisfy the upper threshold, set their NAVs to $\mathcal{D}_{R-RTS}$ provided in R-RTS, and they stay silent during this period, thereby avoiding possible collisions.

(ii) If R-CTS is received after SIFS period, the source node sends the data packet. If R-CTS is not received after SIFS period, the source node updates its CW, backs off and restarts from step (i).

(iii) If R-CACK is received after DATA transmission, S deduces that the data packet has progressed one hop towards D. If a R-ACK message is received following the R-CACK message, S deduces that the packet is successfully delivered at D in one hop.

If R-ACK is received, but R-CACK is not received, S again deduces that D has been reached in single hop. If neither R-CACK nor R-ACK is received, S initiates retransmission with updated CW and returns to step (i).

5.4.3.2 Intermediate Cooperating Nodes

The operation of the cooperating nodes is depicted in Figure 5.14, and summarized below.

Whenever a node receives a R-RTS message, it checks whether it satisfies the FPR and upper threshold criteria, as given in (5.3). If it does, it cooperatively sends the R-CTS message, which is encoded with RDSTC. If the node does not satisfy the FPR or threshold conditions, it sets its NAV according to the duration specified in R-RTS header indicating that the medium is busy and this node will remain silent within this duration. Note that, here, multiple nodes cooperatively, simultaneously and autonomously transmit the R-CTS packet which is encoded with RDSTC.

When a node receives the DATA packet, it sends a R-CACK message cooperatively declaring the forward progress of the DATA packet. Following the R-CACK transmission, the node waits for an SIFS + RIFS period for an R-ACK message from D. If the node does not receive an R-ACK, it deduces that the DATA has not been
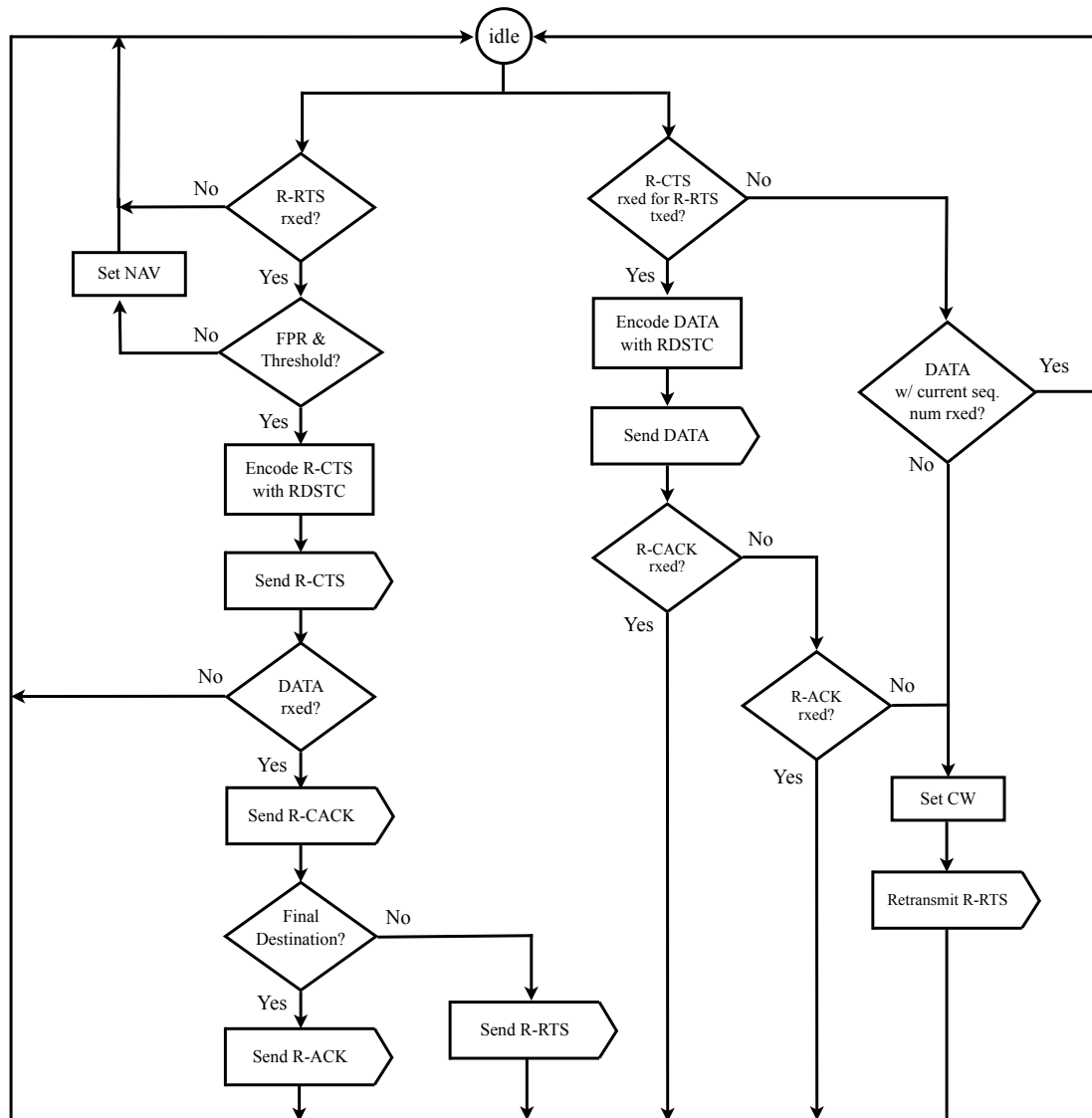
Figure 5.14: Flow chart for the intermediate cooperating nodes and the final destination node.

delivered to D, and it initiates the cooperative transmission of R-RTS for the next hop progress of the DATA packet.

If a node does not receive a DATA packet after SIFS period following R-CTS transmission, it sets its NAV to the duration from the R-RTS packet and returns to the idle state. If the node does not receive a DATA packet, but receives a R-CACK for the data packet with the same sequence number it was expecting, it infers that the

cooperative transmission has been carried out successfully without its participation. In this case, the node updates its NAV according to the duration from the R-CACK and returns to the idle state.

When the node receives an R-CTS message in response to an R-RTS message it has transmitted, it encodes the DATA with RDSTC and sends the DATA cooperatively. If the node receives R-CACK following the DATA transmission, it deduces that the DATA has progressed one hop towards D, and returns to the idle state.

5.4.3.3 Final destination node

The final destination node operates like an intermediate node during the exchange of R-RTS - R-CTS - DATA - R-CACK messages. When this node receives the packet destined to itself, it sends a R-ACK message following an SIFS period after its R-CACK transmission, to declare that the packet is delivered successfully at the destination, so as to prevent further forwarding of the data packet.

The packet exchanges and NAV settings are depicted in Figure 5.10. Furthermore, in Figure 5.11, we depict the cooperative forwarding and cooperative set formation within the packet exchanges of RECOMAC.

Note that, all the nodes that receive a packet and autonomously decide to participate in cooperative transmission, initiate their timers based on the time instant they receive the packet. However, due to different propagation delays, the nodes in the cooperative set receive the packet in different time instants, resulting in different firing times for their timers and yielding asynchronous transmissions. In order to circumvent this problem, we use an extended SIFS period, such that the SIFS specified in IEEE 802.11 standard is extended by an amount of maximum propagation delay, T_{prop}. It is assumed that each node obtains the propagation delay between the sender and itself, then subtracts this value from the total updated SIFS length. This way,

the nodes that receive the packet at different times can have timers that fire at the same time instant. Moreover, as shown in [108], RDSTC can take care of random delays introduced by cooperating nodes and, hence, the assumption that the nodes in the cooperative set are time-synchronized can be relaxed in such cases.

5.4.4 Performance Analysis of RECOMAC

In this section, we present the performance analysis of our RECOMAC architecture in comparison to conventional layered architecture employing regular IEEE 802.11 protocol at the MAC layer and AODV at the routing layer. We denote this conventional architecture as IEEE 802.11+AODV.

AODV is an on-demand route acquisition system, where a route is created when desired by the source node [109]. When a source node wants to send a message to some destination node and it does not already have a valid route to that destination, it initiates a path discovery process to locate the other node. The source node broadcasts a route request (RREQ) packet to its neighbors, which then forward the request to their neighbors, and so on, until either the destination or an intermediate node with a route to the destination is located. AODV utilizes destination sequence numbers to ensure all routes are loop-free and contain the most recent route information. Intermediate nodes can reply to the RREQ only if they already have a route to the destination whose corresponding destination sequence number is greater than or equal to that contained in the RREQ. During the process of forwarding the RREQ packet, intermediate nodes record in their route tables the address of the neighbor from which the first copy of the broadcast packet is received, thereby establishing a reverse path. If additional copies of the same RREQ are later received, these packets are discarded. Once the RREQ reaches the destination or an intermediate node with a fresh enough route, the destination/intermediate node responds by unicast-

ing a route reply (RREP) packet back to the neighbor from which it first received the RREQ packet. As the RREP is routed back along the reverse path, the nodes along this path set up forward route entries in their route tables which point to the node from, which the RREP came. These forward route entries indicate the active forward route. Since the RREP packet is forwarded along the path established by the RREQ packet, AODV only supports the use of symmetric links [62]. Since multiple RREQ packets are received at the destination, yielding multiple possible paths, a route should be selected among those paths. AODV uses a metric to select the best path between the source and the destination node. In our performance comparisons, we consider two metrics for AODV, the hop count and airtime metrics. When AODV uses the hop count metric, an end-to-end path is established based on the minimum hop count, when airtime metric is used, the end-to-end path is established based on the end-to-end link reliability. Since the airtime metric is link aware, it has been defined as the AODV routing metric in wireless mesh network standard, IEEE 802.11s [110].

Table 5.1: System Parameters used in Simulations

DATA	8192 bits	PLCP header	144 bits
RTS	168 bits	Short preamble	432 bits
CTS, ACK	112 bits	Basic rate (used for MAC, PHY headers and control messages)	6 Mbps
R-RTS	304 bits	Data rate	54 Mbps
R-CTS, R-CACK, R-ACK	184 bits	MAC header	272 bits
AODV-hop count RREQ	192 bits	CW min / max	15 / 1023
AODV-hop count RREP	160 bits	Slot time	9 μs
AODV-airtime RREQ	368 bits	SIFS	10 μs
AODV-airtime RREP	344 bits	RIFS	2 μs
RECOMAC LREQ	216 bits	RECOMAC SIFS	12 μs
RECOMAC LREP	296 bits	Max. Transmit power	100 mW

We consider the same network set up and settings as described in Section 5.3.3.

The system parameters used in our simulations are provided in Table 5.1. We use the transmission rates of IEEE 802.11g standard, where control messages (R-RTS, R-CTS, R-CACK, R-ACK, RTS and CTS) and packet headers are transmitted at 6 Mbps and data packets are transmitted at 54 Mbps. We simulate networks with varying number of nodes. For each data point, we create and simulate 20 different network realizations, and the average of the results are presented.

Table 5.2: Source-Destination Connectivity

N	60	80	100	120	140	160	180
AODV-hop count	0.15	0.25	0.70	0.80	1	1	1
AODV-airtime	0	0.45	0.65	0.95	0.95	0.95	1
RECOMAC	1	1	1	1	1	1	1

We have implemented RECOMAC in ns-2 environment, to carry out simulations for performance analysis of RECOMAC in comparison to non-cooperative architecture with IEEE 802.11 and AODV. Our RECOMAC implementation in ns-2 spans the physical and MAC layers, and the routing layer functionality is submerged into our MAC layer model following the descriptions in section 5.4. In the implementation of non-cooperative network, we assume that RTS-CTS exchange is enabled in IEEE 802.11 MAC, and AODV routing is considered with hop count and airtime metrics. Furthermore, packets are subject to channel fading, however it is assumed that during one frame exchange, channel gains do not change.

We observed in our simulations that when the route discovery messages of AODV are subject to fading, AODV initiates route discovery repeatedly without establishing a valid end-to-end route, and thereby leading to zero end-to-end throughput. Because of this, in our simulations for the IEEE 802.11+AODV model, AODV routing packets and MAC packets are assumed to be error-free, i.e., they are not affected by (or they are protected from) fading, whereas data packets undergo Rayleigh fading. However,

175

in RECOMAC model, all control packets (R-RTS, R-CTS, R-CACK, R-ACK) and DATA packets undergo Rayleigh fading. Under these assumptions, in Table 5.2, we provide the fraction of the network realizations in which S and D could establish an end-to-end connection, denoted as source-destination connectivity. It is observed that RECOMAC assures S-D connectivity for all cases, despite the fact that control packets undergo fading. On the other hand, AODV cannot find a valid path between S and D, especially when the network is sparse; AODV can operate when the network is sufficiently dense, i.e., when the number of route alternatives is high. However, as we show in the sequel, this results in dramatically increased routing overhead. In the following experiments, the results are obtained over the cases where the end-to-end connection is established. Due this fact, we do not have data for AODV with airtime metric when $N = 60$.
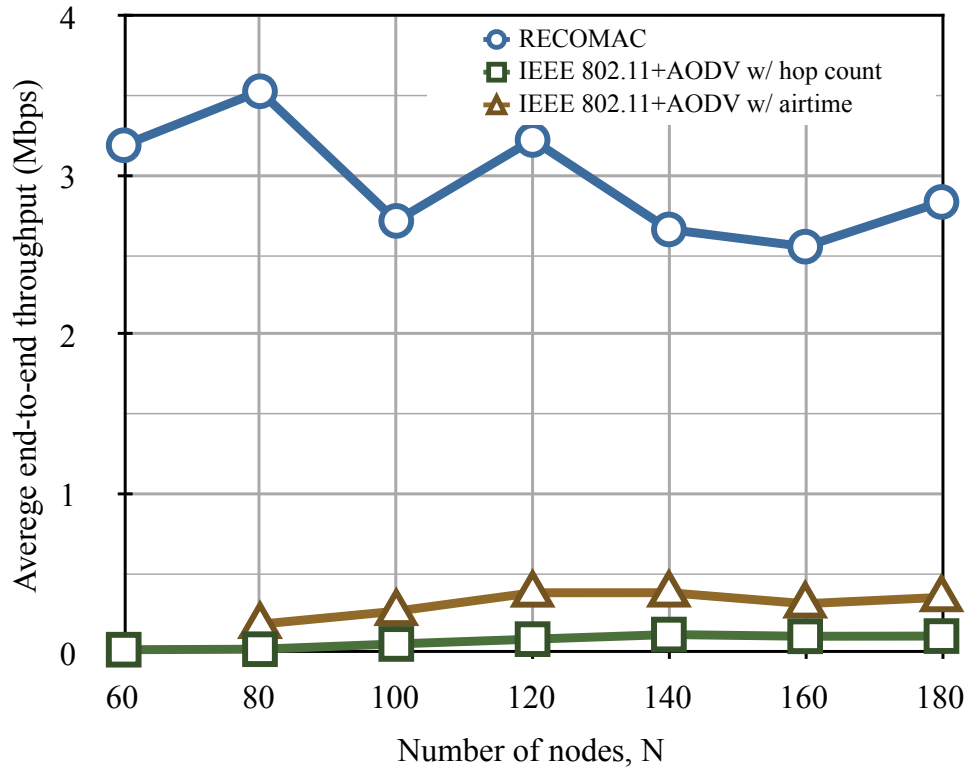

Figure 5.15: The average end-to-end throughput for RECOMAC, IEEE 802.11+AODV with hop count and IEEE 802.11+AODV with airtime metric.

In Fig 5.15, we depict the average end-to-end throughput of RECOMAC architecture, and IEEE 802.11+AODV, AODV implemented with hop count and airtime metrics. It is observed that RECOMAC improves the throughput performance significantly for all network sizes. The performance of AODV with airtime metric is better than AODV with hop count metric, as it updates the path depending on the link quality. The throughput enhancement of RECOMAC is due to robust cooperative transmissions, which prevent packet retransmissions even under channel impairments, and avoid collisions by nature. It is observed that RECOMAC can provide eight times higher end-to-end throughput, as compared to a non-cooperative network based on layered architecture with IEEE 802.11 and AODV (irrespective of routing metric).
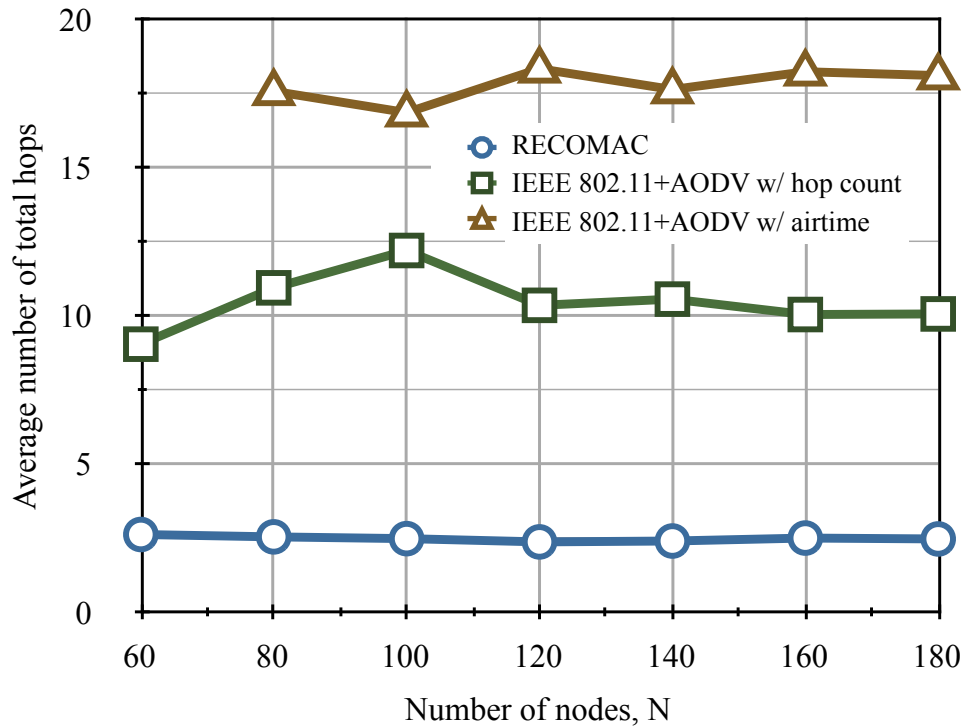

Figure 5.16: The average total number of hops for RECOMAC, IEEE 802.11+AODV with hop count and IEEE 802.11+AODV with airtime metric.

In Figure 5.16, we depict the average number of total hops between S and D. It

is observed that AODV with airtime metric can result in longer routes in search for more reliable ones, while AODV with hop count metric minimizes the hop count for the end-to-end communication. RECOMAC provides the smallest number of total hops, owing to the long haul transmissions enabled by cooperative diversity.
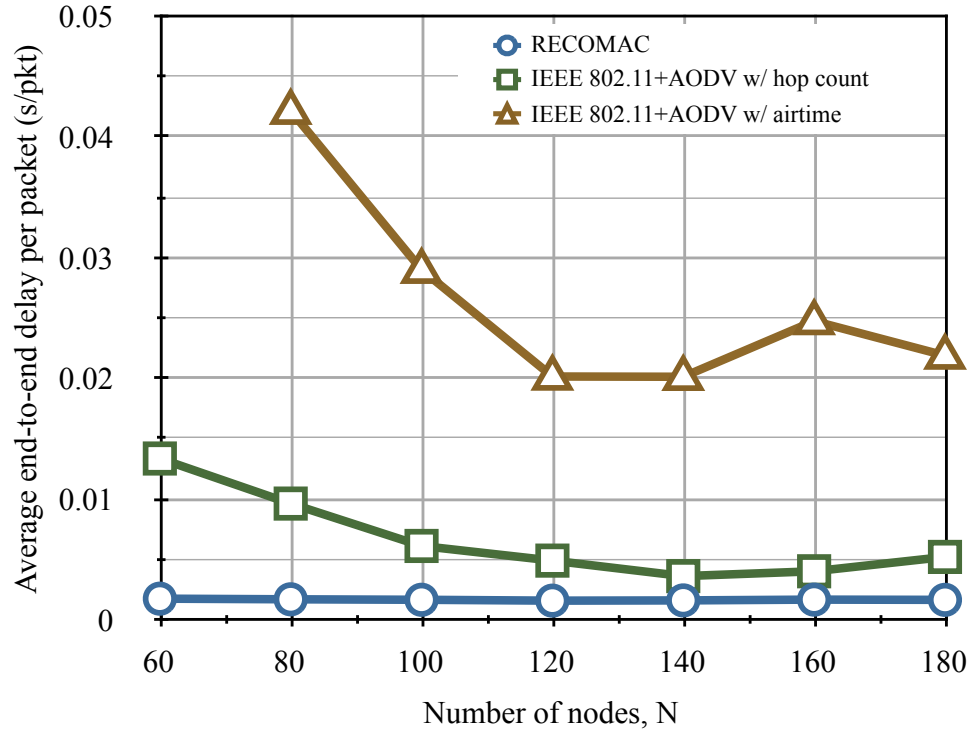

Figure 5.17: The average end-to-end delay per delivered data packet for RECO-MAC, IEEE 802.11+AODV with hop count and IEEE 802.11+AODV with airtime metric.

In Figure 5.17, we depict the average end-to-end delay per delivered packet. It is seen that RECOMAC improves the delay performance by almost five times, because it takes smaller number of hops to reach the destination, packet collisions are avoided by randomized coding and the retransmissions due to channel errors are avoided, owing to improved signal quality as a result of cooperative diversity gain. Even when retransmissions are required, this does not call for reestablishment of the end-to-end route, unlike the conventional layered architecture, IEEE 802.11+AODV. Moreover, in our simulations, we observed that AODV schemes may drop packets at

the MAC layer, due to numerous unsuccessful transmission attempts. In our results, we measure only the delay of successfully delivered packets.
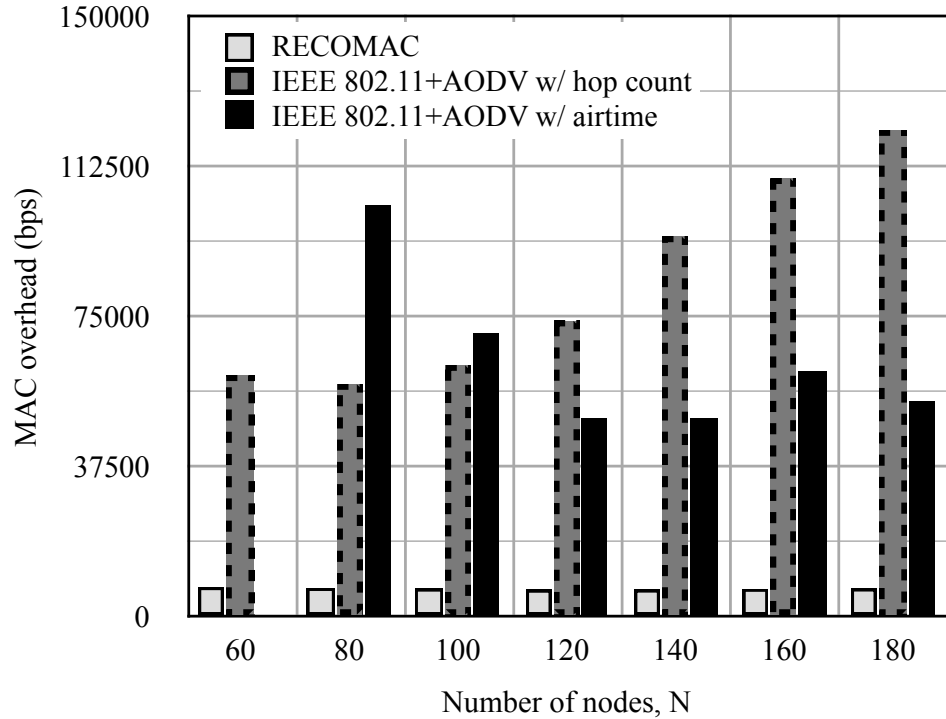

Figure 5.18: The average MAC overhead for RECOMAC, IEEE 802.11+AODV with hop count and IEEE 802.11+AODV with airtime metric.

In Figures 5.18 and 5.19, we provide the amount of MAC and routing overhead caused by the protocols to deliver one data packet to the destination node successfully. It is observed in Figure 5.18 that RECOMAC reduces the MAC messaging overhead significantly as compared to IEEE 802.11+AODV. The fraction of required MAC messaging to the obtained throughput is around 0.0023% for all considered network sizes for RECOMAC, whereas it ranges between 14% and 27% for IEEE 802.11+AODV with airtime metric, and it ranges between 60% and 80% for IEEE 802.11+AODV with hop count metric. This is because of the fact that IEEE 802.11+AODV architecture requires larger number of hops to reach the destination, and at each hop, multiple retransmissions are required due to channel impairments. Furthermore,

in the conventional 802.11+AODV architecture many unsuccessful data delivery attempts are made, requiring repeated route rediscovery phases for which MAC packets are used to coordinate the routing packets. On the other hand, RECOMAC makes use of robust long-haul cooperative transmissions that avoid retransmissions while reducing the total number of hops to reach the destination, thereby MAC messaging is reduced.
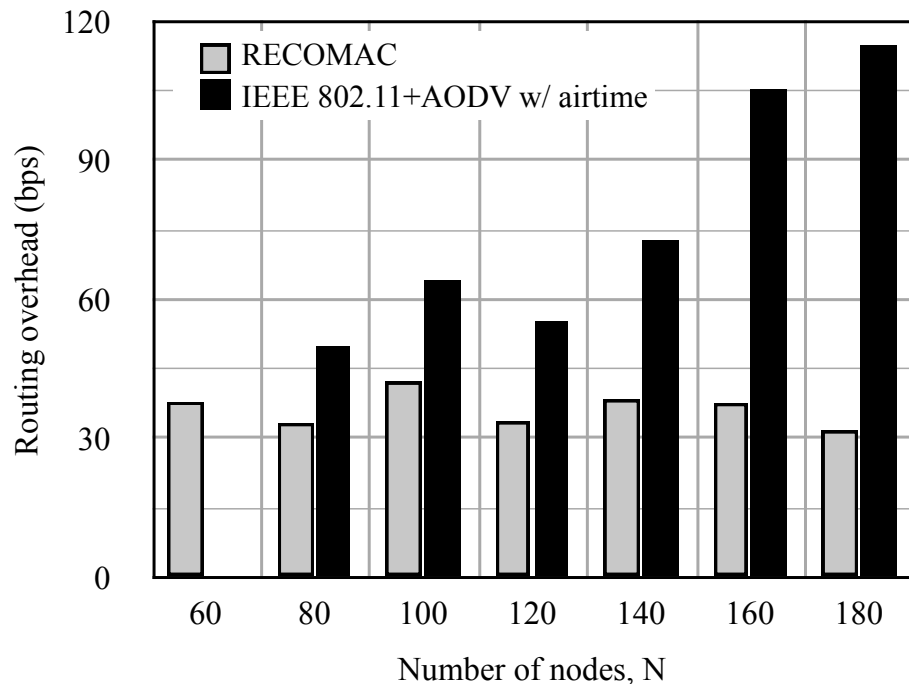
Figure 5.19: The average routing overhead for RECOMAC, IEEE 802.11+AODV with hop count and IEEE 802.11+AODV with airtime metric. Note that for $N = 60$, IEEE 802.11+AODV with airtime does not establish S-D connection.

In Figure 5.19, we depict the routing message overhead of RECOMAC and AODV with airtime metric. (The performance of AODV with hop count is incomparably poorer than the RECOMAC and AODV with airtime metric, hence it is not shown.) The routing message overhead for RECOMAC represents the total messaging (LREP and LREQ) carried out during the destination location discovery phase, and the routing overhead for AODV includes the route discovery phase, i.e., RREQ and RREP

packets. It is observed that the fraction of required route discovery messaging to the obtained throughput is 0.000012% for all considered network sizes for RECOMAC, whereas it ranges between 0.014% and 0.031% for IEEE 802.11+AODV with airtime metric, and it ranges between 4% and 18% for IEEE 802.11+AODV with hop count metric.

In this work, we have provided performance comparisons with the conventional layered architecture, IEEE 802.11+AODV, since both protocols are widely used. Furthermore, it is not possible to make meaningful performance comparisons with other cooperative protocols in the literature [29,35,36,38,70], because these protocols either do not consider an explicit MAC protocol and they assume perfect coordination among the nodes [38, 70], or they consider flawless relay selection and actuation procedures [29,35,36], which obscure the effect of messaging overhead on the overall system performance.

5.5   Discussion

In this chapter, a novel cooperative routing framework is proposed with three cooperative routing schemes and a cross-layer cooperative network architecture, RE-COMAC is presented for application in wireless ad hoc networks. The RECOMAC architecture spans the physical, MAC and routing layers, such that the routing layer functionality is submerged into the MAC layer, as the MAC packet exchanges are exploited for route formation. Our RECOMAC architecture facilitates formation of cooperative sets on the fly in a decentralized and distributed fashion without the need for extra messaging overhead for relay selection and actuation, resulting in opportunistically formed cooperative links that provide robust and reliable end-to-end communication. RECOMAC does not require establishing a prior non-cooperative route before cooperative transmissions, as opposed to the schemes [29, 38]. This

reduces the messaging overhead for route discovery and establishment phases. Furthermore, in RECOMAC architecture, the end-to-end route is defined as series of *regions* in which the relays reside, as opposed to a string of predetermined nodes used in existing methods [29, 38, 70]. Our architecture allows and enables cooperative transmissions of multiple nodes in the routing region. Cooperative forwarding within a region enables progress of the packets towards the direction of the final destination even for sparse networks, where the routing schemes with non-cooperative transmissions can not guarantee source-destination connectivity.

Via realistic implementation of RECOMAC in a network simulator environment, ns-2, and detailed simulations, we evaluate and compare the performance of our architecture in terms of end-to-end throughput and end-to-end delay, to those of non-cooperative networks using well known MAC and ad hoc routing protocols, IEEE 802.11 and AODV, respectively. The routing and MAC overhead is an important cost of end-to-end communication, appropriate quantification of which helps solid comparison between various proposed protocols in the literature. In our analysis, we also quantify the overhead of realizing our cooperative architecture in comparison to the considered non-cooperative architecture. The results demonstrate that under Rayleigh fading and path loss, our cooperative forwarding framework and our cross-layer architecture, RECOMAC, significantly improve the system performance, with eight times higher throughput and ten times lower delay, as compared to non-cooperative layered architecture with IEEE 802.11 and AODV routing. RECOMAC stands out as a promising architecture that can fully exploit cooperative diversity by enabling cooperative transmissions with RDSTC.

The results of this chapter have been submitted for publication in [111, 112].

6   CONCLUSIONS AND FUTURE WORK

In this dissertation, we have proposed a cooperative diversity architecture for wireless networks, by considering cooperation at different network layers.

First, we have presented a new cooperative MAC protocol, COMAC. Through the presented protocol, we have demonstrated and quantified the throughput and energy gains that can be achieved by cooperative transmission in wireless networks. It is shown that the amount of performance improvement depends on the transmission range, data rate and components of energy consumption. Despite the introduced overhead and extra transmissions, cooperative transmission via the COMAC protocol is proven to provide significant throughput enhancements in both point-to-point and multi-point-to-point scenarios, especially for medium to long range transmission. For the same transmission ranges, energy savings of about 50% is obtained over direct transmission, irrespective of increased number of users or circuit energy consumption.

Secondly, we have proposed and analyzed a distributed relay selection and actuation scheme based on random access relay advertisements for our COMAC protocol. The proposed scheme renders simple distributed operation, which makes it suitable especially for densely deployed networks. We have evaluated the throughput performance of COMAC with relay selection through analytical derivation and ns-2 simulations, and we have also observed the energy efficiency. The results are promising as significant throughput enhancements, of up to 79% and energy savings of up to 32% are observed over direct transmission. The COMAC protocol with multiple relays provides a general framework, in which new relay selection metrics can be incorporated for realizing cooperation in wireless networks.

Within the context of cooperative MAC, we have also presented a cross-layer random access method that incorporates cooperative transmissions into the well known slotted ALOHA system. We have derived analytical expressions for the successful packet transmission probability for this protocol and analyzed the effect of random cooperation decision on the system performance. We have shown that by exploiting the robustness of cooperative transmissions against channel impairments, the throughput of the direct ALOHA system in a noisy fading channel can be improved by 30%, via cooperative ALOHA.

Next, we have studied the energy minimal joint cooperator selection and power assignment problem under transmit power constraints such that the cooperative transmissions satisfy a predetermined average BER target. We have derived the average BER of the cooperative system and proposed a simple yet close BER approximation, which can facilitate simple cooperator selection methods with closed form power assignment solutions. We have formulated the joint cooperator selection and power assignment problem, derived and presented the optimal solution (O-CSPA) and we have also proposed a distributed implementation (D-CSPA). The performance of O-CSPA and D-CSPA algorithms are evaluated considering various network topologies, target average BER levels and different power consumption models. Our results demonstrate that smart cooperator selection is essential, as it provides efficient resource allocation with reduced overhead leading to improved system performance. It is further observed that with optimal transmit power assignment, energy dissipated at the transmit amplifiers can be reduced by 80% as compared to using constant transmit power levels, while maintaining long-haul transmissions at the demanded average BER level. Also, it is shown that total energy cost of communication can be reduced by 20% considering current technology in wireless transceivers. As less energy consuming circuitries become available, the energy savings offered by coop-

erative systems can be improved by up to 90%. We also demonstrate that our distributed method, D-CSPA provides similar energy savings with the optimal scheme, O-CSPA, with much lower complexity and with a robust performance even under errors in channel state information. In addition to numerical performance results, we have also obtained the performance of D-CSPA algorithm within the COMAC protocol. For this purpose, D-CSPA algorithm has been implemented in COMAC for relay selection and determination of optimal power levels. Our extensive simulations demonstrate that our distributed algorithm, D-CSPA causes minimal overhead, yields throughput improvement of 4 - 300 times, and an 8 - 800 times decrease in delay, while reducing the energy consumption, as compared to direct transmission.

Last but not least, we have proposed a cooperative routing framework and a cross-layer cooperative network architecture for wireless ad hoc networks, which make use of RDSTC in cooperative transmissions. Our architecture, named as RECOMAC, facilitates formation of cooperative sets on the fly in a decentralized and distributed fashion without the need for extra messaging for relay selection and actuation, resulting in opportunistically formed cooperative links that provide robust and reliable end-to-end communication. Also, RECOMAC does not require establishing a prior non-cooperative route before cooperative transmissions, as opposed to the existing schemes. This reduces the overhead for route discovery and establishment phases. Furthermore, in our architecture, the end-to-end route is defined as series of regions in which the relays reside, as opposed to a string of predetermined nodes used in existing methods. Via realistic implementation of RECOMAC in a network simulator environment, ns-2, and detailed simulations, we evaluate and compare the performance of our architecture in terms of end-to-end throughput and end-to-end delay, to those of non-cooperative networks using well known MAC and ad hoc routing protocols, IEEE 802.11 and AODV, respectively. In our analysis, we also quantify

the overhead of realizing our cooperative architecture in comparison to the considered non-cooperative architecture. Cooperative forwarding within a region is shown to enable progress of the packets towards the direction of the final destination even for sparse networks, where the routing schemes with non-cooperative transmissions can not guarantee source-destination connectivity. The results demonstrate that under Rayleigh fading and path loss, our cooperative forwarding framework and our cross-layer architecture, RECOMAC significantly improve the system performance, with eight times higher throughput and ten times lower delay, as compared to non-cooperative conventional layered architecture with IEEE 802.11 and AODV routing. Therefore, RECOMAC stands out as a promising architecture that can fully exploit cooperative diversity by enabling cooperative transmissions with RDSTC.

Note that, the use of cooperative diversity is essential when the source node cannot communicate directly with the destination node at the required reliability level. When direct transmission satisfies the required level of reliability, the cooperative diversity would not be needed, since the two phase data transmission and messaging overhead associated with the relay selection and actuation processes can obliterate the benefits of cooperation. In this dissertation, it is shown that the source-destination communication can be maintained at the required reliability level even under severe fading conditions and for the distances that direct transmission cannot be carried out. Also, while this dissertation aims at designing a cooperative diversity architecture that spans all the related layers, namely physical, MAC and routing layers, there are still some practical issues that can be considered for future research. For instance, in chapters 3 and 4, relay transmissions have been assumed to be carried out through orthogonal channels realized via orthogonal space-time block codes [42]. However, the design and selection of the best space-time block codes and the bandwidth costs associated with employing specific set of space-time codes are not investigated in this

dissertation. Furthermore, in this dissertation, we assumed that no multiple access interference is present at the receiver due to cooperative transmissions. Besides, in some topologies relay destination channels can be correlated, in which case MISO assumption for cooperative diversity systems is no more valid. The diversity gain in correlated channel case requires substantial work in the physical layer, which can be the subject of another dissertation.

In addition to possible directions listed above, as future work, the protocols proposed in this dissertation can be readily extended to work for different fading distributions, coding and modulation schemes, and multiple access methods, as we also pointed out in the related chapters of this dissertation. Also, throughout this dissertation, we assumed that each node in the network is willing to work towards the benefit of the overall network performance. Incorporation of the incentives for the relay nodes to participate in cooperation and considering the point of view of the cooperating node brings a new problem description, and on this subject, the case where the cooperating node has its own data can be studied and a cooperative diversity architecture can be designed to optimize the system performance from the point of view of the cooperating node.

Bibliography

[1] A. Goldsmith, *Wireless Communications.* 1st ed. New York: Cambridge University Press, 2005.

[2] I. F. Akyildiz, W. Su, Y. Sankarasubramaniam, and E. Cayirci, "Wireless sensor networks: A survey," *Computer Networks*, vol. 38, no. 4, pp. 393–422, Mar. 2002.

[3] J. G. Proakis, *Digital Communications*, 4th ed. New York: McGraw Hill, 2001.

[4] "IEEE Standard 802.11-1997, Wireless lan medium access control (MAC) and physical layer (PHY) specifications."

[5] J. Gutierrez, M. Naeve, E. Callaway, M. Bourgeois, V. Mitter, B. Heile, and E. Corp, "IEEE 802.15.4: a developing standard for low-power low-cost wireless personal area networks," *IEEE Network*, vol. 15, no. 5, pp. 12–19, Sep./Oct. 2001.

[6] A. Sendonaris, E. Erkip, and B. Aazhang, "User cooperation diversity — part I: System description," *IEEE Trans. Commun.*, vol. 51, no. 11, pp. 1927–1938, Nov. 2003.

[7] ——, "User cooperation diversity-part II: Implementation aspects and performance analysis," *IEEE Trans. Commun.*, vol. 51, no. 11, pp. 1939–1948, Nov. 2003.

[8] J. N. Laneman, D. N. C. Tse, and G. W. Wornell, "Cooperative diversity in wireless networks: Efficient protocols and outage behavior," *IEEE Trans. Inf. Theory*, vol. 50, no. 12, pp. 3062–3080, Dec. 2004.

[9] V. Stankovic, A. Host-Madsen, and Z. Xiong, "Cooperative diversity for wireless ad hoc networks," *IEEE Signal Process. Mag.*, vol. 23, no. 5, pp. 37–49, Sep. 2006.

[10] T. M. Cover and A. A. E. Gamal, "Capacity theorems for the relay channel," *IEEE Trans. Inform. Theory*, vol. 25, no. 5, pp. 572–584, Sep. 1979.

[11] A. Nosratinia, T. Hunter, and A. Hedayat, "Cooperative communication in wireless networks," *IEEE Commun. Mag.*, vol. 32, no. 10, pp. 74–80, Oct. 2004.

[12] S. Cui, A. J. Goldsmith, and A. Bahai, "Energy-efficiency of MIMO and cooperative MIMO techniques in sensor networks," *IEEE J. Sel. Areas Commun.*, vol. 22, no. 6, pp. 1089–1098, Aug. 2004.

[13] S. K. Jayaweera, "Virtual MIMO-based cooperative communication for energy-constrained wireless sensor networks," *IEEE Trans. Wireless Commun.*, vol. 5, no. 5, pp. 984–989, May. 2006.

[14] M. Chen, S. Serbetli, and A. Yener, "Distributed power allocation strategies for parallel relay networks," *IEEE Trans. Wireless Commun.*, vol. 7, no. 2, pp. 552–561, Feb. 2008.

[15] Y. Zhao, R. Adve, and T. J. Lim, "Improving amplify-and-forward relay networks: optimal power allocation versus selection," *IEEE Trans. Wireless Commun.*, vol. 6, no. 8, pp. 3114–3123, Aug. 2007.

[16] T. C. Hou and V. O. K. Li, "Transmission range control in multihop packet radio networks," *IEEE Trans. Commun.*, vol. 34, no. 1, pp. 38–44, Jan. 1986.

[17] Y. Li, B. Vucetic, Z. Zhou, and M. Dohler, "Distributed adaptive power allocation for wireless relay networks," *IEEE Trans. Wireless Commun.*, vol. 6, no. 3, pp. 948–958, Mar. 2007.

[18] R. Madan, N. B. Mehta, A. F. Molisch, and J. Zhang, "Energy-efficient cooperative relaying over fading channels with simple relay selection," *IEEE Trans. Wireless Commun.*, vol. 7, no. 8, pp. 3013–3025, Aug. 2008.

[19] J. Luo, R. S. Blum, L. J. Cimini, Greenstein, and A. M. Haimovich, "Decode-and-forward cooperative diversity with power allocation in wireless networks," *IEEE Trans. Wireless Commun.*, vol. 6, no. 3, pp. 793–799, Mar. 2007.

[20] X. Deng and A. M. Haimovich, "Power allocation for cooperative relaying in wireless networks," *IEEE Commun. Lett.*, vol. 9, no. 11, pp. 994–996, Nov. 2005.

[21] S.-H. Chen, U. Mitra, and B. Krishnamachari, "Cooperative communication and routing over fading channels in wireless sensor networks," in *Wireless Commun. and Mobile Comp. Conf.*, vol. 2, Jun. 2005, pp. 1477–1482.

[22] W. Su, A. K. Sadek, and L. K. J. R., "SER performance analysis and optimum power allocation for decode-and-forward cooperation protocol in wireless networks," *IEEE WCNC'05*, vol. 2, pp. 984–989, Mar. 2005.

[23] J. Adeane, M. R. D. Rodrigues, and I. J. Wassell, "Centralised and distributed power allocation algorithms in cooperative networks," in *IEEE Workshop on Signal Proc. Advan. in Wireless Commun. (SPAWC)*, Jun. 2005.

[24] B. Wang, Z. Han, and K. J. R. Liu, "Distributed relay selection and power control for multiuser cooperative communication networks using buyer/seller game," *Proc. IEEE INFOCOM'07*, pp. 544–552, May. 2007.

[25] A. Bletsas, A. Khitsi, D. P. Reed, and A. Lippman, "A simple cooperative diversity method based on network path selection," *IEEE J. Sel. Areas Commun.*, vol. 24, no. 3, pp. 659–672, Mar. 2006.

[26] A. Bletsas, A. Lippman, and D. P. Reed, "A simple distributed method for relay selection in cooperative diversity wireless networks, based on reciprocity and channel Measurements," *IEEE VTC'05*, vol. 3, pp. 1484– 1488, Jun. 2005.

[27] F. A. Onat, Y. Fan, H. Yanikomeroglu, and H. V. Poor, "Threshold based relay selection in cooperative wireless networks," in *IEEE GLOBECOM*, 2008, pp. 1–5.

[28] P. Liu, Z. Tao, S. Narayanan, T. Korakis, and S. S. Panwar, "CoopMAC: A cooperative MAC for wireless LANs," *IEEE J. Sel. Areas Commun.*, vol. 25, no. 2, pp. 340–354, Feb. 2007.

[29] G. Jakllari, S. V. Krishnamurthy, M. Faloutsos, P. V. Krishnamurthy, and O. Ercetin, "A framework for distributed spatio-temporal communications in mobile ad hoc networks," in *Proc. of IEEE INFOCOM*, April 2006, pp. 1–13.

[30] A. Azgin, Y. Altunbasak, and G. AlRegip, "Cooperative mac and routing protocols for wireless ad hoc networks," in *Proc. IEEE GLOBECOM*, vol. 5, Dec. 2005, pp. 2854–2859.

[31] H. Shan, W. Zhuang, and Z. Wang, "Distributed cooperative MAC for multihop wireless networks," *IEEE Commun. Mag.*, vol. 47, no. 2, pp. 126–133, Feb. 2009.

[32] P. Liu, C. Nie, E. Erkip, and S. Panwar, "Robust cooperative relaying in a wireless lan: Cross-layer design and performance analysis," in *Proc. of IEEE GLOBECOM*, 2009, pp. 4107–4112.

[33] C. Nie, P. Lie, T. Korakis, E. Erkip, and E. Panwar, "Coopmax: A cooperative mac with randomized distributed space-time coding for an ieee 802.16 network," in *Proc. of IEEE ICC*, June 2009.

[34] F. Verde, T. Korakis, E. Erkip, and A. Scaglione, "A Simple Recruitment Scheme of Multiple Nodes for Cooperative MAC," *IEEE Trans. Commun.*, vol. 58, no. 9, pp. 2667–2682, Sep. 2010.

[35] B. Zhao and M. C. Valenti, "Practical relay networks: A generalization of hybrid-ARQ," *IEEE J. Sel. Areas Commun.*, vol. 23, no. 1, pp. 7–18, Jan. 2005.

[36] F. Librino, M. Levorato, and M. Zorzi, "Distributed cooperative routing and hybrid arq in mimo-blast ad hoc networks," in *Proc. of IEEE GLOBECOM*, Nov. 2007, pp. 657–662.

[37] A. E. Khandani, J. Abounadi, E. Modiano, and L. Zheng, "Cooperative routing in static wireless networks," *IEEE Trans. Commun.*, vol. 55, no. 11, pp. 2185–2192, Nov. 2007.

[38] M. Dehghan, M. Ghaderi, and D. Goeckel, "Cooperative diversity routing in wireless networks," in *Proc. of WiOpt*, June 2010.

[39] "The network simulator - ns-2." [Online]. Available: http://www.isi.edu/nsnam/ns/

[40] S. Haykin and M. M., *Modern Wireless Communications.* Pearson Prentice Hall, 2005.

[41] T. Eng and L. B. Milstein, "Comparison of diversity combining techniques for rayleigh fading channels," *IEEE Trans. Commun.*, vol. 44, no. 9, pp. 1117–1129, Sep. 1996.

[42] V. Tarokh, H. Jafarkhani, and A. R. Calderbank, "Space-time block codes from orthogonal designs," *IEEE Trans. Inform. Theory*, vol. 45, no. 5, pp. 1456–1467, Jul. 1999.

[43] S. M. Alamouti, "A simple transmit diversity technique for wireless communications," *IEEE J. Sel. Areas Commun.*, vol. 16, no. 8, pp. 1451–1458, Oct. 1998.

[44] A. Papoulis, *Probability, random variables, and stochastic processes*, 2nd ed. McGraw-Hill, 1984.

[45] A. Leon-Garcia and I. Widjaja, *Communication networks*, 1st ed. McGraw-Hill, 2000.

[46] M. K. Simon and M. S. Alouini, *Digital Communication over Fading Channels*, 2nd ed. Wiley, 2005.

[47] ——, *Digital Communications over Fading Channels: A Unified Approach to Performance Analysis.* Wiley, New York, 2000.

[48] L. Zheng and D. N. C. Tse, "Diversity and multiplexing: a fundamental tradeoff in multiple-antenna channels," *IEEE Trans. Inform. Theory*, vol. 49, no. 5, p. 1073, 1096 2003.

[49] T. S. Rappaport, *Wireless Communications: Principles and Practice*, 2nd ed. Upper Saddle River, NJ: Prentice Hall, 2002.

[50] I. E. Telatar, "Capacity of multi-antenna gaussian channels," *Europ. Trans. Telecommun.*, vol. 10, no. 6, pp. 585–595, Nov.-Dec. 1999.

[51] A. Narula, M. D. Trott, and G. W. Wornell, "Performance limits of coded diversity methods for transmitter antenna arrays," *IEEE Trans. Inform. Theory*, vol. 45, no. 7, pp. 2418–2433, Nov. 1999.

[52] F. H. P. Fitzek and M. D. Katz, *Cooperation in Wireless Networks: Principles and Applications.* Springer, 2006.

[53] J. Laneman and G. Wornell, "Distributed space-time-coded protocols for exploiting cooperative diversity in wireless networks," *IEEE Trans. Inf. Theory*, vol. 49, no. 10, pp. 2415–2425, Oct. 2003.

[54] T. E. Hunter and A. Nosratinia, "Distributed protocols for user cooperation in multi-user wireless networks," *IEEE GLOBECOM'04*, vol. 6, pp. 3788–3792, Dec. 2004.

[55] A. Ribeiro, X. Cai, and G. B. Giannakis, "Symbol error probabilities for general cooperative links," *IEEE Trans. Wireless Commun.*, vol. 4, no. 3, pp. 1264–1273, May. 2005.

[56] P. A. Anghel and M. Kaveh, "Exact symbol error probability of a cooperative network in a rayleigh-fading environment," *IEEE Trans. Wireless Commun.*, vol. 3, no. 5, pp. 1416–1421, Sep. 2004.

[57] M. O. Hasna and M. S. Alouini, "End-to-end performance of transmission systems with relays over Rayleigh-fading channels," *IEEE Trans. Wireless Commun.*, vol. 2, no. 6, pp. 1126–1131, Nov. 2003.

[58] A. K. Sadek, W. Su, and K. J. R. Liu, "Performance analysis for multinode decode-and-forward relaying in cooperative wireless networks," in *IEEE ICASSP'05*, vol. 3, Mar. 2005, pp. 521–524.

[59] F. A. Onat, A. Adinoyi, Y. Fan, H. Yanikomeroglu, J. S. Thompson, and I. D. Marsland, "Threshold selection for SNR-based selective digital relaying in cooperative wireless network," *IEEE Trans. Wireless Commun.*, vol. 7, no. 11, pp. 4226–4237, Nov. 2008.

[60] F. A. Onat, Y. Fan, H. Yanikomeroglu, and J. S. Thompson, "Asymptotic BER analysis of threshold digital relaying schemes in cooperative wireless systems," *IEEE Trans. Wireless Commun.*, vol. 7, no. 12, pp. 4938–4947, Dec. 2008.

[61] A. Bletsas, H. Shin, and M. Z. Win, "Cooperative communications with outage-optimal opportunistic relaying," *IEEE Trans. Wireless Commun.*, vol. 6, no. 9, pp. 3450–3460, Sep. 2007.

[62] E. M. Royer and C.-K. Toh, "A review of current routing protocols for ad hoc mobile wireless networks," *IEEE Pers. Commun.*, vol. 6, no. 2, pp. 46–55, Apr. 1999.

[63] J. N. Al-Karaki and A. E. Kamal, "Routing techniques in wireless sensor networks: A survey," *IEEE Wireless Commun.*, vol. 11, no. 6, pp. 6–28, Dec. 2004.

[64] Z. Zhou, S. Zhou, J. H. Cui, and S. Cui, "Energy-efficient cooperative communication based on power control and selective single-relay in wireless sensor networks," *IEEE Trans. Wireless Commun.*, vol. 7, no. 8, pp. 3066–3078, Aug. 2008.

[65] W. Su, A. K. Sadek, and K. J. R. Liu, "Cooperative communication protocols in wireless networks: Performance analysis and optimum power allocation," *Wireless Pers. Commun.*, vol. 44, no. 2, pp. 181–217, Jan. 2008.

[66] L. Song and D. Hatzinakos, "Cooperative transmission in poisson distributed wireless sensor networks: Protocol and outage probability," *IEEE Trans. Wireless Commun.*, vol. 5, no. 10, pp. 2834–2843, Oct. 2006.

[67] V. Mahinthan, L. Cai, J. W. Mark, and X. Shen, "Maximizing cooperative diversity energy gain for wireless networks," *IEEE Trans. Wireless Commun.*, vol. 6, no. 7, pp. 2530–2539, Jul. 2007.

[68] P. Herhold, E. Zimmermann, and G. Fettweis, "A simple cooperative extension to wireless relaying," in *Int. Zurich Seminar on Communications*, 2004, pp. 36–39.

[69] A. Aksu and O. Ercetin, "Reliable multi-hop routing with cooperative transmissions in energy-constrained networks," *IEEE Trans. Wireless Commun.*, vol. 7, no. 8, pp. 2861–2865, Aug. 2008.

[70] L. V. Thanayankizil and M. A. Ingram, "Reactive routing for multi-hop dynamic ad hoc networks based on opportunistic large arrays," in *Proc. of Wireless Mesh and Sensor Networks Workshop, IEEE GLOBECOM*, Dec. 2008.

[71] B. Sirkeci-Mergen and A. Scaglione, "Randomized space-time coding for distributed cooperative communication," *IEEE Trans. Signal Process.*, vol. 55, no. 10, pp. 5003–5017, Oct. 2007.

[72] Z. Lin, E. Erkip, and A. Stefanov, "Cooperative regions and partner choice in coded cooperative systems," *IEEE Trans. Commun.*, vol. 54, no. 7, pp. 1323–1334, Jul. 2006.

[73] Z. Lin and E. Erkip, "Relay search algorithms for coded cooperative systems," in *IEEE GLOBECOM'05*, vol. 3, Nov. 2005, pp. 1314–1319.

[74] I. Maric and R. D. Yates, "Forwarding strategies for gaussian parallel-relay networks," *Proc. IEEE ISIT'04*, pp. 269–274, Jul. 2004.

[75] R. Lin and A. R. Petropulu, "Cooperative transmission for random access wireless networks," *Asilomar Conf.*, vol. 2, pp. 1922–1926, Nov. 2004.

[76] M. K. Tsatsanis, R. Zhang, and S. Banerjee, "Network-assisted diversity for random access wireless networks," *IEEE Trans. Signal Process.*, vol. 48, no. 3, pp. 702–711, Mar. 2000.

[77] "Cisco aironet 1200 series access point data sheet." [Online]. Available: http://www.cisco.com/en/US/products/hw/wireless/

[78] K. Vavelidis, "A dual-band 5.15-5.35 GHz, 2.4-2.5 GHz 0.18 μm CMOS transceiver for 802.11 a/b/g wireless LAN," *IEEE J. Solid-State Circuits*, vol. 39, no. 7, pp. 1180–1184, Jul. 2004.

[79] K. Sohrabi, J. Gao, V. Ailawadhi, and G. J. Pottie, "Protocols for self-organization of a wireless sensor network," *IEEE Pers. Commun.*, vol. 7, no. 5, pp. 16–27, Oct. 2000.

[80] K. Whitehouse, A. Woo, F. Jiang, J. Polastre, and D. Culler, "Exploiting the capture effect for collision detection and recovery," *Proc. of Em-NetS-II*, pp. 45–52, May 2005.

[81] N. Abramson, "The aloha system–another alternative for computer communications," *Proc. of AFIPS Conf., Montvale, NJ*, vol. 44, 1970.

[82] D. Bertsekas and R. Gallager, *Data Networks*, 2nd ed. New Jersey, USA: Prentice Hall, 1992.

[83] D. L. Mills, "Internet time synchronization: The network time protocol," *IEEE Trans. Commun.*, vol. 39, no. 10, pp. 1482–1493, Oct. 1991.

[84] M. S. Gokturk and O. Gurbuz, "Cooperation in wireless sensor networks: Design and performance analysis of a mac protocol," in *IEEE Int. Conf. on Communications, ICC '08.*, May 2008, pp. 4284–4289.

[85] ——, "Cooperative mac protocol with distributed relay actuation," in *Wireless Communications and Networking Conference, 2009. WCNC 2009. IEEE*, April 2009, pp. 1–6.

[86] M. S. Gokturk, O. Ercetin, and O. Gurbuz, "Throughput analysis of aloha with cooperative diversity," *Communications Letters, IEEE*, vol. 12, no. 6, pp. 468–470, June 2008.

[87] W. R. Heinzelman, A. Chandrakasan, and H. Balakrishnan, "Energy-efficient communication protocol for wireless microsensor networks," in *Proc. 33rd Hawaii Int. Conf. on System Sciences*, vol. 2, Jan. 2000, pp. 1–10.

[88] S. Cui, "Cross-layer optimization in energy constrained networks," PhD Dissertation, Stanford University, 2005.

[89] M. Gudmundson, "Correlation model for shadow fading in mobile radio systems," *Electron. Lett.*, vol. 27, no. 23, pp. 2145–2146, Nov. 1991.

[90] "Data sheet for cc2420 2.4 ghz ieee 802.15.4/zigbee-ready rf transceiver." [Online]. Available: http://focus.ti.com/lit/ds/symlink/cc2420.pdf

[91] A. Mainwaring, J. Polastre, R. Szewczyk, D. Culler, and J. Anderson, "Wireless sensor networks for habitat monitoring," in *ACM WSNA '02*, Sep. 2002, pp. 88–97.

[92] W. Kluge, F. Poegel, H. Roller, M. Lange, T. Ferchland, L. Dathe, and D. Eggert, "A fully integrated 2.4-GHz IEEE 802.15.4-compliant transceiver for zigbee applications," *IEEE J. Solid-State Circuits*, vol. 41, no. 12, pp. 2767–2775, Dec. 2006.

[93] R. Min, M. Bhardwaj, S.-H. Cho, N. Ickes, E. Shih, A. Sinha, A. Wang, and A. Chandrakasan, "Energy-centric enabling technologies for wireless sensor networks," *IEEE Wireless Commun.*, vol. 9, no. 4, pp. 28–39, Aug. 2002.

[94] "IEEE Standard 802.15.4-2003, Wireless medium access control (MAC) and physical layer (PHY) specifications for low-rate wireless personal area networks (WPANs)."

[95] M. S. Gokturk and O. Gurbuz, "Cooperation with multiple relays in wireless sensor networks: Optimal cooperator selection and power assignment," *submitted to IEEE Trans. Mobile Comp., under revision.*

[96] L. Badia, M. Levorato, F. Librino, and M. Zorzi, "Cooperation techniques for wireless systems from a networking perspective," *IEEE Wireless Commun.*, vol. 17, no. 2, pp. 89–96, Apr. 2010.

[97] A. E. Khandani, J. Abounadi, E. Modiano, and L. Zheng, "Cooperative routing in wireless networks," in *Allerton Conf. on Communications, Control and Computing*, Oct. 2003.

[98] A. Scaglione and Y.-W. Hong, "Opportunistic large arrays: Cooperative transmission in wireless multihop ad hoc networks to reach far distances," *IEEE Trans. Signal Process.*, vol. 51, no. 8, pp. 2082–2092, Aug. 2003.

[99] E. D. Kaplan, *Understanding GPS: principles and applications.* Artech House, Boston, MA, 1996.

[100] G. Dommety and R. Jain, *Potential networking applications of global positioning systems (GPS).* Technical report TR-24, The Ohio State University, 1996.

[101] J. Proakis, E. Biglieri, and S. Shamai, "Fading channels: information-theoretic and communication aspects," *IEEE Trans. Inf. Theory*, vol. 44, no. 6, pp. 2619–2692, Oct. 1998.

[102] X.-Y. Li, K. Moaveninejad, and O. Frieder, "Regional gossip routing for wireless ad hoc networks," *Mobile Networks and Applications*, vol. 10, no. 1-2, pp. 61–77, 2005.

[103] C. Saad, A. Benslimane, J. Champ, and J.-C. Konig, "Ellipse routing: A geographic routing protocol for mobile sensor networks with uncertain positions," in *IEEE GLOBECOM*, Dec. 2008, pp. 1–5.

[104] T. Q. Duong, O. Alay, E. Erkip, and H.-J. Zepernick, "End-to-end performance of randomized distributed space-time codes," in *Proc. of IEEE PIMRC*, Sept. 2010.

[105] M. Mauve, J. Widmer, and H. Hartenstein, "A survey on position-based routing in mobile ad hoc networks," *IEEE Network*, vol. 15, no. 6, pp. 30–39, Nov./Dec. 2001.

[106] H. Takagi and L. Kleinrock, "Optimal transmission ranges for randomly distributed packet radio terminals," *IEEE Trans. Commun.*, vol. 32, no. 3, pp. 246–257, Mar. 1984.

[107] T. Camp, J. Boleng, and V. Davies, "A survey of mobility models for ad hoc network research," *Wireless Commun. and Mobile Comp. (WCMC): Special issue on mobile ad hoc networking – research, trends and applications*, vol. 2, no. 5, pp. 483–502, Aug. 2002.

[108] M. Sharp, A. Scaglione, and B. Sirkeci-Mergen, "Randomized cooperation in asynchronous dispersive links," *IEEE Trans. Commun.*, vol. 57, no. 1, pp. 64–68, Jan. 2009.

[109] C. E. Perkins and E. M. Royer, "Ad-hoc on-demand distance vector routing," in *Proc. of 2nd IEEE Wksp. on Mobile Comp. Sys. and Apps.*, Feb. 1999, pp. 90–100.

[110] J. D. Camp and E. W. Knightly, "The IEEE 802.11s extended service set mesh networking standard," *IEEE Commun. Mag.*, vol. 46, no. 8, pp. 120–126, Aug. 2008.

[111] M. S. Gokturk, O. Gurbuz, and E. Erkip, "A cross-layer multi-hop cooperative network architecture for wireless ad hoc networks," *submitted to IEEE J. Sel. Areas Commun.*

[112] M. S. Gokturk, E. Erkip, and O. Gurbuz, "A cooperative routing framework based on randomized coding in wireless ad hoc networks," *submitted to IEEE Int. Conf. on Mobile Ad-hoc and Sensor Systems (MASS) 2011.*

Biography

M. Sarper Gokturk received his BS degree in Electrical and Electronics Engineering from the Middle East Technical University, Ankara, Turkey, in 2004. He received his MS degree in Electrical/Telecommunications Engineering from Drexel University, PA, USA, in 2006.

His research interests are in the field of wireless networks, in particular, media access control (MAC), cross layer design, cooperative communication architectures with emphasis on the applications for wireless sensor networks.